technische universität
dortmund

Study of Vegetation Cover Change and Its Driving Forces

By

Yong Xu

A doctorate dissertation submitted to the Faculty of Spatial Planning at TU Dortmund University in partial fulfillment of the requirements for the degree of Doctor of Engineering

Dissertation Committee:

Chairman: Univ.-Prof. Dr. Dietwald Gruehn

Supervisor: Univ.-Prof. Dr. habil. Nguyen Xuan Thinh

Supervisor: Univ.-Prof. Dr.-Ing. Ralf Bill

June 2019, Dortmund

Acknowledgments

First and foremost, I would like to thank the Department of Spatial Information Management and Modelling, School of Spatial Planning, at the University of TU Dortmund for providing the support opportunity, and resources to study and write this thesis.

I am extremely grateful to Prof. Dr. Nguyen Xuan Thinh, my supervisor and dissertation director, for his open mind and flexibility to new thoughts. He gave me chances to create new ideas and to validate it. His optimism, selfless and scientific supervision have fostered my enthusiasm for this study.

I am deeply grateful to my supervisor, Prof. Dr.-Ing. Ralf Bill, University Rostock, for his constructive comments and valuable suggests for my research work. His guidance and advice on my research work benefit me a lot. I am deeply grateful to Prof. Dr. Dietwald Gruehn, the chairman of my disputation, for his invaluable suggestions and support as well.

I have great pleasure in acknowledging my gratitude to Eun Young Park, the head of the English Department, and Dr. Tetyana Müller-Lyaskovets from the University of TU Dortmund. During my Ph.D. study, Eun Young Park guided me to improve my language ability, and Dr. Tetyana Müller-Lyaskovets gave me valuable suggestions for learning English and modifying my dissertation.

Many thanks to all of my colleagues in the Department of Spatial Information Management and Modelling with whom I have interacted during these years, Dr. Yantao Xi, Dr. Cheng Li, Dr. Jie Zhao, Dr. Mu Yang, Dr. Yan Chen, Dr. Kiet Nguyen Huu, Mustafa El-Morshdy, Mahsa Derakhshan, Haniyeh Ebrahimi Salari, and Yuchi Meng. I am grateful to them for their help and support during my study.

A special thanks to my parents and my sisters, for their unconditional love and never-ending support. I would like to express my deepest gratitude and love to them for their support and concern. Finally, I appreciate the financial support from the China Scholarship Council (Grant number: 201506420040) that funded this study.

Abstract

The dynamic change of vegetation cover exerts significant influences on the energetic and chemical circulation worldwide. Systematically monitoring the global vegetation cover change is critical to promote a better understanding of the basic biogeochemical processes, and their possible feedbacks to the global climate system. It is of great practical value to study dynamic vegetation variation related to climate change, human activities, and natural factors to explore the underlying relationships between vegetation cover change and its driving forces and the responding mechanisms of vegetation cover to the variability of the driving forces.

Vegetation degradation is continually proceeding worldwide, but the degradation situation is more serious in developing countries than in developed countries. China is the largest developing country, and it has been experiencing significant socio-economic development, rapid urban expansion, and sharp population growth in eastern China in particular after launching the program of reform and opening-up termed "Socialism with Chinese Characteristics" in China in 1978. The unprecedented socio-economic development, urban expansion, and population growth have led to land use and land cover change, soil fertility decline, vegetation degradation, water contamination, and biodiversity loss in eastern China. Eastern China, a place with a highly developed socioeconomic status than other regions of China, covers seven provinces (*e.g.,* Liaoning, Hebei, Shandong, Jiangsu, Zhejiang, Fujian, and Guangdong) and three municipalities (*e.g.,* Beijing, Tianjin, and Shanghai) with an area of about 1.0277 million km^2.

It is of critical importance for monitoring the dynamic vegetation variation on multi-spatiotemporal scales, exploring the underlying relationship between vegetation cover change and its driving forces (*e.g.,* climate forces, topographic forces, and socio-economic forces), and investigating the time lag effects of vegetation variation in response to climate variables (*e.g.,* precipitation and temperature) in eastern China from 2001 to 2016. To achieve the objectives of this study, the Moderate Resolution Imaging Spectroradiometer Normalized Difference Vegetation Index (NDVI) time series with a 250 m spatial resolution and a 16-day temporal resolution, monthly meteorological data

from meteorological (automatic) base station , Digital Elevation Model data with a 30 m spatial resolution, socio-economic statistical data, and the map of land use types, gross domestic product, and population density in 2000 and 2015 with an 1 km spatial resolution, and the vector map of eastern China at city level were used. A set of mathematical methods such as the maximum value composite method, linear regression analysis, rescaled range analysis, coefficient of variation, Person's correlation coefficient, t-test, and spatial analysis methods (*e.g.,* surface analysis and overlap analysis) were applied in this study.

This study aims at monitoring the dynamic change of vegetation cover and investigating the relationship between vegetation cover and its driving forces on multiple spatiotemporal scales in eastern China from 2001 to 2016. The objectives of this study are fulfilled and the main findings and new results of this study are summarized in following.

The overall annual NDVI displays a distinctive spatial heterogeneity across eastern China, presenting a gradient decrease from the south to the north of eastern China. The spatial distribution of NDVI in spring, summer, and autumn follows a similar pattern, but the overall NDVI value is higher in summer than in spring and autumn. Our calculation indicated that, during the past 16 years, the vegetation cover had gradually increased in eastern China with a magnitude of 0.0003 $year^{-1}$. Areas with a greening trend and areas with a browning trend account for 49% and 33% of the study area, respectively. Spatially, we found that the browning areas are mainly distributed in city centers and the three economic zones and its surrounding areas. Considering the vegetation variation on seasonal scale, NDVI performs an increasing trend in spring and autumn but a decreasing trend in summer.

In this study, we detected that areas expected to show consistency accounting for a larger proportion when compared with the areas expected to show anti-consistency on annual scale, while an opposite phenomenon was found on seasonal scale. In terms of the future changing trend of vegetation cover, areas with certain vegetation degradation will be larger than areas with certain vegetation improvement for eastern China both on annual and seasonal scales in the future. Estimating the vegetation stability on the basis

of variation of coefficient, we found that the vegetation cover is relatively stable in the south of the study area, but it fluctuated wildly in the north of the study area.

Our calculation suggested that temperature can be considered as the dominant climate factor controlling the vegetation growth in eastern China. The relationship is more pronounced between NDVI and temperature than between NDVI and precipitation both on annual and seasonal scales in eastern China for the study period. Moreover, the relationship between NDVI and precipitation is higher in autumn than in spring and summer, while the response of NDVI to temperature is stronger in spring than in autumn, followed by in summer. In this study, we observed, spatially, the overall maximum correlation coefficients between NDVI and precipitation as well as NDVI and temperature are basically higher in the north and lower in the south of the study area both on annual and seasonal scales. Temporally, on annual scale, the NDVI shows no lag time to changes in temperature but a 1-month lag time to precipitation variation. On seasonal scale, the maximum responses of NDVI to changes in precipitation and temperature establish 1-month longer in summer than in spring and autumn. Spatially, the lag time for maximum NDVI response to precipitation and temperature gradually increase from the north to the south of the study area.

Elevation is regarded to be a dominant factor affecting the vertical distribution of vegetation cover. Our findings indicated that both the vegetation cover and vegetation stability increase with the elevation increase and reach its peak at an elevation of about 500 m. The vegetation degradation is more serious at the elevation range of 0 to 100 m than at higher elevation ranges. It is worth noticing that, in this study, our result is against our initial assumptions that the vegetation growth on the north-facing slope is better than the vegetation growth on the south-facing slope. However, we found that the vegetation cover, vegetation cover change, and vegetation stability show no statistical difference on the south-facing slope and north-facing slope. Similar to the responding mechanisms between the elevation-vegetation cover and elevation-vegetation stability, the vegetation cover and vegetation stability show a gradient upward trend with slope range increase. Furthermore, the proportion of the areas with a greening trend shows a “humped” pattern with the slope range increase, and it reaches the peak at the slope range of 6° to 15°.

Our findings indicated that vegetation degradation is generally attributed to socio-economic development, urban expansion, and population growth, particularly in Tianjin, Shanghai, Jiangsu, Zhejiang, Fujian, and Guangdong. However, implementing large-scale reforestation and afforestation programs such as the Natural Forest Conservation Program, Three-North Shelter Forest Program, Beijing and Tianjin Sandstorm Source Controlling Program, and Grain for Green Program contribute to the vegetation greening phenomenon since 1978, in Liaoning, Beijing, Shandong, and Hebei in particular. We further observed that, spatially, the dynamic change of vegetation cover is negatively coupled with socio-economic development, urban expansion, and population growth. Areas with a high-speed socio-economic development, rapid urban expansion, and sharp population growth are along with severe vegetation degradation and strong vegetation oscillation spatially.

Keywords: MODIS NDVI; climate factors; topographic factors; socio-economic factors; coefficient of variation; precipitation; temperature; south-facing slope; socio-economic development; urban expansion; population growth; maximum correlation coefficients; vegetation improvement; vegetation degradation

Table of Contents

List of Figures

List of Tables

List of Abbreviations

Apr	April
Aug	August
AVHRR	Advanced Very High Resolution Radiometer
BTSSR	Beijing–Tianjin Dust and Sandstorm Source Region
BTWSSCP	Beijing and Tianjin Sandstorm Source Controlling Program
C5	Collection 5
C6	Collection 6
CV	Coefficient of Variation
DC	Digital Camera
Dec	December
DEM	Digital Elevation Model
DLI	Development and Life Index
DN	Digital Number
DVI	Difference Vegetation Index
EFS	East-facing Slope
ENVI	Environment for Visualizing Images
ETM+	Enhanced Thematic Mapper Plus
EVI	Enhanced Vegetation Index
Feb	February
GDP	Gross Domestic Product
GGP	Grain for Green Program
GIMMS	Global Inventory Modeling and Mapping Studies
GIS	Geographic Information System
GRACE	Gravity Recovery and Climate Experiment
GRP	Gross Regional Product
HDF	Hierarchical Data Format

HRV	High Resolution Visible
IDL	Interactive Data Language
IPCC	Intergovernmental Panel on Climate Change
Jan	January
Jul	July
Jun	June
LAEA	Lambert Azimuthal Equal Area
LPDAAC	Land Processes Distributed Active Archive Center
Mar	March
May	May
MIR	Mid-infrared
MODIS	Moderate Resolution Imaging Spectroradiometer
MRT	MODIS Reprojection Tool
MSS	Multispectral Scanner
MVC	Maximum Value Composite
NASA	National Aeronautics and Space Administration
NDVI	Normalized Difference Vegetation Index
NDVI_Ann_Ave	Average Annual NDVI
NDVI_Ann_CV	Coefficient of Variation of Annual NDVI
NDVI_Ann_Slope	Annual NDVI Changing Slope
NDVI_Aut_Ave	Average Autumn NDVI
NDVI_Aut_CV	Coefficient of Variation of Autumn NDVI
NDVI_Aut_Slope	Autumn NDVI Changing Slope
NDVI_Spr_Ave	Average Spring NDVI
NDVI_Spr_CV	Coefficient of Variation of Spring NDVI
NDVI_Spr_Slope	Spring NDVI Changing Slope
NDVI_Sum_Ave	Average Summer NDVI
NDVI_Sum_CV	Coefficient of Variation of Summer NDVI

NDVI_Sum_Slope	Summer NDVI Changing Slope
NFCP	Natural Forest Conservation Program
NFS	North-facing Slope
NIR	Near-infrared
NOAA	National Oceanic and Atmospheric Administration
Nov	November
NP_Ann_MCC	Annual Maximum Correlation Coefficient between NDVI and Precipitation
NP_Ann_TimeLag	Annual Time Lag between NDVI and Precipitation
NP_Aut_MCC	Autumn Maximum Correlation Coefficient between NDVI and Precipitation
NP_Aut_TimeLag	Autumn Time Lag between NDVI and Precipitation
NP_MCC	Maximum Correlation Coefficient between NDVI and Precipitation
NP_Spr_MCC	Spring Maximum Correlation Coefficient between NDVI and Precipitation
NP_Spr_TimeLag	Spring Time Lag between NDVI and Precipitation
NP_Sum_MCC	Summer Maximum Correlation Coefficient between NDVI and Precipitation
NP_Sum_TimeLag	Summer Time Lag between NDVI and Precipitation
NP_TimeLag	Time Lag between NDVI and Precipitation
NPP	Net Primary Productivity
NT_Ann_MCC	Annual Maximum Correlation Coefficient between NDVI and Temperature
NT_Ann_TimeLag	Annual Time Lag between NDVI and Temperature
NT_Aut_MCC	Autumn Maximum Correlation Coefficient between NDVI and Temperature
NT_Aut_TimeLag	Autumn Time Lag between NDVI and Temperature
NT_MCC	Maximum Correlation Coefficient between NDVI and Temperature

NT_Spr_MCC	Spring Maximum Correlation Coefficient between NDVI and Temperature
NT_Spr_TimeLag	Spring Time Lag between NDVI and Temperature
NT_Sum_MCC	Summer Maximum Correlation Coefficient between NDVI and Temperature
NT_Sum_TimeLag	Summer Time Lag between NDVI and Temperature
NT_TimeLag	Time Lag between NDVI and Temperature
NUA	New Urban Area
NWFS	Northwest-facing Slope
Oct	October
OUA	Old Urban Area
PCGDP	Per Capita Gross Domestic Product
PD	Population Density
Pre_Ann_Ave	Annual Average Precipitation
Pre_Aut_Ave	Autumn Average Precipitation
Pre_Spr_Ave	Spring Average Precipitation
Pre_Sum_Ave	Summer Average Precipitation
PRM	Parameter
QA	Quality Assurance
RMB	Renminbi
RS	Remote sensing
R/S analysis	Rescaled Range analysis
Sep	September
SFS	South-facing Slope
SPOT VGT	Satellite Pour l'Observation de la Terre Vegetation
SRTM	Shuttle Radar Topography Mission
Tem_Ann_Ave	Annual Average Temperature
Tem_Aut_Ave	Autumn Average Temperature

Tem_Spr_Ave	Spring Average Temperature
Tem_Sum_Ave	Summer Average Temperature
TNSFP	Three-North Shelter Forest Program
TRMM	Tropical Rainfall Measuring Mission
USA	United States of America
UTM	Urchin Tracking Module
VIIRS	Visible Infrared Imaging Radiometer Suite
WFS	West-facing Slope
WGS	World Geodetic System
WHO	World Health Organization

1 Introduction

1.1 Background

Functioned as the bond of the air, soil, and water, vegetation is considered as a sensitive indicator for global environment variation (de Jong et al., 2013). As an important component of the geographical environment, vegetation occupies high proportion in the land surface system and becomes the core and the functional part of the biosphere and the ecosystem (Fabricante et al., 2009). Variation of the vegetation exerts significant influence on the energetic and chemical circulation all over the world. Systematically monitoring the global vegetation cover change is critical to promote a better understanding of the basic biogeochemical processes, and their possible feedbacks to the global climate system (Arneth et al., 2010). Meanwhile, human beings are anticipated to benefit significantly from it when undertaking environment and social-economic activities.

It is of great practical value to study dynamic vegetation variation related to climate changes, human activities, and natural factors to explore the underlying relationships between vegetation cover change and its driving forces and the responding mechanisms of vegetation cover to the variability of driving forces. Environmental and ecological destruction and the intensifying human-land conflict are critical issues that block human beings on the way of sustainable development, as exemplified by the sharp decline of the forests and farmland, the soil erosion and species extinction (Zou and Shen, 2003). These phenomena can be driven by global warming and socio-economic factors.

According to the Fifth Assessment Report of the Intergovernmental Panel on Climate Change (IPCC) (IPCC, 2013), the mean global temperature has increased by 0.85 ℃ over the past 130 years. The relevant research has proved that global warming has exerted certain effects on the vegetation cover variation since the 1980s. Vegetation biomass of the middle and high latitudes in the northern hemisphere has significantly increased. Moreover, the vegetation season commences earlier and the growing season is evidently extended (Myneni et al., 1997, Parmesan and Yohe, 2003). Human activities such as urbanization and the abuse of natural resources have brought in environmental issues, which lead to the decline of the vegetation cover (Guan et al., 2018). Besides,

the distribution of the vegetation cover is closely connected with the natural factors such as topography (Wang et al., 2016b).

Remote sensing (RS) technique, regarded as an alternative to time-consuming and labor-intensive field observation, makes monitoring dynamic vegetation cover possible. It has remarkable economic and social benefits, compared with traditional methods. As an important technique to collect spatial and temporal information, RS data are widely applied to study global and regional vegetation in the perspective of temporal and spatial variation trend (Fensholt and Proud, 2012, Eckert et al., 2015), which establishes the basis of research on vegetation variation monitoring. The emergence of time series Normalized Difference Vegetation Index (NDVI) data from multiple satellite sensors, *e.g.* National Oceanic and Atmospheric Administration (NOAA) Advanced Very High Resolution Radiometer (AVHRR), Moderate Resolution Imaging Spectroradiometer (MODIS), as well as Satellite Pour l'Observation de la Terre Vegetation (SPOT VGT) provides foundation for research on vegetation variation from pixel scale, regional scale to global scale, which makes great progress in vegetation variation research (Zhou et al., 2009, Barbosa et al., 2006, Hazarika et al., 2005).

NDVI is the specific figure reflecting the different reaction of vegetation to visible light, near-infrared reflectance, and soil background, and it is employed to make a quantitative description of the surface vegetation cover and vegetation growth status under certain conditions. It is always applied to monitor the state of vegetation growth, vegetation cover and vegetation dynamic variation. Analysis of terrestrial ecosystem using time series NDVI data is important to monitor vegetation dynamic variation responding to climate change. It is possible to directly express the spatial difference of vegetation cover trends using NDVI data, harvesting an insight on the impact of natural forces and human activities exert to the vegetation variation. The different phases of vegetation index in a given area can be used to monitor the vegetation variation trends (Fensholt and Proud, 2012), the vegetation growth conditions (Jiang et al., 2002), leaf area index (Auslander et al., 2003), net primary productivity (NPP) (Hazarika et al., 2005), and vegetation phenology (Richardson et al., 2010).

Ecosystems in eastern China are particularly fragile and vulnerable due to the rapid urbanization and industrialization and significant economic growth after initiating the

program of reform and opening-up termed "Socialism with Chinese Characteristics" in China in 1978. In addition, four special economic zones are established in Shantou, Shenzhen, and Zhuhai in Guangdong province and Xiamen in Fujian province after implementing this program. On the one hand, this program promoted the progress of the transformation of agricultural society to an industrial society. On the other hand, it led to negative impacts on the local terrestrial ecosystem such as soil erosion, deforestation, over-cultivation, air and water contamination, biodiversity loss, and agricultural land loss.

In this study, the NDVI data from MODIS will be used to study the spatiotemporal characteristics in eastern China, a typical developing coastal area in China. To explore the relationships between the NDVI variation and the driving forces (*e.g.,* climatic factors, socio-economic factors, and topographic factors), monthly temperature and precipitation data, Digital Elevation Model (DEM) data, and socio-economic data are used to analyze vegetation dynamic variation responding to climatic factors, topographic factors, and socio-economic factors. A comprehensive quantitative analysis is made based on various mathematic methods. This study is focused on different temporal scales (monthly, seasonal, annual, and inter-annual) and different spatial scales (pixel, station, and provincial).

1.2 Problem statement and motivation

Over the past three decades, China’s environment has seriously deteriorated, especially in highly developed areas, along with global climate change, complicated geographic conditions, rapid economic growth, high urbanization and industrialization, and further caused tremendous socio-economic impacts (Liu and Diamond, 2005). It has also been recognized that the dynamic variation of vegetation is driven by three major forces: natural forces, climatic forces, and socio-economic forces. Natural forces include stable soil condition, surface roughness, and topographic; climatic forces include surface temperature, precipitation, evapotranspiration, soil moisture, albedo, and cloud; socio-economic forces include transformation of farming methods, policy guidance, population density, Gross Domestic Product (GDP), household consumption, total employment, total investment in fixed assets, urbanization rate, and reforestation projects.

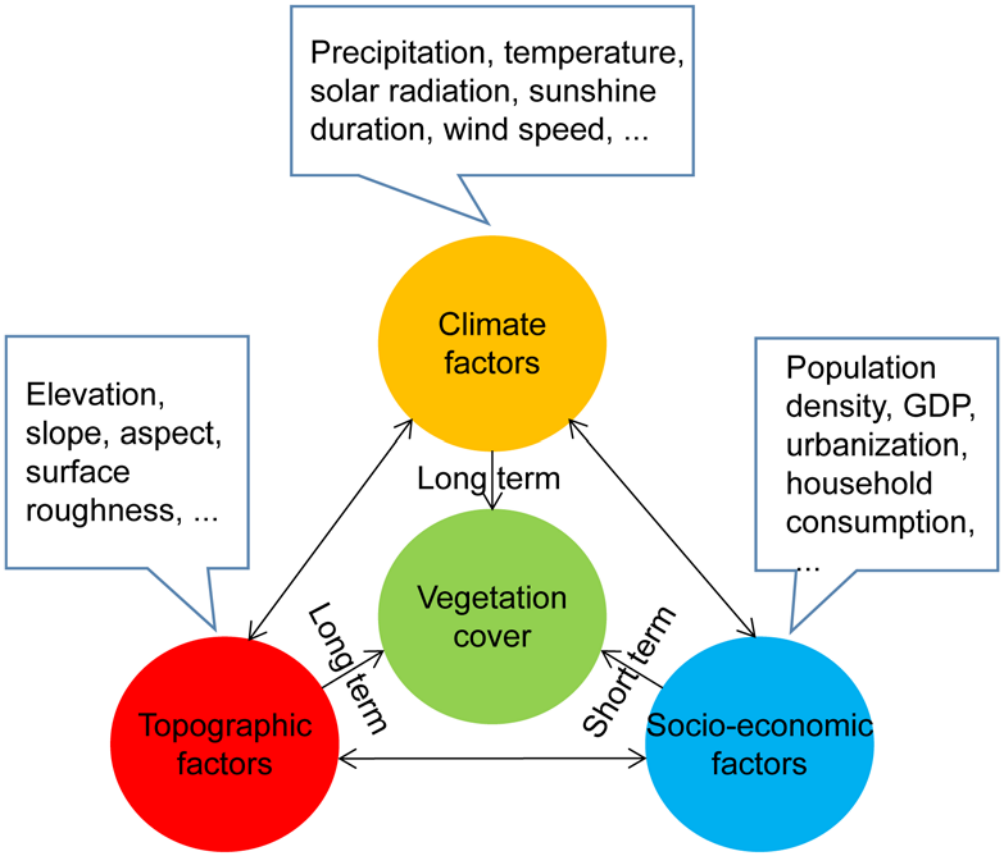

Figure 1-1. The synergism between vegetation cover and its driving forces

In the long term, natural forces and climatic forces are decisive for vegetation evolution. Changes in global climate exert significant influence on terrestrial vegetation system (de Jong et al., 2013). The interaction between climate and vegetation can be found in two aspects: on the one hand, climate determines the spatial distribution of the vegetation, and each type of climate corresponds to one kind of vegetation. On the other hand, different types of vegetation react with the matter and energy and exert influence on the climate. In the short term, the dynamic evolution of vegetation is mainly directly and indirectly influenced by human activities, which exerts a stronger impact on vegetation variation than the impact of climate change and topographic factors on vegetation variation both in speed and extent. The increasing population, developing industrial and the urbanization have proved the decisive socio-economic forces on local, regional and even global scales. It is the consistent irrational exploit of resources that lead to environmental issues. To conclude, long-term climate change determines the overall

pattern of vegetation distribution, while human activities have a direct or indirect impact on the dynamic evolution of local vegetation (Qu et al., 2015).

The capacity to recover from a disturbance can be diminished by vegetation degradation. To alleviate the expansion of degradation and desertification to reinforce the resilience in China's terrestrial ecosystem, the government of China has launched multiple forest conservation and restoration programs. Vegetation reforestation and restoration is an evolving concept in the face of challenges in environmental deterioration and degradation. During the last three decades, the vegetation cover in China has significantly improved at the national level due to the implementation of these reforestation and restoration programs (Lu et al., 2015). It has taken place in the context of rapid social and economic development and dramatic climate changes over the same period (Liu and Diamond, 2008). Although there is an increasing trend of vegetation cover at the large nationwide scale in China over the last three decades (Peng et al., 2011), some decrease trends can be found at the local scale. Because of the impact of rapid urbanization and industrialization boosted the land use and land cover change, the vegetation cover in the Pearl River Delta and Yangtze River Delta has significantly decreased (Qu et al., 2015). The rising urbanization level, structural adjustment of agriculture, and the non-agricultural construction have greatly accelerated the speed of farmland shrinking (Gu et al., 2009).

This study is motivated to explore the spatiotemporal variation characteristics of vegetation cover in eastern China, a typical developing coastal area in China, consisting of seven provinces (Hebei, Liaoning, Jiangsu, Zhejiang, Fujian, Shandong, and Guangdong) and three municipalities (Beijing, Tianjin, and Shanghai). To understand the temporal trends of the regional NDVI, above seven provinces and three municipalities were adopted to be ten independent administrative units. It is interesting to explore vegetation cover variation driven by climate, socio-economic, and natural forces. This study is aimed to analyze the relationships between vegetation cover and the three driving forces in eastern China from three major aspects, such as the changing trend, fluctuation degree, and consistency. The socio-economic driving forces include the total population, density of population, GDP (*e.g.*, primary industry product, secondary industry product, tertiary industry product, and per capita GDP (PCGDP)), urbanization

rate, household consumption (*e.g.*, rural household consumption and urban household consumption), total investment in fixed assets, and total employment. The three topographic factors (*e.g.*, elevation, slope, and aspect) are considered as the natural driving forces. Temperature and precipitation are considered as the two major climatic driving factors. This study will provide a reference for eco-environmental monitoring and protection, as well as vegetation sustainability and promote a better understanding of the interaction between vegetation cover change and its driving forces in eastern China.

1.3 Research objectives and key questions

1.3.1 Research objectives

This study aims at monitoring the NDVI changing trend, NDVI fluctuation degree, and future NDVI changing trend on different spatial and temporal scales in eastern China using the MODIS NDVI time series from 2001 to 2016. It further explores the temporal and spatial interaction between NDVI and its driving forces such as climate force, topographic force, and socio-economic force. In addition, the lag time for maximum NDVI response to climate variation has to be investigated in this study. This study aims at the following objectives:

1) To display the spatial pattern of NDVI value, NDVI stability, and future NDVI changing trend and further explore the spatiotemporal characteristics of NDVI changing trend in eastern China both on annual and seasonal scales from 2001 to 2016.

2) To analyze the relationships between NDVI and precipitation as well as NDVI and temperature both on spatial and temporal scales and further quantitatively investigate the lag time for maximum NDVI response to changes in temperature and precipitation for each administrative unit and 184 meteorological stations.

3) To illustrate the characteristics of spatial coupling of the dynamic change of vegetation cover to topographic factors (*e.g.,* elevation, aspect, and slope) and determine the statistical relationships between vegetation variation and the three topographic factors.

4) To answer the questions: How and to what degree did socio-economic factors influence the vegetation cover, and how is the spatial responding mechanism of vegetation cover change to socio-economic development, urban expansion, and population growth in eastern China over the last two decades.

1.3.2 Research questions

The main challenge of this study is how to quantitatively determine the spatiotemporal change of vegetation cover, climate factors, and socio-economic factors over the last two decades, and how to promote a better understanding of vegetation cover variation in response to its driving forces on different spatial and temporal scales in eastern China effectively. To address these challenges, the following questions are proposed and need to be answered:

1) Which metrics can be used to reflect the long-term vegetation cover variation, and how to quantify the vegetation changing trend and vegetation cover stability?

2) How to quantitatively determine the relationships between NDVI and climate factors, and how to determine the lag time for maximum NDVI response to changes in climate factors? Which climate factor is the dominant factor controlling the vegetation growth in eastern China?

3) How to map the spatial interaction and how to determine the quantitative relationships between vegetation variation and topographic factors and socio-economic factors?

4) Do all the socio-economic factors negatively affect the vegetation growth over eastern China from 2001 to 2016?

5) What is the underlying cause of the spatial heterogeneity of vegetation cover over eastern China?

1.4 Structure of the dissertation

In this section, the structure of the dissertation will be clearly showed up. This dissertation consists of 6 chapters: introduction, theoretical background, the introduction

of the study area, methodology, results and discussion, and summary and conclusion, reflecting the logical framework of this study.

Chapter 1 provides general background information of this study, incorporating research problem statement and motivation, research objectives, and key questions into the introduction, which establishes the critical challenges of this study and the importance of this research topic.

Chapter 2 presents the theoretical background of this study, which provides a solid theoretical infrastructure for this research topic. In addition, this chapter is divided into two parts. Firstly, it reviews that many scholars using different satellite data and implying various mathematical methods to monitor the vegetation cover variation, which has occurred throughout the world across local to national scales. Then this chapter looks back the relationships between vegetation variation and its driving forces on the basis of previous studies.

Chapter 3 is concerned with the study area of eastern China. The geographic, meteorological, and socio-economic characteristics of eastern China are presented in this chapter. Moreover, the database for this study is described, including RS data, meteorological data, DEM data, socio-economic statistical data, as well as other spatial variables.

Chapter 4 describes the methodology initiated in this study. It provides all of the mathematical methods used for quantifying the dynamic change of vegetation cover, climate factors, and socio-economic factors. Furthermore, it establishes that based on various mathematical methods, how to quantitatively determine the correlation of vegetation responses to its driving forces on different spatiotemporal scales in eastern China.

Chapter 5 presents and discusses the main findings generated by the mathematical methods, which are described in chapter 4. To improve the readability of this dissertation, the results of this study are presented in this chapter, being consisted of maps, tables, graphics, and texts. Previous studies are also used to demonstrate and verify the results of this study. Further explanation is released in this chapter when the main findings are not in line with previous works.

Chapter 6 summarizes and discusses the main findings of this study in the context of the whole dissertation. The strengths and limitations of this study are promoted in this chapter. Based on the results of this study, future research related to this study is also presented.

2 Theoretical background

Many scholars have undertaken plenty of exploration on monitoring vegetation variation using NDVI time series. However, no generally accepted conclusion is drawn on the relationships between vegetation variation and the three driving forces (*e.g.,* climatic forces, socio-economic forces, and topographic forces). In this chapter, a brief outline of the strength and limitation of the related mathematical methods used to monitor the vegetation variation and the correlation of vegetation in response to its driving force variation will be then generated. The time lag effects between vegetation growth and climate variation are outlined. Furthermore, the vegetation variation, climate change, urbanization and industrialization processes, and economic growth both on national and regional scales are identified. In addition, the coupled effect of climate forces, topographic forces, and socio-economic forces on vegetation degradation and restoration in different studies were concluded in this chapter.

2.1 Estimation of the vegetation cover based on data processing methods

RS has been regarded as the major means for detecting the vegetation cover. The RS images are capable of reflecting the information and variation trend of vegetation cover on different scales. Multi-source RS images can be used together regardless of the discrepancy among the spatial resolution, spectral resolution, and temporal resolution. Estimating vegetation cover based on multi-spectral RS data requires the development and optimization of mathematical methods, such as linear regression analysis, vegetation index, mixed pixel decomposition, decision tree classification, artificial neural network algorithm, and landscape ecology method. However, this chapter focuses on establishing the vegetation cover variation from regional to global scales based on the method of linear regression analysis, which is determined to be employed to detect the vegetation cover variation in this study.

2.1.1 The overview of different mathematical methods

Regression analysis and mixed pixel decomposition are the two most widely accepted methods (Table 2-1). It has been turned out that non-linear regression analysis is more precise in detecting the turning point of the vegetation variation than linear regression

analysis, but linear regression analysis is more commonly and effectively used for mapping the spatial distribution of long-term vegetation cover variation. Dymond et al. (1992) and Wittich et al. (1995) obtained valuable results of vegetation cover estimation using non-linear regression analysis, while Fensholt and Proud (2012) adopted linear regression analysis and their estimation turned out to be rough on temporal scale but much practical on spatial scale.

Mixed pixel decomposition is favored by scholars for its high accuracy, and the function to eliminate other factors that have impacts on the estimation of vegetation cover such as bare soil and shadows. The combination of data from Landsat, SPOT VGT, NOAA AVHRR, and MODIS optimized the result for mixed pixel decomposition (Gutman and Ignatov, 1998, Al-Abed et al., 2000, Pech et al., 1986, Wu et al., 2015). Dimidiate pixel model was used by many scholars to estimate the vegetation cover in Hai River Basin, Yellow River Basin, Shaanxi Province, Fen River basin, Three Gorges Reservoir Area, Jungar Banner, and Xilinguole in China (Hou et al., 2013, Li et al., 2010, Ma et al., 2012, Tian et al., 2014, Wu et al., 2010, Yuan et al., 2013, Wu et al., 2012). Mid-resolution and high-resolution RS images were applied to monitor the cover of arbor based on the decision tree classification method. The results of this study proved to be of high accuracy (Goetz et al., 2003, Hansen et al., 2002).

The vegetation index method was also employed to monitor the vegetation cover variation in Beer-Sheva and Jing River Basin, but the results turned out to be coarse. The artificial neural network algorithm was employed to calculate the vegetation cover of northwest Pacific and mid-Atlantic oceanic region. Their results turned out to be better than those derived by using regression analysis and mixed pixel decomposition (Atkinson et al., 1997, Boyd et al., 2002). The only restriction of the artificial neural network algorithm is that it requires the accuracy of geometrical registration and availability of training samples. Due to the restriction, it did not be popularized in the research of vegetation cover variation. Mountain ecosystems have been accorded higher priority in global conservation strategies (Brooks et al., 2006). Segmented regression analysis and Sen Slope were employed to detect the vegetation cover variation for mountain protected areas in 5 biodiversity hotspots. The NDVI in five

continental regions showed a moderate greening trend until the middle of the 19th century and shifted to browning trend afterward (Krishnaswamy et al., 2014).

Different research methods may produce different research results. For instance, the conclusion was contrast in two studies using different methods focused on the vegetation variation trend (from 1980s to 2000s) in northwest China on the basis of AVHRR NDVI data (Li et al., 2006, Ma et al., 2003): Ma et al. (2003) adopted the difference ratio and one-dimensional linear regression and concluded that the vegetation cover, on the whole, is on the decline and only local vegetation is optimized. However, Li et al. (2006) employed the landscape ecology method and concluded that the vegetation cover was greatly improved and only locally deteriorated. The contradictory conclusions derived from above two studies can be ascribed to different research methods application. The correct adoption of methods and the verification of the results are therefore both essential to the estimation of vegetation cover.

2.1.2 Vegetation variation on regional scale

As being detected by many scholars that the greening trends of vegetation cover were established in many areas of the world, particularly in Europe, the Sahel, India, and China (Zhang et al., 2017, Julien et al., 2006, Fensholt et al., 2009, Jeyaseelan et al., 2007). It is undeniable that vegetation degradation has continuously swept through many parts of the world such as in Cambodia, Indonesia, and the Philippines (Mather, 2007), while the browning trend has already stalled or even reversed in some areas. For instance, the trend converting from browning to greening started occurring during the 18th century in Western Europe (Mather, 1992) and has also emerged in China and Vietnam around the 1980s (Mather, 2007).

MODIS land cover products proved suitable data resources for identifying the greening or browning trends in vegetation cover from regional to global scales. To promote the view of vegetation cover variation at global level, a linear trend model and a seasonal non-parametric model were combined to detect the changing trend of vegetation cover by using Global Inventory Modeling and Mapping Studies (GIMMS) NDVI dataset. The results of this study pointed out that the vegetation cover change in the northern hemisphere was dominated by a greening trend, while in the southern hemisphere, the

browning trend in tropical Africa, Indonesia/Oceania, and northern Argentina were identified (de Jong et al., 2011).

The linear regression analysis has been popularized to evaluate the vegetation changing trend on the basis of long-term NDVI time series on spatial scale. In the northern hemisphere, the vegetation cover is dominated by a greening trend, which is in line with the results generated by de Jong et al. (2011), and the areas with a significant increase account for more than 50%. However, the vegetation cover in part of central Europe, northern North America, and central Siberia even shifted from greening to browning trends in the growing season (Kong et al., 2017). The Mongolian Plateau is one of the largest steppe ecological environment in Asia as well as in the world. In terms of the regional vegetation variation, the vegetation cover change in the People's Republic of Mongolia and the Inner Mongolia Autonomous Region of China contributes a significant impact on regional climate system as well as the carbon cycle. To generate a map of significant trends in Mongolia, simple linear regression analysis was applied to detect the land degradation and regeneration based on an 11-year (2001 to 2011) MODIS NDVI satellite data record. The results of this study demonstrated that vegetation cover in the north and northeast of Mongolia mainly shows a positive trend, and the negative trends are sparsely located in the center of Mongolia (Eckert et al., 2015).

The MODIS NDVI data has been only available since February 2000, it is impossible to evaluate the vegetation variation before that based on MODIS NDVI data. However, third generation GIMMS NDVI data provided a possibility to extend the research period to the 20th century. Based on greenness anomaly method, the temporal scale of vegetation dynamics in Mongolia and the Inner Mongolia Autonomous Region of China was extended forward 1982 by using third generation GIMMS NDVI data. The changing trend of vegetation cover in Mongolia was investigated and the trend was in line with the results generated by Eckert et al. (2015). The results of this study indicated that the vegetation cover is slightly better in Inner Mongolia than in Mongolia with increasing magnitude of 0.0182 $year^{-1}$ and 0.0176 $year^{-1}$, respectively (Miao et al., 2015).

The continuous upward trend of NDVI in the growing season in Eurasia and North America has been reversed or stalled since the late 1990s due to water shortage (Piao et al., 2011, Wang et al., 2017b, Xu et al., 2017, Bogaert et al., 2002). In contrast, the

NDVI in the growing season (April to October) in China has considerably increased from 1982 to 2010, although the magnitude of the upward trend declined after the early 2000s in comparison with the magnitude of the upward trend from 1982 to 1999. Concerning the spatial pattern of vegetation cover variation, the vegetation cover improved in many parts of southern China over the period of 1982 to 2010, but the vegetation cover kept almost unchanged in northern China for the same period (Peng et al., 2011).

Moreover, Rescaled Range (R/S) analysis was adopted to calculate the Hurst exponent of NDVI time series. The Hurst exponent is widely applied to identify the consistency and the anti-consistency of NDVI time series, which can effectively predict the future changing trend of the vegetation cover (Li et al., 2019, Liu et al., 2017, Liu et al., 2019, Peng et al., 2012, Tong et al., 2018). Previous studies have unitized Hurst exponent to study the consistency and the anti-consistency of the NDVI time series in the Qinghai-Tibet Plateau and Yarlung Zangbo River Basin (Han et al., 2018, Liu et al., 2017, Peng et al., 2012) and the results evidenced that the consistency of the NDVI changing trend is greater than the anti-consistency of the NDVI changing trend in the Qinghai-Tibet Plateau and Yarlung Zangbo River Basin.

However, it is worth mentioning that the same research method may produce different research results. For example, the conclusion was contradictory in two studies using both the same method focused on the future variation trend of vegetation cover in Inner Mongolia (Liu et al., 2019, Tong et al., 2018). Liu et al. (2019) adopted Hurst exponent to identify the consistency of NDVI changing trend based on GIMMS NDVI data from 1982 to 2015 and demonstrated that the areas showing consistency are larger than the areas showing anti-consistency in Inner Mongolia in the future. However, Tong et al. (2018) applied Hurst exponent to study the future variation trend of vegetation cover on the basis of GIMMS NDVI data from 1982 to 2013 and found an opponent result to former study that most of the area exhibits anti-consistency characteristic in Inner Mongolia in the future.

2.1.3 Vegetation variation in different types

Vegetation ecosystem consists of different vegetation types, not only sustaining biodiversity but also producing essential ecological performances. Knowledge of the

dynamics of different vegetation types is critical for developing adaptation strategies to restore vegetation to sustain the fragile ecological system. To investigate the spatiotemporal pattern of vegetation variation in central Asia, linear regression analysis was applied to detect the decreasing and increasing trends of different vegetation types using MODIS NDVI data. The results of this study showed that the decreasing areas are mainly distributed in shrubs and sparse vegetation covered regions (Jiang et al., 2017). The same analysis method was employed to detect the temporal trends and spatial patterns of land use and land cover change in northern China, which not only reinforced the understanding of the spatiotemporal dynamics of vegetation variation but also expounded the underlying mechanisms of long-term land use transformation. The results of this study suggested that the forest and closed shrub land in northern China increased greatly from 2001 to 2013. Furthermore, the urban areas gained 23129 km^2 due to a great number of people migrated from rural to urban areas, which promoted the urbanization processes, particularly in the north China plain and northeast China plain (Wang et al., 2016a).

Temperate grasslands are known as an important role in regional climate change and preventing and managing soil erosion. To better understand patterns of NDVI change for temperate grasslands, mostly located in northern China, Piao et al. (2006b) detected the temporal variation of NDVI. The mean NDVI for temperate grasslands was firmly increased in the growing season (April to October), and the magnitude of the upward trend was slightly greater in spring and autumn than in summer from 1982 to 1999. In terms of each grassland type in different seasons, the magnitude of the increase for temperate meadow was greater in spring than in summer and autumn, whereas an opposite result was observed in both temperate steppe and temperate desert steppe.

Furthermore, the coefficient of variation (CV) of NDVI can be considered as a very useful and efficient indicator for identifying the amplitude of the inter-annual vegetation cover oscillation. To investigate the degree of the vegetation fluctuation, NDVI CV was applied to quantify temporal vegetation cover variation and to express the magnitude of inter-annual variability in 5 biome groups (forest, grassland, desert, alpine vegetation, and cropland) over China for the last two decades of the 20^{th} century (Fang et al., 2001).

2.1.4 Vegetation variation in response to multiple reforestation programs

China’s government has invested enormous funds and made great efforts in vegetation deterioration mitigation, poverty eradication, livelihoods improvement, and rural economy restructure. Reduced government ability of natural resources management (China’s Cultural Revolution) accelerated the unrestricted forest harvesting activities and promoted environment degradation and deterioration from 1966 to 1976. Soon after, a set of large-scale ecological restoration program such as Grain for Green Program (GGP), Beijing and Tianjin Sandstorm Source Controlling Program (BTWSSCP), Natural Forest Conservation Program (NFCP), and Three-North Shelter Forest Program (TNSFP) has been initiated to alleviate the vulnerable terrestrial ecosystem (Bryan et al., 2018).

The NDVI changing trend can be used to evaluate the effectiveness of the ecological restoration programs. The slope of the linear regression was proposed to assess the vegetation variation after implementing the GGP, BTWSSCP, and TNSFP in Horqin Sandy Land, China. The results of this study showed that the vegetation cover in 76% of the sand dune areas was improved, particularly in Naiman Banner, Hure Banner and the south of Horqin Left Back Banner (Zhang et al., 2012). Reforestation and restoration programs would be the most effective way to upgrade vegetation cover on regional scale at short-term. After implementing the TNSFP for more than two decades, linear regression analysis was applied to explore the greening and browning trends using GIMMS NDVI data. The results of this study pointed out that the vegetation cover has remarkably improved over most of the TNSFP region, particularly in eastern regions of China and in the northern Piedmont of Tianshan Mountains (Duan et al., 2011).

The linear regression analysis was also employed to quantify the magnitude of vegetation restoration in the Shaanxi-Gansu-Ningxia Region after implementing the GGP for 10 years. A remarkable upward trend of vegetation cover was observed in most areas of this region, particularly in Yulin in Shaanxi province. The magnitude of vegetation improvement was significantly greater in the Shaanxi-Gansu-Ningxia Region than in northern China, which has launched the TNSFP approximately two decades. Areas distributed in the east of this region experienced significant fluctuation was identified, which might be caused by initiating the GGP in this area (Li et al., 2013).

The NFCP maintains natural forests by way of logging bans and afforestation activities, while the GGP transforms farmland to forest land or grassland through relative grain and financial allowance to farmers. The NFCP has made great achievement in natural forest restoration and soil conservation. For instance, the timber logging in the northeast of China and Inner Mongolia reduced by 11 million m^3 from 1997 to 2005, which led to immeasurable ecological and socio-economic effects. To offset the market demand for timber, China's government enhanced the total import volume of 29.4 million m^3 in 2005 (Liu et al., 2008b).

2.1.5 Comparing different data sources for vegetation monitoring

The NDVI data derived from Terra MODIS and SPOT VGT are considered to be a more precise and robust data source to assess the long-term vegetation trends than AVHRR GIMMS NDVI data. GIMMS NDVI was employed to detect the vegetation variation in Dahra, Senegal from 2000 to 2007 using linear regression analysis, while Terra MODIS and SPOT VGT are used as reference datasets to evaluate the accuracy of the GIMMS NDVI. The results of this study exhibited that the vegetation variation trend derived from SPOT VGT NDVI is greater than Terra MODIS and AVHRR GIMMS NDVI data. Furthermore, the slope value derived from GIMMS NDVI data was in line with the MODIS NDVI in semi-arid areas (Fensholt et al., 2009).

To verify whether the results and the method of this study can be popularized on global scale. Linear regression analysis was again employed to perform the vegetation cover change spanning from 2000 to 2010 on global scale, comparing the global Terra MODIS NDVI and GIMMS NDVI time series data. The results of this study showed that the temporal trends derived from GIMMS NDVI are in line with the trends generated from MODIS NDVI data. However, more areas of positive trends were produced by the MODIS NDVI data in arctic regions than GIMMS NDVI data (Fensholt and Proud, 2012). By exceeding the study area from regional to global, Fensholt et al. (2012) verified that the accuracy of variation patterns derived from MODIS NDVI dataset is higher than GIMMS NDVI data when it was used to monitor the vegetation cover variation from regional to global scales.

It is critical to monitor the global vegetation variation accurately by using different RS imageries for a better understanding of the functions and processes of the vulnerable ecological system. Zhang et al. (2017) attempted to carry out the global vegetation cover trend from 2001 to 2015 by means of comparing the MODIS NDVI and MODIS Enhanced Vegetation Index (EVI) data derived from Collection 6 (C6) and Collection 5 (C5). After applying the linear regression analysis at pixel level to both MODIS NDVI and MODIS EVI data and found that the global vegetation cover established a significant increasing trend in Terra-C6 EVI, while a contrasting phenomenon was observed in Terra-C5 EVI. Based on Terra-C5 NDVI and EVI, a huge number of browning areas was detected in tropical regions. However, it was not identified in Terra-C6 NDVI and EVI.

Figure 2-1. Estimation of the vegetation variation based on different methods

Study Area	Data Source	Method	Reference
Global	GIMMS NDVI	Linear Regression Analysis	de Jong et al., 2011
Global	GIMMS NDVI, MODIS NDVI		Fensholt and Proud, 2012
Northern hemisphere	GIMMS NDVI		Kong et al., 2017
Central Asia	MODIS NDVI		Jiang et al., 2017
China	GIMMS NDVI		Peng et al., 2011
Western Germany	AVHRR NDVI		Wittich et al., 1995
South Island	SPOT VGT		Dymond et al., 1992
Mongolia	MODIS NDVI		Eckert et al., 2015
Dahra	MODIS NDVI, SPOT VGT		Fensholt et al., 2009
Horqin Sandy Land	SPOT VGT		Zhang et al., 2012
Beer-Sheva, Israel	MODIS NDVI, Kodak DC-40	Vegetation Index Method	Gitelson et al., 2002
Jing River Basin	MODIS NDVI		Guo et al., 2006

Australian	Landsat MSS	Pixel Decomposition Model	Pech et al., 1986
Global	AVHRR NDVI		Gutman et al., 1998
Syrian Coast	SPOT VGT		Al-Abed et al., 2000
Three Gorges Reservoir Area	MODIS NDVI		Wu et al., 2012
Mid-Atlantic Region	IKONOS		Goetz et al., 2003
Western Province, Zambia	MODIS NDVI, IKONOS, LandSat ETM+		Hansen et al., 2004
United Kingdom	AVHRR NDVI, SPOT HRV	Artificial Neural Network	Atkinson et al., 1997
United States, Pacific Northwest	AVHRR NDVI		Boyd et al., 2002
Eurasia, North America	GIMMS NDVI	Landscape Ecology Methods	Bogaert et al., 2002
Northwest China	AVHRR NDVI		Li et al., 2006

2.2 Study on driving forces of vegetation variation

Many scholars have accumulated very good experience and carried out rewarding research on the correlation between vegetation cover change and multiple driving forces, such as climatic forces, topographic forces, and socio-economic forces. Vegetation cover shows apparent spatial heterogeneity. The spatial pattern of different vegetation species varies from each other. Even in the same region, different vegetation cover represents different inter-annual and seasonal characteristics, which results from the influence of climatic forces, topography forces, and socio-economic forces. Vegetation cover has a time lag in response to changes in temperature and precipitation and is, to a certain degree, subject to topographic factors (*e.g.,* elevation, slope, and aspect) and socio-economic activities (*e.g.,* population density, GDP, and urbanization).

2.2.1 The correlation between NDVI and climatic factors

Spatiotemporal variation of vegetation cover of territorial ecosystems has been intimately associated with climate change. The unique spatiotemporal pattern of climate variations may lead to a distinct spatial and temporal pattern of vegetation cover regarding the generally recognized interaction between vegetation growth and climate change (de Jong et al., 2013). Previous literature on the correlation between NDVI and climate factors were mainly focused on precipitation and temperature. However, the reaction of NDVI to precipitation and temperature variation is varied from different vegetation types as well as on different spatial scales. Many scholars pointed out that NDVI is either dominated by a single climate factor (precipitation or temperature) or the combined effect of precipitation and temperature. Moreover, the lag time for maximum NDVI response to precipitation and temperature variations has been proven in many parts of the world.

2.2.1.1 The dominant effect of precipitation or temperature variation to NDVI

Vegetation is always considered to be a sensitive indicator in the study of the vulnerable biosphere and global climate change (Salim et al., 2008). Temperature and precipitation act as the most direct and significant factors for vegetation growth (Chen, 2001, Lin et al., 2017, Zhao et al., 2001). Many scholars have announced that NDVI is closely related to precipitation, which is the main factor limiting the growth of vegetation, particularly in arid and semi-arid regions (Fensholt et al., 2012, Bao et al., 2014). The inter-annual vegetation cover in arid and semi-arid regions in the middle north and northwest parts of China was dominant by precipitation, except that the vegetation variation was ascribed to changes in temperature. An analogous phenomenon was observed in spring and autumn that temperature favored the vegetation growth. Abundant precipitation promoted the vegetation growth in summer, but high temperature negatively affected the vegetation growth (Liang et al., 2015).

The response relation between vegetation cover and precipitation in Sahelian on inter-annual, annual and seasonal scales has been analyzed. The results of this study showed that, apart from the inter-annual scale, the vegetation cover responded to precipitation intimately both on the annual and seasonal scales (Anyamba and Tucker, 2005). NDVI is recognized as a surrogate of vegetation cover and reflects the vegetation

growth status. Duan et al. (2012) calculated the relationships between NDVI-precipitation and NDVI temperature to determine the primary climate factor controlling the vegetation cover variation in the TNSFP region. The results of this study suggested that vegetation growth and plant photosynthesis are dominated by precipitation from 1982 to 2006, particularly in northwestern China (Duan et al., 2011). In Sudan, the vegetation growth is highly positively correlated with precipitation, particularly during the heavy precipitation, whereas the relationship between NDVI and precipitation was complicated rather than a linear trend (Salim et al., 2008).

Many scholars have declared that temperature is the main factor affecting the spatial and temporal pattern of vegetation cover in many parts of the world. Understanding the interaction between ecosystems and climate factors on regional, continental, and global scales is crucial to detect the sensitivity of vegetation growth responding to changes in climate effectively. The vegetation cover was remarkably influenced by a summer temperature increase in the Arctic, except in recently deglaciated areas, particularly, the vegetated and graminoid vegetation types were positively responded to the warming summer temperature (Raynolds et al., 2008). The vegetation cover in the northern hemisphere has been generally increased over the last three decades (Peng et al., 2013, Kong et al., 2017).

The impact of climate change on vegetation growth has been intensively debated and the patterns of the interaction are complicated, which is varied on different spatial and temporal scales. The onset and cessation of the growing season, which are greatly sensitive to temperature change and potentially influence the vegetation growth. As suggested by Kong et al. (2017), temperature is considered as a dominant factor affecting the vegetation growth in the northern hemisphere, particularly in North America and Siberia. The vegetation growth in central Canada, eastern of the United States of America (USA), and western Africa was primarily correlated to soil moisture, which is closely related to precipitation and underground water storage. The vegetation growth is highly related to the upward trends of temperature and solar radiation in southeastern China, while precipitation alleviates the negative impact of soil moisture downtrend on vegetation variation.

The change of vegetation cover in response to climate variation is varied in different ecosystem types. The warming temperature can prospectively extend the growing season, and a greening trend can be anticipated (Buermann et al., 2014, Garonna et al., 2014). As being proved that the NDVI in the growing season showed an upward trend in all types of ecosystems except for desert ecosystem in the context of an increasing trend in temperature at the same time in China, indicating a significant relationship between temperature and NDVI for all ecosystems in the growing season (Peng et al., 2011).

China is one of the largest countries in the world and covers 9.597 million km² territory. Due to the width range of territory, different types of climate coexist in China and refer various functions for vegetation growth in the corresponding ecosystem (Cui, 2010, Dai and Zhang, 2010, Guo et al., 2008, Wang et al., 2014). Guo et al. (2008), Dai et al. (2010), Cui et al. (2011), and Wang et al. (2014) analyzed the correlation coefficients between NDVI and precipitation as well as NDVI and temperature in northwestern China, Qilian Mountains, eastern China, and southern China on the basis of NDVI data and meteorological data. Results have shown distinctive spatiotemporal distributions of NDVI responding to temperature and precipitation. Furthermore, the correlation coefficient with temperature is generally higher than that with precipitation. Bao et al. (2014) focused on investigating the correlation between NDVI and precipitation as well as NDVI and temperature in Mongolia plains from 1982 to 2010. Results of this study demonstrated that NDVI had a positive correlation with temperature and precipitation before the 1990s, but it turned out to be a negative one after the 1990s. There are distinct spatial differences in the distribution of NDVI responding to temperature and precipitation.

The vegetation cover increased in southern China continuously because of plenty of forest inventories and multiple large-scale afforestation activities (Pan et al., 2011, Peng et al., 2011). In addition, an increasing trend in temperature during the last several decades stimulated the vegetation growth in southern China, where is not a water-limited ecosystem (Lin et al., 2010). Hence, temperature can be regarded as a primary climate factor for vegetation growth over southern China. Due to the apparent annual and seasonal behaviors of vegetation growth, vegetation status is always considered to be a sensitive indicator on the research of the evolution of ecosystem processes under the impact of climate change and human activities. NPP is always considered as a good

proxy of vegetation growth and adopted to detect the spatiotemporal pattern of vegetation evolution related to its driving forces. For example, in the Huai River Basin and heavy industry areas, covering Harbin, Changchun, and Shenyang in the northeast of China, positive correlations were found between NPP-sunshine duration and NPP-accumulated temperature. In addition, the precipitation is determined to be a negative factor affecting the vegetation growth in the Huai River Basin (Salim et al., 2008).

The temperature and precipitation interact to propose complex and various constraints on vegetation growth throughout the world. Global climate change was regarded as the main factor affecting mountain ecosystems. The relationships between vegetation cover and climate factors are varied in different mountain ecosystems. A positive relationship between NDVI and temperature was found over the mountain preserved areas located in Africa and Southeast Asia, while temperature showed a negative impact on mountain vegetation in Central America, South America, and South Asia. Furthermore, precipitation presented a weaker influence or no influence on mountain ecosystems (Krishnaswamy et al., 2014). The Namoi catchment, located in eastern Australia, is a typical semi-arid riparian area with diverse plant species. In general, the maximum temperature was the main factor negatively affecting the vegetation growth over Namoi. In addition, more precipitation was needed during the warmer months than cooler months to reach the same NDVI value over this riparian zone (Fu and Burgher, 2015). However, the climate factors were not the determining factors controlling the vegetation growth in North America and Africa, places the NDVI showed no relationship or only a weak relationship to climate change (Fang et al., 2001).

2.2.1.2 The combined effect of precipitation and temperature to NDVI

Many scholars have exhibited that the vegetation growth is neither dominated by the precipitation or temperature, while it has been further proposed that the manifestations of these two factors are usually lumped together. It has been demonstrated that inter-annual changes of vegetation cover were closely related to changes in temperature during spring and summer in the middle and high latitudes in the northern hemisphere, while in semi-arid areas, apart from the temperature, the precipitation is also an important factor (Ichii et al., 2001). The vegetation greening and browning trends are intimately associated with moisture stress generated by temperature and precipitation

variations. For instance, warming temperature cooperated with no significant increase in the precipitation had a negative impact on plant growth in northwestern Canada and the positive relationship between tree-ring width and temperature has weakened (D'Arrigo et al., 2004). The cooling temperature could also promote vegetation growth in low-latitude ecosystems by the way of decreasing evapotranspiration and respiration rate. Meanwhile, the increasing temperature has alleviated several serious climate constraints to vegetation growth as well and led to an improvement in NPP in many parts of the world (Nemani et al., 2003).

Many studies have demonstrated that vegetation cover appears an upward trend in many parts of China from 1982 to 2010 at national level due to a long-term warming trend (Peng et al., 2011). Regarding the vegetation growth on seasonal scale, the magnitude of the increasing trend in vegetation growth is greater in spring than in summer and autumn (Piao et al., 2003). The warming temperature not only prolonged the growing season of vegetation growth but also promoted the photosynthesis rate in plants (Piao et al., 2006a). However, a downward trend swept in the northern hemisphere, covering parts of China, caused by the widespread drought stress and less moisture availability has been evidenced since the 1990s (Jeong et al., 2011, Park and Sohn, 2010). For example, in northern China, the NDVI in the growing season significantly increased before the 1990s due to temperature and precipitation increases. However, the NDVI in the growing season presented a downtrend afterward because of the prolonged drought season caused by global warming and precipitation decrease (Peng et al., 2011).

Previous climate changes have not only converted vegetation behavior, but they also have influenced the nature of vegetation-climate relationships. Due to climate change, the sensitivity of vegetation to temperature variation has reduced or shifted in temperate latitudes (Barber et al., 2000). A global assessment demonstrated that the greening trend was closely related to warming and/or increased precipitation, while the browning trend was ascribed to increased temperature and/or decreased precipitation (Xiao and Moody, 2005).

2.2.1.3 The impact of climate factors on different vegetation types

Correlation analysis between NDVI and climate factors is essential for exploring the interaction between global climate change and the processes in terrestrial ecosystems (Potter and Brooks, 1998). Maps of greening and browning trends of vegetation cover were produced under the impact of the temperature, precipitation, and incident solar radiation variation on global scale. The results of this study showed that over 50% of the spatial vegetation variation could be ascribed to the variation of climate factors. The most remarkable greening and browning trends were distributed in Argentina and Australia. This study further proved that the pattern of different land use types in response to climate change was heterogeneous. The forests establish a negative relationship to temperature variation under the warming conditions and a significant positive relationship was observed in shrub lands responding to precipitation variation (de Jong et al., 2013).

Effective green leaf area index, indicating the growth of vegetation, was highly correlated with precipitation variation in European shrubland, whereas changes in annual temperature could not explain the differences in effective green leaf area index, except for a negative correlation was revealed at the north of European (Mänd et al., 2010). NOAA AVHRR NDVI data was applied to research how the precipitation affects different types of vegetation in southern Israel and found that vegetation in the sample region was sensitive to the precipitation (Schmidt and Gitelson, 2000).

Trends in the growing season for precipitation, temperature, and NDVI follow each other fairly well in China, with an increasing trend in whole over the temperate grasslands. In terms of each grassland types, the relationship between temperature and NDVI for temperate meadow was significantly greater than that of precipitation, whereas a contrasting phenomenon was found in temperate desert steppe, indicating that precipitation is the key factor affecting the temperate desert steep and the temperate meadow is potentially controlled by temperature in the growing season (Piao et al., 2006b). The vegetation growth in the alpine meadow of the Three-River Source Region on the Qinghai-Tibetan Plateau was inconsiderable with temperature variation before 1995, whereas the relationship was converted from insignificant to significant after 1995 (Xu et al., 2011).

2.2.1.4 The time lag effect of NDVI in response to climate factors

Owing to the spatiotemporal heterogeneity of terrestrial ecosystems, the diverse spatiotemporal patterns of vegetation cover is fairly correlated with climate forces and presents complicated time lag effects from regional to global scales. However, most of the studies only concentrated on the influence of the concurrent climatic forces and did not pay attention to the time lag effects of climatic forces on plant growth. Regarding the time lag effects of vegetation growth is pretty crucial for a better understanding and quantifying the vegetation evolution in the context of global warming and drought wide spreading. For instance, 64% of the vegetation cover change was dominated by the climate characteristics, which was 11% greater than neglecting the time lag effect on vegetation growth on global scale, which improved the accuracy and precision of the study and provided a reference to natural vegetation management and conservation (Wu et al., 2015).

Zeng et al. (2013) employed Pearson's correlation analysis to detect the time lag effects between NDVI and precipitation as well as NDVI and temperature on global scale. The results of this study showed that vegetation growth was mostly influenced by 1-month preceding precipitation and concurrent temperature. In addition, the correlations between NDVI and precipitation as well as NDVI and temperature were more complicated on regional scale. The time lag effects of NDVI and precipitation as well as NDVI and temperature were variedly extending from 0 up to 6 months and from 0 to 4 months on regional scale, respectively. For example, the vegetation growth in central North America, central Eurasia, India, and the Sahel was closely correlated to the precipitation when the precipitation preceded NDVI by 1 month, while in Central Europe, the vegetation presented the largest correlations when the temperature preceded NDVI by 3 to 4 months.

The time lag effects of NDVI in response to precipitation implied that most of the vegetation in high latitude regions in the northern hemisphere exhibited an appreciable correlation with the concurrent precipitation, while the vegetation in arid and semiarid showed a 1-month time lag to changes in precipitation (Rundquist and Harrington, 2000). Furthermore, most of the vegetation in the Qinghai–Tibet Plateau, southern Australia, and southern South America showed no time lag effects to temperature, and the

vegetation growth was considerably influenced by the concurrent temperature (Wu et al., 2015).

To gain an overall impression of the delay mechanisms of the response of vegetation growth to climate change on the annual and seasonal scales, NDVI has been exhibited to demonstrate variation in vegetation productivity responding to climate variation. The relationships between NDVI and precipitation as well as NDVI and temperature in Kansas were carried out and found that a high correlation between the average value of NDVI in the growing season and precipitation during the current growing season and 7 preceding months (15 months duration) (Wang et al., 2003). The NDVI in response to precipitation variation appears obvious annual and seasonal features across northern Patagonia. In northern Patagonia, the annual NDVI was significantly correlated with previous precipitation. Furthermore, the seasonal NDVI showed a similar reaction to precipitation variation. No significant relationship could be found between NDVI and concurrent precipitation both on the annual and seasonal time scales (Fabricante et al., 2009).

Distinct time lag effects of vegetation growth responding to precipitation variability were found in western and central North America that the vegetation growth in summer was highly influenced by precipitation derived from spring even winter in last year (Zeng et al., 2013). In Central Eurasia, the vegetation growth presented seasonal behaviors to climate characteristics. Vegetation growth in summer was significantly affected by precipitation, indicating that precipitation is the key factor controlling the vegetation behaviors. However, the vegetation growth in spring was mostly related to the temperature. These results suggested a time lag effect existed between vegetation growth and climate factors (Xu et al., 2017).

Climate change influences vegetation cover variation by controlling the metabolism rate in the process of vegetation growth (Parmesan and Yohe, 2003). In other words, climate change is accountable for the renovation of vegetation cover on a certain level. The restriction of water-heat climate conditions is in charge of the spatial pattern of vegetation. The spatiotemporal characteristics of vegetation cover response to temperature and precipitation on the annual and seasonal scale in eastern China were detected by Cui et al. (2010). The conclusion of this study exhibited that NDVI showed a

10 days lag to the variation of temperature, and a 30 days lag to precipitation generally. Summer is the primary season for plant growth, especially in the northern hemisphere due to relatively high temperature and abundant precipitation. For instance, the maximum NDVI value is greater in August than other months in northeastern China, whereas the highest temperature and precipitation are in July preceding maximum NDVI by 1 month (Yang et al., 2009).

Terrestrial ecosystems display complex behavior on different spatial and temporal scales in the response of different vegetation types to climatic change. Better understanding of the mechanism of vegetation growth responses to climate change is a decisive demand for evaluating the dynamics of the future terrestrial ecosystem (Wang et al., 2011). Inspect the relationships for diverse vegetation types, it has been demonstrated that the relationships between forests and precipitation were significantly weaker than that of grasslands, shrublands, croplands, and savannas (Zeng et al., 2013).

Different vegetation types exhibited distinct time lag effects of vegetation growth responding to temperature or precipitation variation (Shen et al., 2013). Moreover, the same vegetation type also presented different time lag effects of vegetation growth in response to temperature and precipitation. For instance, the majority of global forest ecosystem has no obvious time lag effect to temperature in whole, whereas more than 60% of the evergreen needle leaf forest and the deciduous broadleaf forest showed 1- and 2- month time lags to temperature, respectively. The time lag effects of shrubs response to temperature exhibited an obvious spatial pattern in different latitude regions. The shrubs in high latitude regions in the northern hemisphere were mostly correlated with the concurrent temperature, while a 1-month time lag was examined in low and middle latitude regions. Wood savanna and savanna greatly reacted to temperature when the temperature preceded NDVI by approximately 2 months. The cropland showed the minimum time lag effects to temperature, and more than 74% of the cropland mostly correlated with the concurrent temperature (Wu et al., 2015). In terms of the time lag effects of different vegetation types to precipitation, shrubs presented 1-month time lag to precipitation in high latitude regions and an approximately 2-month time lag in low latitude regions. The grasslands and deserts exhibited the closest relationships with precipitation in summer (Xu et al., 2017).

2.2.2 The correlation between NDVI and topographic factors

Topographic factors, including elevation, aspect, and slope, are intently related to the spatial and temporal patterns of the vegetation cover at a certain level. In the northern hemisphere, plants on the south-facing slope (SFS) obtain more solar radiation than on the north-facing slope (NFS), which may lead to both inhibition and promotion for effective energy and mass transfer to the plant and result in differences in vegetation growth consequently. There is an opposite phenomenon in the southern hemisphere (Auslander et al., 2003, Rasmussen et al., 2015). Under the influence of the combined functions of light condition, water stress, and heat energy, the NDVI value was greater on the NFS than on the SFS for both wet and dry seasons in the Guadalupe Valley, located in the northwest of Mexico. Furthermore, the NDVI value was higher in wet seasons than in dry seasons, implying a better vegetation development and growth in wet seasons due to the contradiction and balance between water demand and water availability for vegetation growth (Toro Guerrero et al., 2016). It has been demonstrated previously that the patterns of vegetation cover in response to different aspects were uneven both on spatial and temporal scales for the Santa Monica Mountains in California. The NDVI value was on the NFS higher than on the SFS, particularly in May, July, and September (Deng et al., 2009).

Topographic factors are the major factors affecting the spatial distribution of the vegetation for mountain areas in the long-term. Moreover, it was highly expected that elevation contributes much more to vegetation variation in comparison with the effects of aspect and slope on vegetation variation (Busing and White, 1993). It was observed that the vegetation growth and vegetation indices improved along with the increase in elevation in the Darab Mountain, Iran. During the elevation range of 1500 to 3000 m, the vegetation cover was apparently better than below areas. The vegetation indices such as NDVI, EVI and Difference Vegetation Index (DVI) reached the maximum value in the vertical zone of 3000 m. In terms of the vegetation cover on different aspects, the vegetation cover was much better on the northwest-facing slope (NWFS) than other aspects because the shady aspect reduced the evapotranspiration and maintained the soil moisture to favor the vegetation growth in this semi-arid region (Mokarram and Sathyamoorthy, 2015).

Moreover, in the mountain regions of semi-arid Central Asia, elevation and aspect are still considered to be the principal factors influencing the spatial distribution and growth status of vegetation. The upper forest line started at 1800 m in the west and raised to 2200 m in the east in the northern front ridge, holding a vertical range of 200 m to the lower forest line, whereas the upper forest line lied at an elevation of 2400 m in the southern mountain ridge. When the slope degree is less than 5º, no significant effects of the topographic pattern was observed in vegetation distribution. This underlying cause of the differences in vegetation distribution and growth to topographic factors originally comes from the natural environmental conditions (Klinge et al., 2015). In the Upper Uruguay River Basin, Brazil, the processes of intensification and extensification of forest management were significantly correlated with the distance from water bodies, while the processes of intensification were simultaneously related to the elevation range (de Freitas et al., 2013). The vegetation recovery was affected by the magnitude of the elevation in northern Arizona. The vegetation rehabilitation and regeneration in higher elevation areas were weaker than that of in lower elevation areas (Kim, 2013).

The vegetation structure was intimately correlated with the aspects of the Mediterranean zone in Chile. The floristic composition on the east-facing slope (EFS), west-facing slope (WFS), and SFS is likely homologous that the number of evergreen species and the plant size in these three aspects were larger than on the NFS. A set of xeromorphic species was found on the NFS, which can be explained by species invasion. Moreover, a large number of hygrophilous species was detected on the SFS, but it was curbed by the unbalanced water demand and supply (Armesto and Martínez, 1978). The resilience of the terrestrial ecosystem and the surfaces of potential vegetation growth are likely linked with the species richness and species diversity, which not only enhanced the ecological diversity but also reinforced the vegetation resilience and afforded a possibility to combat the disturbances from natural disasters and human activities. The species richness and species diversity for different aspects in different climate zones such as Mediterranean, semiarid, arid, and extreme-arid were disparate. For instance, an inverse phenomenon was observed in the Mediterranean zone, where the species richness and species diversity on the SFS was greater than that on the NFS. In arid and extreme-arid zones, the species richness was remarkably lower on the SFS than that on the NFS. In

terms of vegetation cover on different aspects for different climate zones, vegetation cover was significantly greater on the NFS than that on the SFS, except for no remarkable differences were observed on the SFS and the NFS in the extreme-arid zone (Kutiel and Lavee, 1999).

In the northern hemisphere, the microclimate on the SFS and the NFS is different in light, heat and water conditions, which further influences the vegetation growth status such as the height of the plant and plant physiological characteristics (*e.g.*, the size of the leaf and the density of the gall). Due to the effect of solar radiation, NFS is cooler and wetter than SFS. Auslander et al. (2003) analyzed the relationships between plant traits and aspects on different sites in Israel and found that the leaf size and plant height were greatly related to the aspects. The leaf size/plant height was remarkably larger/taller on the NFS than on the SFS. The leaf size was not closely related to the site and slope. In contrast to the leaf size on different aspects, on the one hand, the falling density was greater on the SFS than on the NFS. On the other hand, the gall density varied at different sites, particularly in Keziv, the gall density on the SFS was 16 times greater than on the NFS.

Vegetation acts as an essential role in maintaining and rehabilitating fragile terrestrial ecosystems. The relationships between vegetation restoration and topographic factors vary from region to global scales. It is pivotal to comprehend the mechanism of vegetation restoration in response to topographic factors to improve the fragile ecological environment, especially in opencast coal mine dumps. Topographic factors (*e.g.*, elevation, aspect, and slope) exert a large impact on plant group composition, structure, density, species richness, as well as species distribution. The progress of vegetation restoration was greatly influenced by the slope variation in Shanxi Pingshuo Antaibao opencast coal mine dumps. A positive relationship was performed between slope/aspect and surface biomass and herb cover, whereas an opposite relationship was obtained between slope/aspect and canopy density. The impact of elevation on vegetation improvement did not show a distinct difference due to the maximum height difference of the elevation is only 125 m in this coal mining area. Though the progress of the vegetation restoration exhibited a considerable connection to local topographic factors, the soil factors dominated the progress in this region (Wang et al., 2016b). However, it

has been demonstrated that the spatial pattern of vegetation diversity and growth status were highly related to the aspect and elevation (more than 300 m) for Longjiao Mountain forest areas in China (Wang et al., 2006).

Topography factors could also influence the progress of vegetation restoration by affecting soil properties and fertility. Daqing Mountain is a nature reserve located in the center of Inner Mongolia, a place an arid and semi-arid transition zone is. The vegetation cover in Daqing Mountain showed a distinct spatial distribution with the changes in elevation and aspects. The NDVI value was higher on the NFS than on the SFS in all elevations. Typically, the vegetation cover on the SFS was dominated by grassland and shrubland. With an increase in elevation on the NFS, the vegetation cover transited from grassland to woodland. Both on the NFS and SFS, the vegetation appeared a significant vertical distribution and it was noticeably improved with the elevation increase when the elevation under 1400 m (Jin et al., 2015).

Climate change on micro-scale is determined by topographic factors and plant species composition. With the elevation ranging from 147 m to 7000 m in the Yarlung Zangbo River Basin, China, the vegetation cover responded to changes in climate derived from elevation variation and hence exhibited a unique vertical and horizontal pattern. It has been verified that the NDVI has been improved in the Yarlung Zangbo River Basin from 1999 to 2003, and the most obvious enhancement was observed when the elevation is lower than 500 m. The magnitude of the upward trend slightly increased for the elevation from 500 to 2000 m, and then the increasing trend stalled or even reversed when the elevation reaches 4000 m, which was ascribed to a combination function of an overall precipitation reduction and temperature warming in this region, especially at the elevation over than 2500 m (Li et al., 2015a).

The vegetation cover showed a considerable relationship with the elevation and slope variation in Henan. The greatest vegetation cover was distributed in lower elevation areas and the vegetation cover decreased remarkably with the elevation increase. The overall vegetation cover had decreased from 2000 to 2003, areas with an elevation ranging from 200 to 600 m in particular. The better vegetation covers were mainly distributed in smaller slope degrees. The vegetation cover reduces with the rise in the

slope degree. Furthermore, the vegetation cover presented no obvious differences in different aspects (Li et al., 2015b).

2.2.3 The correlation between NDVI and socio-economic factors

The spatial pattern of browning and greening trends appeared in many parts of the world alternately, implying that they could not be fairly related to climate forces (de Jong et al., 2013). Along with climatic forces and topographic forces, changes in vegetation cover might be caused by socio-economic forces, affecting the interactions of the atmosphere, hydrosphere, geosphere, and biosphere of the Earth's ecosystems and the land cover and land use change. Socio-economic factors mainly consist of human-induced land use and land cover change, urbanization, economic development, and population growth or a combination effect. By 2050, approximately 66% of the world population is projected to live in urban areas, as reported by the World Health Organization (WHO). Urbanization has sobering impacts (*e.g.*, deplete resources, produce water and air contamination, and convert cultivable lands to urban areas) on local ecosystems, but these adverse impacts are complicated on different spatial and temporal scales. Identifying the negative and positive interactions between socio-economic forces and terrestrial ecosystems are essential for managing and maintaining the urban and economic development as well as biodiversity conservation appropriately.

Due to the frequency of human activities, the human-induced land cover and land use changes are continually proceeding in developing countries than in developed countries. Especially in developing counties, the ecosystem and environment are more sensitive to human-induced effects. The World Bank released a report in 2007, which announced that a considerable number of megacities would be settled in developing countries by 2020, which mostly caused by population growth and economic development in urban areas and may further exacerbate the vulnerable ecosystem degradation (Bank, 2007). A severe degradation trend was detected in Zimbabwe on national scale, particularly in the heavily-utilized, communal areas, which was primarily ascribed to human-induced land use and land cover change (Prince et al., 2009). As the main performance of socio-economic activities, human-induced land use and land cover change, converting from tropical forests to rubber and palm oil, might be related to the extension of vegetation browning in Indonesia and other parts of Southeast Asia (Koh et al., 2011, Mann, 2009).

The intact vegetation cover in South Africa was negatively associated with the scale of the settlement and the amount of settlement population because the construction of new settlements and intensive human agriculture activities in rural areas resulted in the sharp conversion of surrounding natural vegetation (Coetzer et al., 2013). The vegetation cover has been devastated to satisfy the processes of urbanization and industrialization in the context of frequency exploration and exploitation activities of oil and gas in northern West Siberia. Especially in the south of this region, urbanization has reduced the vegetation cover not only within the recently expanded urban areas but also the surrounding areas, particularly with a distance approximately 5 to 10 km around the urban areas. However, the vegetation cover in many cities of this region within or near the old urban areas presented an increasing trend, which was ascribed to the succession and evolution of generative plants developing under a warming context (Esau et al., 2016).

The degradation of the ecosystem and environment is highly connected with population density, PCGDP, and urbanization and industrialization level. For instance, the total population and PCGDP were the absolute factors accelerating the environmental degradation in Nigeria. The coastal areas in southern Nigeria, a region experienced significant environmental degradation was ascribed to the high population density and intensive socio-economic activities recently or previously, while a contrasting phenomenon was found in northern Nigeria, a region with low population density and inferior economic development (Madu, 2009). The above research verified the hypothesis proposed by Dietz et al. (2007) that population and PCGDP are the primary factors influencing the terrestrial ecosystem stability and environment security. For example, Dhaka, the capital of Bangladesh, has experienced massive population growth, dramatic urban sprawl, and significant economic development since the 1980s, which converted a large number of non-urban areas (*e.g.*, water bodies, cultivated land, vegetation, and wetlands) to urban areas and built plenty of roads and infrastructure. These urbanization processes further resulted in a deterioration in local ecosystems, alteration in plant behavior and degradation in vegetation cover (Dewan and Yamaguchi, 2009).

The environment and ecological problems derived from vegetation destruction are very serious. Vegetation variation trend varies from region to region under the impacts of human interruptions. In China, the primary challenge we faced is how to effectively distinguish the effects on vegetation variation caused by climate changes and human activities in different ecosystems. Especially, the effects of human activities on vegetation variation are hard to be distinctly segregated due to the heterogeneity of vegetation on different spatial and temporal scales and the close relationships with localized climate characteristics (Buyantuyev and Wu, 2009, Wessels et al., 2007). For instance, the urbanization and industrialization were demonstrated to be the pivotal driving forces accelerating the vegetation browning in the east part of the Qilian Mountains and oasis areas by way of exorbitant exploitation and depletion the natural resources. Particularly, the vegetation growth not only within the urban areas but also within the distance of 0 to 4 km to urban areas was highly disturbed or even remarkably curbed by human activities due to immense construction works and land use transformation from the non-urban area toward urban settlement (Guan et al., 2018).

After investigating the links between socio-economic variation and vegetation dynamic in 32 residential communities over southeastern Australia, the result of this study demonstrated that the vegetation cover was closely related to socio-economic development, particularly in recent years. The housing density was negatively correlated with community vegetation cover, whereas education level, income, home ownership, as well as immigration status produced positive effects to vegetation dynamics (Luck et al., 2009). In addition, Buyantuyev and Wu (2009) demonstrated that in the Phoenix metropolitan region, USA, a large amount of natural vegetation was transferred into agricultural lands and urban areas parallel with rapid urbanization and strong socio-economic variables. The spatial vegetation heterogeneity and vegetation cover were improved by human-modified land covers and landscapes. Meanwhile, the vegetation cover in the eastern and southern America has been remarkably improved due to successful forest management (Hicke et al., 2002).

China has experienced rapid urbanization and industrialization since the 1980s, leading to 6% of the national land went through remarkably vegetation change. For example, in most of the big cities (the capital city of each province) of China, the urban development

intensity was negatively correlated with the vegetation cover (Zhou et al., 2014). In Yangtze River Delta and Pearl River Delta, in particular, places have suffered significant vegetation deterioration and degradation because tremendous economic growth and urban development boosted a huge amount of forests and farmlands to convert into built-up land (Qu et al., 2015).

China has experienced explosive economic growth in recent decades. Particularly in eastern China, with the rapid progress of industrialization and urbanization, the gross regional product (GRP) has gone through enormous growth after implementing the program of reform and opening-up. In terms of NPP in eastern China, it showed a negative correlation to the magnitude of GRP growth, indicating a negative impact of economic growth on vegetation succession and evolution. The vegetation deterioration was mostly ascribed to a large amount of farmland converted into urban areas to satisfy the huge residence demand for immigration and the development of industrialization and urbanization (Piao et al., 2010). Meanwhile, the tremendous economic development accompanied by a lower NPP in many parts of China, especially in eastern China, which can be regarded as an admonition that it is undesirable to develop the economy at the cost of the ecosystem deterioration (Wang et al., 2017b).

The vegetation restoration programs such as the GGP, TNSFP, the BTWSSCP, and NFCP have remarkably alleviated land desertification, land conversion, and vegetation deterioration in many parts of China and obtained great achievement in ecological construction, forest conservation, and environmental protection since 1978 (Zhang et al., 2016). In terms of vegetation restoration in Shaanxi-Gansu-Ningxia Region, it benefited significantly from the program of GGP, which converted massive of croplands into forest land and grassland and closed hillsides to promote afforestation with sustained professional services and technical support (Li et al., 2013). The ecological protection and restoration program of NFCP was launched in 2005 in the Three-River Source Region, which restricted the livestock numbers and alleviated the grazing intensity. It has been evidenced that the vegetation cover improved significantly in many parts of the Three-River Source Region after implementing the program NFCP, and this program can be regarded as a key promoting factor for vegetation restoration and evolution (Xu et al., 2011).

The forest biomass in northeastern China has been increased due to effective forest management and afforestation policy implementation. Afforestation and reforestation activities have a great impact on biomass dynamics (Zhang and Liang, 2014). Furthermore, the vegetation cover has significantly improved in the upstream of Yangtze River basin from 2001 to 2010 because of the reforestation and forest protection program boosted the land use and land cover change, and they finally resulted in a remarkable enhancement in terrestrial ecosystem productivity. However, it has been demonstrated that a considerable amount of croplands transformed into urban areas, which brought negative impacts on vegetation cover, but this negative impact offset by the transformation of shrublands to forests soon (Zhang and Liang, 2014).

Most of the deteriorated vegetation can be rehabilitated by effectively sound land use policies or regularized management that convert farmlands to forest land, close hillsides to facilitate afforestation and maintain stocking rates at a reasonable range. For example, human activities (*e.g.,* overgrazing, cultivation, and urbanization) were observed to be the key driving factor affecting the vegetation cover in Inner Mongolia from 1981 to 2006. Particularly, after launching the household production responsibility policy in the 1980s, the stocking rates have extraordinarily increased at the cost of vegetation cover degradation and deterioration. In addition, new institutional arrangements (*e.g.*, BTWSSCP and GGP) for grasslands protection and restoration were practiced in 2000, which has inhibited or even shifted the upward trend of stocking rates, leading to enormous vegetation enhancement in Inner Mongolia (Li et al., 2012). In most areas of China, the vegetation cover may negatively relate to population density, agriculture activities, urban expansion, as well as economic development, while it benefited significantly from the implementation of multiple afforestation and conservation programs (Qu et al., 2015).

3 Introduction of the study area

This chapter primarily introduces the study area of eastern China, including the socio-economic status, geographic features, land cover and land use change, population growth, and climate variation. To carry out the objectives of this study, the MODIS NDVI data, monthly meteorological data, DEM data, socio-economic statistical data, as well as other vector data and raster data applied in this study are further introduced in this chapter.

3.1 Study area

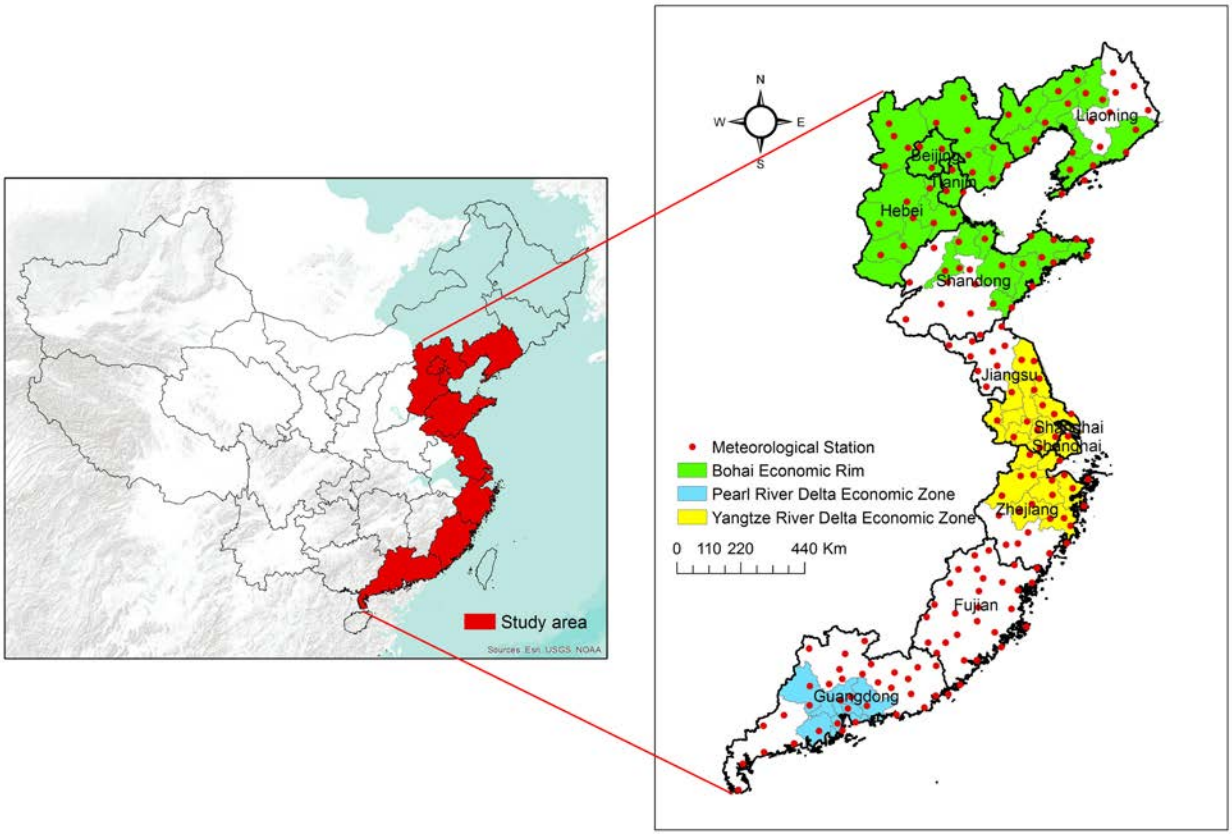

Figure 3-1. The geographical boundary of the study area, the location of the meteorological station, and the location of the three economic zones

This study is focused on eastern China, extending from 109°39′ to 125°46' E longitude and 20°13′ to 43°26' N latitude. Eastern China, a place exhibits high spatial differences on the distribution of fundamental natural resources, is composed of seven provinces (*e.g.*, Liaoning, Hebei, Shandong, Jiangsu, Zhejiang, Fujian, and Guangdong) and three

municipalities (*e.g.*, Beijing, Tianjin, and Shanghai) spanning a total area of about 1.0277 million km^2 (Figure 3-1). Eastern China is a highly developed region in China due to the deep influence of the program of reform and opening-up termed "Socialism with Chinese Characteristics" launched in China in 1978. Especially, Beijing is the capital of the People's Republic of China, the political center of China, and the cultural center of China. Moreover, Beijing is also considered as a key transportation hub of the world. In addition, Shanghai is recognized as one of the most import economic centers of China, and it takes an essential role in Chinese economic reform and development. Jiangsu is one of the most socially, economically and culturally developed provinces in the whole China, ranking at the top list of PCGDP and Development and Life Index (DLI).

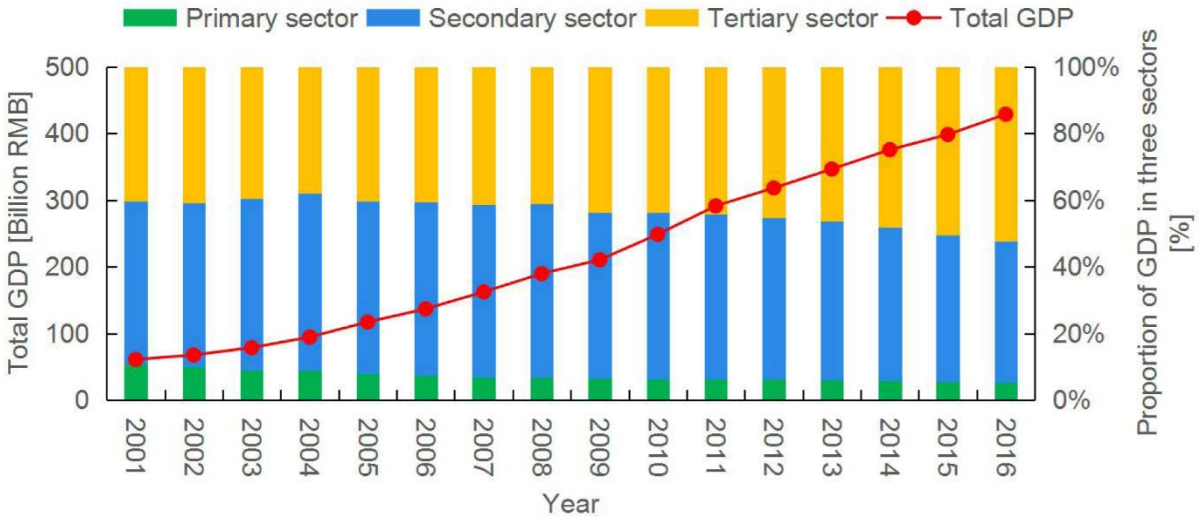

Figure 3-2. The total GDP of eastern China and the proportion of primary, secondary, and tertiary industry products from 2001 to 2016

Source: Own illustration; Based on Statistical Yearbook of China, 2002-2017

Figure 3-2 shows that the total GDP in eastern China had significantly increased from 60.847 billion Renminbi (RMB) in 2001 to 428.38 billion RMB in 2016 with a considerable increase rate of 23 billion RMB year^{-1}. The proportion of the primary sector had continuously decreased from 10.7% of the total GDP in 2001 to 5.4% of the total GDP in 2016. The proportion of the secondary sector presented a small increase from 2001 to 2004, and the increasing trend was curbed or even reversed afterward. The proportion of the secondary sector reached a maximum magnitude in 2004 with a proportion of 53.1%

of the total GDP. The tertiary sector showed an upward trend from 2001 to 2016 and contributed over half of the total GDP of eastern China in 2016 (Statistical Yearbook of China, 2002-2017).

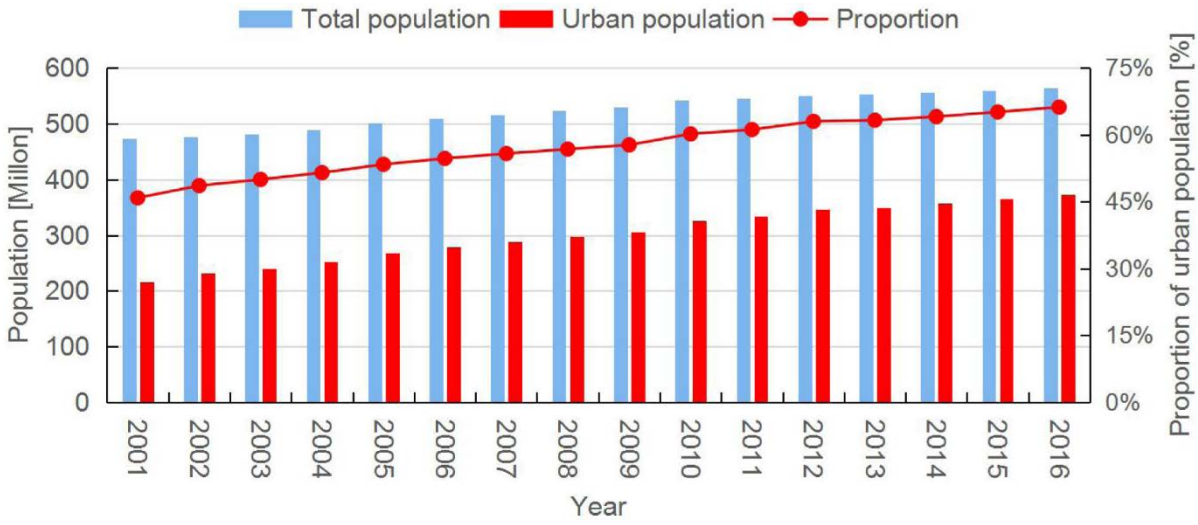

Figure 3-3. The total population, urban population, and proportion of the urban population of eastern China

Source: Own illustration; Based on Statistical Yearbook of China, 2002-2017

After launching the policy of reform and opening-up, rapid urbanization and magnificent economic growth have taken place over the whole of China, particularly in eastern China. The population in eastern China accounts for approximately 40.8% of the total population in China in 2016, while eastern China accounts for only 10.7% of China's terrain. Figure 3-3 shows that along with the rapid urbanization and dramatic economic growth, the total population in eastern China had increased by approximately 19.3% from 472.74 million in 2001 to 564.12 million in 2016 because a large amount of population had migrated from rural areas to urban areas to satisfy the work labor demand under the background of the rapid pace of industrialization. The significant amount of immigration came from the neighbor provinces or other regions of China. In these provinces and regions, with the development of agricultural intensification and mechanization system, a large amount of surplus labor existed in rural areas, particularly in the middle and southwest of China. Figure 3-3 shows that the urban population had constantly increased from 2001 to 2016 and reached about 373.4 million in 2016. In

addition, the urbanization rate had promoted by 20.3% from 45.9% in 2001 to 66.2% in 2016 in eastern China, which are significantly greater than the magnitude of 37.7% in 2001 and 57.4% in 2016 in China (Statistical Yearbook of China, 2002-2017).

The three China's largest economic zones such as the Pearl River Delta, Yangtze River Delta, and Bohai Economic RIM are located in eastern China, where the socio-economic status, urbanization rate, and population density are much higher than other regions of the study area. The urbanization rate of the three economic zones has reached the top level nationwide. Particularly, Jiangsu has formed an increasing gradient of urbanization level from the north to the south. In recent years, the growing urbanization, industrialization, and traffic infrastructure construction have led to the expansion of urban areas and the shrink of farmland and forest land in eastern China remarkably. Human activities result in more negative impacts on vegetation cover, especially in the middle-lower reaches of the Yangtze River and Pearl River, where have become the least vegetation-covered areas.

Topographically, eastern China spreads from the south to the north along with the eastern coastline in China. The Yangtze River and Yellow River are the major rivers in eastern China, which are the longest and second longest rivers in Asia, respectively. Apart from this, The Huai River Basin acts as a climate transition zone, and it is located in Jiangsu province. The Huai River is considered as the geographical dividing line between the northern and southern China, where present two distinct types of climatic characteristics. The landscape of eastern China is varied, and the elevation of eastern China ranges from -281 to 2849 m (Figure 3-4). Vast plain areas are located in the middle of eastern China with an elevation ranging from 0 to 40 m, particularly in Jiangsu, Shandong, Tianjin, and southern Hebei. High elevation areas are distributed in the south and north parts of eastern China, particularly in part of Fujian, Zhejiang, and the northern Hebei. Figure 3-4 shows that the elevation is significantly lower in the middle of Liaoning than in the east and west, while the elevation is greater in the middle of Shandong than the surrounding areas.

A remarkable land use and land cover change has been detected in eastern China, including the transformation of farmland to urban areas in the three economic zones and city center, the deterioration in grassland due to overgrazing, as well as the reforestation

and afforestation in the northwest of Hebei and Beijing as a result of the implementation of a serious of ecological conservation and forest restoration programs. The major land use types in eastern China are farmland, forest land, grassland, built-up land, and water body (Figure 3-5). The farmland is mainly located in the middle of eastern China, covering 42.2% of the study area, such as Jiangsu, Shandong, and Hebei. Especially in Jiangsu, the landscape is mostly flat, with its plain area covering 68.8% of the whole province, including the Yangtze-Thai Lake Plain, Coastal Plain, and Lixiahe Plain. Affected by intensive agriculture planting pattern for years, eastern China enjoys a relatively high rate of vegetation cover, which is relatively higher in Shandong, Jiangsu, and Zhejiang in the growing season. Due to the abundant agricultural products, Jiangsu and Zhejiang have long enjoyed its reputation as “a land flowing with milk and honey”.

Low vegetation cover mainly distributes in the outskirts and center of cities and the eastern coastal areas. Densely interconnected water channels and dotted waters are distributed in the south of the Huai River Basin. These surface water and groundwater resources primarily satisfy the water demand of the inhabitant consumption, vegetation growth, and the processes of the urbanization and industrialization. In addition, to ease the water shortage in the north of the Huai River Basin, the South-to-North Water Diversion Project was put into action in 2002 to channel water from the Yangtze River to Beijing, Tianjin, and Hebei to secure the domestic, municipal, and industrial water supply in these regions. Forest lands account for more than 35.6% of the study area, which mostly and coincidentally spread at the high elevation areas. These areas are sparsely distributed in Guangdong, Fujian, and Zhejiang and wide-ranging in the north of Hebei and east of Liaoning.

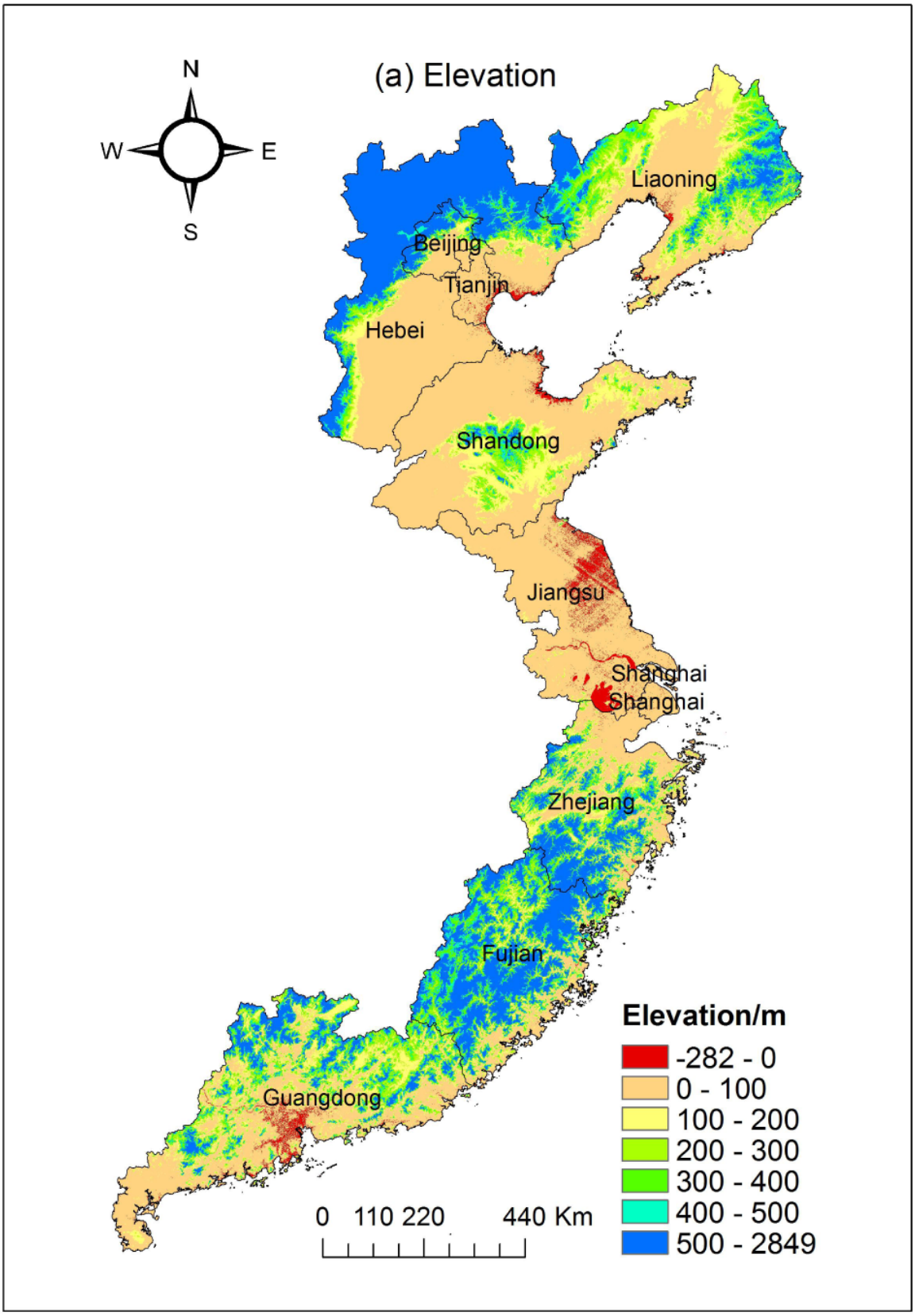

Figure 3-4. The elevation of eastern China

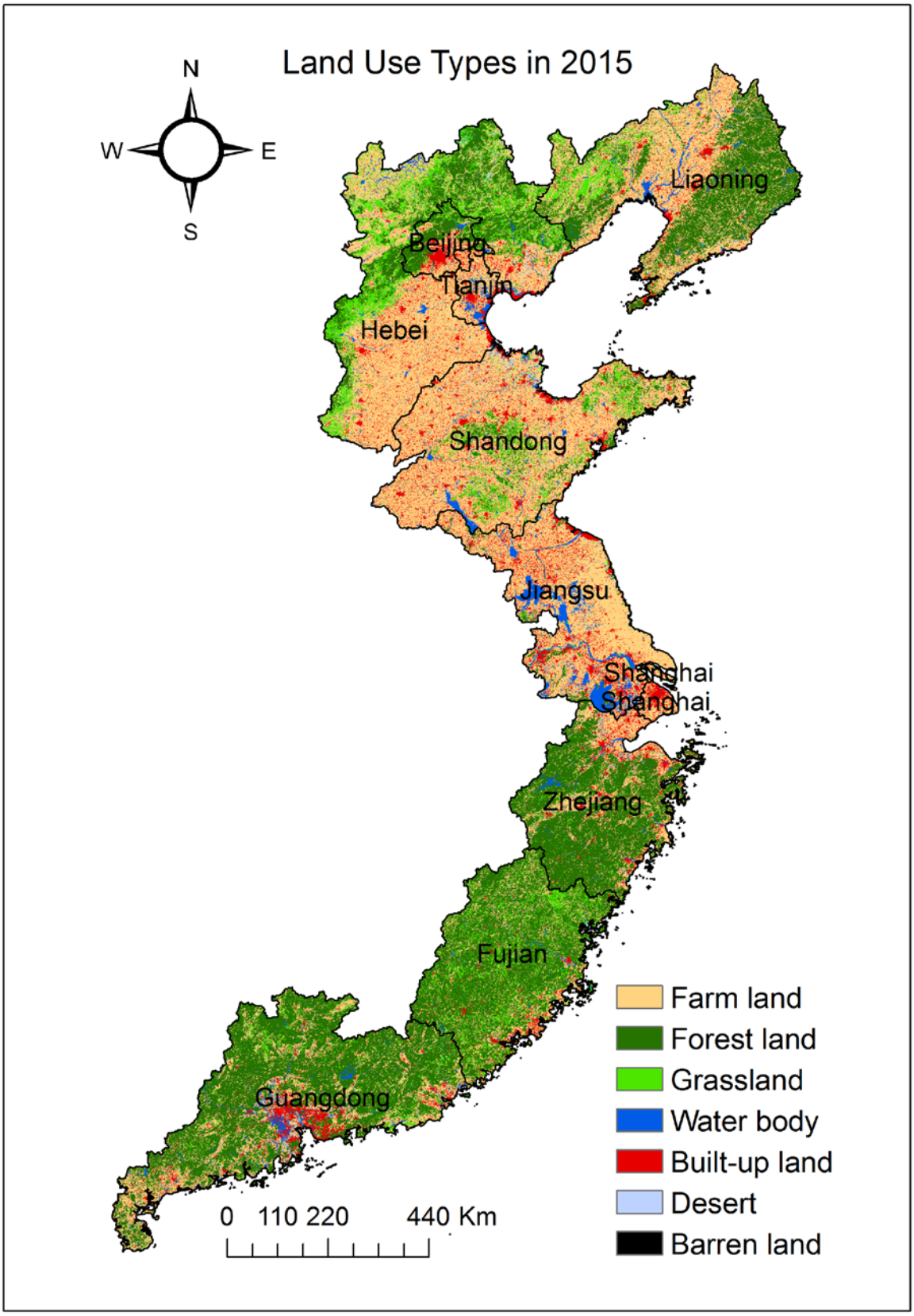

Figure 3-5. The land use types of eastern China in 2015

Eastern China is located in the East Asian monsoon climate zone, which is sensitive and vulnerable to climate variation (Cui, 2010). The Huai River is located in the north of Jiangsu. Areas located in the south of the Huai River are dominated by humid climate, and areas located in the north of the Huai River are under the control of sub-humid climate and semi-arid climate (Yin et al., 2018). Figure 3-6 shows that the precipitation increases from January to July/August and decreases afterward. Precipitation is primarily concentrated in summer. The monthly temperature shows a similar variation pattern to precipitation, but it reaches the highest temperature in July. The average annual temperature ranges from 15 to 16.5 ℃ in eastern China, and the accumulated annual precipitation within the study area varies widely from 1000 to 1500 mm, all of which are beneficial for vegetation growth.

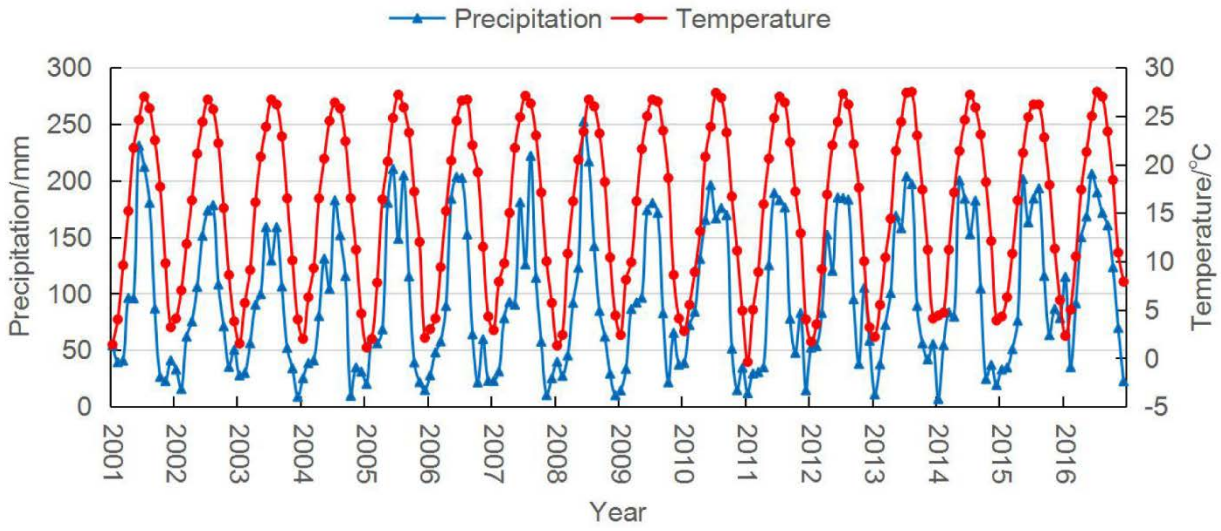

Figure 3-6. The monthly precipitation and temperature in eastern China from 2001 to 2016

Source: Own illustration; Based on monthly in situ observed temperature and precipitation data, 2001-2016

Spatially, due to the influence of monsoon climate, an apparent south-to-north precipitation gradient leads to a downward trend in accumulated annual precipitation from more than 2000 mm (Guangdong) in the south of eastern China to less than 400 mm (Hebei) in the north (Figure A-5(a)). The accumulated mean annual precipitation is distinctly heterogeneity in eastern China. Jiangsu can be regarded as a transition zone

of the humid region to sub-humid/semi-arid region. Due to the conversion of the climate zone, the precipitation converts from “rich” to “poor” from the humid region to the sub-humid/semi-arid region. The precipitation in Guangdong, Zhejiang, and Fujian is remarkably higher than in other provinces and municipalities. The annual and seasonal temperatures situated at different latitudes are mainly influenced by the angle of solar radiation and elevation. The mean annual temperature decreases with the latitude increase in the study area. Figure A-6(a) shows that the highest temperature occurs in Guangdong with a magnitude of more than 24 ℃ and the lowest temperature exhibits in Liaoning. It is worth mentioning that the temperature in the middle of Shandong and the middle and north of Fujian is lower than the surrounding areas because the altitude of the sensor of these meteorological stations is relatively higher than the surrounding meteorological stations.

3.2 Data

To explore the spatiotemporal variation of vegetation cover and the driving forces that influence the vegetation variation, the following datasets are required: MODIS NDVI dataset, the vector map of eastern China, monthly meteorological dataset from meteorological (automatic) base station, DEM data, the map of land use types, the map of GDP, the map of population density, and socio-economic statistical data. Detailed information about the data sources is listed in Table 3-1. The study period was determined by the availability of RS data, which is available from February 2000 to the present. To obtain a completed annual MODIS NDVI data to secure the accuracy of this study, the study period is determined from January 2001 to December 2016. All of the raster layers and the vector layers applied in this study are reprojected to the coordinate system of World Geodetic System (WGS) 84, Urchin Tracking Module (UTM) Zone 50 N and the spatial reference system of WGS 84 by using the MODIS Reprojection Tool (MRT) software and ArcGIS 10.3 platform.

Table 3-1. The list of data sources

Category	Data	Scale	Year	Sources
MODIS13Q1	MODIS NDVI	250 m spatial resolution; 16-day temporal resolution	2001-2016	National Aeronautics and Space Administration (NASA)
Climate Data	Precipitation	Monthly in situ observed from meteorological (automatic) base station	2000-2016	China Meteorological Administration and State Information Center
	Temperature			
Topographic Data	DEM	30 m spatial resolution	-	Shuttle Radar Topography Mission (SRTM)
Socio-economic Data	GDP	Administrative unit	2001-2016	National Bureau of Statistics of China
	Primary Industry Product			
	Secondary Industry Product			
	Tertiary Industry Product			
	Total Investment in Fixed Assets			
	PCGDP			
	Household Consumption			
	Rural Household Consumption			
	Urban Household Consumption			
	Population			
	Total Employment			
	Population Density			
	Urbanization Rate			

Spatial Socio-economic Data	GDP Map	1 km spatial resolution	2000, 2015	Resource and Environment Data Cloud Platform
	Land Use Map			
	Population Density Map			
Vector Map	The Vector Map of China at City Level	1:1 000 000	2015	

3.2.1 MODIS NDVI Data

NDVI can be considered as a measure of the "greenness" of terrestrial landscapes. NDVI has been widely employed in vegetation variation detection and practical application evaluation from regional to global scales. The MOD13Q1 NDVI data adopted in this study is released by National Aeronautics and Space Administration (NASA) (*https://ladsweb.modaps.eosdis.nasa.gov/*), spanning from January 2001 to December 2016, with a 250 m spatial resolution, a 16-day temporal resolution, and a total of 23 temporal images in a whole year. Each temporal image is mosaicked by six MODIS tiles (h26v04, h26v05, h27v04, h27v05, h28v05, and h28v06) derived from MOD13Q1 C6, which covers the whole study area. It has been demonstrated that the accuracy of the MODIS NDVI C6 is higher than the MODIS NDVI C5 due to sensor degradation of C5 (Zhang et al., 2017, Li et al., 2018). The MODIS NDVI C6 dataset has been processed by geometric precision correction and radiation correction.

A batch processing procedure is applied to MODIS data for projection and format conversion, including the use of the MRT tool, the projection transformation tool, and Cygwin. After mosaicking and re-projecting, the regional MODIS data is extracted in a batch using the vector map of the study region on the basis of the Environment for Visualizing Images (ENVI) 5.3 platform. To obtain the maximum value of monthly NDVI data for each pixel, the maximum value composite (MVC) approach is applied to select the maximum value over a certain time interval. After that, the maximum value of monthly NDVI over such an interval is likely to be a cloud-free value. Finally, the NDVI is calculated from the initial Digital Number (DN) in MOD13Q1, which ranges from -3000 to 10000. As the range of NDVI value is between -1 and 1, the calculation of NDVI is accomplished by multiplying the DN by a scaling factor 0.0001.

When NDVI value is higher than 0.4, it indicates that lands covered by green, leafy vegetation, otherwise, indicating that lands where there is only a few or even no vegetation cover. Figure 3-7 (a) and (b) reflect the spatial pattern of vegetation cover in eastern China in 2001 and 2016, respectively, and the vegetation cover indicates by DN. The greenish color indicates where higher vegetation cover has, and the reddish color indicates where the lower vegetation cover or no vegetation is dominated.

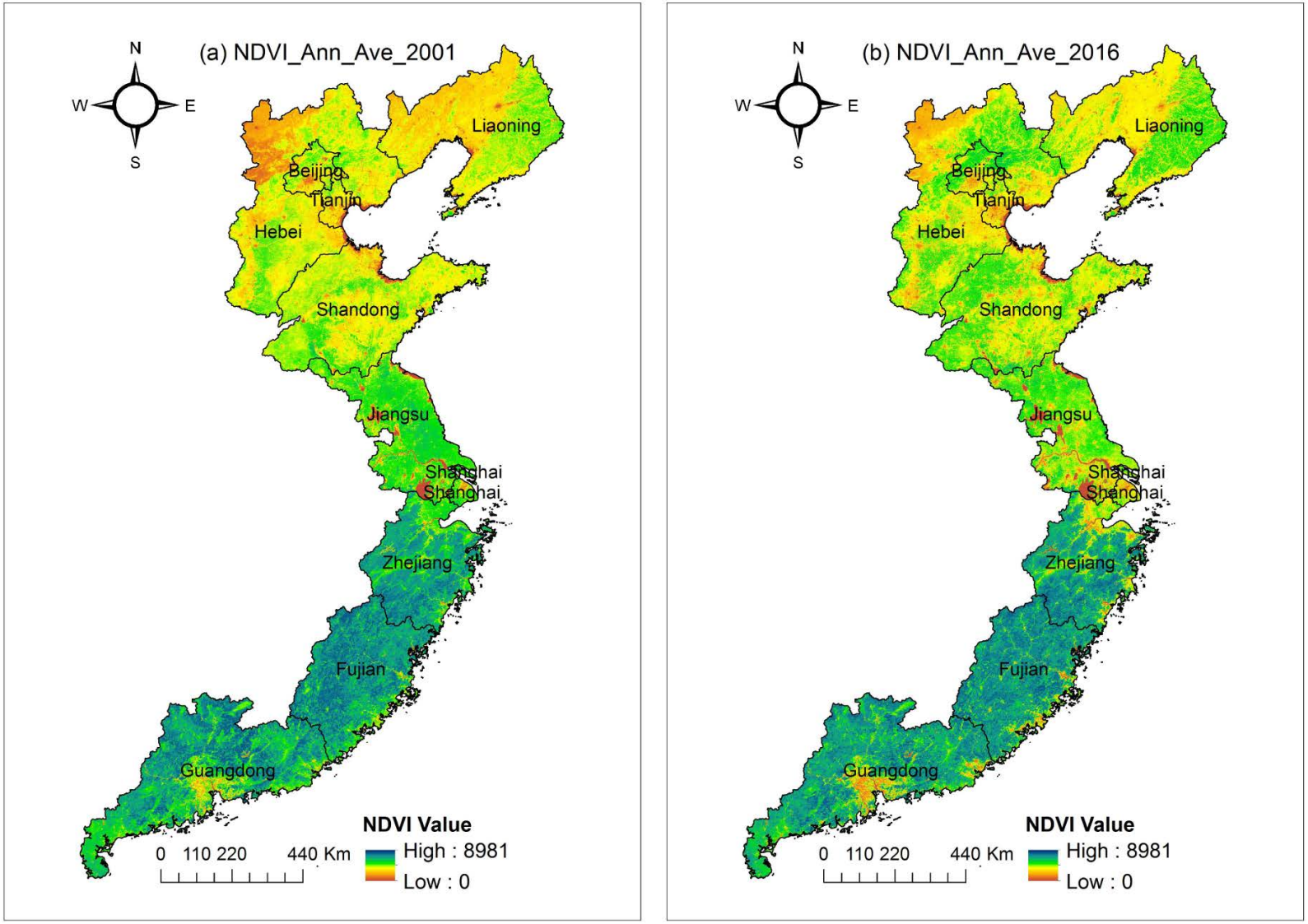

Figure 3-7. The spatial pattern of MODIS NDVI in eastern China in 2001 and 2016

3.2.2 Meteorological data

Due to the effect of East Asian monsoon, the climate shows a complex pattern in eastern China, which results in significant impacts on vegetation evolution and succession. To display the interaction pattern between vegetation cover and climate factors, the temperature and precipitation are employed in this study. The meteorological dataset includes temperature and precipitation, covering from October 2000 to December 2016. This study uses monthly in situ observed temperature and precipitation data from meteorological (automatic) base station. The meteorological data can be downloaded from the China Meteorological Science Data Sharing Service System (*http://data.cma.cn/*) provided by the China Meteorological Administration and State Information Center. This dataset is under high-quality control. The temperature data hold a precision of 0.1 degrees, and the precipitation data hold a precision of 0.1mm.

204 meteorological stations are located in the study area. Due to the availability of the time period of the meteorological dataset and the location of the station, 184 stations are selected for this study. For instance, the station of Bohai A platform which is located on the sea and there is no vegetation cover within a distance of 5 km, which is meaningless to detect the interaction between vegetation cover and climate factors for this meteorological station. Furthermore, the meteorological dataset of Shengzhou is only available from 2007 to 2008, which is unsuitable for analyzing the relationships between vegetation cover and climate variables.

3.2.3 DEM data

DEM is a surrogate of the Earth's terrestrial surface topography. It can be applied to acquire topographic features, geomorphometric parameters, morphometric variables or even terrain information (Prasannakumar et al., 2011). DEM can be freely downloaded from Shuttle Radar Topography Mission (SRTM) (*https://gdex.cr.usgs.gov/gdex/*). Three types of SRTM-DEM products are available, the SRTM 1', SRTM 3' and SRTM-GTOPO30 with a spatial resolution of 1 arc second (30 m), 3 arc seconds (90 m), and 30 arc seconds (1 km), respectively (Global Land Cover Facilities website 2005) (Prasannakumar et al., 2011). The DEM data with a 30 m spatial resolution is applied in this study, covering the whole of China. The DEM data from SRTM is accessed as tiles

at each 1º× 1º grid. The individual DEM tiles are spliced into an integrated map covering the whole study region. After splicing and re-projecting, the integrated map is extracted by the vector map of the study region using the ArcGIS 10.3 platform.

Eastern China is a coastal region with high variability in elevation and terrain nature. The vegetation growth is assumed to closely relate to the topographical differences due to the influence of topography on heat, water, and light conditions. In this study, three factors (*e.g.*, elevation, slope, and aspect) are considered as the natural topographic driving factors influencing the dynamic change of vegetation cover. The three factors can be obtained by implementing surface analysis based on the ArcGIS 10.3 platform.

3.2.4 Socio-economic statistical data

The vegetation change is closely related to socio-economic development, urban expansion, and population growth. The socio-economic factors are the most obvious way reflecting the status of social and economic development. Hence, it is essential to adopt the socio-economic factors to analyze the relationships between NDVI and socio-economic factors. The socio-economic data derived from Statistical Yearbook of China (2002 to 2017) is published by the National Bureau of Statistics of China *(http://www.stats.gov.cn/tjsj/ndsj/)*. The socio-economic datasets are categorized into three classes: general economic vitality, household consumption, and human population. The general economic vitality includes GDP, primary industry product, secondary industry product, tertiary industry product, PCGDP, and total investment in fixed assets. Household consumption is composed of household consumption, rural household consumption, and urban household consumption. Moreover, the human population consists of urbanization, population density, total population, and total employment. All of these datasets are collected for each province and municipality from 2001 to 2016. The 13 statistical datasets can represent the major socio-economic driving forces that contribute to the spatiotemporal distribution and variation of vegetation cover. Detailed statistical data can be seen in appendix B. To detect the relationships between the socio-economic factors and the annual NDVI, the statistical datasets are pre-processed.

Table 3-2. The socio-economic statistical data from 2001 to 2016

Category	Factor	Unit	Year
General Economic Vitality	GDP	100 million RMB	2001-2016
	Primary Industry Product		
	Secondary Industry Product		
	Tertiary Industry Product		
	Total Investment in Fixed Assets		
	PCGDP	RMB	
Household Consumption	Household Consumption		
	Rural Household Consumption		
	Urban Household Consumption		
Human Population	Population	Ten thousand	
	Total Employment		
	Population Density	People per sq. km	
	Urbanization Rate	%	

3.2.5 Vector map and raster map of the study region

The vector map of China is obtained from the Resource and Environment Data Cloud Platform (*http://www.resdc.cn/Default.aspx*). This map contains the administrative divisions at city scale, which is highly controlled for precision and quality. The vector map of eastern China is extracted from the vector map of China at the city level, and it can be used as a mask for the extraction of NDVI, the raster map of topographic factors (*e.g.*, elevation, aspect, and slope), the raster map of socio-economic factors (*e.g.*, GDP, urban areas, and population density), as well as the raster map of climate factors (*e.g.*, precipitation and temperature) at different levels.

The raster map of land use types, population density, and GDP is generated with a 5-year interval with a spatial resolution of 1 km provided by Resource and Environment Data Cloud Platform (*http://www.resdc.cn/Default.aspx*). These raster maps are available for every five years. Thus, the raster map of land use types, population density,

and GDP in 2000 and 2015 is applied in this study to detect the spatial interaction between annual NDVI and the topographic factors from 2001 to 2016. All of the raster datasets cover the whole of China. The land use types, population density, and GDP can be extracted by the vector map of eastern China.

Table 3-3. The land use types

Land Use Type	Description
Farmland	Paddy field and dry land
Forest Land	Dense forest land (with forest land), shrubland, sparse forest land, and other forest lands
Grassland	High-cover grassland, medium-cover grassland, and low-cover grassland
Water Body	Wetlands, canals, lakes, reservoirs, glaciers, permanent snow, and beaches
Built-up Land	Urban areas, rural residential areas, as well as industrial and mining areas
Desert	Sandy land, Gobi, saline-alkali land, and alpine desert
Barren Land	Barren land and bare rock gravel

4 Methodology

The dynamic change of vegetation cover and the spatiotemporal pattern of vegetation growth in response to its driving forces are complicated because the climate system varies from regional to global scales, from different topographical conditions, and from frequency of disturbances derived from human activities (Buermann et al., 2014, Gamon et al., 2013, Nemani et al., 2003, Zhang et al., 2013b, Buyantuyev and Wu, 2009, Liu et al., 2008b, Liu and Diamond, 2008). This study proposes a practical framework for monitoring the spatiotemporal vegetation cover change, estimating the vegetation stability, and predicting the future variation trend of vegetation cover in eastern China, and further presents a series of mathematical methods to analyze the spatiotemporal dynamics of NDVI and the relationships between NDVI and its driving factors (*e.g.*, climate factors, topographic factors, and socio-economic factors). In this study, MODIS NDVI was used as a representation of vegetation productivity, which indicates the biomass of the vegetation during the study period in eastern China.

The framework consists of four sections. A set of mathematical methods and analysis modules are applied to achieve the research objectives of this study. Section 4.1 exhibits the quantification of spatiotemporal pattern of vegetation cover change. Regarding the MODIS NDVI data, MVC method, geographical mean value calculation, linear regression analysis, stability analysis, and R/S analysis were adopted to display the distribution pattern, changing trend, future changing trend, and fluctuation degree on spatiotemporal scales.

Section 4.2 exhibits the pattern of NDVI in response to climate change both on spatial and temporal scales. In this section, the linear regression analysis was applied to analyze the changing trend of the climate factors, and Pearson’s correlation analysis was adopted to determine the correlation coefficients between NDVI and the climate factors both on annual and seasonal scales. Furthermore, t-test was employed to test the significance level of the correlation coefficients. Moreover, the lag time for maximum NDVI response to climate variation was investigated, and the spatial characteristics of the lag time for maximum NDVI response to climate variation were displayed both on annual and seasonal scales.

Section 4.3 exhibits the spatial pattern of NDVI in response to topographic variation. The surface analysis module was utilized to acquire the raster data of the elevation, aspect, and slope. The raster data of elevation, aspect, and slope were further used to overlap the map of the annual NDVI, changing slope of the annual NDVI, as well as the CV of the annual NDVI.

Section 4.4 reveals the interplay between the annual NDVI and socio-economic development. Pearson's correlation analysis was applied to explore the strength of the relationships between the annual NDVI and the socio-economic factors. In this section, we further analyzed the spatial coupling features of NDVI variation referring to changes in socio-economic factors. Buffer analysis and overlay analysis were employed to detect the spatial pattern of the annual NDVI responding to socio-economic development, urban expansion, and population growth in eastern China for the study period.

With the support of Geographic Information System (GIS) and RS technologies, the spatiotemporal variation of vegetation cover and its driving forces are analyzed. The flow charts of data processing and analysis are as follows:

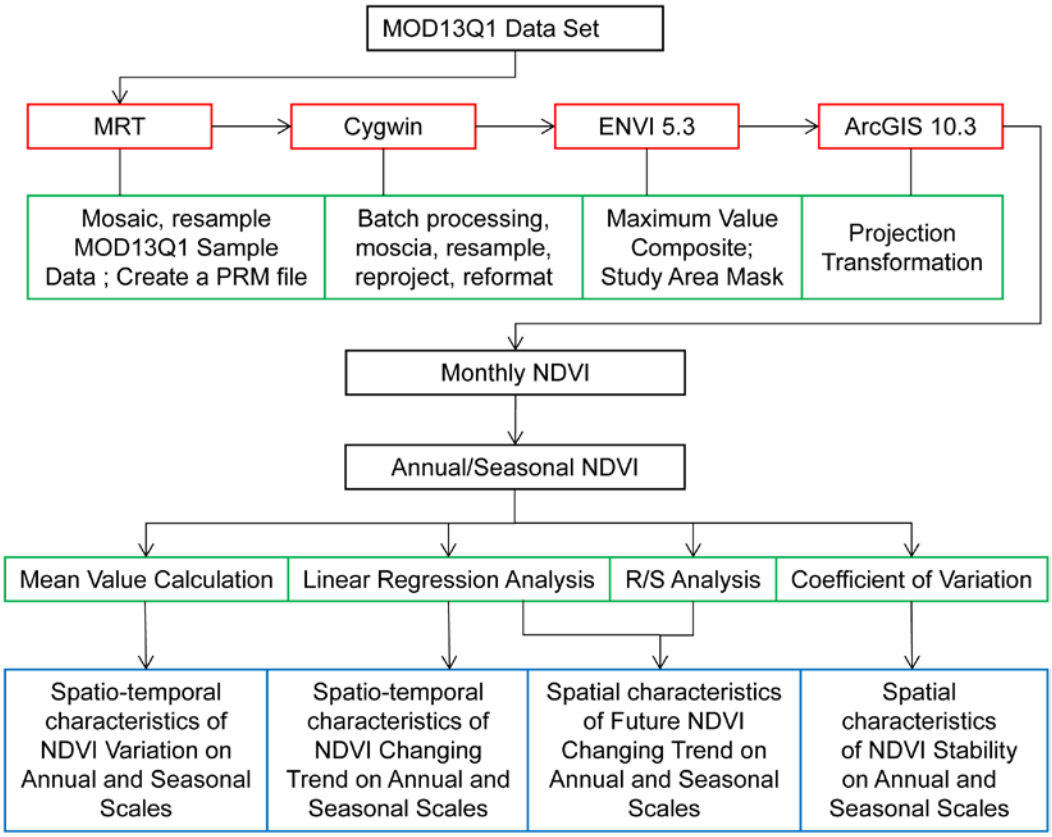

Figure 4-1. The workflow for calculation of the spatiotemporal variation of NDVI

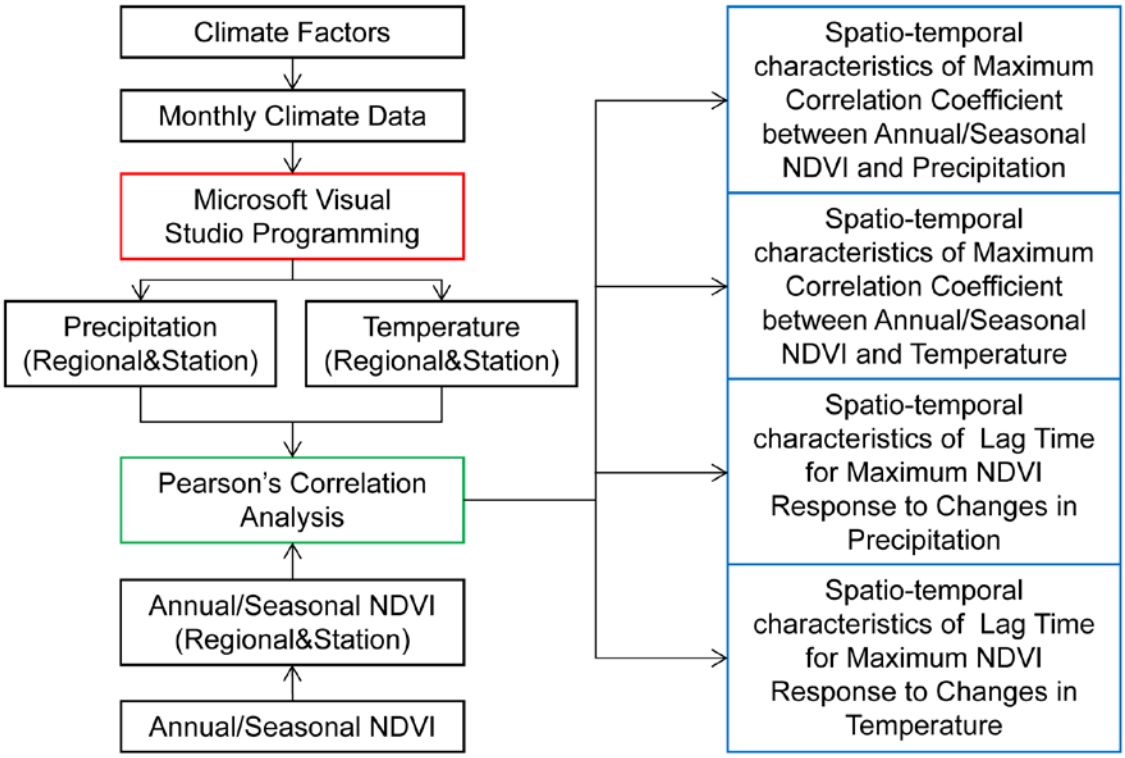

Figure 4-2. The workflow for calculation of the relationship between NDVI and climate factors

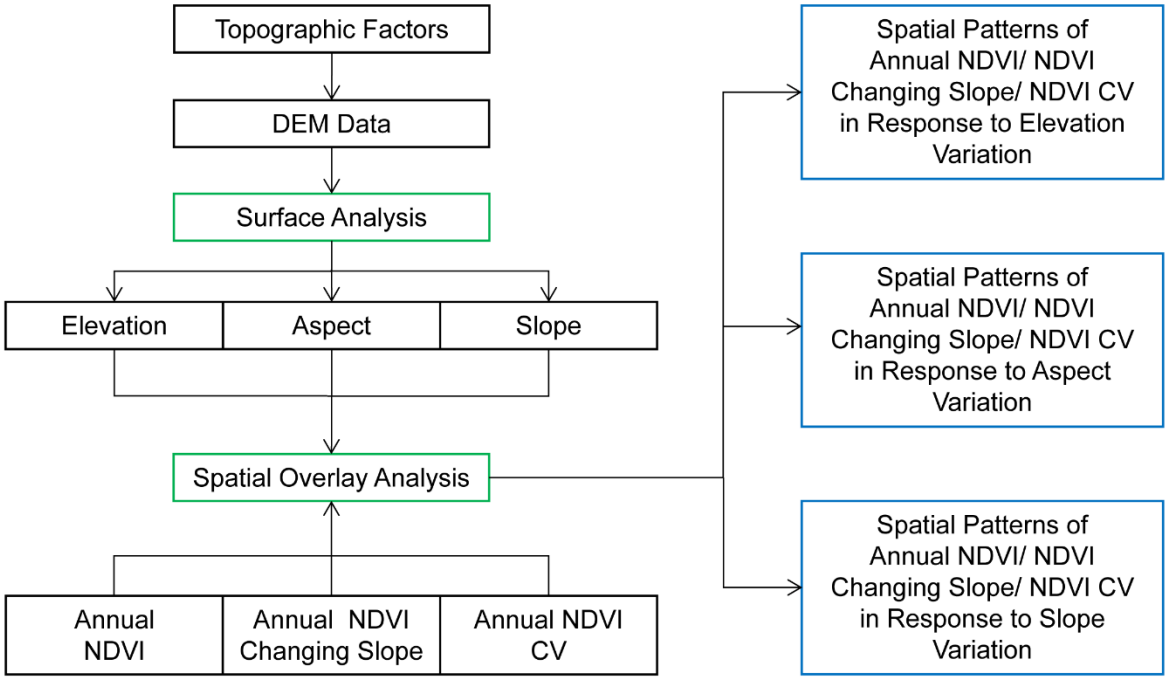

Figure 4-3. The workflow for investigation of interaction between NDVI and topographic factors

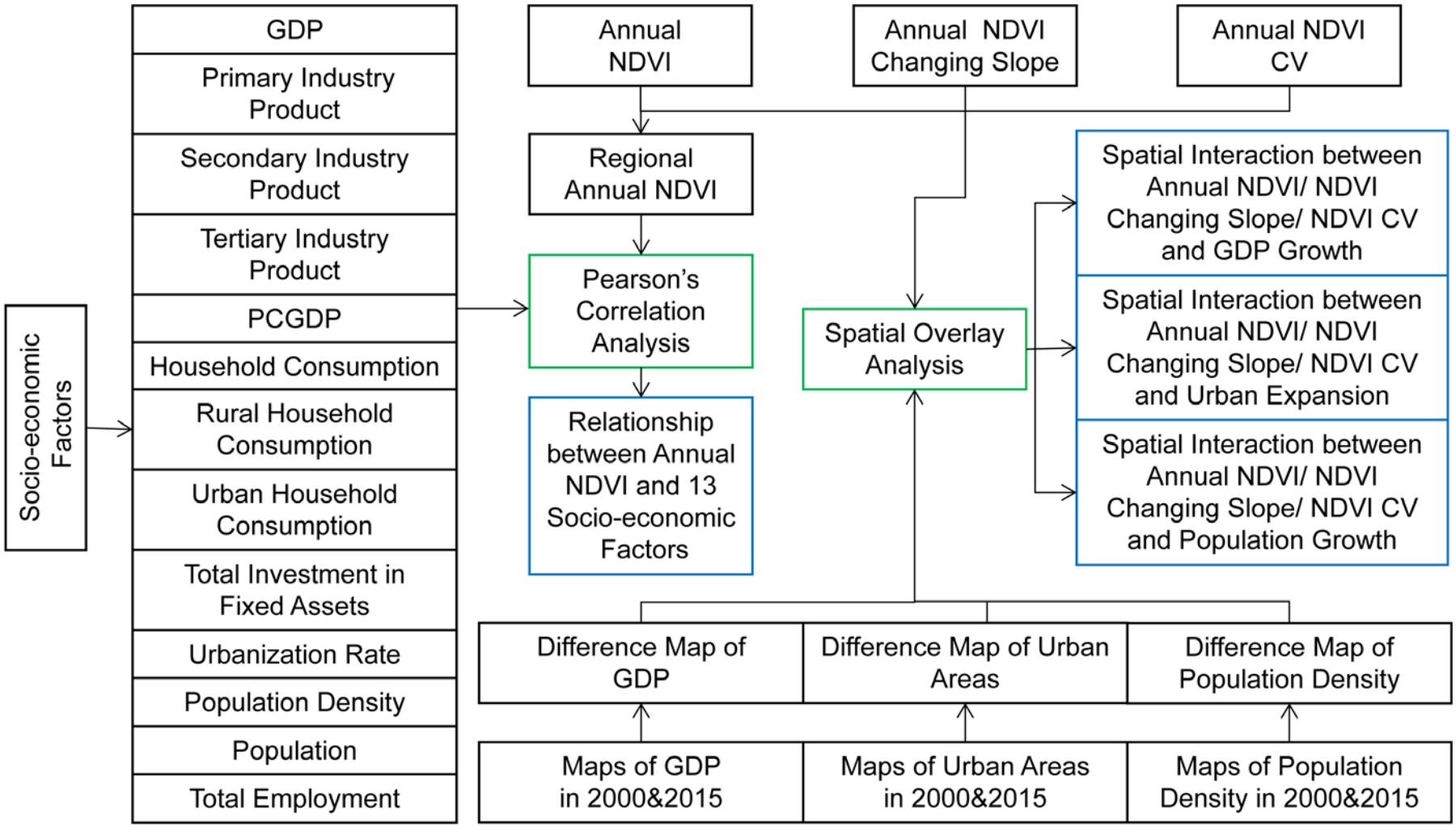

Figure 4-4. The workflow for calculation of the relationship between NDVI and socio-economic factors

4.1 Quantification of spatiotemporal pattern of vegetation cover change

4.1.1 The pre-processing of the MOD13Q1 dataset

It is essential to mention that the monthly mean NDVI can be applied to quantify the vegetation vitality (Zhang et al., 2017). In this study, monthly mean NDVI is used to estimate the vegetation activity both on spatial (pixel and regional) and temporal (inter-annual, seasonal, and annual) scales. The NDVI data applied in this study is derived from MODI3Q1 products, which can be directly used to monitor the vegetation productivity over a specified area. Monthly mean NDVI is the most basic data employed to quantify the dynamic change of vegetation cover. To obtain the monthly mean NDVI dataset, a series of pre-processing has to be executed.

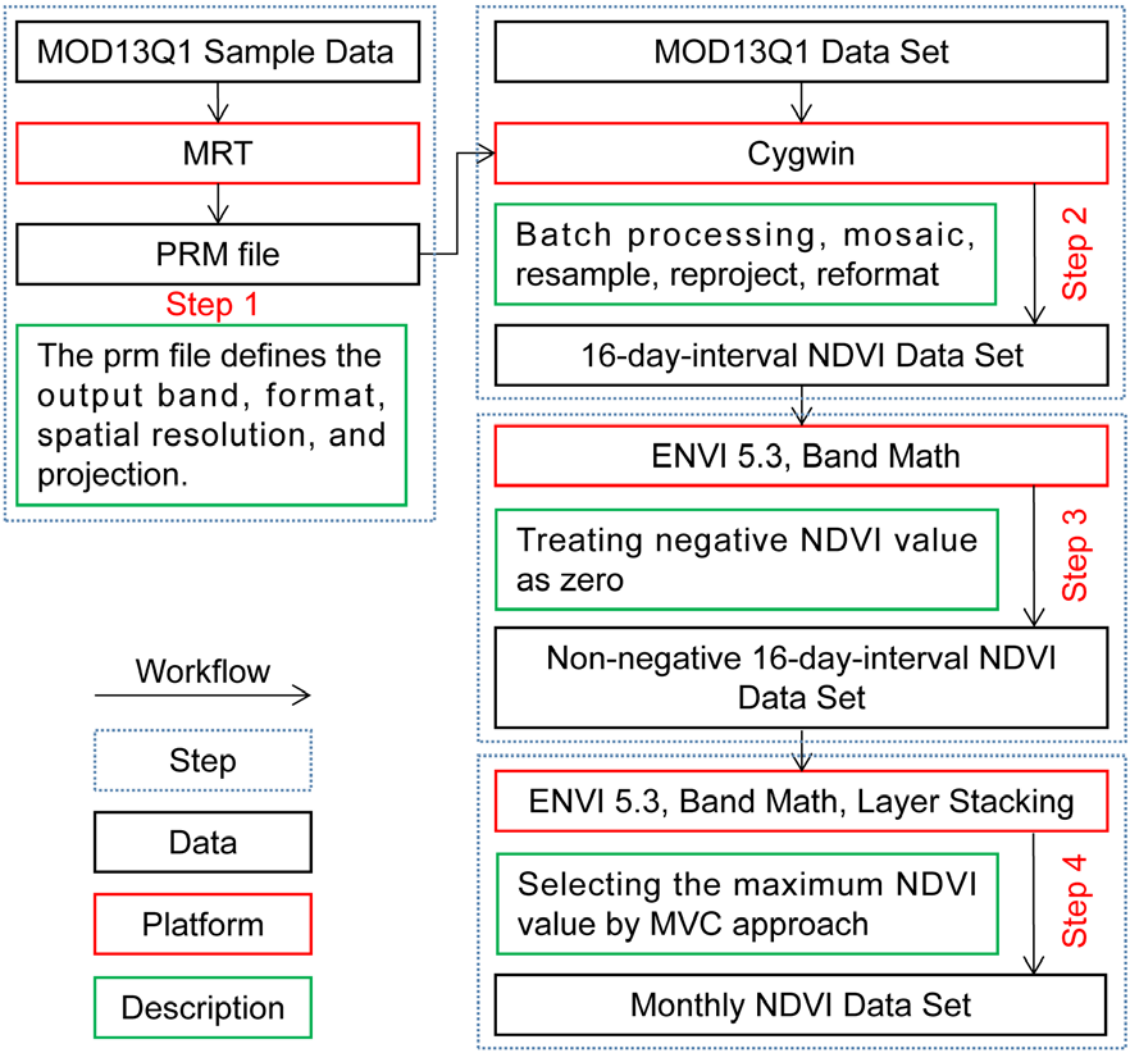

Figure 4-5. The workflow of MOD13Q1 dataset pre-processing

As shown in Figure 4-5, the workflow of the pre-processing work is divided into four steps. In step 1, a parameter file (PRM) was produced in the background of the MOD13Q1 sample data by using MRT software. The PRM file was used as a template file in batch processing of the MOD13Q1 dataset. Step 2 illustrates the workflow of the batch processing of the MOD13Q1 dataset, in which the band of NDVI was selected and mosaicked covering the entire study area. Step 3 treated all of the negative NDVI value as zero, which decreases the uncertainty of the estimation of the vegetation activity and enhances the accuracy of the NDVI time series. The maximum NDVI value in each pixel was composited in step 4 using the MVC approach. Eventually, the monthly NDVI dataset was generated on the basis of the above processing steps.

The MOD13Q1 dataset was stored by the format of Hierarchical Data Format (HDF), which contains NDVI, EVI, pixel quality assurance (QA), and Blue, Red, near-Infrared (NIR) and mid-Infrared (MIR) reflectances (Huete et al., 2002). In this study, the MRT, which is available for free to all registered users and is developed to support higher level MODIS Land products, was employed to produce a PRM file. Six HDF tiles acquired during the same period were used as the MOD13Q1 sample data, which was utilized to produce the PRM file. The PRM file defines the band, format, spatial resolution, and spatial projection of the output MODIS NDVI dataset, and it will be used in step 2, batch processing of MOD13Q1 dataset.

Cygwin is a set of GNU and Open Source tools, which supports functionality comparable to a Linux distribution on Windows. It can be used to produce the NDVI images systematically by creating a batch processing program. In terms of the rules of naming MOD13Q1 HDF files, the file's name was combined by the product type, data acquisition time, tile identify, dataset version, and data production time. According to the data acquisition time of the HDF files, every six files acquired for the same period were identified, mosaicked, and then resampled automatically based on Cygwin programming. To keep the consistency of the NDVI dataset, the NDVI band was extracted. The format was reformatted from HDF to GeoTIFF, and the spatial projection was then reprojected to Lambert Azimuthal Equal Area (LAEA), while the spatial resolution kept no change with a resolution of 250 m. 23 images of each year, 368 images in total from 2001 to

2016, were produced, but it cannot be directly used to reflect the monthly vegetation activity. It has to be further processed.

In this study, vegetation activity was quantified based on monthly mean NDVI, while some negative monthly NDVI values were existed due to the influence of cloud, water, snow, and ice. Because of the meaningless of the negative monthly NDVI value for vegetation dynamics analysis over vegetation covered region, all of the negative monthly NDVI values were treated as zero by applying the module of Band Math on the basis of ENVI 5.3 platform before adopting MVC approach.

The MVC approach was used to select the maximum NDVI value over a certain time period on pixel scale to remove the influences from residual cloud, residual mist, cloud shadow, and terrain shadow with the aid of ENVI 5.3 platform, the module of Layer Stacking and Band Math (Zhang et al., 2012). The formula is as follows：

$$NDVI_{\mathrm{i}} = Max(NDVI_{ij}) \quad (1)$$

where $NDVI_{\mathrm{i}}$ is the NDVI value of the month i, $NDVI_{\mathrm{ij}}$ is the NDVI value of the j period (16-day interval) among the month i. The maximum NDVI value of each month in each pixel is selected to compose the maximum NDVI time series. This method is also effective to remove the interference from the cloud, atmosphere, and solar altitude. After compositing, the monthly NDVI dataset was extracted by the vector map of the study area on the basis of ENVI 5.3 platform, the module of Batch Extraction. Then, the monthly NDVI dataset was reprojected to WGS_1984_UTM_Zone_50N projection to maintain the data consistency with the aid of ArcGIS 10.3 platform, the module of Projections and Transformations.

Each year encompasses 23 NDVI time-series images. The monthly composed NDVI images are composited by one or two images, which depends on whether the year is a leap year or non-leap year. The study period ranges from 2001 to 2016, in which only 2004, 2008, 2012, and 2016 are leap years. Table 4-1 shows that the NDVI images in November in leap years and in October in non-leap years are composed by only one image. Except that, the NDVI images in the other 11 months are composited by two

images (Testa et al., 2017). The detailed information of the composite periods of the NDVI images was categorized in Table 4-1.

Figure 4-6(a), (b), and (c) display the spatial patterns of the NDVI, representing by DN, on 14th September 2014, 30th September 2014, and September 2014 in eastern China, respectively. Figure 4-6(c) was composited by Figure 4-6(a) and (b) using the MVC approach. Figure 4-6(c) shows that the NDVI value gradually decreases from the south to the north of eastern China. Especially, the NDVI values are significantly lower in the Pearl River Delta and Yangtze River Delta than the surrounding areas. Comparing the NDVI value in the Figure 4-6(a), (b), and (c), the NDVI value is greater in the northern part of eastern China in the Figure 4-6 (c) than in Figure 4-6; meanwhile, the NDVI value is higher in the southern part in Figure 4-6(c) than in the Figure 4-6(b). The spatial differences pictured in Figure 4-6(a), (b), and (c) can be ascribed to the functionality of the MVC approach.

Table 4-1. The composite periods of the NDVI images

Category	Number	Date in a leap year	Month in a leap year	Date in a non-leap year	Month in a non-leap year
1	001	01. Jan	January	01. Jan	January
2	017	17. Jan		17. Jan	
3	033	02. Feb	February	02. Feb	February
4	049	18. Feb		18. Feb	
5	065	05. Mar	March	06. Mar	March
6	081	21. Mar		22. Mar	
7	097	06. Apr	April	07. Apr	April
8	113	22. Apr		23. Apr	
9	129	08. May	May	09. May	May
10	145	24. May		25. May	
11	161	09. Jun	June	10. Jun	June
12	177	25. Jun		26. Jun	
13	193	11. Jul	July	12. Jul	July
14	209	27. Jul		28. Jul	
15	225	12. Aug	August	13. Aug	August
16	241	28. Aug		29. Aug	
17	257	13. Sep	September	14. Sep	September
18	273	29. Sep		30. Sep	
19	289	15. Oct	October	16. Oct	October
20	305	31. Oct		01. Nov	November
21	321	16. Nov	November	17. Nov	
22	337	02. Dec	December	03. Dec	December
23	353	18. Dec		19. Dec	

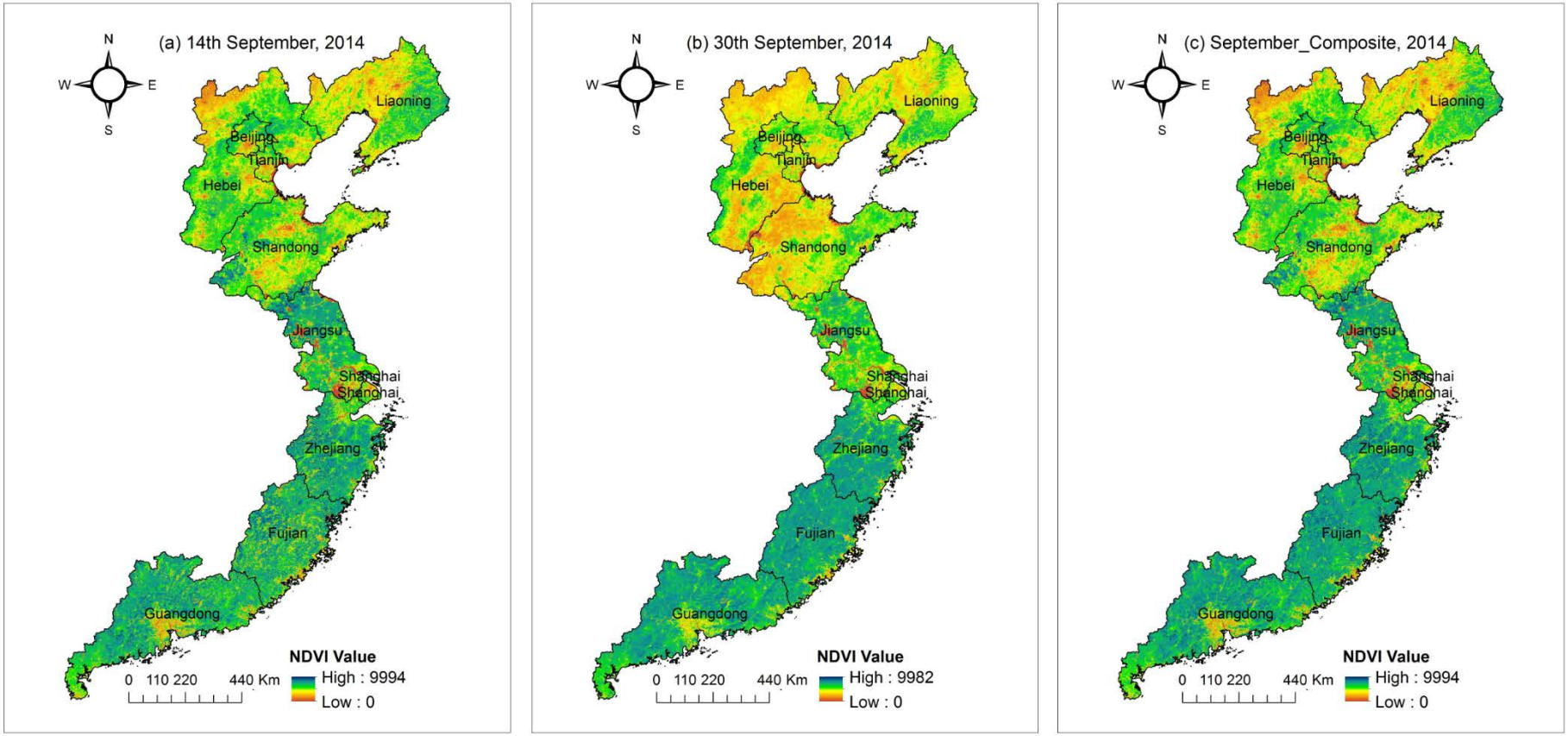

Figure 4-6. The spatial pattern of MODIS NDVI on 14th September, 2014 (a), 30th September, 2014 (b), and September_Composite, 2014 (c) in eastern China

Figure 4-6(a) and (b) display the spatial pattern of NDVI on 14th September 2014 and 30th September 2014 in eastern China, respectively. Figure 4-6(c) is composited by Figure 4-6(a) and Figure 4-6(b) using the MVC approach.

4.1.2 Estimation of the spatiotemporal pattern of NDVI

This study aims to explore the spatial and temporal patterns of the vegetation cover in eastern China. As mentioned previously, in this study, monthly mean NDVI was used as the main sources for monitoring the dynamic change of vegetation cover to exhibit the geographical distribution characteristics of vegetation activity on different spatial and temporal scales. A set of mathematical methods and data processing platforms are utilized to achieve the objectives of this study. Before monitoring the vegetation activity, the DN has to be converted to unitless NDVI value using the formula (2). The scale factor is available on the web page of Land Processes Distributed Active Archive Center (LPDAAC) (https://lpdaac.usgs.gov). The formula is as follows:

$$NDVI = DN * 0.0001 \tag{2}$$

The spatial distribution pattern of the seasonal vegetation activity was monitored using the time series of the mean NDVI in each season (spring: March to May, summer: June to August, autumn: September to November, winter: December to next February). With the exception of winter, the mean NDVI in spring, summer, and autumn were adopted to reflect the seasonal vegetation vitality. In the north of eastern China, lands were dominated by deciduous forest, and it might be covered by snow in winter. Furthermore, in the middle part of eastern China, the cropland was withered or harvested in late autumn. Due to the above reasons, the NDVI change in winter was not considered in this study. The calculation of seasonal NDVI ($\overline{NDVI_s}$) follows the formula below, taking the summer as an example:

$$\overline{NDVI_s} = (\sum_{i=6}^{8} NDVI_i) / 3, i = 6,7,8 \tag{3}$$

where $\overline{NDVI_s}$ is the mean NDVI of summer, $NDVI_{\mathrm{i}}$ is the largest NDVI composite of the month i, and i is the month number, ranging from 6 to 8. Similarly, the mean NDVI of spring and autumn in each year was obtained based on the formula (3). Figure 4-8(a) displays the spatial distribution of the summer NDVI in 2014, which is produced by using ArcGIS 10.3 platform, the module of Map Algebra, applying the formula (3).

Annual variation of the NDVI was an essential component for temporal analysis of vegetation cover. This study utilized the mean annual time series ($\overline{NDVI_y}$) for the spatial and temporal analysis of the annual NDVI. The calculation of mean annual NDVI ($\overline{NDVI_y}$) follows the formula below:

$$\overline{NDVI_y} = (\sum_{i=1}^{12} NDVI_i)/12, i = 1,2,3,...,12 \quad (4)$$

where $\overline{NDVI_y}$ is the mean annual NDVI, $NDVI_i$ is the largest NDVI composite of the month i, i represents the number of the month, which ranges from 1 to 12. Figure 4-8(b) shows the annual NDVI calculated against the background of applying the formula (5), displaying the spatial pattern of the annual NDVI in eastern China in 2014.

Multi-annual monthly mean NDVI, multi-annual seasonal mean NDVI, as well as multi-annual mean NDVI can not only be applied to reflect the surface biomass, but they can also be employed to display the spatial dynamic of general vegetation activity on monthly, seasonal, and annual scales, respectively. In this study, multi-annual monthly mean NDVI was defined on the basis of the average NDVI for 16 years at a certain month. The formula is as follows：

$$\overline{NDVI_j} = \frac{\sum_{i=1}^{16} NDVI_{ij}}{16} \quad (5)$$

where $\overline{NDVI_j}$ is the multi-annual monthly mean NDVI of the month j, $NDVI_{ij}$ is the largest monthly composite NDVI of the month j in the year i, j represents the number of the month, ranging from 1 to 12. i is the number of the year, extending from 1 to 16.

The multi-annual seasonal mean NDVI was calculated based on the formula (3) and formula (5) under the support of ArcGIS 10.3 platform, the module of Map Algebra. Similarly, using the formula (4) and formula (5), the multi-annual mean NDVI was acquired. To quantitatively evaluate the vegetation cover on different spatial and temporal scales, the NDVI value was reclassified into five classes based on ArcGIS 10.3

platform, the module of Reclass (Table 4-2, Figure 4-8). The method of generating regional mean NDVI would be issued further.

Table 4-2. The thresholds for the classification of NDVI value

Category	Range	Description
1	0≤NDVI≤0.2	The NDVI value is higher than 0.4, indicating that lands covered by green, leafy vegetation, otherwise, indicating that there is only a few or even no vegetation cover in this region.
2	0.2<NDVI≤0.4	
3	0.4<NDVI≤0.6	
4	0.6<NDVI≤0.8	
5	0.8<NDVI≤1	

To understand the temporal trends of the regional NDVI, the ten administrative units (Beijing, Tianjin, Hebei, Liaoning, Shanghai, Jiangsu, Zhejiang, Fujian, Shandong, and Guangdong) and eastern China were adopted to be 11 independent regions (units). Thus, the regional NDVI change and the relationships between regional NDVI and its driving forces were carried out. To show the general characteristics of the vegetation activity on regional scale, the regional-average NDVI time series datasets were generated, which can be used to analyze the vegetation variation in different provinces and municipalities quantitatively. The formula is as follows:

$$\overline{NDVI_r} = \frac{1}{N}\sum_{i=1}^{N} NDVI_i, i = 1,2,3,...,N \quad (6)$$

where N is the total number of the pixels in a specified region, $\overline{NDVI_r}$ represents the regional-average NDVI, $NDVI_i$ is the maximum value of each pixel, and i is the pixel number. It is worth mentioning that the calculation of $\overline{NDVI_s}$, $\overline{NDVI_y}$ and $\overline{NDVI_j}$ is focused on temporal scale, while $\overline{NDVI_r}$ is calculated based on spatial scale. That is to say, we can further calculate the regional-average $\overline{NDVI_s}$, $\overline{NDVI_y}$ and $\overline{NDVI_j}$ based on the above mean value calculation method.

Figure 4-8(a) and (b) show the mean summer NDVI and mean annual NDVI in eastern China in 2014, respectively. Figure 4-7(a) and (b) illustrate the percentage of the regional summer NDVI and annual regional NDVI in different categories of each

administrative unit. The calculation of Figure 4-7(a) was based on the formula (3) and formula (6), while the calculation of Figure 4-7(b) was based on the formula (4) and formula (6).

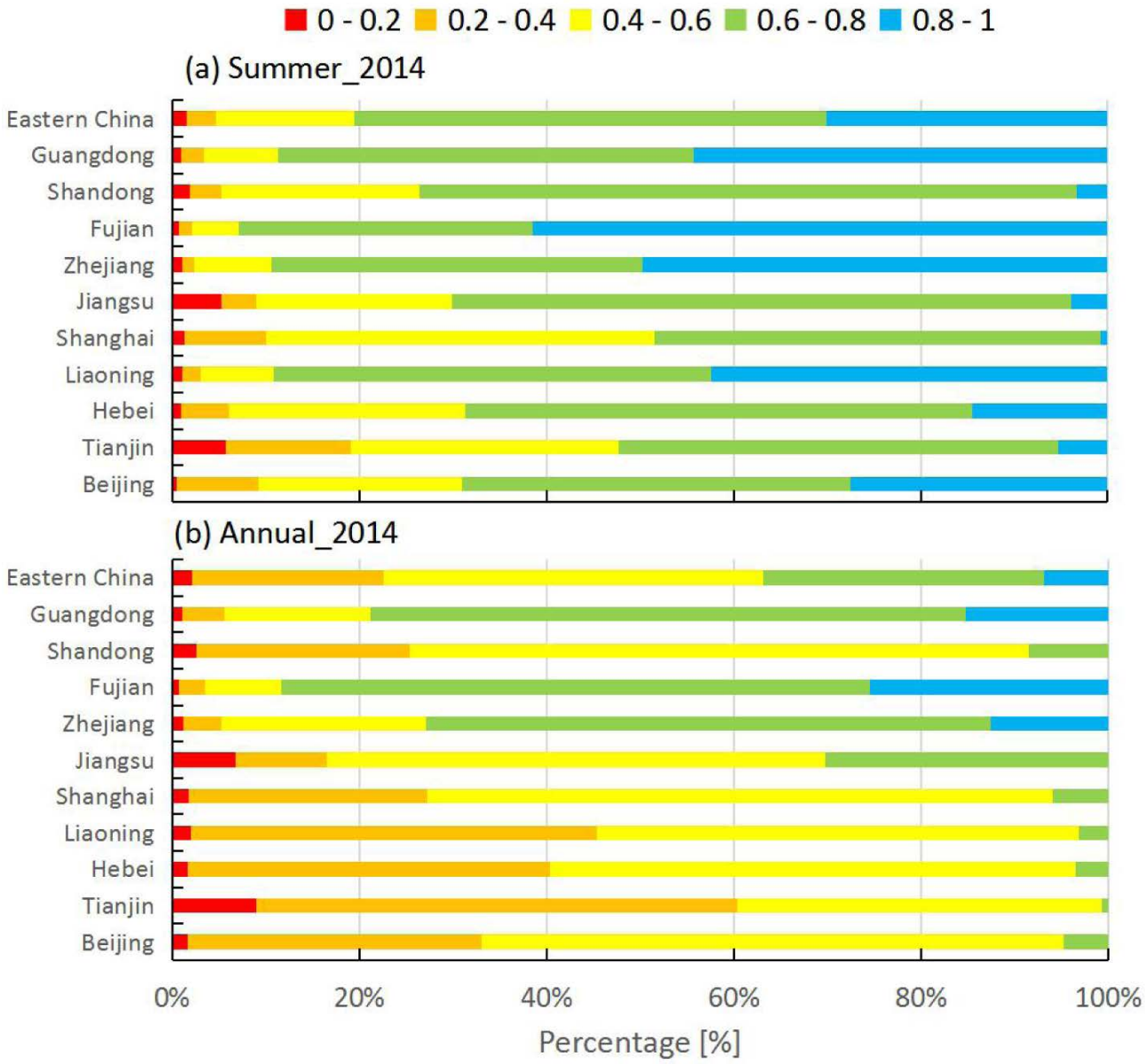

Figure 4-7. The statistical results of the percentage of regional summer NDVI and annual NDVI in 2014

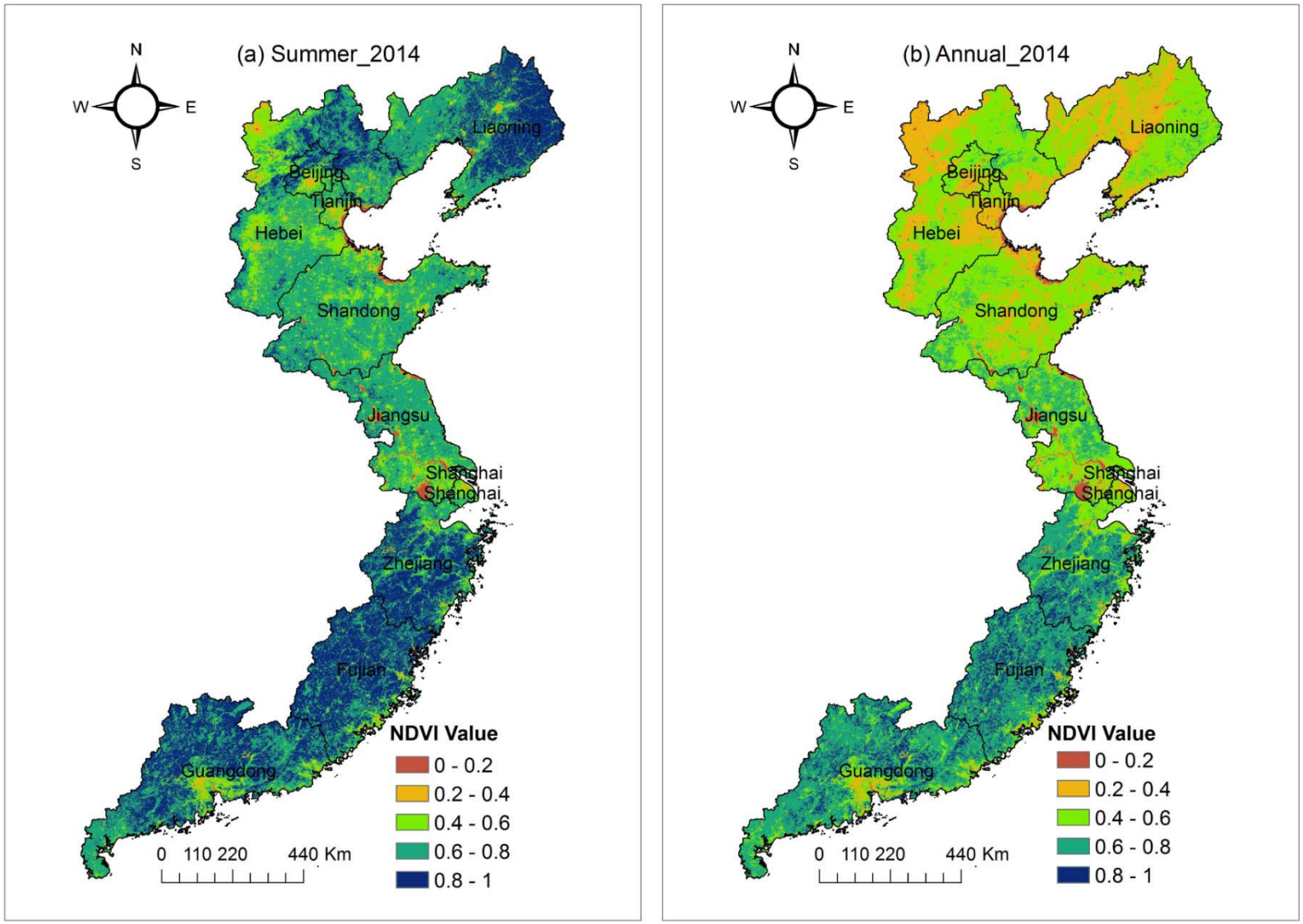

Figure 4-8. The spatial pattern of summer NDVI and annual NDVI in 2014

4.1.3 Estimation of the spatiotemporal pattern of NDVI changing trend

Depending on the periodical variation of ground vegetation biomass, NDVI time series indicates a strong seasonal and annual change of vegetation activity (Jong et al., 2012). To estimate the spatiotemporal pattern of NDVI changing trend in eastern China, the spatial and temporal fluctuation of the seasonal and annual NDVI was analyzed using linear regression analysis method (Zhang et al., 2012). Vegetation variation (greening and browning) can be reflected by the changing trend of the NDVI value, and the changing trend is defined in the background of the slope of the linear regression. NDVI changing slope is a widely used proxy, evaluating the strength of the NDVI changing trend.

The dynamic change of vegetation cover was detected both on spatial (pixel and regional) and temporal (seasonal and annual) scales. Taking the calculation of the changing slope of the annual NDVI as an example. Similarly, the changing slope of the seasonal NDVI can be obtained in the background of the same methods. The workflow of the annual NDVI time series processing consists of 3 steps. In step 1, the annual NDVI images were stacked into a 16 image-long annual NDVI time-series based on the ENVI 5.3 platform, the module of Layer Stacking. Particularly, the 16 annual NDVI images were acquired previously, deriving from the formula (4).

In step 2, the annual NDVI time-series images were processed by linear regression analysis method. With a set of variables which vary with testing time processed by linear regression analysis, the changing trend of each grid can be estimated. The changing slope of the mean annual vegetation cover can be obtained by applying linear regression analysis on the pixel scale. Thus, the changing trend and spatiotemporal distribution of vegetation cover were revealed. Specifically, the changing slope of the annual NDVI was computed using formula (7) (Zhang et al., 2012):

$$Slope = \frac{n \times \sum_{i=1}^{n} (i \times NDVI_i) - \sum_{i=1}^{n} i \sum_{i=1}^{n} NDVI_i}{n \times \sum_{i=1}^{n} i^2 - (\sum_{i=1}^{n} i)^2} \quad (7)$$

where n represents the total number of the years, $NDVI_i$ is the NDVI value in the year i.

Slope is the vegetation changing rate. If the $Slope$ > 0, it means, there is a trend of greening during n years; if $Slope$ < 0, then a trend of browning. The larger the absolute value of $Slope$ is, the more obvious change of vegetation cover occurs. With the support of ENVI Interactive Data Language (IDL) programming, each pixel is processed by linear regression analysis. The changing trend of each pixel is obtained, and then it was turned into the GeoTIFF format, which depicts the spatial features of vegetation cover change.

Step 3 qualitatively evaluated the changing trend of vegetation cover, the changing slope was classified into five classes: significant decrease, slight decrease, unchanged, slight increase, and significant increase (Table 4-3).

Table 4-3. The thresholds for the classification of NDVI changing slope

Category	Range [year^{-1}]	Description
1	Slope≤-0.009	Significant Decrease
2	-0.009< Slope ≤-0.003	Slight Decrease
3	-0.003< Slope ≤0.003	Unchanged
4	0.003< Slope ≤0.009	Slight Increase
5	Slope >0.009	Significant Increase

The regional NDVI changing trend reflects the overall picture of vegetation dynamic variation in a specified regional. Taking the calculation of the changing slope of the regional annual NDVI as an example, similarly, the changing slope of the seasonal NDVI can be computed by the seasonal NDVI dataset instead of implementing the annual NDVI dataset. In this study, the 11 independent regions (units) were adopted to analyze the regional annual NDVI change. Based on the formula (6), 11 regional annual NDVI time series were computed and then extracted by using annual NDVI images and the vector map of eastern China. Each annual NDVI image generates 11 corresponding regional annual NDVI data with the aid of ArcGIS 10.3 platform, the module of Extraction. The 11 generated regional annual NDVI datasets were then analyzed by linear regression analysis method. The 11 generated regional annual NDVI will then be applied

to create curves to illustrate the annual NDVI changing trend on regional scale on the basis of Microsoft Excel, the module of insert.

4.1.4 Estimation of the spatial pattern of future vegetation changing trend

In this study, R/S analysis method is applied to study the consistency of vegetation cover on the basis of NDVI time series. R/S analysis method is initially proposed by Hurst when analyzing the hydrologic data of the Nile (Hurst, 1951) and further developed into an analysis theory by Mandelbrot and Wallis to analyze time series (Mandelbrot and Wallis, 1969). This method is extensively applied in many fields (*e.g.,* hydrology, economics, climatology and geology). Based on the R/S analysis method, it is possible to predict future changing trend against the background of the current changing trends. Fundamental principle of R/S analysis method:

To define a time series $\{NDVI(\tau)\}, \tau = 1,2,...,n$

To define the mean sequence of the time series,

$$\overline{NDVI}_{(\tau)} = \frac{1}{\tau}\sum_{t=1}^{\tau} NDVI(t) \ , \tau = 1,2,...,n \tag{8}$$

To calculate the accumulated deviation,

$$X(t,\tau) = \sum_{t=1}^{\tau}(NDVI(t) - \overline{NDVI(\tau)}) \ , 1 \le t \le \tau \tag{9}$$

To generate the range sequence,

$$R(\tau) = \max_{1\le t\le \tau} X(t,\tau) - \min_{1\le t\le \tau} X(t,\tau) \ , \tau = 1,2,...,n \tag{10}$$

To generate the standard deviation sequence,

$$S(\tau) = \left[\frac{1}{\tau}\sum_{t=1}^{\tau}(NDVI(t) - \overline{NDVI(\tau)})^2\right]^{\frac{1}{2}}, \tau = 1,2,...,n \tag{11}$$

A non-dimensional ratio (R/S) is introduced to rescale R.

$$\frac{R(\tau)}{S(\tau)} = \frac{\max\limits_{1\le t\le \tau} X(t,\tau) - \min\limits_{1\le t\le \tau} X(t,\tau)}{\left[\frac{1}{\tau}\sum_{t=1}^{\tau}(NDVI(t) - \overline{NDVI(\tau)})^2\right]^{\frac{1}{2}}}, \quad (12)$$

If there is a number H fitting the formula $R/S = (c\tau)^H$ (c is a constant), then there are Hurst phenomena in time series $\{NDVI(\tau)\}$, and H is called the Hurst exponent. In the double logarithm coordinate ($\ln \tau$, $\ln R/S$), the least-squares fitting is used to get the Hurst exponent of each pixel. Hurst exponent ranges from 0 to 1. There are three situations:

(1) When $0 < H < 0.5$, there is a negative correlation between the past and future changing trends of NDVI, which indicates that the NDVI will reverse the current changing trends in the future.

(2) When H = 0.5, it indicates that the current changing trend and the future changing trend of NDVI are independent.

(3) When $0.5 < H < 1$, there is a positive correlation between the past and future changing trends of NDVI, which indicates that the NDVI will remain the current changing trends in the future.

Applying R/S analysis and linear regression analysis to every pixel, the spatial characteristics of the future changing trend of NDVI can be illustrated. To monitor the future changing trend of vegetation cover for eastern China, the NDVI changing slopes were reclassified into three classes: decrease (significant and slight decreases), unchanged, and increase (significant and slight increases) and the Hurst exponent was classified into two types: $0 < H < 0.5$ and $0.5 < H < 1$. Then the reclassified NDVI changing trend was overlapped on the Hurst exponent maps to exhibit the spatial characteristics of future NDVI changing trend.

It is worth mentioning, as detailed in Table 4-4 that (1) areas expected to switch the decreasing trend can be considered as vegetation improvement in the future; (2) areas expected to remain the decreasing trend can be considered as vegetation consistent degradation in the future; (3) areas expected to remain the increasing trend can be

considered as vegetation consistent improvement in the future; (4) areas expected to shift the increasing trend can be considered as vegetation consistent improvement in the future; (5) areas expected to experience unchanged can be considered as vegetation unchanged in the future; and (6) areas predicted to switch from unchanged to a decreasing trend (degradation) or an increasing trend (improvement) can be considered as uncertainty vegetation changing trend in the future. In this study, to quantitatively analyze the improvement area and degradation area in eastern China in the future, we only took the areas with a certain future changing trend (1-5) into consideration.

Table 4-4. Predicted future vegetation changing trends

NDVI Slope& Hurst Exponent	Decrease	Unchanged	Increase
0＜H＜0.5	Consistent Degradation	Unchanged	Consistent Improvement
0.5＜H＜1	Improvement	Improvement/ Degradation	Degradation

4.1.5 Estimation of the spatial pattern of NDVI stability

The NDVI CV was applied to capture the terrestrial landscape ecosystem's resilience and stability to changes in its driving forces. The stability of the vegetation cover in the corresponding region during different years can be revealed from the CV of NDVI on pixel scale. In this study, the NDVI CV value was considered as a measure of the NDVI variability related to the mean NDVI value both on the annual and seasonal scales. Its stability in time series can be estimated using the following formulas (Barbosa et al., 2006) :

$$Cv = \frac{\sigma}{\overline{NDVI}} \tag{13}$$

$$\sigma = \sqrt{\frac{\sum_{i=1}^{n}(NDVI_i - \overline{NDVI})^2}{n-1}} \tag{14}$$

where Cv represents the CV of the NDVI time series, σ is the standard deviation of the NDVI images from 2001 to 2016, $\overline{NDVI}$ is the mean NDVI value for a given time period.

n represents the total number of the years. $NDVI_i$ is the NDVI value in the given year i. Cv indicates the dispersion degree of data distribution. Larger Cv indicates higher dispersion degree and higher stability.

To statistically analyze the stability of the vegetation cover both on spatial and temporal scales, the NDVI CV value was reclassified into four classes based on ArcGIS 10.3 platform, the module of Reclass (Table 4-5). After reclassification, 11 NDVI CV maps at the administrative unit level were extracted to analyze the percentage of the NDVI CV in different categories for each administrative unit.

Table 4-5. The thresholds for the classification of NDVI CV

Category	Range	Description
1	0≤CV≤0.05	The larger value of NDVI CV indicates a stronger fluctuation occurring in vegetation cover.
2	0.05<CV≤0.1	
3	0.1<CV≤0.15	
4	0.15<CV≤1	

4.2 The spatiotemporal characteristics of NDVI in response to climate factors

4.2.1 The pre-processing of meteorological data

Changes in either water availability or temperature might induce changes in vegetation activity (de Jong et al., 2013). For many parts of China, the water availability is determined by the amount of precipitation, water storage, and snowmelt. In this study, precipitation and temperature are regarded as two main climate factors affecting the vegetation activity in eastern China. To analyze the relationships between NDVI and precipitation as well as NDVI and temperature, the monthly precipitation and temperature data have to be processed. The monthly precipitation and temperature datasets cover 204 meteorological stations, whereas only 184 meteorological stations are adopted to generate the correlation coefficients between NDVI and precipitation as well as NDVI and temperature due to data availability. On the basis of the Microsoft

Visual Studio programming, the monthly precipitation and temperature datasets will be selected based on the identification code of the 184 meteorological stations.

In this study, the seasonal and annual temperatures are defined against the background of the mean temperature during a corresponding time period, which are acquired by applying the formulas (3) and (4), respectively, as introduced previously. However, the annual and seasonal precipitations are the amount of the accumulated precipitation over specified time periods. The calculation of seasonal precipitation (PRE_s) follows the formula below, taking the summer as an example:

$$PRE_s = (\sum_{i=6}^{8} PRE_i), i = 6,7,8 \quad (15)$$

where PRE_s is the amount of the precipitation of summer, PRE_i represents the amount of the precipitation of the month i, and i indicates the month number, ranging from 6 to 8. The accumulated precipitation in spring and autumn in each year can be computed based on the formula (15).

The accumulated annual precipitation reflects the total amount of the precipitation during an entire year, which is beneficial for plant growth and plant succession. The calculation of the accumulated annual precipitation (PRE_y) follows the formula (16):

$$PRE_y = (\sum_{i=1}^{12} PRE_i), i = 1,2,3,...,12 \quad (16)$$

where PRE_y is the amount of the annual precipitation, PRE_i is the amount of precipitation in the given month i, and i represents the number of the month, extending from 1 to 12.

Regional mean precipitation and temperature are measured as the amount of mean precipitation and the mean temperature of all meteorological stations over a specified region. The calculation of the regional mean precipitation and temperature follow the formula below, taking the regional mean temperature as an example:

$$\overline{TEM_m} = \frac{1}{N}\sum_{i=1}^{N} TEM_i, i = 1,2,3,\ldots, N \quad (17)$$

where $\overline{TEM_m}$ is the regional mean temperature, TEM_i indicates the temperature in the given meteorological station i, i ranges from 1 to N, and N is the total number of the meteorological stations within a specified region.

To explore the spatiotemporal characteristics of climate change and the spatiotemporal patterns of NDVI in response to climate variation, as shown in Table 4-5, the following datasets are acquired to achieve the objectives of this study. All of the datasets are obtained on the basis of the following formulas and platforms.

Table 4-6. Used formulas for pre-processing of precipitation and temperature with the help of Microsoft Visual Studio programming

	Dataset	Used Formula
1	Monthly Precipitation/Temperature	-
2	Seasonal Precipitation/Temperature	Based on the formula (15)/(3)
3	Annual Precipitation/Temperature	Based on the formula (16)/(4)
4	Regional Monthly Precipitation/Temperature	Based on the formula (17)
5	Regional Seasonal Precipitation/Temperature	Based on the formulas (15) and (17)/(3) and (17)
6	Regional Annual Precipitation/Temperature	Based on the formulas (16) and (17)/(4) and (17)
7	Multi-annual Monthly Mean Precipitation/Temperature	Based on the formula (5)
8	Multi-annual Seasonal Mean Precipitation/Temperature	Based on the formulas (5) and (15)/(3) and (5)
9	Multi-annual Mean Precipitation/Temperature	Based on the formulas (5) and (16)/(4) and (5)

4.2.2 The spatiotemporal characteristics of maximum NDVI response to climate factors

Climate change generates great impacts on vegetation growth in Earth's landscape ecosystems. Due to the spatial heterogeneity of ecosystems, vegetation in response to climate variation performs diverse spatial and temporal patterns and time lag effects (Wu et al., 2015). This study intends to explore the relationships between NDVI and precipitation as well as NDVI and temperature and further investigate the lag time for maximum NDVI response to precipitation and temperature on multiple spatial and temporal scales on the basis of NDVI time series, monthly precipitation dataset, as well as monthly temperature dataset.

To detect the relationships between NDVI and climate variables and investigate the lag time for maximum NDVI response to climate variables for each meteorological station (184 meteorological stations) and each administrative unit (ten administrative units and eastern China), the NDVI time series of each meteorological station and each administrative unit has to be produced. To obtain the monthly NDVI dataset of each station, the monthly NDVI dataset was downscaled to a 3 km spatial resolution NDVI dataset in ArcGIS 10.3, the module of Raster, which averaged all of the pixels value in the 3 km output pixel. Based on the geographical location of the 184 meteorological stations, the NDVI value in each 3 km × 3 km surrounding areas was then extracted to form 184 monthly NDVI time series datasets from January 2001 to December 2016. Based on the formula (6), the NDVI time series of the 11 administrative units was calculated and formed into 11 NDVI time series afterward. Above calculating processes were achieved based on ArcGIS 10.3.

The analysis of vegetation activity in response to precipitation and temperature was carried out in 3 aspects: (1) the temporal characteristics of NDVI in response to changes in precipitation and temperature, (2) the spatial patterns of NDVI in response to precipitation and temperature variation, (3) the spatiotemporal mechanisms of the lag time for maximum NDVI response to precipitation and temperature. To achieve these three objectives, particularly quantitatively investigating the maximum correlation coefficients between NDVI and precipitation as well as NDVI and temperature, the Pearson's correlation analysis is regarded as a common methodology of quantifying the strength of the relationships between NDVI and precipitation as well as NDVI and

temperature at different time lags (Kileshye Onema and Taigbenu, 2009). A t-test is further applied to test the significant statistical relationship. The correlation coefficient at different time lag periods can be computed. The formula is as follows:

$$R_{xy} = \frac{\sum_{i=1}^{n}(x_i - \bar{x})(y_i - \bar{y})}{\sqrt{\sum_{i=1}^{n}(x_i - \bar{x})^2}\sqrt{\sum_{i=1}^{n}(y_i - \bar{y})^2}} \quad (18)$$

where R_{xy} is the correlation coefficient between x and y, n represents the total number of years, i is the year number, x_i and y_i are the value of impact factors in the given year i, $\bar{x}$ and $\bar{y}$ are the mean values of impact factors during the study period. The R_{xy} ranges from 0 to 1. The larger the correlation coefficient is, the higher the correlation is.

Previous studies have demonstrated that the time lag effects of NDVI in response to changes in precipitation and temperature take place in precipitation and temperature preceding NDVI by 0 to 3 months primarily (Cui, 2010, Wu et al., 2015, Anderson et al., 2010). Considering the time lag effects of NDVI in response to precipitation and temperature variation (Braswell et al., 1997), not only the concurrent monthly precipitation and temperature are taken into account, but also the preceding precipitation and temperature of 1 to 3 months are considered to explore the relationships between NDVI and precipitation as well as NDVI and temperature in this study. Moreover, the correlation coefficients between NDVI and precipitation as well as NDVI and temperature are detected both on seasonal and annual scales. The impacts of precipitation and temperature on NDVI are expected to show finite time lags due to variability in the temporal response of NDVI to temperature and precipitation variations.

To investigate the lag time for maximum NDVI in regard to climate variables, I examined the relationships between NDVI and precipitation as well as NDVI and temperature at different time lags (0 to 3 months) by shifting temperature and precipitation series 1 month backward at a time. For instance, as shown in Table 4-6, to explore the temporal characteristic of the annual NDVI in response to changes in the temperature of previous 0 to 3 months in Beijing, the monthly NDVI dataset of Beijing from January 2001 to December 2016 was selected and formed into an NDVI time series. Similarly, the

monthly temperature from January 2001 to December 2016, December 2000 to November 2016, November 2000 to October 2016, as well as October 2000 to September 2016 in Beijing were selected and formed into four temperature time series. The correlation coefficients between NDVI and the temperature of previous 0 to 3 months were calculated on the basis of the formula (18), respectively. The maximum correlation coefficient of these four correlation coefficients was picked, which indicates the maximum response of NDVI to temperature variation in Beijing. In addition, the corresponding month of the maximum correlation coefficient determines the lag time for maximum NDVI response to temperature on annual scale in Beijing. Similarly, the response of annual NDVI to precipitation of previous 0 to 3 months and the seasonal NDVI to precipitation and temperature of previous 0 to 3 months were computed by implementing the same methods.

To reveal the spatial characteristic of NDVI in response to climate variables, the relationships between NDVI and precipitation as well as NDVI and temperature on each meteorological station are investigated. Utilizing the method, which was mentioned previously, the correlation coefficients between NDVI and the precipitation and temperature of previous 0 to 3 months of each station were computed for the whole year, spring, summer, and autumn, respectively. The maximum correlation coefficients of NDVI and precipitation as well as NDVI and temperature of each meteorological station were selected and the lag time was identified according to the corresponding month of the maximum correlation coefficient. In the background of the location of the 184 meteorological stations, the maximum correlation coefficients and its corresponding lag time of each station were displayed based on ArcGIS 10.3 platform, respectively. Thus, the lag time for maximum NDVI response to precipitation and temperature were performed both on annual and seasonal scales.

Table 4-7. Data for the calculation of the correlation coefficient between NDVI and temperature of previous 0 to 3 months on annual scale in Beijing

0-month lag				1-month lag			
Temperature[℃]		NDVI		Temperature[℃]		NDVI	
Data	Value	Data	Value	Data	Value	Data	Value
01.2001	-6.55	**01.2001**	0.191	**12.2000**	-3.6	**01.2001**	0.191
02.2001	-2.05	**02.2001**	0.184	**01.2001**	-6.55	**02.2001**	0.184
03.2001	6.35	**03.2001**	0.204	**02.2001**	-2.05	**03.2001**	0.204
...	...	**...**	...	**...**	...	**...**	...
10.2016	13.35	**10.2016**	0.372	**09.2016**	20.5	**10.2016**	0.372
11.2016	4.5	**11.2016**	0.284	**10.2016**	13.35	**11.2016**	0.284
12.2016	-3.45	**12.2016**	0.216	**11.2016**	4.5	**12.2016**	0.216
2-month lag				**3-month lag**			
Temperature[℃]		**NDVI**		**Temperature[℃]**		**NDVI**	
Data	Value	Data	Value	Data	Value	Data	Value
11.2000	4.5	**01.2001**	0.191	**10.2000**	12.3	**01.2001**	0.191
12.2000	-3.6	**02.2001**	0.184	**11.2000**	4.5	**02.2001**	0.184
01.2001	6.35	**03.2001**	0.204	**12.2000**	-3.6	**03.2001**	0.204
...	...	**...**	...	**...**	...	**...**	...
08.2016	25.45	**10.2016**	0.372	**07.2016**	27.1	**10.2016**	0.372
09.2016	20.5	**11.2016**	0.284	**08.2016**	25.45	**11.2016**	0.284
10.2016	13.35	**12.2016**	0.216	**09.2016**	20.5	**12.2016**	0.216

4.3 The spatial characteristics of annual NDVI in response to topographic factors

The three primary topographic factors (*e.g.,* elevation, aspect, and slope) affect the spatial pattern of the vegetation activity by controlling the solar radiation and microclimate (Mokarram and Sathyamoorthy, 2015, Allen and Peet, 1990). Elevation is considered to be the most important topographic factor. The synergistic effects of elevation-aspect and elevation-slope determine the vertical structure of the vegetation biomass (Busing and White, 1993). To explore the spatial interaction between the annual

NDVI and topographic factors, the three topographic factors such as elevation, aspect, and slope, have to be acquired on the basis of the DEM data.

The DEM tiles, covering the study area, were merged and reformatted into GeoTIFF format and then reprojected into the projection of WGS_1984_UTM_Zone_50N under the support of ArcGIS 10.3. Elevation is derived from the DEM dataset. To illustrate the spatial interplay between the annual NDVI and elevation and to statistically analyze the vertical annual NDVI variation along with the elevation increase, the elevation was categorized into seven classes using ArcGIS 10.3, the module of Reclass (Table 4-8). The proportion of each elevation range was acquired on the basis of the zonal statistic.

Table 4-8. The thresholds for the classification of the elevation

Category	Range [m]	Percentage	Description
1	-282≤ Elevation ≤0	2%	The elevation is the most important topographic factors dominating the vertical distribution of vegetation by affecting water availability and temperature.
2	0< Elevation ≤100	45%	
3	100< Elevation ≤200	11%	
4	200< Elevation ≤300	8%	
5	300< Elevation ≤400	7%	
6	400< Elevation ≤500	6%	
7	500≤ Elevation ≤2849	21%	

The two significant features of Earth's land surface are aspect and slope. They play important roles in the processes of surface morphology evolution, self-organizing ecological restoration, and soil erosion (Prasannakumar et al., 2011). Aspects reflect the direction of the slopes, which face a certain area. Aspects are expressed by degrees from the north, a clockwise direction forming an entire circle, ranging from -1° to 360° (Bennie et al., 2008). The aspect-value of -1° indicates the flat areas. Aspect data is derived from the DEM data with the aid of ArcGIS 10.3, the module of Raster Surface Analysis. Differences in the NDVI values on the NFS and SFS are analyzed in this study. NFS corresponds to slope directions to the northwest (292.5° to 337.5°), north (337.5° to 22.5°), and northeast (22.5° to 67.5°). SFS consists of slope directions of the southwest (202.5° to 247.5°), south (157.5° to 202.5°), and southeast (112.5° to 157.5°) (Toro

Guerrero et al., 2016) (Table 4-9). Areas on the NFS account for 29% of the study area and areas on the SFS occupy 37% of the study area. Figure 4-9 displays the spatial pattern of the NFS and SFS. In addition, the flat (-1°), EFS (67.5° to 112.5°), and WFS (247.5° to 292.5°) were not adopted into this study.

Table 4-9. The thresholds for the classification of the aspects

Category	Aspect	Range [°]	Percentage	Description
1	NFS	Northeast (22.5°–67.5°)	29%	The NFS and SFS affect vegetation activity by accepting unbalanced solar radiation and sunshine duration.
		North (337.5°–22.5°)		
		Northwest (292.5°–337.5°)		
2	SFS	Southeast (112.5°–157.5°)	37%	
		South (157.5°–202.5°)		
		Southwest (202.5°–247.5°)		

A slope angle is an essential factor in determining the steepness of slopes. In this study, the slope data is derived from the DEM data extension from 0° to 90° based on ArcGIS 10.3 platform, the module of Raster Surface Analysis. Human disturbances and agricultural activities are particularly intense within the areas with slope degree ranging from 0 to 15°, and the areas with slope degree ranging from 15 to 25° are appropriate for forest succession and restoration. To statistically analyze the spatial mechanism of the dynamic NDVI change at different slope ranges, as shown in Table 4-9, the slopes were categorized into five classes using ArcGIS 10.3 platform, the module of Reclass. Figure 4-10 illustrates the spatial pattern of the slopes. Table 4-10 shows that the proportion of the slope ranges decreases with slope degree increase.

Table 4-10. The thresholds for the classification of the slopes

Category	Range [°]	Percentage	Description
1	0°≤ Slope ≤2°	30%	The larger the value of the slope is, the steeper is the slope. The frequency of human disturbances and agricultural activities decrease as the degree of a slope angle increases.
2	2°< Slope ≤6°	25%	
3	6°< Slope ≤15°	18%	
4	15°< Slope ≤25°	17%	
5	25°< Slope ≤90°	11%	

In this study, three vegetation metrics (*e.g.,* annual NDVI, annual NDVI changing slope, and annual NDVI CV) are utilized to explain the dynamic change of vegetation cover. The topographical factors affect the geographical distribution of NDVI by interplay with vegetation activity. The three topographic factors do not drive NDVI in similar ways, potentially performing synergistic associations when driving vegetation activity. To display the spatial pattern of the annual NDVI in different categories of the elevation, aspect, and slope ranges, the datasets of elevation, aspect, and slope are adopted to be overlapped on the three vegetation metrics, respectively (Zhang et al., 2015). For instance, the annual NDVI was extracted on the basis of the reclassified elevation, aspect, and slope datasets not only to display the spatial dynamic of the annual NDVI along with the elevation, aspect, and slope gradient, but also to statistically analyze the changing characteristics of the annual NDVI in terms of in different categories of elevation, aspect, and slope ranges. Theoretically, on the basis of the above methods, the spatial interaction between the three vegetation metrics (*e.g.,* annual NDVI, annual NDVI changing slope, and annual NDVI CV) and the three topographic factors (*e.g.,* elevation, aspect, and slope) was illustrated, and then their quantitative relationships were determined, respectively.

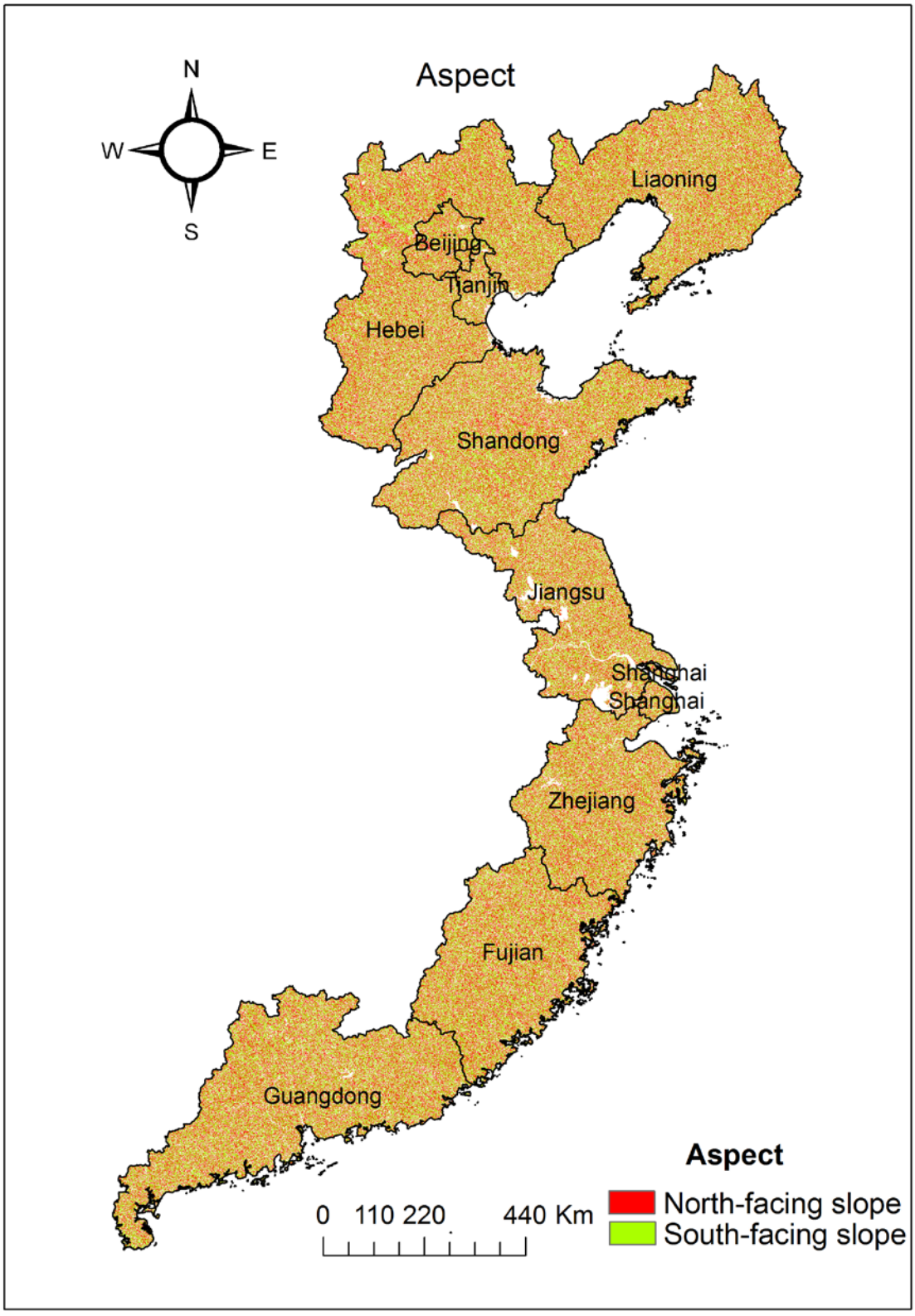

Figure 4-9. The spatial pattern of aspect in eastern China

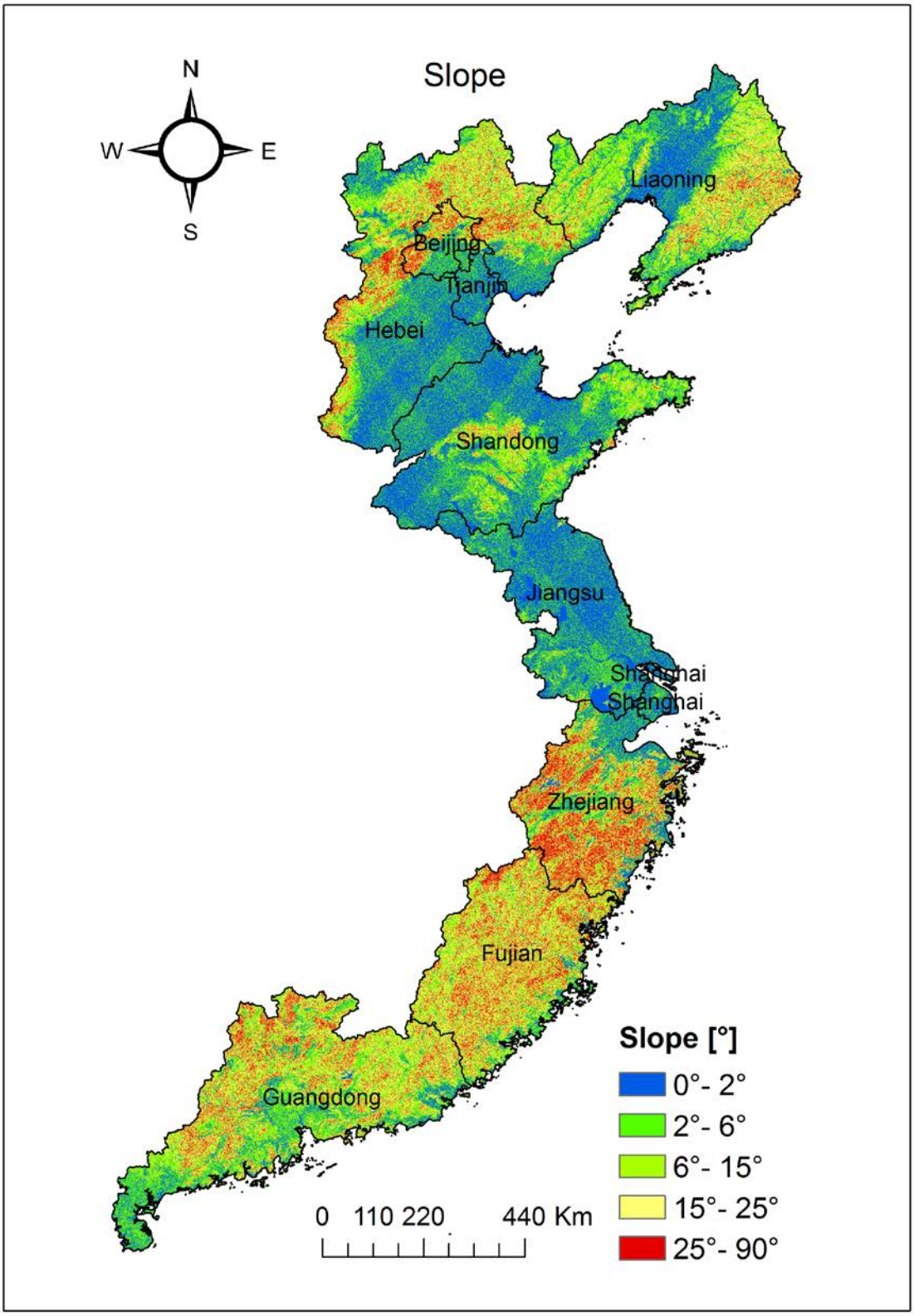

Figure 4-10. The spatial pattern of slope in eastern China

4.4 The spatiotemporal characteristics of annual NDVI in response to socio-economic factors

Along with the accelerating process of urbanization and industrialization, the economic status has been promoted significantly, which resulted in vegetation deterioration and environmental exacerbation in many parts of the world, particularly in developing countries (Dewan and Yamaguchi, 2009). In this study, the 13 socio-economic factors are regarded as the socio-economic forces and categorized into three classes: general economic vitality, including GDP, primary industry product, secondary industry product, tertiary industry product, total investment in fixed assets, and PCGDP; household consumption, covering household consumption, rural household consumption, and urban household consumption; and human population, encompassing total population, total employment, population density, and urbanization. These socio-economic factors are utilized to indicate economic development, urban expansion, and population growth in eastern China.

To explore the relationships between annual NDVI and the 13 socio-economic factors on temporal scale, a 16-data-long (each year a data) time series of each socio-economic factor in each administrative unit was formed. Meanwhile, based on the formulas (4) and (6), annual NDVI in each administrative unit was computed and then formed a 16-data-long dataset. On the basis of the datasets of the annual NDVI and the 13 socio-economic factors, Pearson's correlation coefficient was implemented to quantify the strength of the relationships between annual NDVI and the 13 socio-economic factors.

Scholars have demonstrated that negative impacts of urbanization on NDVI have gradually declined from urban centers toward rural areas, particularly in metropolitan areas (Zhou et al., 2016, Zhou et al., 2014, Dewan and Yamaguchi, 2009). To observe how the spatial feedback mechanism of NDVI reacts to urban expansion from urban centers toward marginal urban areas, the urban areas were categorized into two types: old urban areas and new urban areas. Old urban areas are defined in the background of the conditions before 2001. As new developments have taken place, the urban areas which were generated from 2001 to 2015 were considered to be the new urban areas in this study. Furthermore, the urban areas in 2000 and 2015 were merged together to

produce merged urban areas. Based on the merged urban areas, a set of buffers extending outward from 0 to 5 km, 5 to 10 km, and 10 to 15 km from the urban edge was created (Figure 4-11(a)), respectively, to observe the spatial mechanism of vegetation cover change in the marginal urban areas.

In this study, the three vegetation metrics (*e.g.,* annual NDVI, annual NDVI changing slope, and annual NDVI CV) in the old urban areas, new urban areas, and the three surrounding buffer areas were extracted to illustrate the spatial interaction of vegetation change to each corresponding area. The statistical data of the three vegetation metrics in each corresponding area was adopted to quantitatively and comparably analyze the magnitude of the NDVI cover change and vegetation stability extension from the urban centers toward the surrounding areas. The above data processing steps were accomplished under the support of ArcGIS 10.3, based on different functioning modules.

Economic development and population growth are projected to promote rapid changes in vegetation activity and increase spatial heterogeneity in vegetation cover. GDP is a surrogate for the economic performance of a specified region. Population density indicates the potential frequency of human activities in a community. The GDP and population density map are available both in 2000 and 2015 with a 1 km spatial resolution. These four maps were utilized to detect the spatial coupling between economic development and population growth and vegetation variation.

For example, the GDP maps of 2000 and 2015 were used to generate a GDP difference map from 2000 to 2015 (Figure 4-11(b)), which illustrates the differences of the spatial distribution of the economic development in eastern China. This GDP difference map is quantified by the Chinese currency (RMB). The GDP difference map was categorized into five classes. Then the reclassified GDP difference map was overlapped on the three vegetation metric maps to exhibit the spatial characteristics of NDVI change in response to GDP variation. The annual NDVI, annual NDVI changing slope, and annual NDVI CV in each GDP category were extracted, respectively. The corresponding statistical data of the three vegetation metrics in each GDP difference category was further generated. Using the above all methods, the spatial characteristics of the three vegetation metrics with regard to population growth were performed.

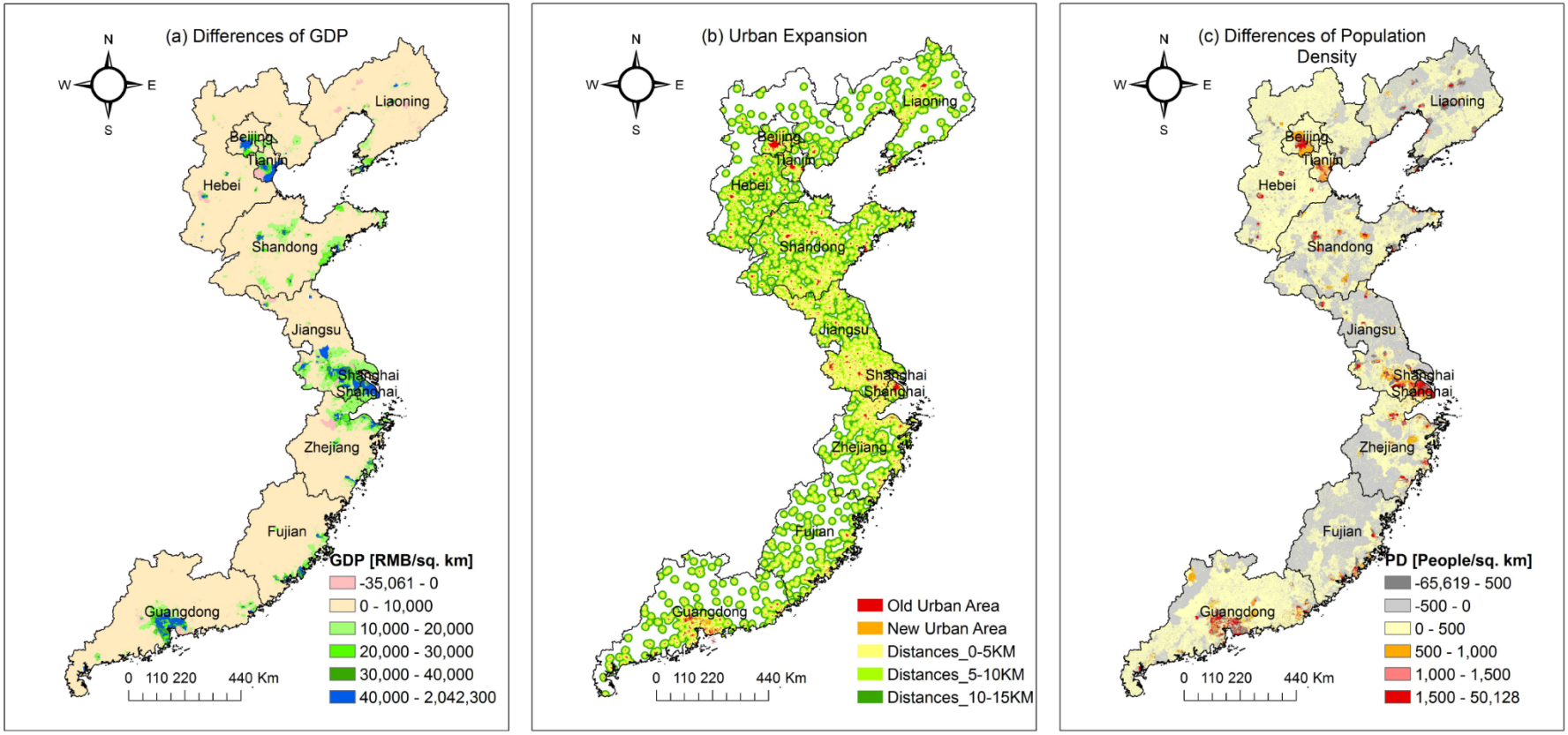

Figure 4-11. Spatial distribution of the differences in socio-economic development, urban expansion, and population growth in eastern China from 2000 to 201

5 Results and discussion

In the former chapters, the objective, theoretical background, and methodology of this study are introduced. To provide a better understanding of NDVI in response to climate factors, topographic factors, as well as socio-economic factors, the mathematical methods are employed to carry out the objectives of this study on the basis of the MODIS NDVI data, meteorological data, DEM data, socio-economic data, as well as other raster and vector data. This chapter, which consists of 4 sections, presents and discusses the main findings of this study. Section 5.1 exhibits the spatiotemporal variation of NDVI both on annual and seasonal scales. Section 5.2 presents the relationships between NDVI and climate factors and the lag time for maximum NDVI response to changes in climate factors. Section 5.3 displays the spatial interaction between annual NDVI and topographic factors. Section 5.4 shows the impacts of socio-economic development, urban expansion, and population growth on vegetation cover change both on spatial and temporal scales.

5.1 The spatiotemporal variation of vegetation cover in eastern China

5.1.1 The temporal variation of NDVI

5.1.1.1 The temporal variation of monthly NDVI

On the basis of the 16-year (2001 to 2016) regional average monthly NDVI, the monthly patterns of the NDVI variations of the ten administrative units and the entire study area are shown in Figure 5-1, indicating the dynamic changes of average vegetation productivity from January to December over eastern China. These patterns are against the background of the average monthly values of all NDVI pixels in each corresponding administrative unit. Each point represents the monthly climatological average from 2001 to 2016. Figure 5-1 reflects the dynamic changes of monthly NDVI from January to December in the ten administrative units and the entire study area. The monthly NDVI value ranges from 0.376 to 0.741 over the study area, and the maximum and minimum NDVI values take place in January and July, respectively.

The trends of the monthly NDVI in Liaoning, Beijing, Tianjin, Hebei, and Shandong follow each other fairly well, presenting that a monotonic upward trend occurs from January

toward July and then the NDVI value decreases steadily from July toward December, but differ remarkably in amplitude. However, the monthly NDVI in Jiangsu, Shanghai, Zhejiang, Fujian, and Guangdong increases continually and reaches a peak in August, then the increasing trend reverses and presents a steady downward trend afterward.

It is worth mentioning that the monthly NDVI in Jiangsu exhibits a downward trend from April to June and then increases from June to August, which is caused by a unique crop rotation system in Jiangsu. The agriculture activity in Jiangsu is dominated by winter wheat/paddy rice and rapeseed/paddy rice double cropping rotation. The winter wheat and rapeseed crops are harvested in late May and early June, which result in dropping in NDVI value in May and June immediately. Soon, the farmlands are irrigated, plowed, and then transplanted by paddy rice. The NDVI value in these areas enhances fairly with the rice growth within a short period of time (Xiao et al., 2010). Above explanation demonstrates why the NDVI value presents a valley in June in Jiangsu.

The maximum NDVI value of each administrative unit is generally greater than 0.7, particularly in Fujian, the maximum NDVI value reaches 0.791 in August. Exceptionally, the maximum NDVI value in Tianjin appears in July, which is only 0.635. The minimum NDVI value in Beijing, Tianjin, Fujian, and Guangzhou exhibits in February. Apart from that, the minimum NDVI value in other administrative units presents in January. The minimum NDVI value is only 0.160 in Tianjin, while it reaches 0.633 in Fujian. In addition, the monthly NDVI value from January to December is significantly higher in Zhejiang, Fujian, and Guangdong than in other administrative units for the corresponding period. Furthermore, the amplitude of the monthly NDVI value is obviously weaker in these three administrative units than in other administrative units. The maximum amplitude of the monthly NDVI value takes place in Liaoning with an interval of 0.607, and the minimum amplitude of the monthly NDVI value takes place in Fujian with an interval of 0.157.

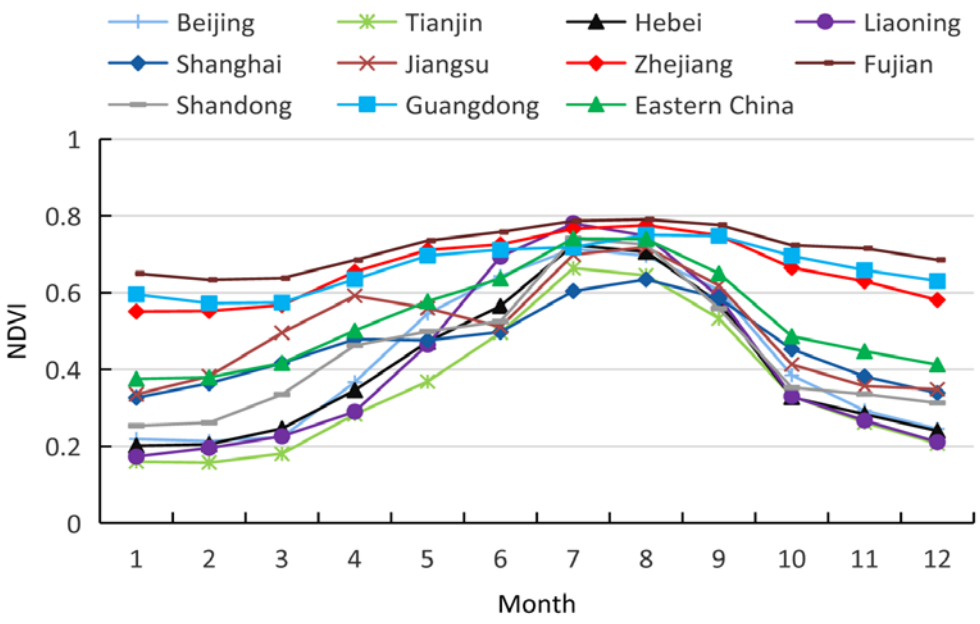

Figure 5-1. The temporal variation of regional monthly NDVI

5.1.1.2 The temporal variation of annual NDVI

The variations of the annual and seasonal NDVI in eastern China, covering the ten administrative units, from 2001 to 2016 were computed to illustrate the dynamic change of vegetation cover over eastern China for the study period. Each point relates to a mean NDVI value measured on the basis of the values of all the pixels located in the corresponding administrative unit. Against the background of the linear regression analysis method, the temporal variation of the NDVI for different administrative units is shown in Figure 5-2 and Table 5-1. The annual NDVI shows a slightly increasing trend with a changing value of 0.0003 year^{-1} in eastern China. The maximum NDVI value takes place in 2014 with a magnitude of 0.543, and the minimum NDVI value shows in 2001 and 2015, exhibiting a 0.024 difference to the maximum NDVI value.

Considering the temporal variation of the annual NDVI in each administrative unit, from Figure 5-3 and Table 5-1, it can be seen that the annual NDVI in different administrative units presents distinct increasing and decreasing trends. More specifically, the annual NDVI exhibits increasing trends in Beijing, Hebei, Liaoning, and Shandong but decreasing trends in Tianjin, Shanghai, Jiangsu, Zhejiang, Fujian, and Guangdong. It is worth noticing that the magnitude of the increasing trends is slightly larger in Beijing,

Hebei, and Liaoning than in Shandong. Particularly, the magnitude of the absolute changing slope values is 0.0036 $year^{-1}$ in Shanghai and 0.0031 $year^{-1}$ in Jiangsu, implying that the vegetation cover had remarkably decreased in Shanghai and Jiangsu for the study period.

5.1.1.3 The temporal variation of seasonal NDVI

The maximum NDVI value appears both in 2014 with a magnitude of 0.519 in spring and 0.542 in autumn, respectively, whereas the NDVI value ranges from 0.675 in 2015 and 0.716 in 2013 in summer. Generally, the NDVI value is higher in summer than in autumn, followed by in spring in eastern China, except that the NDVI value in 2002 is slightly lower in autumn than in spring. In terms of the NDVI changing trend in eastern China on seasonal scale, Figure 5-2 and Table 5-1 show that the NDVI value presents an upward trend in spring and autumn but a downward trend in summer. The magnitude of the changing trend is largely greater in summer (-0.0013 $year^{-1}$) than in spring (+0.0003 $year^{-1}$) but almost the same as in autumn (+0.0012 $year^{-1}$), indicating that the dynamic change of vegetation cover is significantly stronger in summer and autumn than in spring. This result is not fully in line with the results distributed by Piao et al. (2003). Piao et al. (2003) investigated the seasonal NDVI changing trend over China and demonstrated that NDVI increased in all season, with an increasing changing trend of 0.0018 $year^{-1}$ in spring, 0.0012 $year^{-1}$ in summer, and 0.0009 $year^{-1}$ in autumn，respectively (Piao et al., 2003).

The opposite changing trend in summer between Piao et al. (2003) and our study might be caused by the differences of the data source, study period, as well as the study area. Piao et al. (2003) focused on monitoring the vegetation changing trend from 1982 to 1999 over China on the basis of GIMMS NDVI with an 8 km spatial resolution, but we detected the dynamic change of vegetation cover in eastern China based on MODIS NDVI with a 250 m spatial resolution. On the one hand, the NDVI data derived from MODIS is recognized to be a more precise and robust data source to assess the long-term vegetation trends than GIMMS NDVI data. On the other hand, eastern China is a highly developed region in China, the socio-economic status, urbanization rate, and population density are much higher than in other regions of China, particularly in the 21st

century, which is at the cost of local ecological deterioration and vegetation degradation. The explanations provided above answer why the vegetation changing trend in summer in our study is not in line with the result generated by Piao et al. (2003).

Furthermore, many scholars have demonstrated that the length of the growing season has profoundly extended in the northern hemisphere (Linderholm, 2006, Myneni et al., 1997, Karlsen et al., 2008). Eastern China is located in the mid- to the high-latitudes northern hemisphere. The NDVI value in eastern China had experienced an increasing trend in spring and autumn during the study period. This result is highly in line with previous studies. The growing season extension is attributed to the advance in the start of the growing season in spring and prolonged the growing season in autumn for these areas (Parmesan and Yohe, 2003, Gill et al., 2015).

NDVI exhibits seasonal variation for each administrative unit distinctly. Regarding the temporal variation of the seasonal NDVI in each administrative unit, Figure 5-3 and Table 5-1 show that the NDVI in spring presents an increasing trend in Beijing, Tianjin, Hebei, Liaoning, and Shandong, while an opponent changing trend is observed in Shanghai, Jiangsu, Zhejiang, Fujian, and Guangdong. The magnitude of the increasing trend is slightly higher in Beijing (0.0039 $year^{-1}$) than in Hebei, Liaoning, and Shandong but considerably higher than in Tianjin. The magnitude of the decreasing trend is double or even triple higher in Shanghai than in Jiangsu, Zhejiang, Fujian, and Guangdong, indicating that a more serious vegetation degradation had swept most parts of Shanghai and reduced the vegetation activities consequently from 2001 to 2016.

Results of the NDVI change for each administrative unit in summer are given in Figure 5-3 and Table 5-1. In summer, the NDVI in Beijing, Hebei, and Liaoning shows an upward trend, while the magnitude of the increasing trend is triple higher in Liaoning than in the two former administrative units. The magnitude of the decreasing trend of the NDVI is remarkably stronger in Shanghai and Jiangsu than in Tianjin, Zhejiang, Fujian, Shandong, and Guangdong. Especially, the magnitude of the decreasing trend reaches 0.0075 $year^{-1}$ in Jiangsu, implying that an even more critical vegetation deterioration had happened in Jiangsu for summer from 2001 to 2016.

The number of the administrative units experienced a vegetation browning trend is less in autumn (three administrative units) than in spring (five administrative units) and summer (seven administrative units). In autumn, the decreasing trends in Zhejiang and Guangdong can be neglected. The increasing rate of NDVI in autumn reaches 0.0046 $year^{-1}$ in Beijing, while the magnitude of the changing trend in Shandong, Hebei, Liaoning, Fujian Tianjin, and Jiangsu gradually increases from -0.0024 $year^{-1}$ to less than -0.00001 $year^{-1}$ (Figure 5-3 and Table 5-1).

Combining the view of the seasonal NDVI in the ten administrative units, Figure 5-3 shows that the NDVI is generally higher in summer than in autumn, followed by in spring. Particularly noteworthy point is that the NDVI in Jiangsu is obviously higher in spring than in autumn (Figure 5-3(f)), and the NDVI in spring and autumn in Shandong is interlaced (Figure 5-3(i)). This phenomenon in Jiangsu and Zhejiang is caused by crop harvesting taking place in later October in Jiangsu and Shandong (Xiao et al., 2010). Crop harvesting results in vegetation cover decrease over vast farmlands. It is worth notifying that the maximum NDVI in spring, summer, and autumn occurs in Fujian with a magnitude of 0.703, 0.790, and 0.754, respectively (Figure 5-3(h)), suggesting a superior vegetation cover and a more stable vegetation activity in Fujian than in other administrative units.

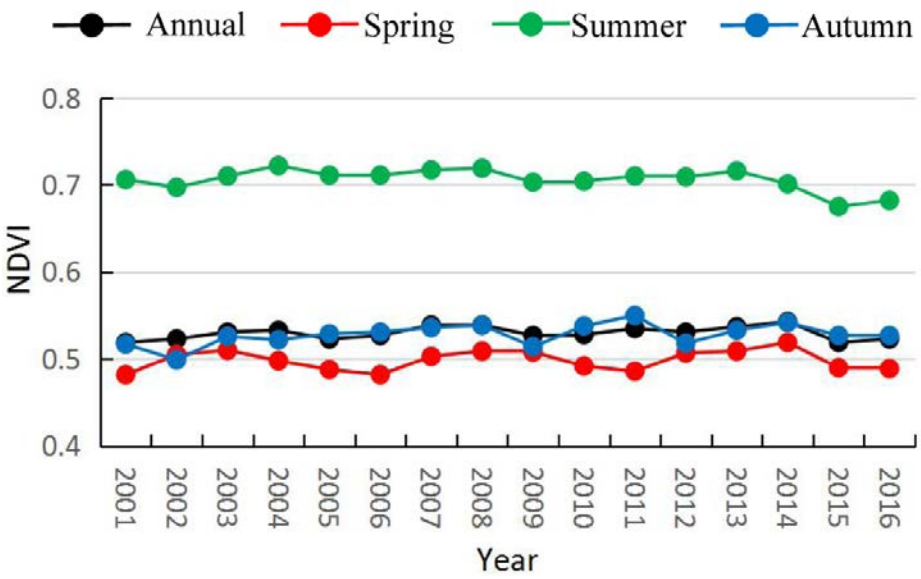

Figure 5-2. The temporal variation of annual and seasonal NDVI from 2001 to 2016 for eastern China

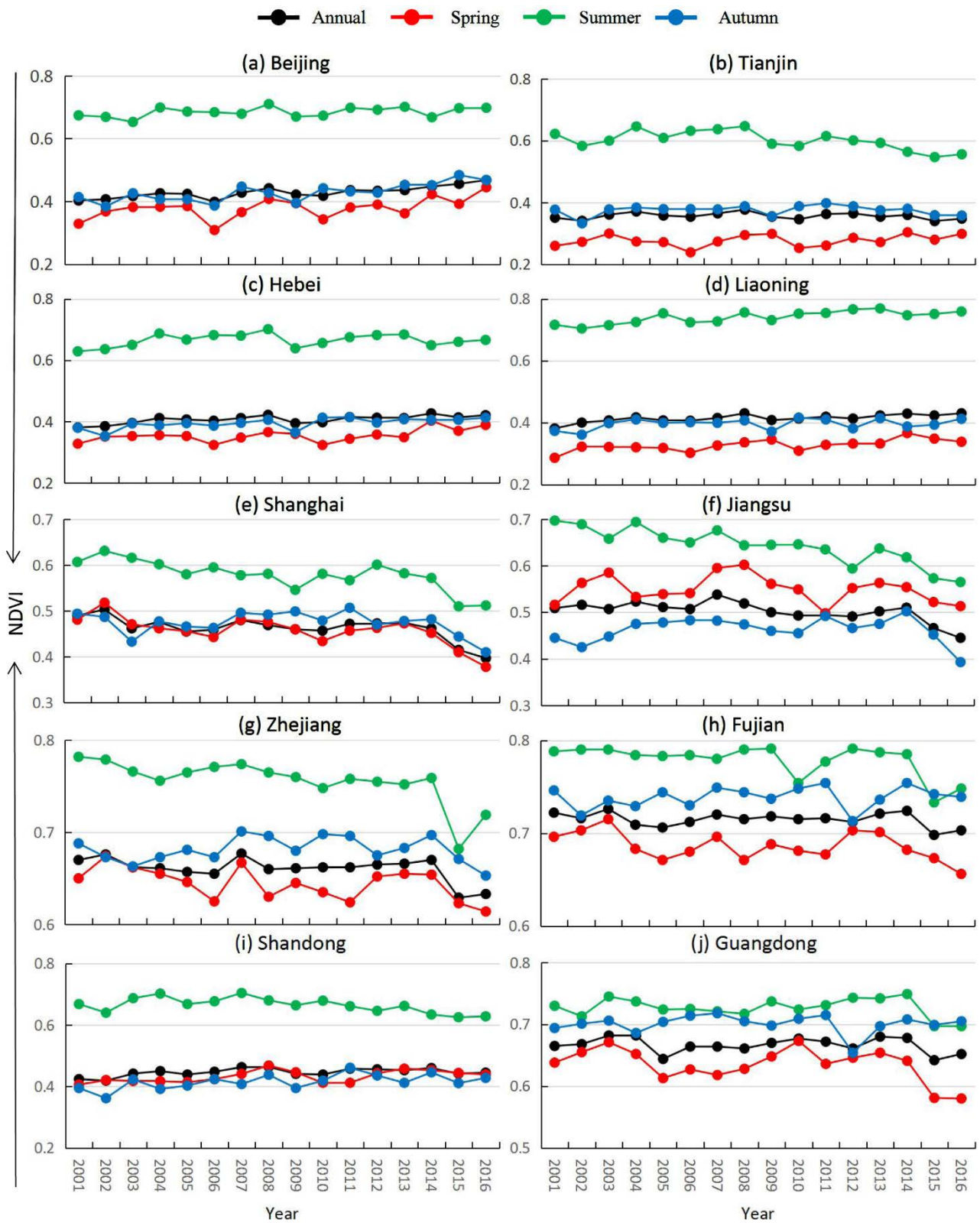

Figure 5-3. The temporal variation of annual and seasonal NDVI in ten administrative units from 2001 to 2016

Table 5-1. The equation and R-squared value of annual and seasonal NDVI of eastern China and ten administrative units (Unit: year^{-1})

Administrative unit	The equation and R-squared value of annual and seasonal NDVI			
	Annual	Spring	Summer	Autumn
Beijing	y = 0.0033x + 0.4009 R^2 = 0.6995	y = 0.0039x + 0.3459 R^2 = 0.2985	y = 0.0014x + 0.6724 R^2 = 0.1835	y = 0.0046x + 0.3891 R^2 = 0.5877
Tianjin	y = -0.0003x + 0.3594 R^2 = 0.0199	y = 0.0013x + 0.2669 R^2 = 0.1008	y = -0.004x + 0.6352 R^2 = 0.374	y = 0.0002x + 0.373 R^2 = 0.0043
Hebei	y = 0.002x + 0.3902 R^2 = 0.5228	y = 0.0025x + 0.3334 R^2 = 0.3184	y = 0.0011x + 0.6556 R^2 = 0.0667	y = 0.0024x + 0.3744 R^2 = 0.4416
Liaoning	y = 0.0021x + 0.3962 R^2 = 0.6036	y = 0.0028x + 0.303 R^2 = 0.4988	y = 0.0034x + 0.7119 R^2 = 0.6416	y = 0.0013x + 0.3851 R^2 = 0.1255
Shanghai	y = -0.0036x + 0.4933 R^2 = 0.4431	y = -0.0046x + 0.4959 R^2 = 0.4715	y = -0.0054x + 0.6248 R^2 = 0.5974	y = -0.0016x + 0.4869 R^2 = 0.083
Jiangsu	y = -0.0031x + 0.5285 R^2 = 0.456	y = -0.0014x + 0.561 R^2 = 0.0516	y = -0.0075x + 0.7059 R^2 = 0.8066	y = 5E-05x + 0.4624 R^2 = 7E-05
Zhejiang	y = -0.0015x + 0.6727 R^2 = 0.2812	y = -0.002x + 0.6611 R^2 = 0.2864	y = -0.0037x + 0.7874 R^2 = 0.5276	y = -6E-05x + 0.6818 R^2 = 0.0004
Fujian	y = -0.0006x + 0.7194 R^2 = 0.1215	y = -0.0015x + 0.6986 R^2 = 0.2122	y = -0.0021x + 0.7963 R^2 = 0.3246	y = 0.0005x + 0.7342 R^2 = 0.0468
Shandong	y = 0.0013x + 0.435 R^2 = 0.2464	y = 0.0023x + 0.4125 R^2 = 0.3402	y = -0.003x + 0.6899 R^2 = 0.3522	y = 0.0029x + 0.3912 R^2 = 0.3275
Guangdong	y = -0.0006x + 0.6712 R^2 = 0.0473	y = -0.0025x + 0.6561 R^2 = 0.1902	y = -0.0006x + 0.7323 R^2 = 0.0357	y = -0.0002x + 0.7023 R^2 = 0.0031
Eastern China	y = 0.0003x + 0.527 R^2 = 0.0458	y = 0.0003x + 0.4957 R^2 = 0.0188	y = -0.0013x + 0.7167 R^2 = 0.2342	y = 0.0012x + 0.5182 R^2 = 0.1985

5.1.2 The spatial pattern of vegetation cover

5.1.2.1 The spatial pattern of annual NDVI

Mean NDVI is a simple graphical indicator, which can be used to reflect the general spatial characteristics of vegetation vitality and to estimate the overall above-ground vegetation biomass over a certain region during a corresponding period of time. In this study, the multi-year mean annual NDVI from 2001 to 2016 is utilized to monitor the spatial heterogeneities of the vegetation cover over eastern China. The NDVI values are divided into five classes: 0 to 0.2, 0.2 to 0.4, 0.4 to 0.6, 0.6 to 0.8, and 0.8 to 1. Higher NDVI value indicates a higher possible density of green leaves, and lower NDVI value represents a sparse vegetation cover or even no vegetation over a specified region. In this study, the annual NDVI displays a distinct and uneven spatial distribution over eastern China (Figure 5-5(a)). The proportion of each category of the annual NDVI for each administrative unit is computed against the background of the map of the mean annual NDVI and the administrative map. Figure 5-4(a) provides the proportion of the mean annual NDVI value in each category for eastern China and the ten administrative units.

From Figure 5-5(a), it can be seen that the mean annual NDVI exhibits a clear spatial differentiation in eastern China, showing a gradient decline from the south to the north of the study area. Areas with high NDVI values are mainly located in Zhejiang, Fujian, and Guangdong, while areas distributed in the west of Liaoning, east of Beijing, Tianjin, Hebei, and Shanghai are dominated by low NDVI values. Most of the areas with moderate NDVI values are distributed in Jiangsu, a place regarded to be a transitional zone of the southern part of eastern China to the northern part. In other words, the NDVI value is converted from high NDVI value to low NDVI value, and the NDVI values in Jiangsu are in between the two areas. Moreover, the NDVI values are significantly lower in the center of the Pearl River Delta and Yangtze River Delta than its surrounding areas.

The spatial pattern of the annual NDVI is closely correlated with the land use types. The land use type in Zhejiang, Fujian, and Guangdong is largely characterized as forest land dominated by evergreen broadleaf forest. NDVI values are therefore remarkably higher in these three administrative units than in other administrative units. Figure 5-4(a) shows

that the annual NDVI values from 0.6 to 1 accounts for 88% in Fujian, 71% in Zhejiang, and 77% in Guangdong, respectively, which is significantly higher than in other administrative units.

The main terrestrial land use type in Jiangsu is farmland (Xiao et al., 2010). The annual NDVI in this region is dominated by moderate NDVI values, ranging from 0.4 to 0.6, which takes 67% of the total corresponding area. Additionally, the land use and land cover types in the east of Liaoning are monopolized by temperate coniferous-broadleaved mixed forests, deciduous broadleaf forests, and woods and shrubs, whereas the land use and land cover types in the west of Liaoning are mostly possessed by typical and desert steppes. The farmland and meadow steppes are distributed in the middle of Liaoning (Gao and Yu, 1998, Wang et al., 2015a, Wang et al., 2017a). Due to the distinct spatial pattern of the land use types in Liaoning, the NDVI values in the east of Liaoning are greater than in the west part, and the lowest NDVI value is presented in the middle part. Figure 5-4(a) shows that the proportion of the NDVI values ranging from 0 to 0.4 accounts for 36% in Beijing, 62% in Tianjin, 44% in Hebei, and 53% in Liaoning, separately, which is far above the average level for the entire study area (24%). It is worth noticing that all of these four above administrative units are located in the Bohai Economic Rim, a place with a highly developed socio-economic status. In addition, the pace of urbanization and industrialization has been accelerated since 1978 when the program of reform and opening-up put into action in China (Qu et al., 2015, Zhou et al., 2014, Zhou et al., 2016).

5.1.2.2 The spatial pattern of seasonal NDVI

Multi-year mean seasonal NDVI can reflect the spatial features of the regional vegetation cover for each season. The distribution pattern of the mean NDVI in spring, summer, and autumn display noticeable spatial discrepancy in eastern China from 2001 to 2016 (Figure 5-5(b) and Figure 5-6(a) and (b)). In terms of the NDVI value in spring, Figure 5-5(b) shows that the NDVI values from Guangdong toward Jiangsu are incontestably higher than in other administrative units, particularly in Tianjin, the middle of Shandong, as well as in the west of Hebei and Liaoning. Overall, the NDVI values ranging from 0 to 0.4 account for 34% of the study area in spring, which takes one-third of the study area,

and the proportion is greater than in summer and autumn. Moreover, the proportion of the NDVI values spanning from 0.8 to 1 takes only 1% of the study area.

Inspection of the NDVI value in each category in spring for each administrative unit, results are given in Figure 5-4(b), a homologous phenomenon is observed that the proportion of the NDVI values ranging from 0.6 to 0.8 is larger in Fujian (71%), Zhejiang (65%), and Guangdong (69%) than in other administrative units. In particular, more than 95% of the NDVI values in Beijing, Tianjin, Hebei, Liaoning, and Shanghai are lower than 0.6, indicating that a lower vegetation density spreads in these five administrative units. In addition, the NDVI values ranging from 0.2 to 0.4 in Beijing, Tianjin, Hebei, and Liaoning account for more than 50% of the corresponding areas, especially this proportion reaches 66% in Tianjin.

The vegetation cover situation dramatically upgraded in summer (Figure 5-5(b)). The best vegetation cover displays in Zhejiang, Fujian, Guangdong, the east of Liaoning, and the north of Hebei. However, the vegetation cover is relatively poor in the west of Hebei, Shanghai, and the coastal areas of Guangdong, where the NDVI values are significantly lower than the surrounding areas. As detailed in Figure 5-4(c) that the proportion of the NDVI values ranging from 0.6 to 0.8, and from 0.8 to1 accounts for 59% and 26% of the study area, respectively. In addition, the magnitude of the NDVI values ranging from 0 to 0.4 occupies only 3% of the study area. The conclusions provided above suggest a considerable high vegetation cover in summer in eastern China. Comparing to Figure 5-4(b) and (c) shows that the vegetation vitality in the ten administrative units has considerably improved from spring to summer. For instance, the proportion of the NDVI values ranging from 0.6 to 1 increased by 75% in Beijing, 64% in Tianjin, 71% in Hebei, and 90%, respectively, in Liaoning from spring to summer.

The spatial distribution of multi-year mean NDVI in autumn is shown in Figure 5-6(b). The vegetation cover markedly and gradually reduces from the south of Guangdong to the north of Liaoning, and the NDVI value reaches the lowest value in the north of Hebei and Liaoning. Comparison of the vegetation cover in the north of eastern China (the east of Liaoning and north of Hebei) and the south of eastern China (Zhejiang, Fujian, and Guangdong) in summer and autumn, the NDVI values in the north of eastern China are

dramatically declined. This phenomenon can be ascribed to the structure of the local vegetation types and the related features of plant growth behavior.

Figure 5-4(d) shows that the vegetation cover in eastern China is dominated by moderate vegetation cover. Areas with the NDVI value ranging from 0.4 to 0.6 occupy 41% of the study area. Comparing to the Figure 5-4(c) and (d) suggests that the proportion of the high NDVI values (from 0.6 to 1) rapidly decreased from summer to autumn in seven of the ten administrative units, except for Zhejiang, Fujian, and Guangdong presenting a slight decrease. Figure 5-4(b) and (d) show that the proportion of the NDVI values in each category for Beijing, Tianjin, Hebei, Liaoning, and Shanghai is homologous, but the proportion of the NDVI values ranging from 0.6 to 1 in Shandong and Jiangsu in spring exceeds by 68% and 44% in autumn, respectively, suggesting a better vegetation situation in autumn in Shandong and Jiangsu than in spring, which can be explained by the harvest activities in autumn in these regions.

The spatial patterns of vegetation cover in spring, summer, and autumn follow the same pattern: namely, the NDVI value is higher in the east of Liaoning, northwest of Hebei, Zhejiang, Fujian, as well as in Guangdong than in other regions of the study area (Figure 5-4(b), (c), and (d)). The most intensive variation of vegetation activity appears in the west of Liaoning, north of Hebei, middle of Shandong, and entire Jiangsu. The vegetation cover shows unique seasonal characteristics in these regions, which are different from other parts of the study area. Above results are generated by the combined effects of local climate systems, topographic forces, as well as intensive human intervention.

Generally, the overall NDVI values in summer are higher than in autumn, followed by spring. The vegetation cover displays a significant downward trend from the south to the north of eastern China in all seasons with the exception of the NDVI values in Jiangsu and the west part of Shandong where the NDVI values in spring are noticeably larger than in autumn. This phenomenon is attributed to the land use types and the agriculture rotation system in Jiangsu and Shandong (Xiao et al., 2010). The vegetation cover in Jiangsu and Shandong is dominated by agricultural plants, which are significantly influenced by effective man-management during the processes of crop sowing, growing to harvesting. The rapeseed and winter wheat are harvested from the second half of May

to early June (spring), then the farmlands are plowed and flooded, and then replanted to paddy rice and spring wheat. Therefore, a downward trend of NDVI value can be found from May to June but increases in July in Jiangsu at once. In addition, the spring wheat and paddy rice harvesting take place from early September to late October (autumn), resulting in a decline in NDVI values instantly in Jiangsu and Shandong (Hu et al., 2017, Huang et al., 2012). The explanation provided above answers the question of why the NDVI values in Jiangsu and the west of Shandong are lower in autumn than in spring.

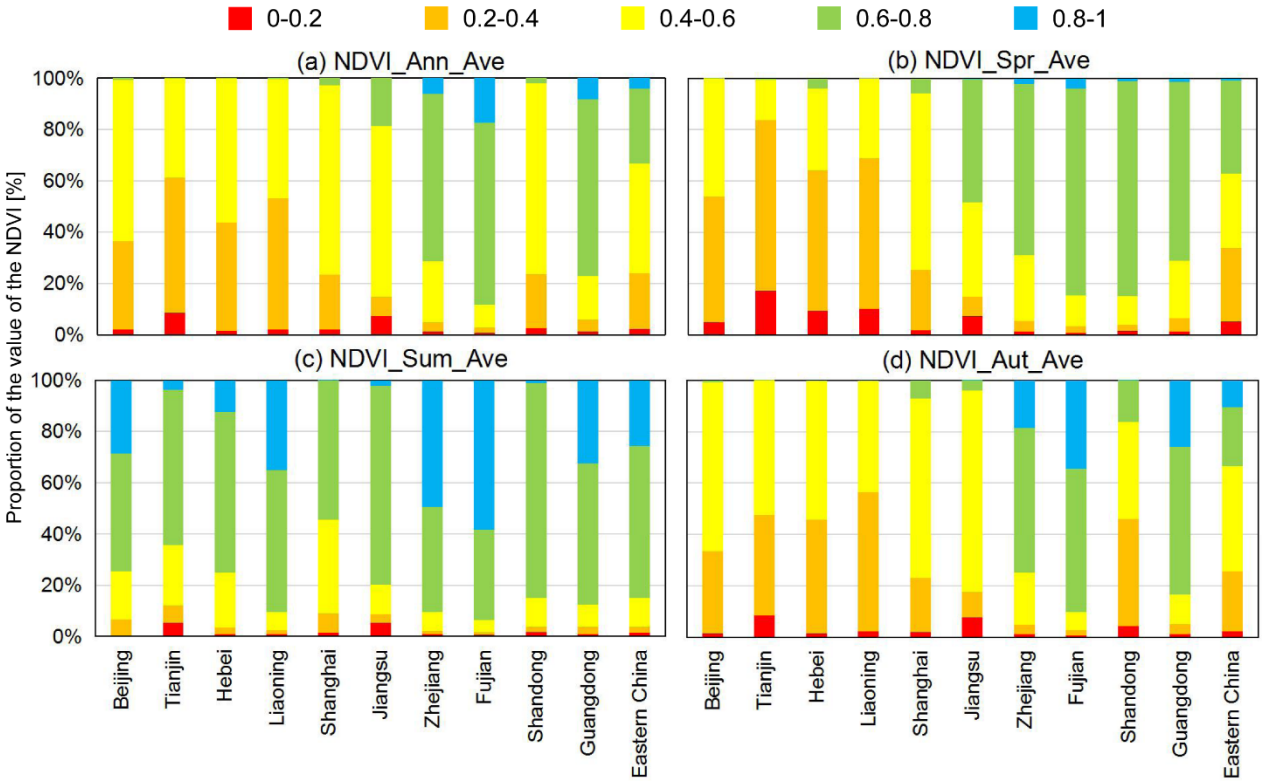

Figure 5-4. The statistical results of the annual and seasonal NDVI for eastern China and the ten administrative units

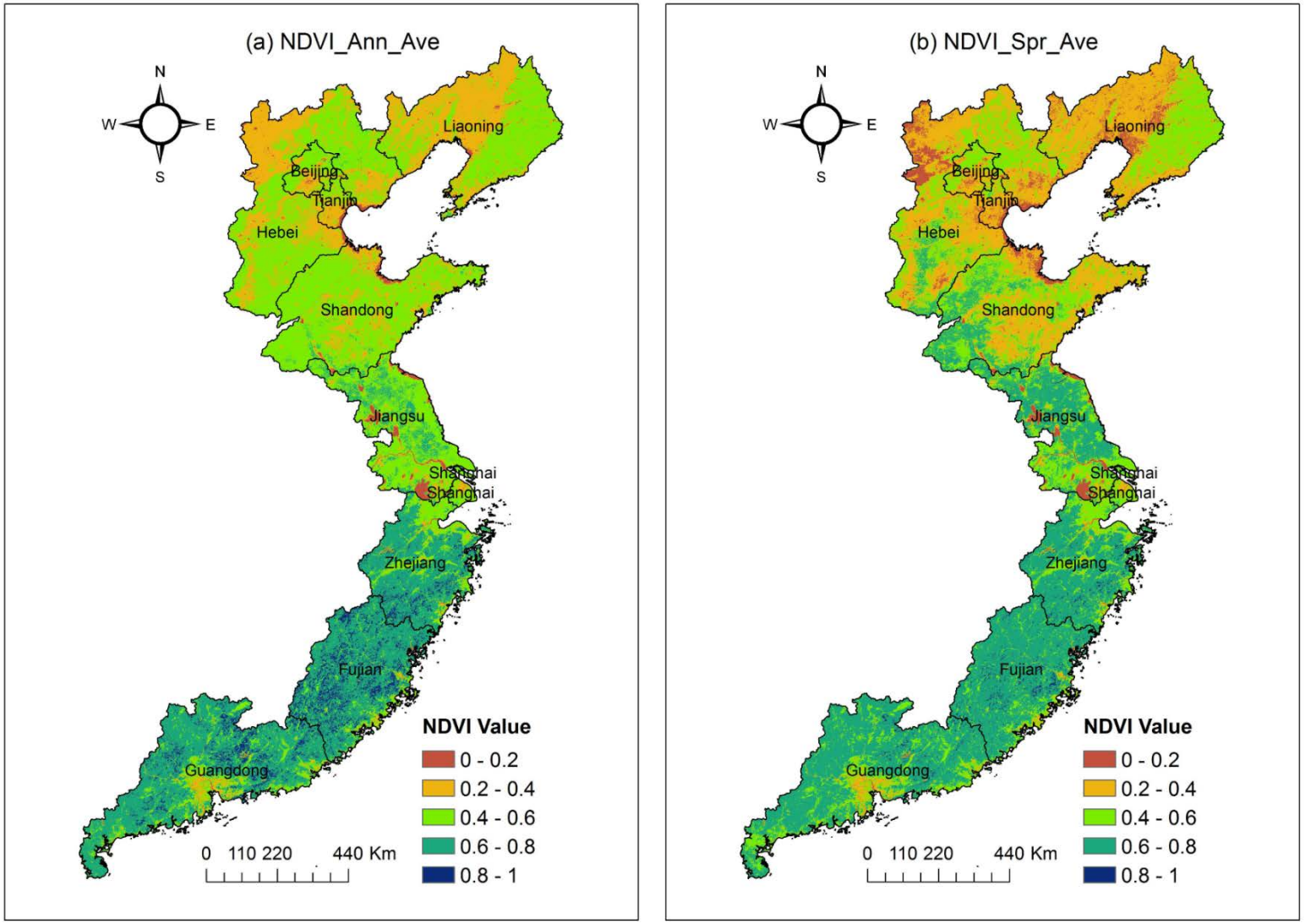

Figure 5-5. The spatial patterns of the annual and spring NDVI in eastern China from 2001 to 2016

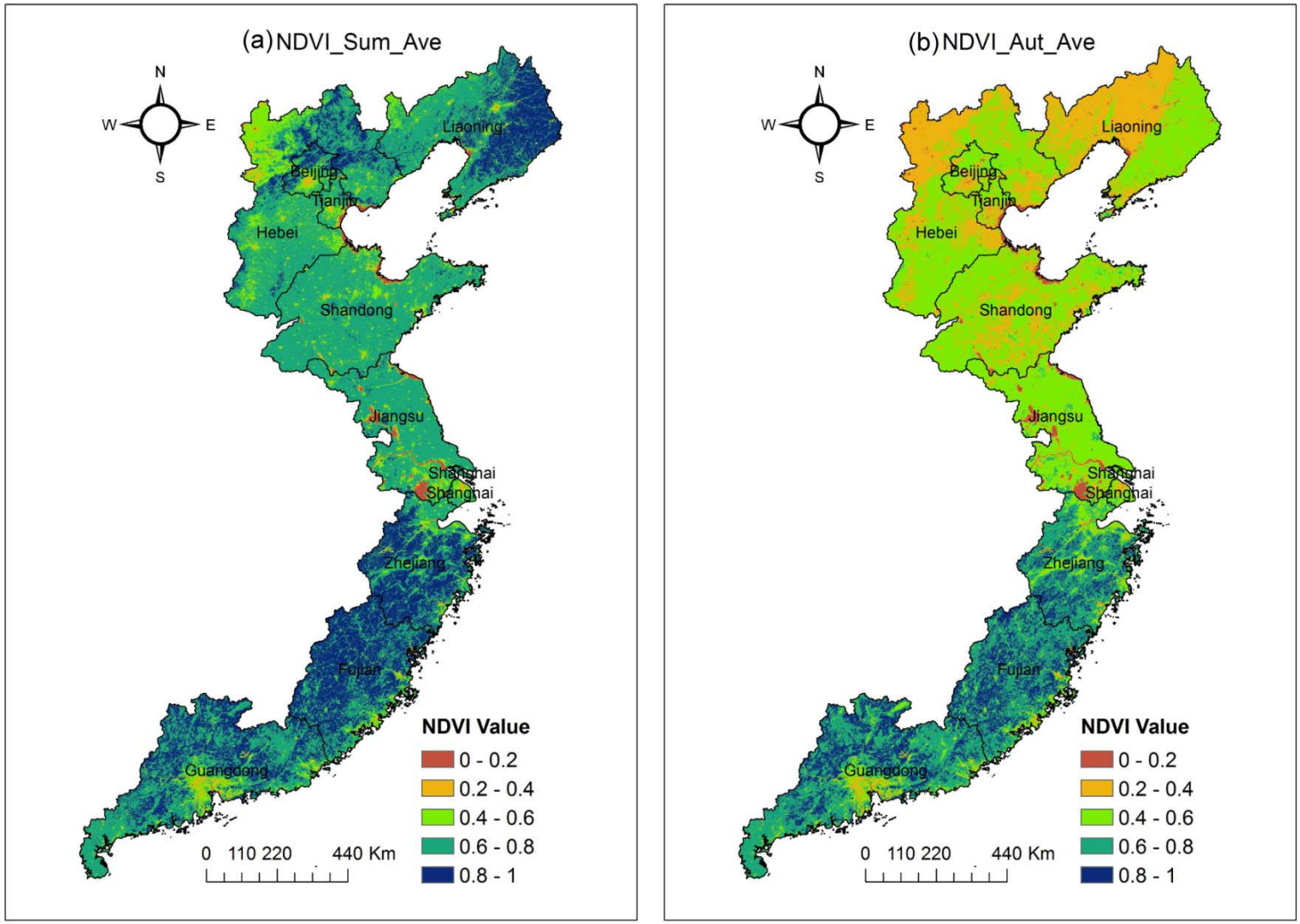

Figure 5-6. The spatial patterns of summer and autumn NDVI in eastern China from 2001 to 2016

5.1.3 The spatial pattern of vegetation changing trend

5.1.3.1 The spatial pattern of annual NDVI change

On the basis of the 16-year annual NDVI time series with the aid of ENVI IDL programming, the changing slope of the annual NDVI on each pixel was computed, which can be used to illustrate the spatial characteristics of the annual NDVI dynamic over eastern China from 2001 to 2016. Figure 5-8(a) shows that vegetation cover had experienced a significant degradation in many regions of the study area for the study period. An impressive decreasing trend is found in Jiangsu, Shanghai, the junction areas of Hebei, Tianjin, and Beijing, and many parts of Zhejiang, Fujian, and Guangdong, and the decreasing trend cannot be ignored. The overall vegetation cover in eastern China had gradually increased for the study period, and the vegetation change exhibited evident regional characteristics and obvious spatial heterogeneous. To quantitatively analyze the degree of the vegetation restoration or deterioration in eastern China from 2001 to 2016, the vegetation changing slope was classified into five classes in the background of the magnitude of the annual NDVI changing slope: significant decrease, slight decrease, unchanged, slight increase, and significant increase (Table 4-3).

Figure 5-8(a) shows that the vegetation cover had improved across many regions of the study area during the study period, particularly in the east and west of Liaoning, north of Hebei, Beijing, as well as in the middle and north of Shandong. This improvement is ascribed to the implementation of diverse afforestation and reforestation programs in the north of China, such as the GGP, NFCP, BTWSSCP, and TNSFP. These Programs have been carried out since 1978 and they have achieved enormous positive results in desertification prevention, soil and water protection, vegetation rehabilitation, and ecological conservation (Miao et al., 2015, Gutiérrez Rodríguez et al., 2016, Zhang et al., 2016, Viña et al., 2016, Lu et al., 2015, Piao et al., 2015, Cao et al., 2011, Bryan et al., 2018, Li et al., 2015c). In addition, the improvement of vegetation cover in Beijing is tightly correlated with the 2008 Olympic Games. After winning the right to host the 2008 Olympic Games in 2001, the local government returned some of the lands back to forests. Therefore, the vegetation cover in Beijing in 2008 reached 51.6%, which is also an essential factor for explaining why the vegetation cover enhanced in Beijing within a relatively short period of time (Duan et al., 2011).

The vegetation cover in the north of Zhejiang, west of Fujian, as well as in entire Shanghai, Jiangsu, and Tianjin is more sensitive and fragile. The vegetation browning trend is more serious in these areas than in other regions of the study area. These browning areas are distinctively spatially coupled with the areas with sharp population growth, rapid urban expansion, and high-speed economic development of the last three decades. All of these disturbing developments are at the cost of land use change, soil fertility decline, vegetation degradation, water contamination, and biodiversity loss (He, 2009, Liu et al., 2008b, Lu et al., 2015). We further noticed that all of these browning areas are located within the three largest China's economic zones (the Pearl River Delta, the Yangtze River Delta, and the Bohai Economic RIM), which play irreplaceable roles in China's socio-economic development.

Along with the effects of socio-economic development, vegetation degradation is also closely associated with changes in local climate systems. For instance, NDVI had gradually declined from 1982 to 2003. It was largely affected by prolonged drought seasons, which were generated by an annual mean temperature increase and an accumulated annual precipitation decrease, both taking place at the same time (Liu et al., 2008a).

Figure 5-7(a) shows that the vegetation cover in 33% of the study area exhibits a decreasing trend, in which 10% of these areas had undergone a significant decrease mainly distributed in Shanghai, the south of Jiangsu and sparsely distributed in Zhejiang, Fujian, Tianjin, and Hebei. Areas with vegetation cover remaining unchanged account for 18% of the study area, which is evenly spaced over the entire study area. Moreover, the vegetation cover in nearly half of the study area (49%) had improved, in which accounting for 29% of these areas had experienced a significant improvement. These improved areas are mostly concentrated in Beijing, Liaoning, the northwest of Hebei, and middle of Shandong.

From 2001 to 2016, the changing trend of the annual NDVI varies from different administrative units. A higher proportion of the significant increase exists for Tianjin, Shanghai, Jiangsu, Zhejiang, and Fujian (Figure 5-7(a)). Areas with slight increases account for 52% in Shanghai and 48% in Jiangsu. Areas with remaining unchanged and a slight increase account for almost the same proportion for all of the administrative units.

Besides, more administrative units with an NDVI enhancement are quantitatively identified. Areas with significant increases account for 69%, 50%, and 56% in Beijing, Hebei, and Liaoning, respectively, and these proportions are evidently larger than in other administrative units. Particularly, areas with a significant increase account for only 2% in Shanghai and 4% Jiangsu.

5.1.3.2 The spatial pattern of seasonal NDVI change

To facilitate the analysis of the characteristics of the spatial pattern of the seasonal NDVI changing trend from 2001 to 2016, the linear regression analysis method was applied to detect the changing trend of the seasonal NDVI at pixel level in eastern China during the corresponding period. Three changing slope maps of the seasonal NDVI were reclassified into five classes under the support of ArcGIS 10.3 platform. Figure 5-8(b) and Figure 5-9(a) and (b) display the spatial characteristics of the NDVI change in spring, summer, as well as in autumn, respectively.

Figure 5-8(b) shows that the NDVI changing trend presents prodigious spatial variabilities in eastern China in spring. NDVI increases slightly over large areas of the northern part of the study area, extending from Shandong to Liaoning. Areas with a slightly decreasing trend are widespread from the north of Guangdong to the south of Jiangsu. Meanwhile, vegetation cover in 38% of the study area had remained unchanged during the study period, which mostly coexists with the areas with a slight decrease but vaster geographical region, stretching from Guangdong to the north of Shandong. NDVI in approximately 10% of the study area shows a significant increase, and these areas are concentrated in the middle of Liaoning and north of Hebei.

Figure 5-9(a) displays a distinct spatial pattern of the NDVI change in summer in eastern China. Comparison of the NDVI change between spring and summer, as evidenced in Figure 5-7(b) and (c), the vegetation degradation is even more critical in summer than in spring. Especially, areas with a slightly decreasing trend account for 33% of the study areas in summer, but account for only 22% of the study area in spring. Areas with a slight decrease take the second largest proportion in summer, and these areas extend from Fujian to the south of Hebei. Moreover, areas with an increasing trend are primarily distributed in Liaoning and the north of Beijing and Hebei, which account for 25% of the

study area, in which 7% of these areas had experienced a significant improvement predominantly distributed in the east of Liaoning and sparsely distributed in the north of Beijing and Hebei. NDVI in 40% of the study area had remained unchanged in summer, which is mostly located in the north of Guangdong, middle of Shandong, as well as in the southeast of Hebei.

The vegetation cover had widely and slightly enhanced over many parts of the study area in autumn (Figure 5-7(d)). Comparison of the spatial patterns of the NDVI change between autumn and the two former seasons, Figure 5-7(d) shows that areas with a decreasing trend and areas with an increasing trend are alternately distributed in eastern China in autumn. In autumn, NDVI remaining unchanged accounts for 40% of the study area, which is in the same proportion as in summer but slightly higher than in spring. The slightly greening areas, that is, areas with a slight increase, account for 36% of the study area mostly distributed in the middle of Shandong, north of Hebei, west of Liaoning, and Beijing. The proportion of the slightly increased areas is considerably higher in autumn than in the two former seasons. The proportion of the areas with significant and slight decreases in autumn is about half of that in summer, indicating a comparable improvement in vegetation activity in autumn when compared with in summer. Generally, the vegetation cover had diffusely increased in autumn in most areas of eastern China from 2001 to 2016, and areas with a significant and slight vegetation deterioration only take place in around one-fifth of the study area.

Figure 5-7(b), (c), and (d) reveal the proportion of different categories of the seasonal NDVI changing slope for different administrative units simultaneously. The proportion in different categories of the NDVI changing slope varies in each administrative unit in spring (Figure 5-7(b)). It can be seen that the vegetation cover in Beijing, Tianjin, Hebei, Liaoning, and Shandong had undergone a vegetation greening surplus (a positive difference between the proportion of significant and slight increases and the proportion of significant and slight decreases) in spring from 2001 to 2016. Particularly, areas with an increasing trend account for 73% of the study area in Liaoning, followed by Beijing (64%). Areas remaining unchanged account for 68% in Guangdong and 54% in Jiangsu. These proportions are remarkably higher than in other administrative units, suggesting a more stable vegetation cover in Guangdong and Jiangsu in spring for the study period. A

higher proportion of the areas with a slightly decreasing trend exhibits in Shanghai, Zhejiang, as well as in Fujian with a magnitude of 53%, 40%, and 35% of the corresponding total areas, respectively.

In summer the proportion of the areas with significantly and slightly decreasing trends is higher than the proportion of the areas with significantly and slightly increasing trends in seven of the ten administrative units, except for Beijing, Hebei, and Liaoning, implying that a serious vegetation degradation had swept most of the study area in summer (Figure 5-7(a)). Figure 5-7(a) shows that the top five administrative units ranked by a vegetation browning surplus (a negative difference between the proportion of significant and slight increases and the proportion of significant and slight decreases) in descending order are Jiangsu, Shanghai, Zhejiang, Shandong, and Fujian. The proportion of the areas with a slight decrease increased by 42% in Jiangsu and 28% in Shandong from spring to summer.

However, areas with significant and slight increases in vegetation cover account for 54% in Beijing, 44% in Hebei, and 72% in Liaoning, respectively. All of these administrative units benefited significantly from a huge investment in initiating various vegetation restoration programs in the north of China. These programs not only turned some of croplands into forest lands and grasslands, but they also afforested a huge number of unused lands and barren lands into forest lands (Cao et al., 2017, Liu et al., 2008b, Lu et al., 2011, Lu et al., 2015).

Furthermore, the vegetation cover change is also closely associated with climate variability. Piao et al. (2011) demonstrated that the vegetation degradation in the southeast of China was basically influenced by the decreasing autumn precipitation, whereas the enhancement of vegetation cover in boreal regions is caused by the warming autumn temperature (Dragoni et al., 2011, Vesala et al., 2010). It is worth noticing that both vegetation degradation and vegetation restoration are more significant on annual scale than on seasonal scale, which can be attributed to the cumulative effects of positive and negative influences from each season.

The proportion of the areas with a slight decrease in nine out of the ten administrative units is lower in autumn than in the two former seasons, except for Liaoning (Figure

5-7(b), (c), and (d)). As detailed in Figure 5-7(d), areas with significant and slight increases in Beijing, Hebei, and Shandong sprawl over more than 50% of the corresponding total areas, respectively. The proportion of the areas with significantly and slightly increasing trends reaches 81% in Beijing in particular. Except for Beijing, areas with vegetation cover remaining unchanged take an equivalent proportion in other administrative units. It is worth noticing that both vegetation degradation and vegetation restoration are significant on annual scale than in all three seasons, which can be attributed to the accumulative effects of positive and negative influences from each season.

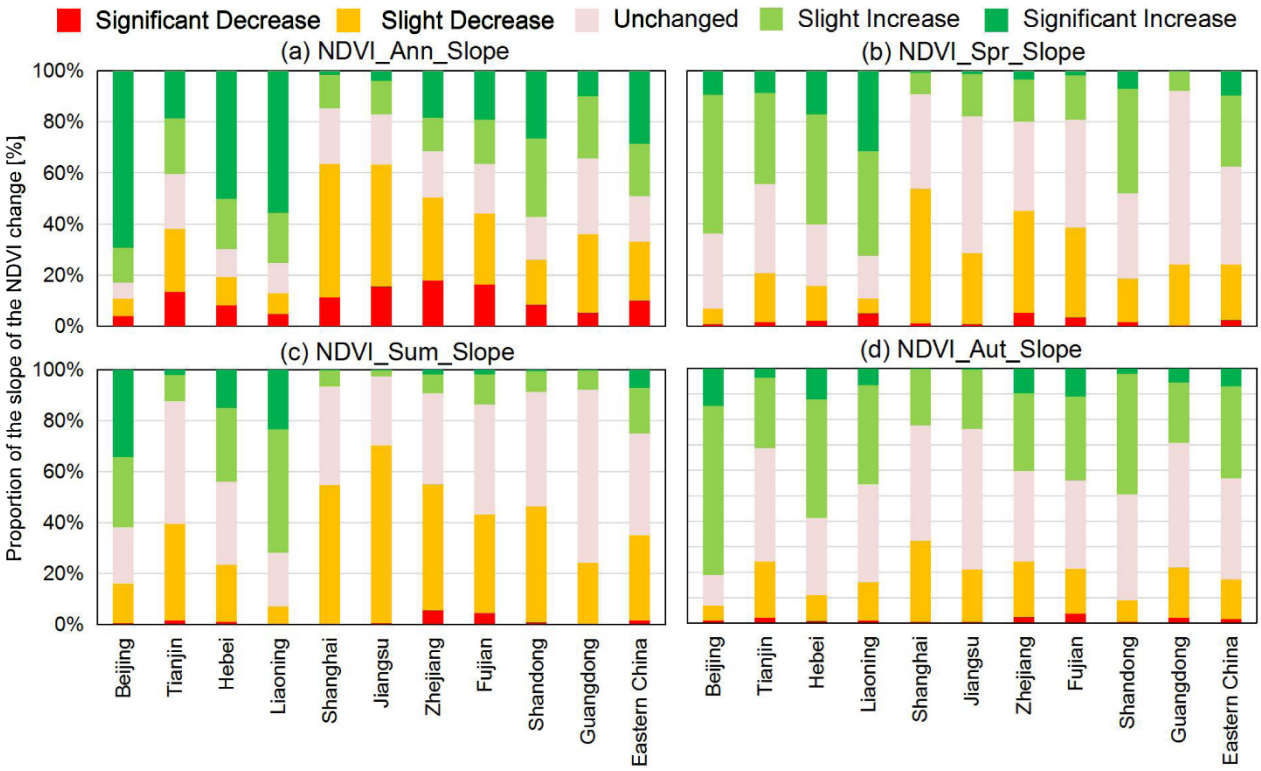

Figure 5-7. The statistical results of the annual and seasonal NDVI change for eastern China and the ten administrative units

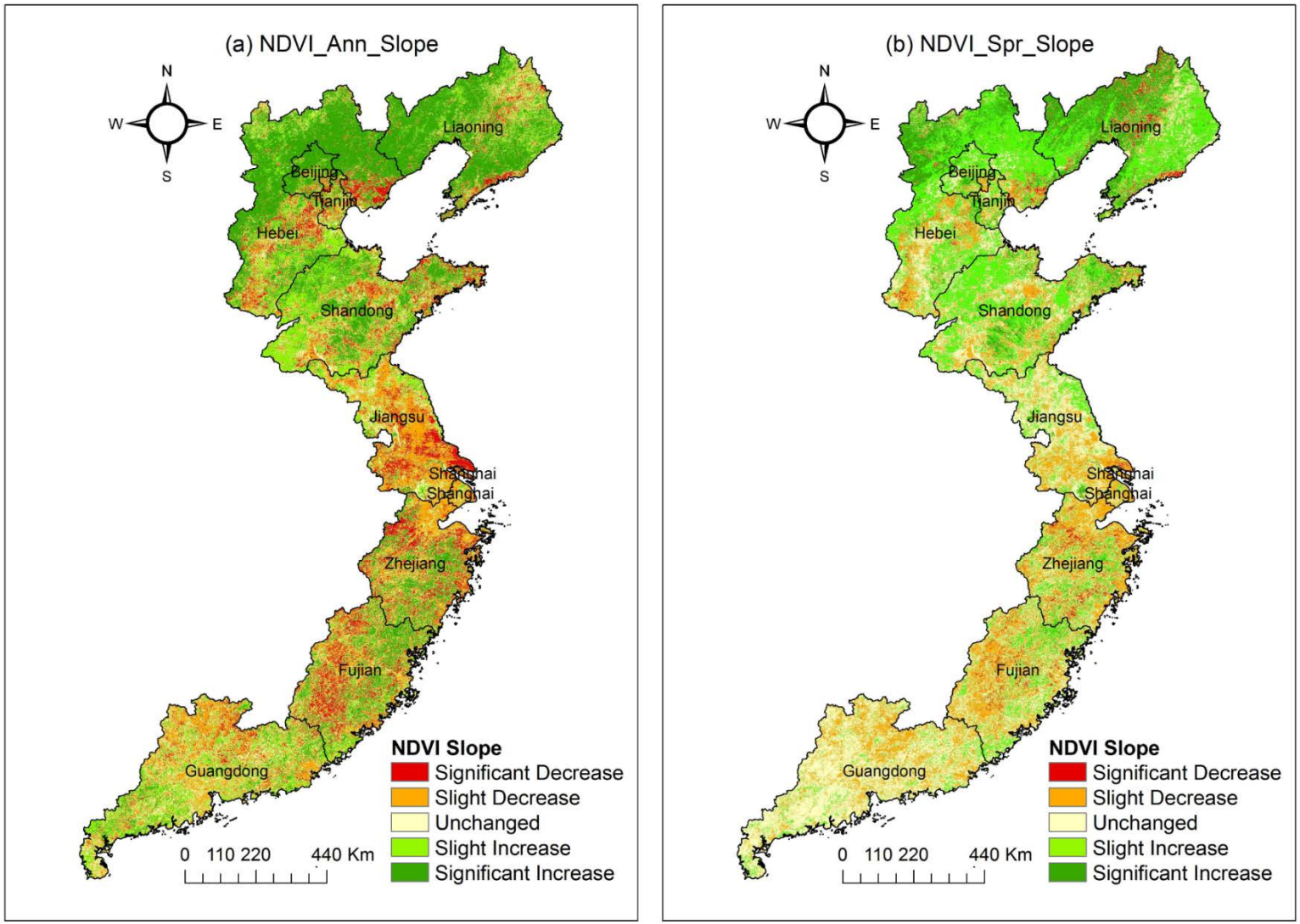

Figure 5-8. The change trends of the annual and spring NDVI in eastern China from 2001 to 2016

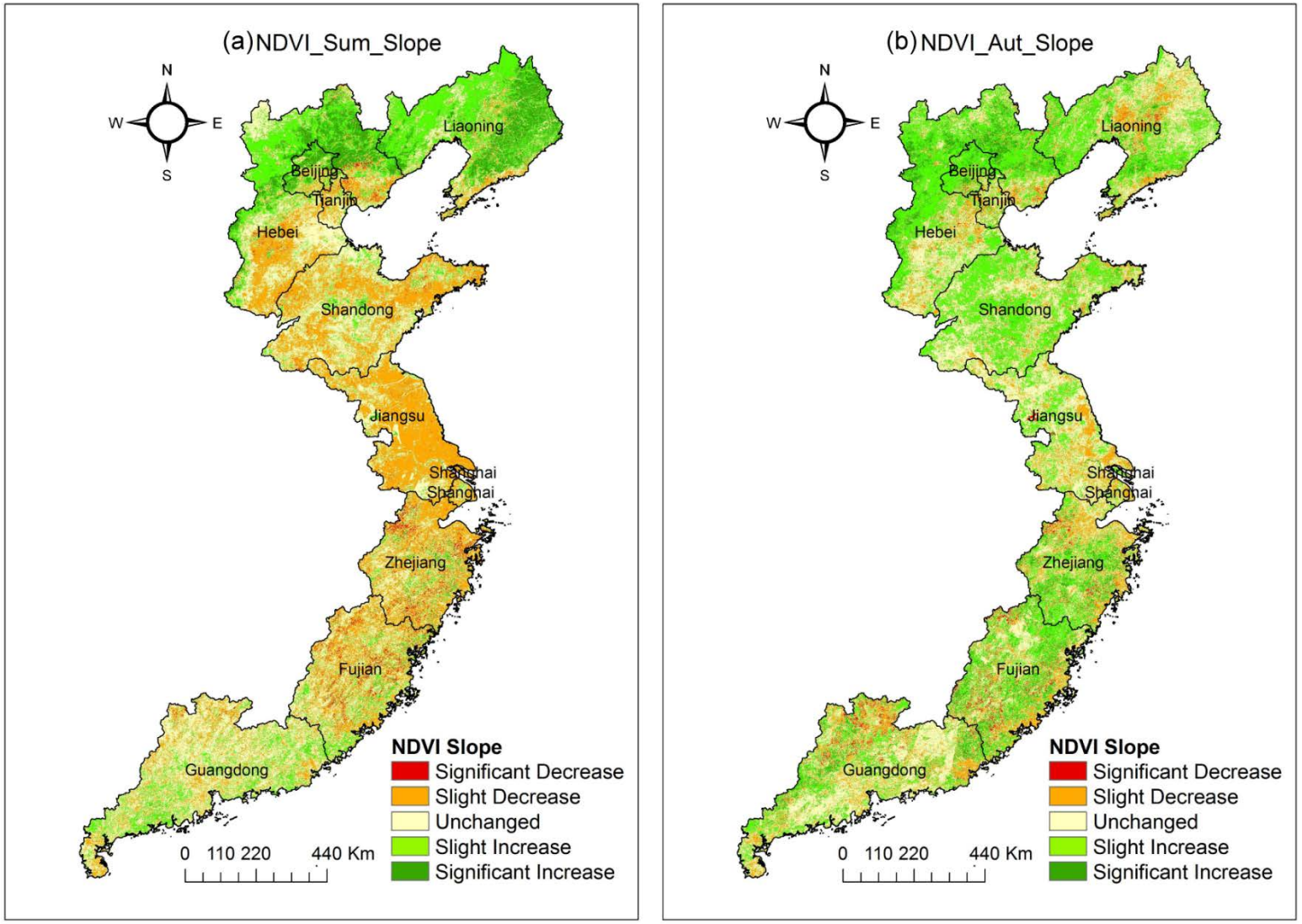

Figure 5-9. The change trends of the summer and autumn NDVI in eastern China from 2001 to 2016

5.1.4 The spatial pattern of the future vegetation changing trend

5.1.4.1 The spatial pattern of the future annual NDVI changing trend

It is of great practical value to apply R/S analysis to study the consistency of the vegetation cover and further to predict the future changing trend of vegetation cover in eastern China. Hurst exponent can be used to indicate the consistency of the NDVI time series. In this study, firstly, R/S analysis was applied to generate the Hurst exponent for every pixel against the background of the 16-year NDVI time series with the aid of MATLAB programming. Then overlay analysis was used to overlap the results of the NDVI changing trend and Hurst exponent of NDVI time series. Thus the spatial pattern of the future changing trend of NDVI was displayed both on annual and seasonal scales (Figure 5-11 and Figure 5-12). Furthermore, zone analysis was applied to generate the statistical results of the future changing trend of NDVI for eastern China and the ten administrative units (Figure 5-10).

Hurst exponent ranges from 0 to 1. When Hurst exponent is greater than 0.5, indicating that NDVI will remain the current changing trend in the future, and when Hurst exponent is lower than 0.5, indicating that NDVI will shift the current changing trend in the future. It is worth noticing that, on annual scale, the mean Hurst exponent of the study area is 0.51, suggesting a weak consistency of NDVI time series for eastern China. Moreover, the areas expected to maintain the current changing trends (57%) are larger than the areas expected to shift the current changing trends (43%) for eastern China.

Figure 5-11(a) displays the spatial characteristics of the future changing trend of the annual NDVI. The future changing trend of the annual NDVI shows distinctive spatial heterogeneity over the study area. Figure 5-10(a) and Figure 5-11(a) show that the consistent improvement area accounts for the largest proportion (25%) of the study area, which spreads from Shandong to Liaoning. The improvement area accounts for 12% of the study area. The consistent degradation area accounts for 21% of the study area, which is concentrated in the north of Jiangsu and scattered over the study area. The degradation area accounts for 24% of the study area, which is primarily distributed in Liaoning and the north of Beijing and Hebei. Areas expected to experience unchanged in the future accounting for 11% of the study area, and areas with uncertain future

changing trend accounting for only 7% of the study area. Above results suggest that the areas with certain vegetation degradation will be larger than the areas with certain vegetation improvement in eastern China in the future.

From the perspective of the future changing trend of the annual NDVI for each administrative unit, the proportion of the areas expected to degrade in the future in nine of the ten administrative units (except for Shandong) is larger than the proportion of the areas expected to improve in the future. Particularly in Beijing and Liaoning, the degraded area expected to reach half of the corresponding area in the future.

5.1.4.2 The spatial pattern of the future seasonal NDVI changing trend

In terms of the future changing trend of the seasonal NDVI in eastern China, accounting for 53% in spring, 57% in summer, and 60% in autumn of the study area predicted to reverse the current changing trends in the future, and accounting for 47% in spring, 43% in summer, and 40% in autumn of the study area predicted to maintain the current changing trends in the future. Above results generated two statements that (1) the areas expected to remain the current changing trend are slightly greater than the areas expected to switch the current changing trend in all seasons; and (2) the areas expected to switch the current changing trend in the future are largest in autumn, followed by summer and then spring.

As displayed in Figure 5-11(b), in spring, the consistent improvement area is located in the middle of Liaoning and the junction area of Hebei and Shandong, accounting for 15% of the study area. The improvement area is sparsely scattered from the south of Jiangsu to Guangdong, accounting for 11% of the study area. The degradation area accounts for the largest proportion (23%), which is mainly distributed in the north of Hebei and Beijing and the east and west of Liaoning. The consistent degradation area accounts for 13% of the study area.

Figure 5-12(a) shows in summer the consistent improvement area accounts for the smallest proportion (11%), which is sparsely scattered from Shandong to Liaoning. The improvement area in Jiangsu is larger than in other regions of the study area. The degradation area and the consistent degradation area account for 32% of the study area,

which is primarily located in Tianjin, the junction area of Shandong and Hebei, the north of Beijing and Hebei, and the east of Liaoning.

Figure 5-12(b) displays that in autumn the improvement area and consistent improvement area account for 24% of the study area, which is primarily located in the junction area of Fujian and Zhejiang and sparsely scattered over the study area. The degradation area takes the largest proportion (28%), which is predominantly located in the middle and north of Shandong, north of Beijing and Hebei, and west of Liaoning. The consistent degradation area accounts for only 8% of the study area.

Regarding the future changing trend of the seasonal NDVI for each administrative unit, the proportion of the areas expected to degrade in the future in eight of the ten administrative units in spring (except for Shandong and Zhejiang), in six of the ten administrative units in summer (except for Shanghai, Jiangsu, Zhejiang, and Fujian), and in seven of the ten administrative units in autumn (except for Shanghai, Zhejiang, and Fujian) is larger than the proportion of the areas expected to improve in the future. It is worth noticing that areas expected to degrade in the future in Beijing reaching 52% in spring, 54% in summer, and 66% in autumn, indicating that the current improving trend of vegetation cover in Beijing may reverse and a server vegetation degradation may occur in the future.

Above results suggest that the areas with certain vegetation degradation will be larger than the areas with certain vegetation improvement for eastern China both on annual and seasonal scales in the future. This result is in line with the results generated by Li et al. (2019). Li et al. (2019) demonstrated that areas with an increasing trend and an anti-persistence characteristic account for the largest proportion both on annual and seasonal scales in the 400 mm annual precipitation fluctuation zone, China, indicating a server vegetation degradation in the future in this region.

However, our result is not in line with the results generated by Tong et al. (2018). Tong et al. (2018) evidenced that the areas with vegetation improvement are larger than the areas with vegetation degradation in the Mongolian Plateau in the future, particularly in Inner Mongolia. Inner Mongolia located in the north of China, the vegetation cover has significantly improved in recent years due to large-scale reforestation and afforestation

programs implementation and practical ecological management in this region (Tong et al., 2018, Zhang et al., 2016, Duan et al., 2011). However, eastern China is located in the eastern coastal area of China, a region has highly developed in the last three decades. Although the vegetation cover has restored in this region in recent decades, the tolerance and resilience of terrestrial ecosystem are limited. Therefore, the continued socio-economic development, urban expansion, and population growth may result in vegetation degradation in eastern China in the future. Above explanation may answer the question of why the areas with vegetation degradation predicted to be larger than the areas with vegetation improvement in eastern China in the future.

Along with rapid urbanization and industrialization occurring in eastern China, environmental concerns have become increasingly serious in recent decades in this region. Large-scale reforestation and afforestation programs have exerted great impacts on regional vegetation restoration and rehabilitation, in the north of the study area in particular, but the terrestrial ecosystem in more regions is becoming more vulnerable and unstable. To prevent the environmental degradation in eastern China effectively, the large-scale reforestation and afforestation programs should be continuously implemented, and, meanwhile, it is urgent to put new vegetation-protection programs into action to protect existing vegetation cover and alleviate the environmental deterioration, particularly in the south of eastern China.

The transformation of land use functions (*e.g.*, forest land, grassland, shrubland, and farmland to built-up land) and enhanced human activities contributed to vegetation degradation directly and inevitably. Therefore, appropriate ecological-conservation policies should be formulated by authorities and put into practice to regulate inappropriate land use change. These policies can not only protect existing vegetated areas but provide a sustainability way to further enhance vegetation resource inventory, particularly in the areas with vegetation degradation currently and the areas expected to degrade in the future.

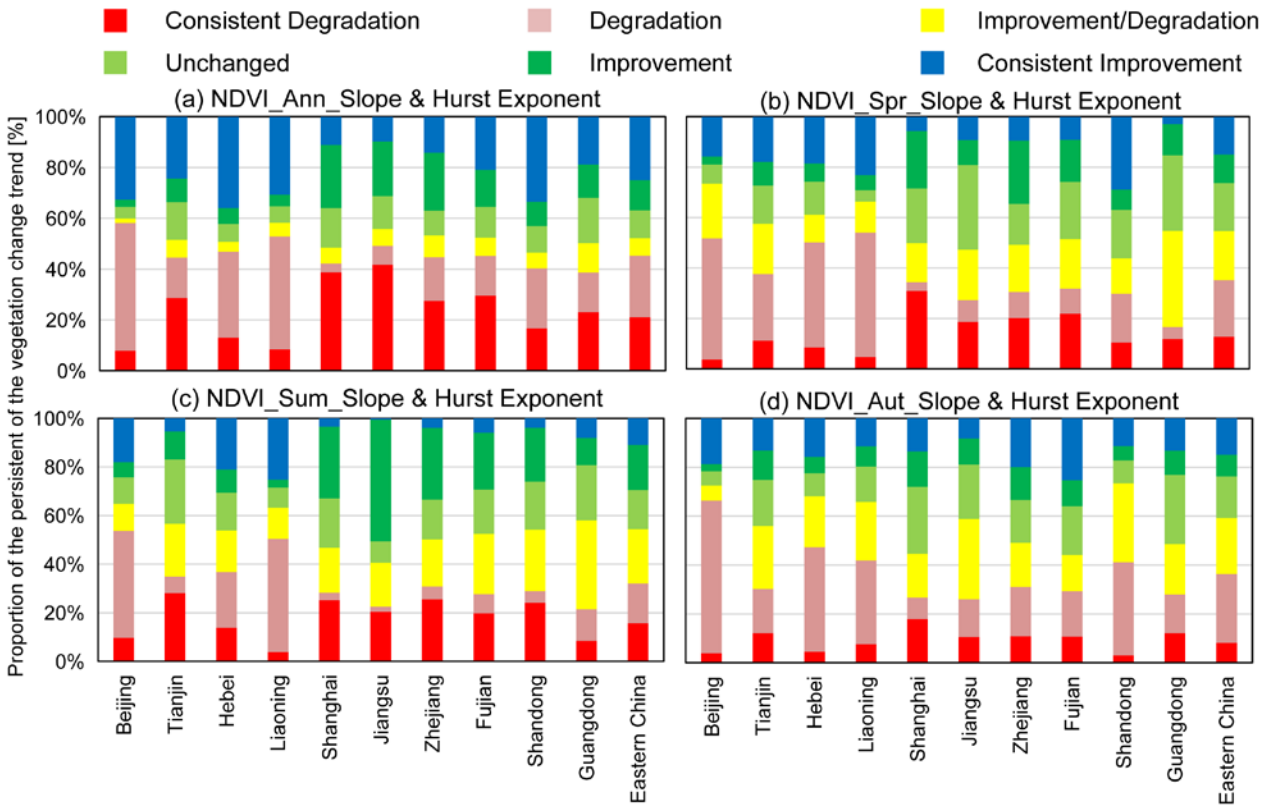

Figure 5-10. The statistical results of the future changing trends of annual and seasonal NDVI for eastern China and the ten administrative units

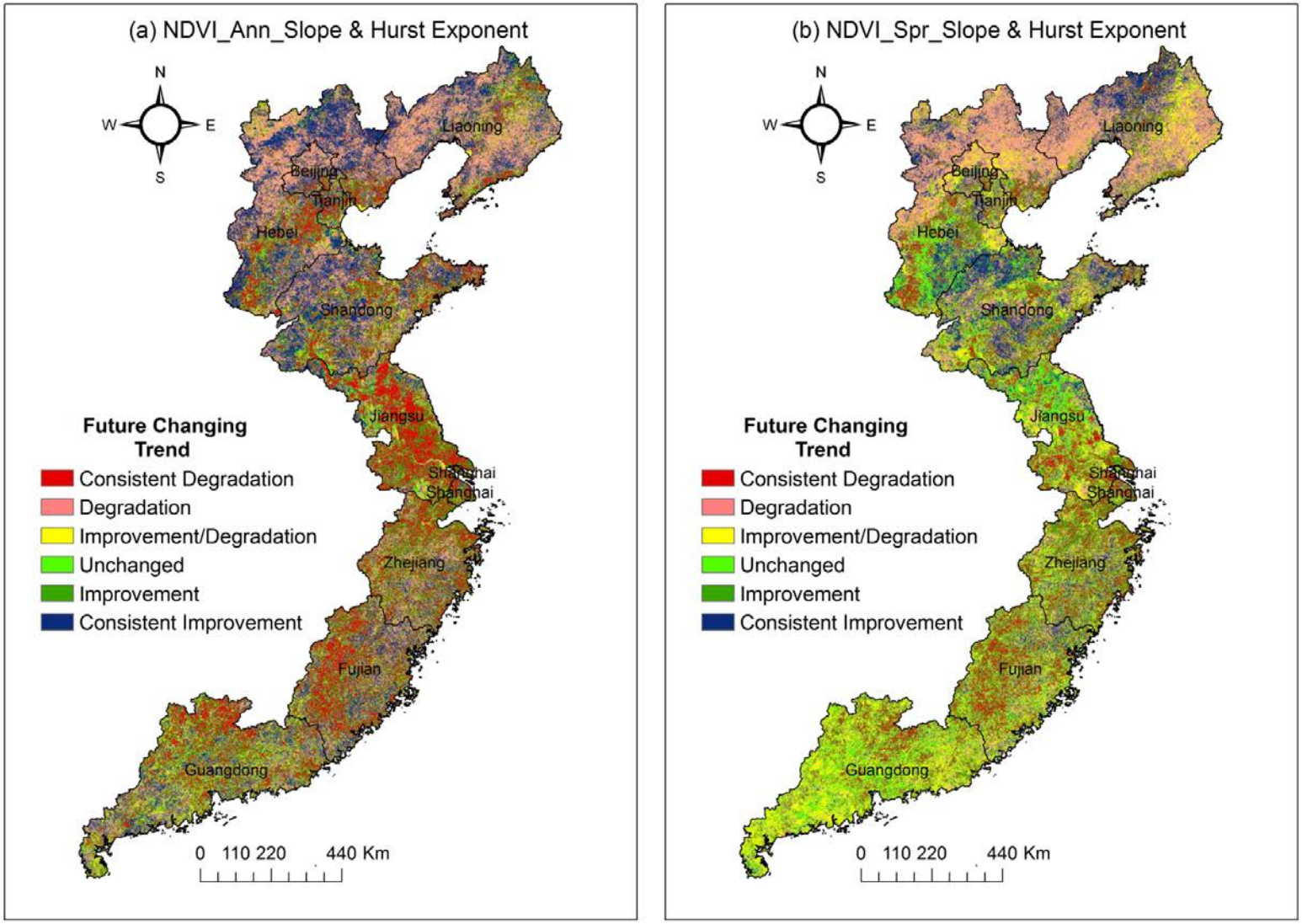

Figure 5-11. The spatial patterns of the future changing trends of the annual NDVI and spring NDVI in eastern China

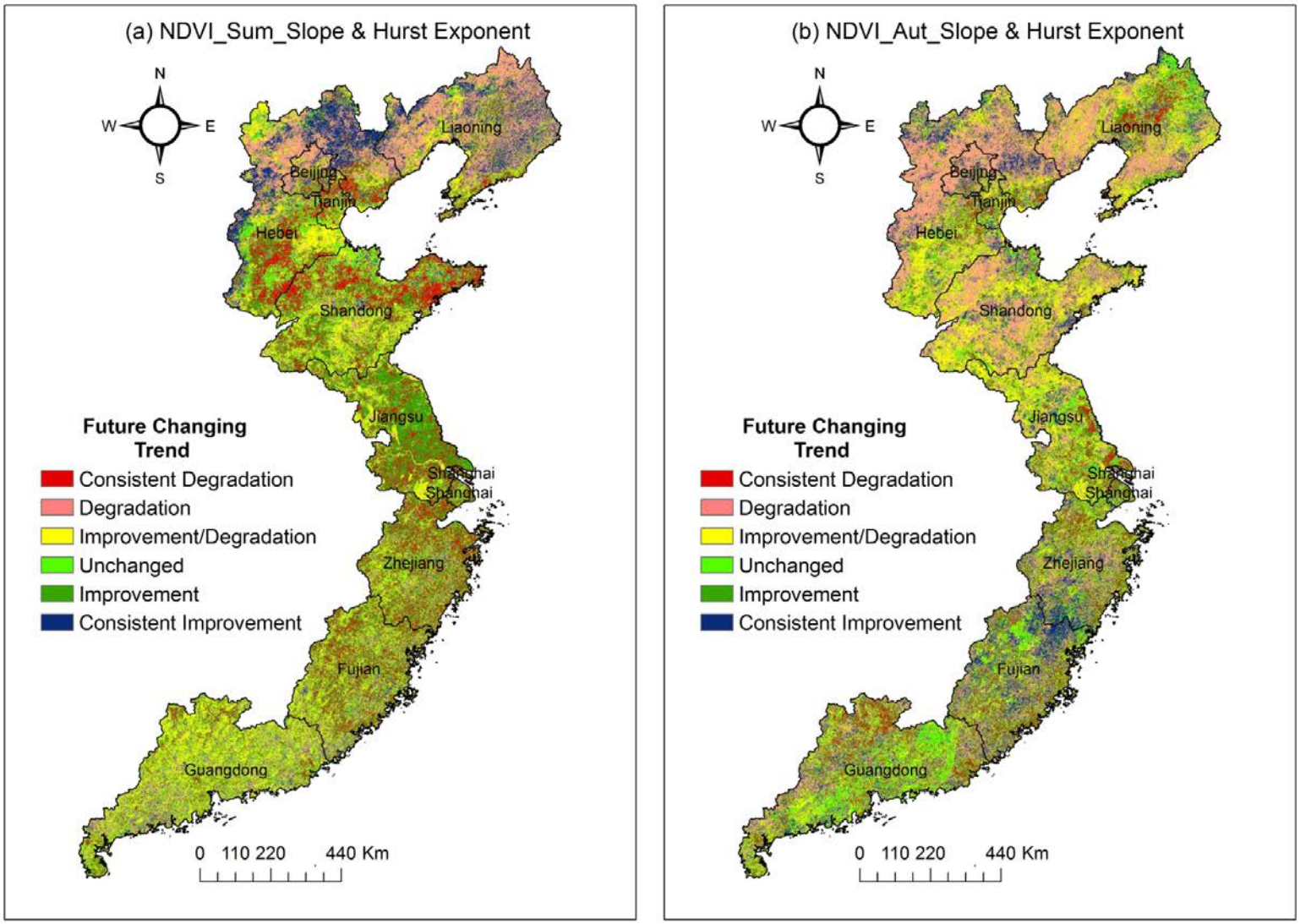

Figure 5-12. The spatial patterns of the future changing trends of summer NDVI and autumn NDVI in eastern China

5.1.5 The spatial pattern of vegetation stability

5.1.5.1 The spatial pattern of annual vegetation stability

The fluctuation of the vegetation cover is largely influenced by the overall vegetation activity over a certain period. In this study, NDVI CV is applied as an indicator to measure the overall vegetation stability in eastern China from 2001 to 2016. To quantitatively determine the degree of the vegetation variability, the NDVI CV was divided into four classes, as shown in Table 4-4. A larger value of the NDVI CV tends to show a stronger fluctuation in vegetation activity, and a smaller value indicates a stable vegetation cover (Barbosa et al., 2006). The proportion of the annual NDVI CV in each category for the ten administrative units and the study area is simultaneously calculated based on the map of the NDVI CV and the vector map of the study area. The proportion of the annual NDVI CV in different categories for the study area and the ten administrative units are detailed in Figure 5-13(a).

Figure 5-14(a) illustrates the spatial pattern of the annual NDVI CV across the study area, which indicates the variability of the vegetation cover for the study period. The annual NDVI CV shows distinct spatial differences in the northern and southern parts of the study area, suggesting that the vegetation cover is comparatively stable in the south than in the north of the study area. Areas with the annual NDVI CV values ranging from 0 to 0.05 are densely distributed in the east of Liaoning, Zhejiang, Fujian, and Guangdong and sparsely located in the north of Beijing and Hebei, which account for 45% of the entire study area. These areas are mostly dominated by stable forest land. Many scholars have demonstrated that the forest land has a better sustainable ability in ecological resilience in resisting disturbances from regional climate change and frequency of human activities (Wang et al., 2015b, Gazol et al., 2018, Cui et al., 2013).

Areas with the NDVI CV values ranging from 0.05 to 0.1 account for 43% of the study area, which stretch from Jiangsu to the east of Liaoning. However, the NDVI CV values in Shanghai, Tianjin, the eastern coastal areas of Guangdong, south of Jiangsu, as well as in the northwest of Hebei range from 0.1 to 1, indicating that an intensive vegetation oscillation had occurred in these areas during the study period. It is worth noting that an NDVI CV value suggests the magnitude of the NDVI fluctuation, but it does not indicate

the oscillation direction of the vegetation activity. Higher NDVI CV value indicates a stronger positive or negative NDVI changing trend. It is clear that the areas in Shanghai, Tianjin, the eastern coastal areas of Guangdong, and in the south of Jiangsu had experienced a negative NDVI fluctuation due to the rapid urban expansion and socio-economic development that occurred in these areas in recent decades. These changes happened at the cost of tremendous ecological degradation. Another reason for these changes was the usage of farmlands and forest lands as urban areas (Qu et al., 2015, Zhao et al., 2017, Zhou et al., 2016).

A set of vegetation afforestation and reforestation programs has been launched in the north of China, covering most areas of Hebei, Beijing, and Liaoning. Due to effective regional forest management, not only the negative effects derived from socio-economic advancement were offset, but the vegetation cover in these areas also had comprehensively improved (Zhang et al., 2016, Bryan et al., 2018, Cao, 2011). High NDVI CV values in these areas can be basically considered as a positive NDVI fluctuation. All explanations provided above account for the higher NDVI CV value in these areas. In addition, they explain why the spatial pattern of the NDVI CV value shows a poor spatial coupling with the spatial patterns of the annual NDVI value and annual NDVI changing slope.

In terms of the proportion of the annual NDVI CV in different categories for each administrative units, inspection of Figure 5-13(a), it shows that higher proportion of the annual NDVI CV values ranging from 0 to 0.05 takes place in Liaoning, Zhejiang, Fujian, and Guangdong. Particularly, this proportion reaches 72% in Zhejiang and 80% in Fujian, implying that the vegetation stability in these two administrative units is better than in other administrative units. Proportion of the annual NDVI CV values ranging from 0.15 to 1 in Tianjin, Jiangsu, and Shanghai occupies around 15% of their total corresponding areas, which are higher than in other administrative units (the proportion of the annual NDVI CV values ranging from 0.15 to 1 in other administrative units is less than 5%). This phenomenon is caused by vulnerable vegetation growth conditions such as high-speed urbanization, industrialization, and population growth in these regions.

5.1.5.2 The spatial pattern of seasonal vegetation stability

The spatial characteristics of the seasonal vegetation stability were carried out in this study at pixel level to evaluate the fluctuation of the vegetation activity over eastern China from 2001 to 2016. The spatial distribution of the NDVI CV in spring, summer, and autumn shows an apparent spatial heterogeneous across the entire study area. Particularly, obvious seasonal differences are displayed in the north of the study area. Figure 5-14(b) and Figure 5-15(a) and (b) display the spatial distribution pattern of the NDVI CV in spring, summer, and autumn, respectively.

In spring the NDVI CV values are lower in the middle than in the southern and northern parts of the study area (Figure 5-14(b)), indicating that a stronger vegetation fluctuation had taken place in the southern and northern parts of the study area over the study period. Areas with the NDVI CV values ranging from 0.15 to 1 account for 16% of the study area, which is mostly distributed in the center of the three economic zones. Areas with the NDVI CV values ranging from 0 to 0.05 are mainly distributed in Zhejiang and the north of Fujian, which account for 12% of the study area. The NDVI CV values in Liaoning display a distinct geographical difference between the east and the west: namely, higher values are concentrated in the west part, and lower values are located in the east part, indicating an unbalanced vegetation oscillation.

Comparison of Figure 5-14(b) and Figure 5-15(a) show that the overall vegetation activity is more stable in summer than in spring, except for the northwest of Hebei, a place where the NDVI CV values are higher in summer than in spring. Areas with the NDVI CV values ranging from 0 to 0.05 in summer account for 31% of the study area, and this proportion is higher than in spring by 19%. Moreover, the NDVI CV values in the center of the three economic zones range from 0.15 to 1, which are considerably higher than the surrounding areas. Figure 5-14(b) and Figure 5-15(b) show that the NDVI CV values in autumn present a similar spatial pattern to spring, but the amplitude of the vegetation variability is slightly lower in autumn than in spring. With an exception of the NDVI CV values in the northwest of Shandong is higher in autumn than in spring. Comparison of the overall vegetation stability in spring, summer, and in autumn, we noticed that the vegetation activity shows a clear geographical distribution difference in

all seasons, but the overall vegetation stability is better in summer than in autumn, followed by in spring.

Figure 5-13(b), (c), and (d) illustrate the proportion of the season NDVI CV in different categories for eastern China and the ten administrative units. Figure 5-13(b) shows that the proportion of the NDVI CV values ranging from 0.15 to 1 in Tianjin reaches 47% in spring, which is higher than in other administrative units, particularly in Liaoning, Zhejiang, and Fujian, where the proportion of the NDVI CV values ranging from 0.15 to 1 is only 8%, 7%, and 5%, respectively. However, the proportion of the NDVI CV values ranging from 0 to 0.05 accounts for 54% in Fujian and 38% in Zhejiang. Figure 5-13(b) and (c) illustrate that in summer the proportion of the NDVI CV values ranging from 0 to 0.05 is enhanced in nine out of the ten administrative units in comparison with the proportion of the NDVI CV values ranging from 0 to 0.05 in spring. However, the proportion of the NDVI CV values ranging from 0 to 0.05 in Shanghai and Jiangsu is still relatively low with a magnitude of 1% and 6%, respectively. An analogous pattern of the proportion of the NDVI CV in each category is observed in spring and autumn, except for the proportion of the NDVI CV values ranging from 0 to 0.05 in Guangdong and from 0.05 to 0.1 in Tianjin are greater in autumn than in spring, respectively.

Fang et al. (2001) evaluated the fluctuation of the NDVI of the forest, grassland, desert, alpine vegetation, and cropland on annual scale in China from 1982 to 1999 and Peng et al. (2015) assessed the vegetation stability of different regions of eastern China from 1999 to 2008 on the basis of CV. Fang et al. (2001) and Peng et al. (2015) concentrated on evaluating the overall vegetation fluctuation characteristics. However, in this study, CV is utilized to spatially quantify the magnitude of the vegetation variability both on annual and seasonal scales. Not only the spatial characteristics of the vegetation stability were displayed, but also the magnitude of the vegetation fluctuation for each pixel and each administrative unit was quantified against the background of CV, which comprehensively explored the vegetation stability in eastern China.

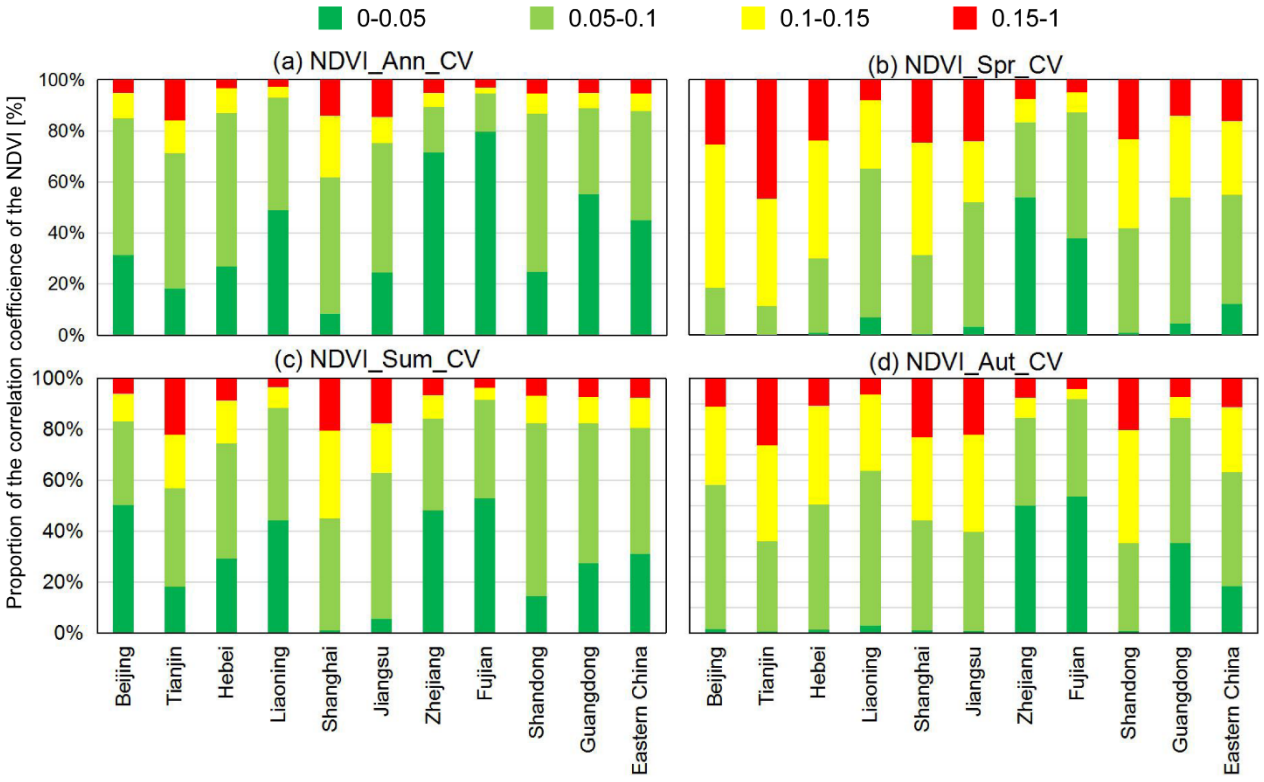

Figure 5-13. The statistical results of the coefficient of variation of annual and seasonal NDVI for eastern China and the ten administrative units

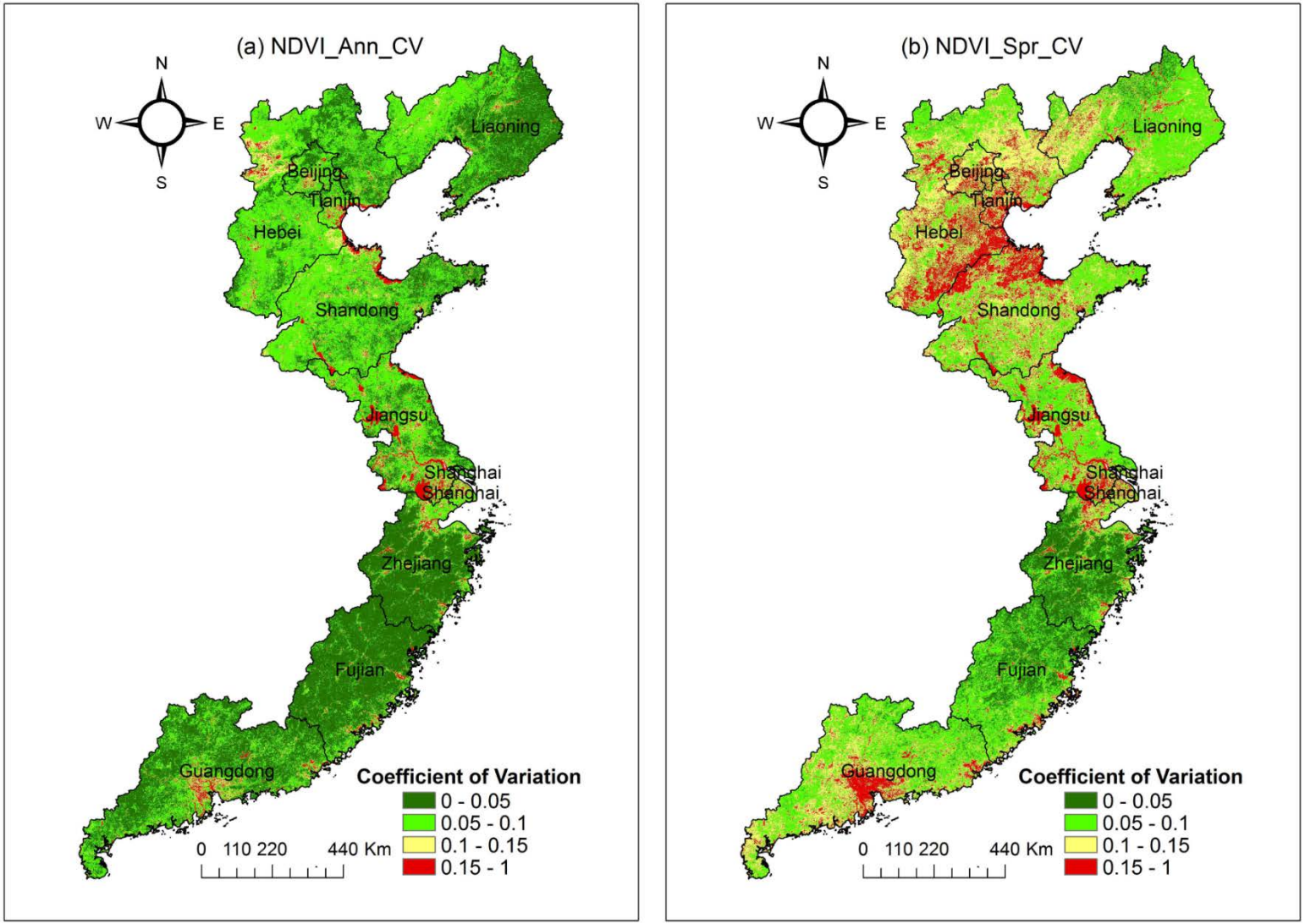

Figure 5-14. The spatial patterns of the coefficient of variation of the annual and spring NDVI in eastern China from 2001 to 2016

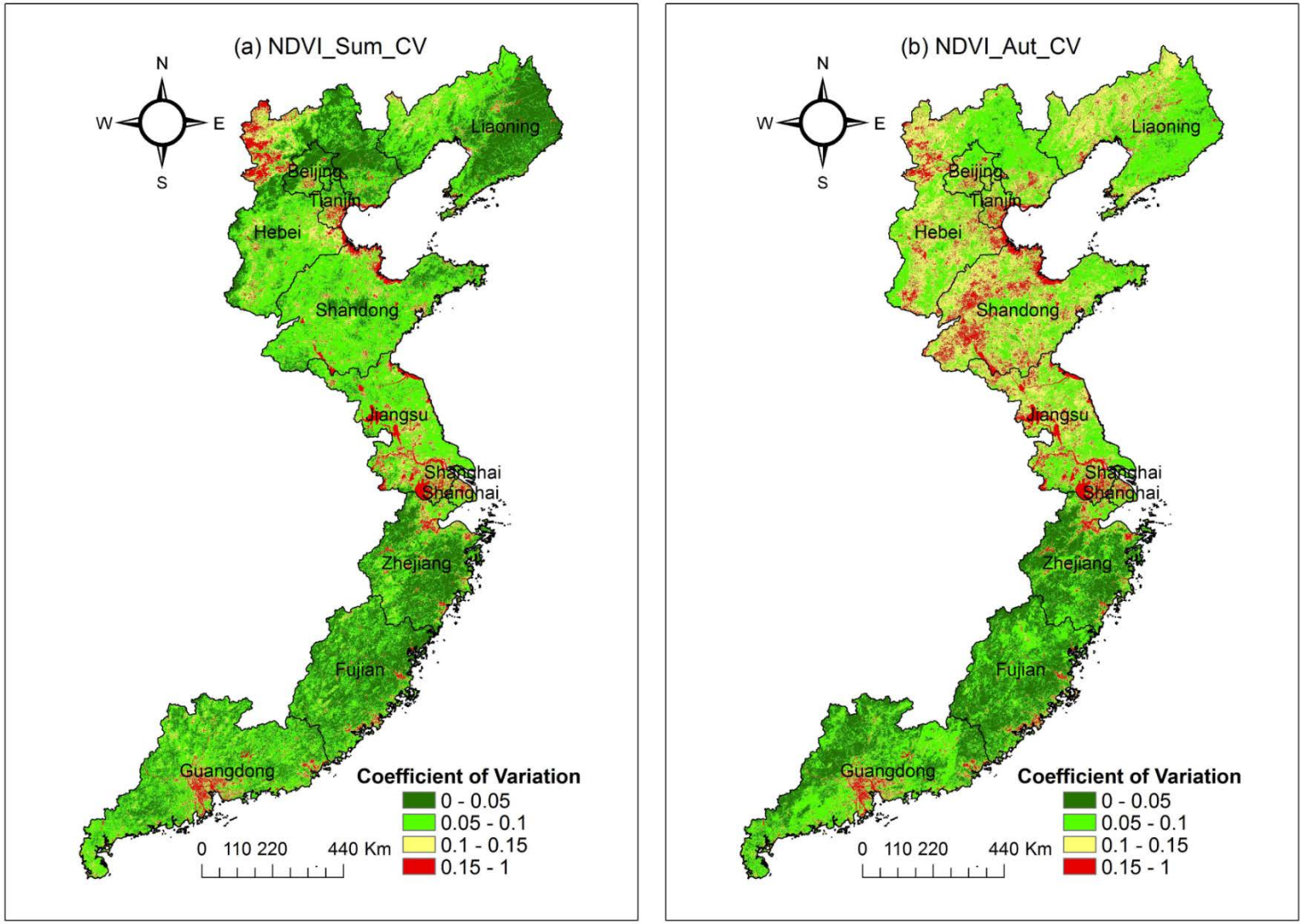

Figure 5-15. The spatial patterns of the coefficient of variation of summer and autumn NDVI in eastern China from 2001 to 201

5.2 The relationship between NDVI and climate factors in eastern China

5.2.1 The temporal characteristics of NDVI in response to climate factors

Climatic factors could have diverse impacts on vegetation growth for different regions (Albani et al., 2006, Brown and de Beurs, 2008). Among these factors, precipitation and temperature are regarded as primary factors determining the rate of respiration and photosynthesis in plants, thereby affecting the vegetation vitality (Biebl and Mcroy, 1971). In this study, the relationships between NDVI and precipitation as well as NDVI and temperature were investigated for NDVI and the precipitation and temperature of previous 0 to 3 months on the basis of eastern China, the ten administrative units, and the 184 meteorological stations both on annual and seasonal scales. The maximum correlation coefficients between NDVI and precipitation as well as NDVI and temperature were selected based on four correlation coefficients, and the lag time for maximum NDVI response to changes in precipitation and temperature was determined on the basis of the corresponding time period of the maximum correlation coefficient.

The relationships between NDVI and precipitation as well as NDVI and temperature on annual scale present in Table 5-2 and Table 5-3, respectively. In eastern China, the maximum correlation coefficients between the annual NDVI and temperature are generally higher than that of between the annual NDVI and precipitation during the same period. The annual NDVI has the largest correlation with the precipitation of previous 1 month with a correlation coefficient of 0.872 in eastern China, while the annual NDVI is mostly affected by the concurrent temperature (the temperature of previous 0 month) with a correlation coefficient of 0.945 (Table 5-2, Table 5-3, and Table 5-4), therefore, suggesting that the maximum response of annual NDVI to precipitation presents a 1-month time lag, and the maximum response of annual NDVI to temperature shows a 0-month time lag in eastern China.

The maximum correlation coefficients between NDVI and precipitation as well as NDVI and temperature in spring, summer, and autumn were computed for the study area, and all of the maximum correlation coefficients are statistically significant at the $p<0.01$ level. The maximum correlation coefficients of NDVI in response to precipitation are higher in autumn than in spring and summer, whereas the maximum correlation coefficients of

NDVI in response to temperature are larger in spring than in autumn, followed by in summer. It is worth noting that the lowest maximum correlation coefficients between NDVI and precipitation as well as NDVI and temperature are both reported in summer, indicating that the response of NDVI to changes in precipitation and temperature is weaker in summer than in spring and autumn.

Table 5-2 and Table 5-3 indicate that in spring, summer, and autumn the maximum response of NDVI to temperature is more noticeable than the maximum response of NDVI to precipitation in eastern China. In spring and autumn, NDVI shows the maximum relationship with the precipitation of previous 1 month and the temperature of previous 0 month, respectively (Table 5-4), indicating a 1-month lag time between NDVI and precipitation and no time lag between NDVI and temperature both in spring and autumn. However, a 2-month lag time between NDVI and precipitation and a 1-month lag time between NDVI and temperature are reported in summer over the study area.

The maximum response of annual NDVI to temperature is more pronounced than the maximum response of annual NDVI to precipitation: namely, temperature is the dominant factor controlling the vegetation activity in eastern China. This conclusion is in line with former studies. For instance, Cui (2010) examined the relationships between NDVI and precipitation as well as NDVI and temperature for eastern China and found that the maximum response of NDVI to the variation of temperature was stronger than that of between NDVI and precipitation. Chen et al. (2001) analyzed the impact of the variations of precipitation and temperature on NDVI over China. The results of this study demonstrated that temperature was regarded as the main climate driving factor affecting vegetation growth in the eastern coastal areas of China. Peng et al. (2015) computed the correlation coefficients between NDVI and precipitation as well as NDVI and temperature in 210 meteorological stations in eastern China, and the results showed that the absolute value of the correlation coefficients between NDVI and temperature was higher than that of between NDVI and precipitation in 120 meteorological stations. Consequently, the temperature was considered as the primary driving factor of vegetation change in eastern China. Peng et al. (2011) investigated the changing trending of vegetation growth and its climate driving factors in China. The result pointed out that the vegetation

activity in the growing season (April to October) in the east of China was dominated by temperature.

The maximum response of NDVI to temperature is considerably pronounced in spring and autumn in comparison with the maximum response of NDVI to temperature in summer in northern mid- to high-latitudes (Zeng et al., 2013, Mao et al., 2012). Figure 5-2, Figure A-1, Table 5-1, and Table A-2 indicate that in spring and autumn changes of both NDVI and temperature followed each other fairly well in eastern China with a similar upward trend during the study period. The temperature in spring and autumn had increased with a magnitude of 0.0418℃ $year^{-1}$ and 0.0738℃ $year^{-1}$, respectively, from 2001 to 2016. Meanwhile, the NDVI in spring and autumn had changed with an increasing rate of 0.0003 $year^{-1}$ and 0.0012 $year^{-1}$, individually. Many scholars have demonstrated that temperature changes at the beginning and end of the growing season have significant impacts on vegetation variability (Angert et al., 2005, Piao et al., 2008). The rise in spring and autumn temperatures has extended the growing season and further enhanced the vegetation productivity in the northern hemisphere in the context of global warming (Richardson et al., 2010, Piao et al., 2008, Zhang et al., 2013b). Thus the above views are further confirmed by upward trends of NDVI and temperature for spring and autumn and the corresponding correlation coefficients between NDVI and temperature in eastern China.

Figure A-2 and Table A-2 show that the temperature had increased with a magnitude of 0.0381℃ $year^{-1}$ in summer from 2001 to 2016. Meanwhile, the NDVI had declined with a changing rate of 0.0013 $year^{-1}$ across eastern China. These results are in line with most of the previous studies, which evidenced that recent warmer and drier summer climatic conditions led to a decline in plants growth over Eurasia and the northern hemisphere (Angert et al., 2005, Piao et al., 2011, Park and Sohn, 2010, Lotsch et al., 2005). Temperature in summer resulted in an increase in evapotranspiration rate and in a decline in soil moisture, thereby in reducing or even curbing the vegetation activity in eastern China. It has to be mentioned that, considering the correlation coefficients between NDVI and temperature on seasonal scale, Cui (2010) pointed out that the highest correlation coefficients are in autumn, while a different phenomenon was found in our study. We found that the correlation coefficient between NDVI and temperature is

higher in spring than in autumn, followed by in summer, which is not in line with the results generated by Cui (2010).

The lag time for maximum NDVI response to precipitation is more apparent than the lag time for maximum NDVI response to temperature, and the lag time between NDVI and precipitation as well as NDVI and temperature is apparently longer in summer than in spring and autumn. The conclusions provided above are in line with the results of previous studies. Cui (2010) analyzed the lag time for maximum NDVI response to precipitation and temperature in eastern China and demonstrated that the NDVI was mostly related to the temperature with a time lag of 10 days, but the NDVI primarily reacted to the precipitation with a lag of about 30 days on annual scale. Cui (2010) further revealed the lag time for maximum NDVI response to climate factors on seasonal scale. The lag time for maximum NDVI response to precipitation and temperature was longer in summer than in spring and autumn. For instance, the maximum correlation coefficients between NDVI and temperature were acquired when the temperature preceding NDVI by 20 days in spring and autumn but 40 days in summer. Liang et al. (2015) firstly investigated the spatial and temporal patterns of NPP in China and then calculated the relationships between NPP and precipitation as well as NPP and temperature. The results of this study suggested that no obvious time lag effects were observed in NPP responses to temperature, while NPP presented an obvious lag time to changes in precipitation. Zeng et al. (2013) detected the time lag effects between NDVI and climate factors on global scale and turned out that vegetation growth was mostly influenced by 1-month preceding precipitation and concurrent temperature. In addition, in northern Patagonia, the annual and seasonal NDVI were significantly related to previous precipitation. Moreover, no significant relationship was detected between NDVI and concurrent precipitation (Fabricante et al., 2009).

For a better understanding of the seasonal characteristics of NDVI change in regard to climate variation, the maximum correlation coefficients between NDVI and precipitation as well as NDVI and temperature for each administrative units were carried out in spring, summer, and autumn. Table 5-2 shows that all of the maximum correlation coefficients between NDVI and temperature are statistically significant at the $p<0.01$ level. All of the maximum correlation coefficients between NDVI and precipitation are statistically

significant at the $p<0.01$ level, except for the correlation coefficients in Jiangsu and Shanghai for spring and in Shanghai, Zhejiang, and Fujian for summer (Table 5-3).

We noticed that the maximum correlation coefficients between NDVI and temperature are generally greater in spring than in autumn (in seven out of the ten administrative units in spring are greater than in autumn) (Table 5-3). However, the maximum correlation coefficients between NDVI and precipitation in nine out of the ten administrative units are greater in autumn than in spring except for in Fujian (Table 5-2). Noteworthy point is that the maximum correlation coefficients between NDVI and temperature are generally higher than that of between NDVI and precipitation for the same period, implying that temperature plays a more important role in controlling vegetation growth, and it appears to be a better climate driving factor for explanation the dynamic changes of vegetation in the ten administrative units.

Comparison of the lag time between NDVI and precipitation as well as NDVI and temperature in the ten administrative units, the lag time for maximum NDVI response to precipitation is significantly pronounced than the lag time for maximum NDVI response to temperature, particularly in summer and autumn (Table 5-4). In spring and autumn, the NDVI is mostly correlated with the concurrent temperature, except for Liaoning, a place where the NDVI is influenced by the temperature of previous 1 month in spring. Furthermore, distinct and complex lag time is shown in summer for maximum NDVI response to temperature in the ten administrative units. NDVI in Beijing, Tianjin, Hebei, Jiangsu, Shanghai, Zhejiang, as well as in Fujian is closely associated with the temperature of previous 2 months, while NDVI in Liaoning and Shandong presents 0-month and 1-month lag time to changes in temperature, respectively.

In terms of the lag time for maximum NDVI response to precipitation and temperature, the lag time is more complex and apparent for maximum NDVI response to changes in precipitation. 2-month lag time is observed in Zhejiang for spring and in Shanghai, Zhejiang, and Fujian for summer. In addition, NDVI shows a 1-month lag time to precipitation in nine out of the ten administrative units in autumn except for Beijing. It is north notifying that NDVI in Guangdong is mostly affected by the preceding temperature and precipitation of 3 months.

Table 5-2. The maximum correlation coefficient between NDVI and precipitation for eastern China and the ten administrative units

NP_MCC	Beijing	Tianjin	Hebei	Liaoning	Shanghai	Jiangsu	Zhejiang	Fujian	Shandong	Guangdong	Eastern China
Annual	0.808 **	0.817 **	0.887 **	0.822 **	0.463 **	0.609 **	0.543 **	0.591 **	0.837 **	0.641 **	0.872 **
Spring	0.623 **	0.621 **	0.749 **	0.653 **	0.182	0.290 *	0.417 **	0.543 **	0.656 **	0.491 **	0.715 **
Summer	0.547 **	0.565 **	0.648 **	0.574 **	0.230	0.536 **	0.237	0.155	0.704 **	0.482 **	0.620 **
Autumn	0.687 **	0.725 **	0.778 **	0.811 **	0.472 **	0.588 **	0.559 **	0.540 **	0.732 **	0.567 **	0.852 **
* Significant at P < 0.05 * *Significant at P < 0.01											

Table 5-3. The maximum correlation coefficient between NDVI and temperature for eastern China and the ten administrative units

NT_MCC	Beijing	Tianjin	Hebei	Liaoning	Shanghai	Jiangsu	Zhejiang	Fujian	Shandong	Guangdong	Eastern China
Annual	0.935 **	0.912 **	0.921 **	0.919 **	0.883 **	0.825 **	0.943 **	0.876 **	0.897 **	0.854 **	0.945 **
Spring	0.943 **	0.956 **	0.960 **	0.928 **	0.533 **	0.523 **	0.942 **	0.875 **	0.902 **	0.779 **	0.967 **
Summer	0.642 **	0.724 **	0.812 **	0.680 **	0.772 **	0.816 **	0.558 **	0.482 **	0.834 **	0.553 **	0.849 **
Autumn	0.905 **	0.917 **	0.878 **	0.892 **	0.889 **	0.883 **	0.87 **	0.729 **	0.804 **	0.804 **	0.897 **
* Significant at P < 0.05 * *Significant at P < 0.01											

Table 5-4. The lag time for maximum NDVI response to precipitation and temperature for eastern China and the ten administrative units

NP_TimeLag	Beijing	Tianjin	Hebei	Liaoning	Shanghai	Jiangsu	Zhejiang	Fujian	Shandong	Guangdong	Eastern China
Annual											
Spring											
Summer											
Autumn											

NT_TimeLag	Beijing	Tianjin	Hebei	Liaoning	Shanghai	Jiangsu	Zhejiang	Fujian	Shandong	Guangdong	Eastern China
Annual											
Spring											
Summer											
Autumn											

5.2.2 The spatial pattern of maximum NDVI in response to climate factors

5.2.2.1 The spatial pattern of maximum NDVI in response to precipitation

To explore the spatial characteristics of NDVI in response to climate variability both on annual and seasonal scales, the correlation coefficients between NDVI and the precipitation and temperature of previous 0 to 3 months for each meteorological station were calculated on the basis of the monthly NDVI time series and the data of the monthly precipitation and temperature of 184 selected meteorological stations. Then, the maximum correlation coefficients between NDVI and precipitation as well as NDVI and temperature for each meteorological station were selected and displayed to monitor the spatial pattern of maximum NDVI in response to climate variables. The significant level of each maximum correlation coefficient was tested by t-test. The spatial pattern of the maximum correlation coefficients reports the spatial characteristics of the driving effects of precipitation and temperature on NDVI change. Hence, the operating mechanisms of the driving forces of precipitation and temperature on vegetation growth are illustrated in Figure 5-17, Figure 5-18, Figure 5-20, and Figure 5-21, respectively.

Figure 5-17(a) shows that the maximum correlation coefficients of the annual NDVI to precipitation display a distinct spatial pattern in eastern China. Geographically, the response of the annual NDVI to precipitation is more pronounced in the north of eastern China than in the south. The annual NDVI is positively associated with the precipitation at all of the meteorological stations, and 97% of the maximum correlation coefficients are statistically significant at the $p<0.01$ level, as shown in Figure 5-16(b). Figure 5-17(a) and Figure 5-16(a) show that the maximum correlation coefficients between the annual NDVI and precipitation ranging from 0.75 to 1 account for 4% of the total meteorological stations, which are mainly distributed in the north of Hebei. Areas expansion from the north of Jiangsu to Liaoning, except for the north of Hebei, are dominated by the maximum correlation coefficients ranging from 0.5 to 0.75, which account for 44% of the total meteorological stations. However, the maximum correlation coefficients distributed from the middle of Jiangsu to Guangdong basically range from 0.25 to 0.5, which occupy 45% of the total meteorological stations.

Figure 5-17(b) and Figure 5-18(a) and (b) display the spatial pattern of the seasonal maximum correlation coefficients between NDVI and precipitation. The maximum correlation coefficients between NDVI and precipitation are generally larger in spring and autumn than in summer. The spatial distribution of the maximum correlation coefficients in spring and autumn is homologous. As shown in Figure 5-16(b), accounting for about 50% and 58% of the maximum correlation coefficients in spring and autumn are statistically significant at the $p<0.01$ level, respectively. However, in summer, only 21% of the maximum correlation coefficients are statistically significant at the $p<0.01$ level.

In spring and autumn, the maximum correlation coefficients of NDVI in response to precipitation in most of the meteorological stations located in the north of the study area, covering Liaoning, Hebei, Beijing, Tianjin, as well as in Shandong, are larger than 0.5. The maximum correlation coefficients of NDVI in response to precipitation located in the south of the study area, including Jiangsu, Shanghai, Zhejiang, Fujian, and Guangdong, are generally from 0 to 0.5. In spring, the NDVI is slightly and negatively correlated with the precipitation in five meteorological stations, which are located in the eastern coastal areas of eastern China. In summer, the maximum correlation coefficients between NDVI and precipitation from 0 to 0.25 and from 0.25 to 0.5 account for 46% and 40% of the total meteorological stations (Figure 5-16(a)), respectively, which coexist across Liaoning, Jiangsu, Shanghai, Fujian, Zhejiang, as well as in Guangdong. Moreover, the negative maximum correlation coefficients of NDVI in response to precipitation account for 6% of the total meteorological stations in summer (Figure 5-16(a)), which are mainly distributed in the southwest of Fujian and the junction areas of Jiangsu and Zhejiang.

Spatially, the maximum correlation coefficients of NDVI in response to precipitation are generally higher in the north and lower in the south of the study area, suggesting that precipitation plays a higher-level control on vegetation growth in the north of the study area. This result is in agreement with the views of previous studies that NDVI in the north of eastern China is closely and positively correlated with the precipitation (Duan et al., 2011, Cui, 2010, Peng et al., 2015). Areas located in the north of eastern China are controlled by sub-humid and semi-arid climate. Thus, precipitation plays a vital role in vegetation growth (Yin et al., 2018). Figure A-3 and Table A-1 show that precipitation had considerably increased in Liaoning, Beijing, Tianjin, as well as in Hebei from 2001 to

2016. Part of the increased precipitation could directly retain in the soil and then improve the soil moisture. Consequently, the soil moisture could provide enough water to promote the photosynthetic rates, thereby improving vegetation productivity (Duan et al., 2011, Yang et al., 2014). In contrast, areas located in the south of eastern China (from Guangdong to the south of Jiangsu) are controlled by a humid climate. Thus, the relationship between NDVI and precipitation is less pronounced in the south of the study area due to sufficient precipitation throughout a year (Table A-1 and Figure A-5).

In addition, precipitation is relatively rich in the south of eastern China and poor in the north of eastern China. Due to the sufficient precipitation in the south of eastern China, the water supply could satisfy the demand for vegetation activities. Therefore, the precipitation is not the decisive factor determining the vegetation growth in this region (Cui, 2010, Xu et al., 2003). All explanations provided above demonstrate why the maximum correlation coefficients between NDVI and precipitation are relatively lower in the south than in the north of eastern China for all three seasons.

Temporally, the maximum correlation coefficients of NDVI in response to precipitation are generally higher in spring and autumn than in summer, suggesting that the impact of precipitation on vegetation growth is less pronounced in summer than in spring and autumn. The uneven precipitation in spring, summer, and autumn is the underlying cause of the differences in the seasonal maximum correlation coefficient. Precipitation is more plentiful in summer than in spring and autumn, particularly in the south of the study area. In summer, the relatively richer precipitation is basically sufficient for vegetation growth across the study area. The excessive precipitation could not continually improve the photosynthesis rate of plants, but it instead increased the surface latent heat flux of evaporation. The increasing evaporation resulted in an increase in cloud cover, thereby curbing the photosynthesis and respiration in plants (Liang et al., 2015, Piao et al., 2006a). These explanations answer the questions why NDVI in response to precipitation in more pronounced in spring and autumn than in summer and why in some meteorological stations in the south of the study area the maximum correlation coefficients between NDVI and precipitation are negative. These conclusions are also confirmed in previous studies (Zhao et al., 2001, Cui, 2010).

Additionally, the maximum correlation coefficients between NDVI and precipitation in all seasons are comparatively lower in Guangdong, Fujian, Zhejiang, Shanghai, and Jiangsu. On the one hand, densely interconnected water channels are distributed in these administrative units. On the other hand, farmland in these regions is dominated by irrigated crops. The water demand for vegetation growth can, therefore, supply by a large area of artificial irrigation and surface water resources at a certain level, which reduces the sensitivity of the vegetation growth to changes in precipitation.

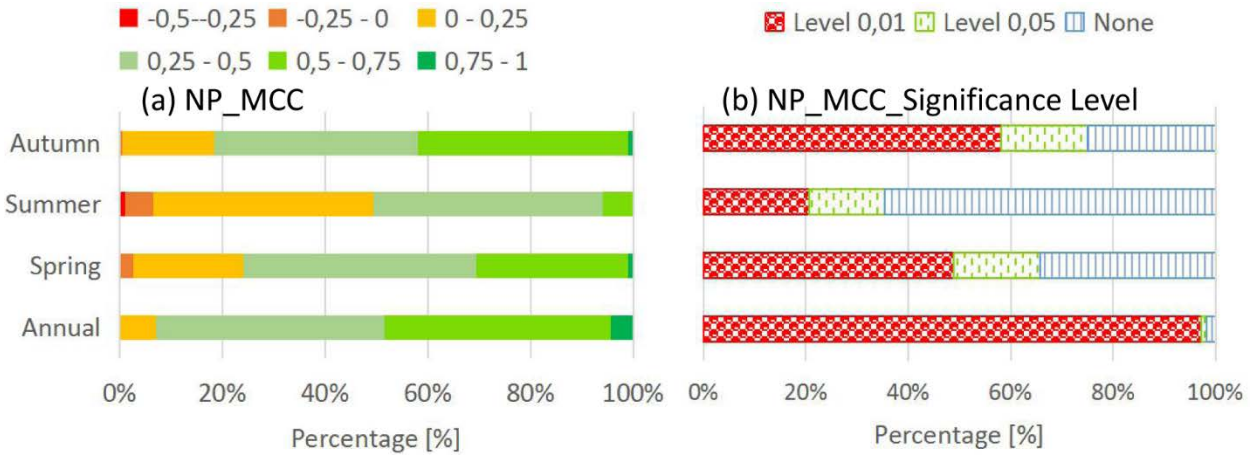

Figure 5-16. The statistical results of the maximum correlation coefficient between NDVI and precipitation and the significance level of the maximum correlation coefficient on annual and seasonal scales

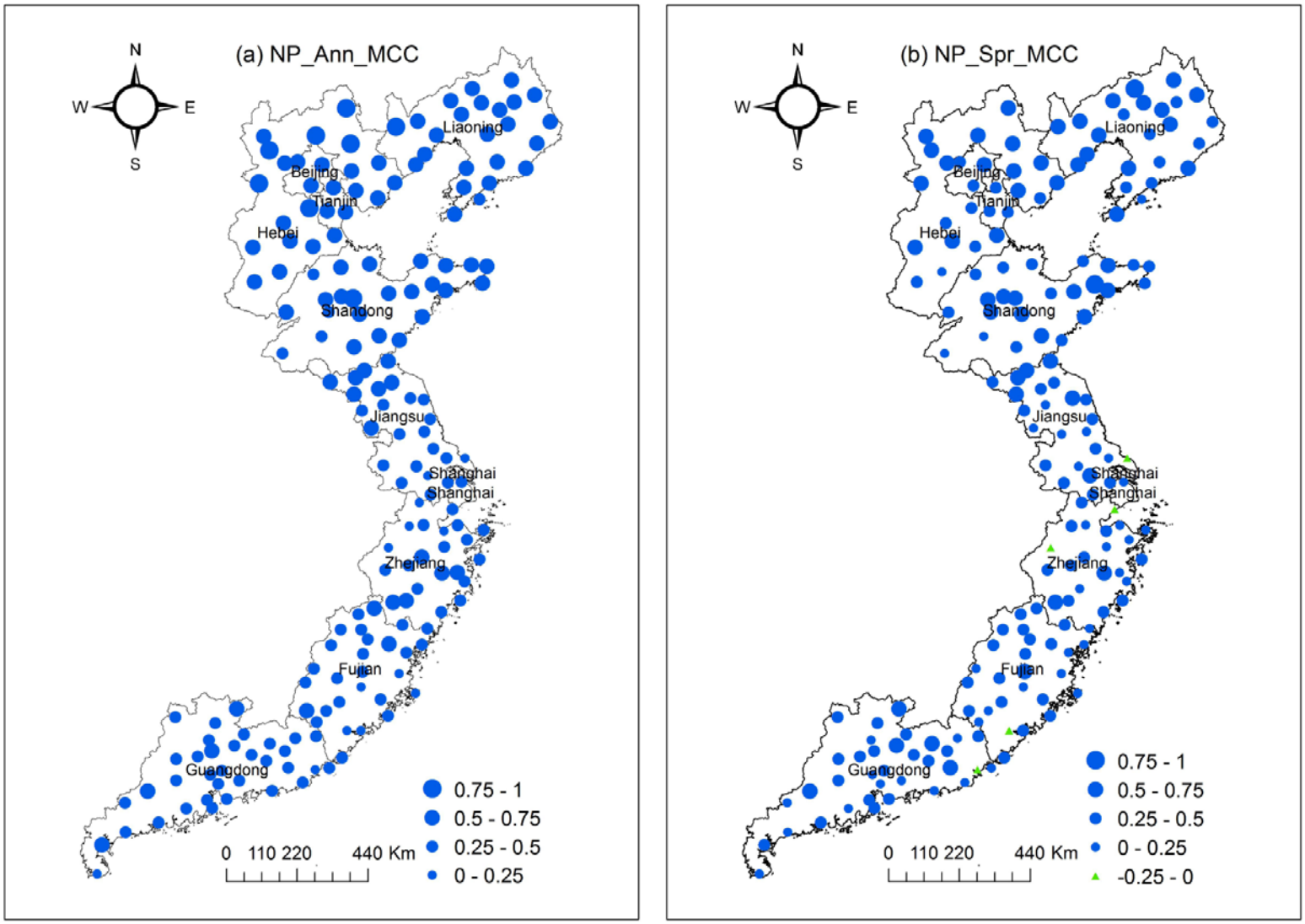

Figure 5-17. Spatial distribution of the maximum correlation coefficient between annual NDVI and precipitation (a) as well as spring NDVI and precipitation (b)

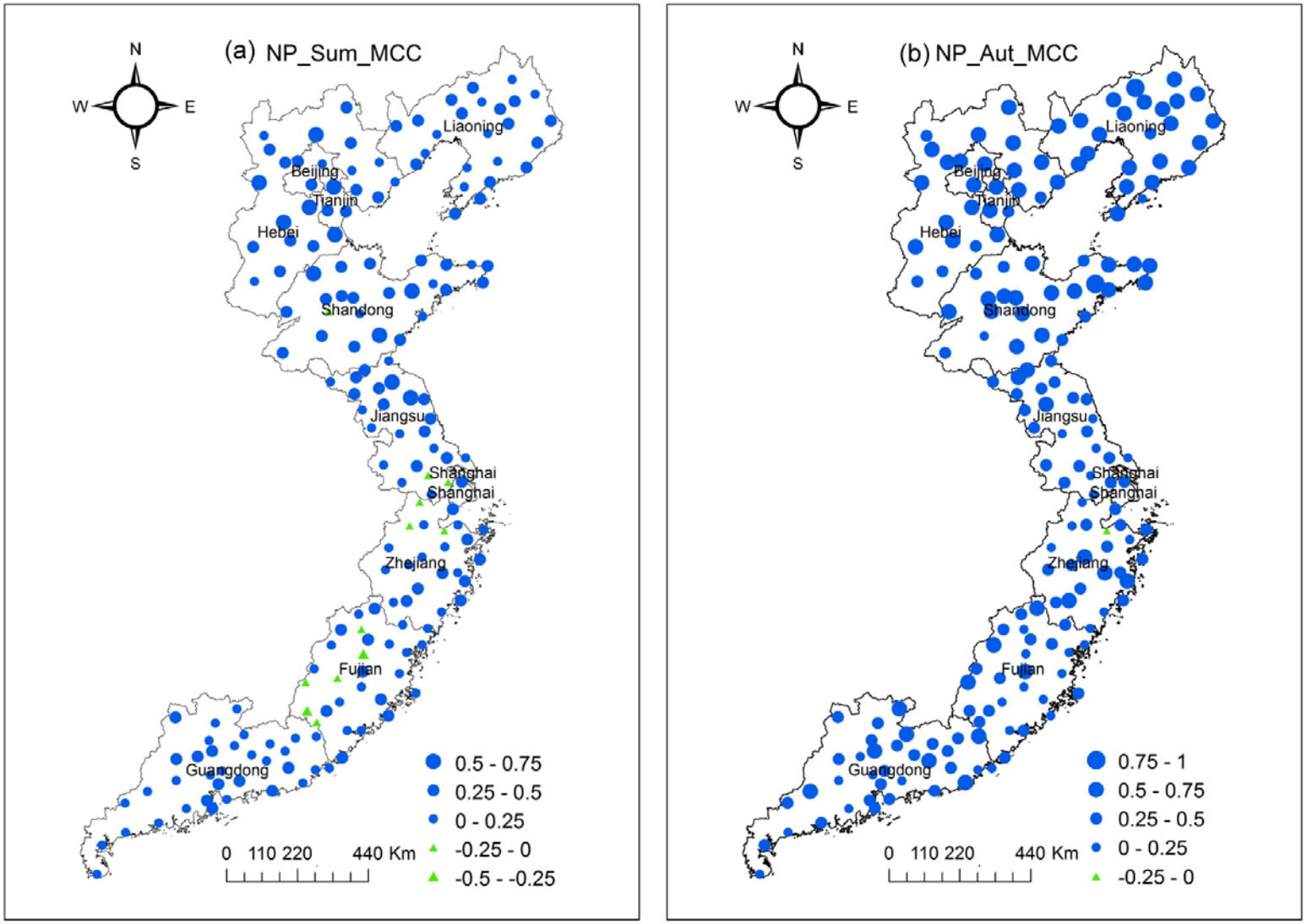

Figure 5-18. Spatial distribution of the maximum correlation coefficient between summer NDVI and precipitation (a) as well as autumn NDVI and precipitation (b)

5.2.2.2 The spatial pattern of maximum NDVI in response to temperature

Similar to the spatial distribution of the maximum correlation coefficients between the annual NDVI and precipitation, the maximum correlation coefficients of the annual NDVI in response to temperature distributed from the north of Jiangsu toward Liaoning are more pronounced than that of distributed from the middle of Jiangsu toward Guangdong. The annual NDVI and temperature present a positive relationship at all of the meteorological stations, and 100% of the maximum correlation coefficients between the annual NDVI and temperature are statistically significant at the level of $p<0.01$ (Figure 5-19(b)). In terms of the dominant factor in each meteorological station, 183 out of 184 meteorological stations are primarily controlled by temperature on annual scale.

Comparison of the maximum correlation coefficients between the annual NDVI and precipitation as well as the annual NDVI and temperature (Figure 5-17(a) and Figure 5-20(a)), temperature shows a stronger regulation on the annual NDVI variation than the effects of precipitation on the annual NDVI across the study area. The maximum correlation coefficients between the annual NDVI and temperature ranging from 0.75 to 1 account for around 45% of the total meteorological stations, which exceeds the proportion of the maximum correlation coefficients between the annual NDVI and precipitation ranging from 0.75 to 1 by 41%. These meteorological stations are mainly distributed from the north of Jiangsu to Liaoning and in the east of Zhejiang. The maximum correlation coefficients between the annual NDVI and temperature ranging from 0.5 to 0.75 account for around 42% of the meteorological stations, which are mostly distributed from the middle of Jiangsu to Guangdong. Only 13% of the maximum correlation coefficients are lower than 0.5, which are generally located in the eastern coastal areas of Fujian and Guangdong (Figure 5-19(a) and Figure 5-20(a)).

In spring and autumn, the maximum correlation coefficients of NDVI in response to temperature are basically positive and display a similar spatial pattern (Figure 5-20(b) and Figure 5-21(b)). As detailed in Figure 5-19(b), 74% and 85% of the maximum correlation coefficients between NDVI and temperature in spring and autumn are statistically significant at the $p<0.01$ level, respectively. The overall relationship between NDVI and temperature in summer is relatively weaker or even negative across eastern China. The meteorological stations located in Jiangsu and the junction areas of

Shandong and Hebei, the maximum correlation coefficients between NDVI and temperature in these meteorological stations are higher than the surrounding meteorological stations (5-18(a)). Moreover, only 35% of the maximum correlation coefficients pass the $p<0.01$ significant level in summer. It is worth mentioning that the vegetation cover variation is decisively controlled by temperature at 160 meteorological stations in spring, 124 meteorological stations in summer, and 170 meteorological stations in autumn.

Similarly, in spring and autumn, the maximum correlation coefficients between NDVI and temperature distributed in Shandong, Hebei, Tianjin, Beijing, as well as Liaoning are higher than 0.75 (Figure 5-20(b) and Figure 5-21(b)). However, the maximum correlation coefficients between NDVI and temperature distributed in the north of Jiangsu are generally greater in autumn than in spring. In summer, the maximum correlation coefficients of NDVI in response to temperature ranging from 0.75 to 1 account for around 8% of the total meteorological stations mainly distributed in Jiangsu and the junction areas of Shandong, Hebei, and Tianjin. The maximum correlation coefficients between NDVI and temperature are relatively lower in Zhejiang, Fujian, and Guangdong. Figure 5-21(a) shows that in some meteorological stations of the three administrative units, NDVI is negatively related to the temperature, which accounts for 6% of the total meteorological stations.

Geographically, the maximum correlation coefficients between NDVI and temperature gradually decrease with the decrease in latitude in eastern China both on annual and seasonal scales. This phenomenon has been evidenced by previous studies (Peng et al., 2015, Lin et al., 2007, Li and Shi, 2000). Li and Shi (2000) pointed out that the correlation coefficients between NDVI and temperature increased from the southeastern to the northwestern of China. Lin et al. (2007) further concluded that the seasonal variability of NDVI in Hunan was mostly affected by temperature, and the impact of temperature on NDVI enlarged from the south toward the north of Hunan. Temperature plays an essential role in affecting the rate of vegetation growth and development but differs in plant species (Hatfield and Prueger, 2015).

We further displayed the spatial pattern of the correlation coefficients between NDVI and precipitation as well as NDVI and temperature both on annual and seasonal scales.

However, distinctive spatial differences of the correlation coefficients between NDVI and precipitation as well as NDVI and temperature are observed between our results and the results derived from Cui (2010) and Li et al. (2019). For instance, Li et al. (2019) evidenced that NDVI is negatively associated with temperature in the junction area of Shandong and Hebei, but an opposite correlation was observed in the same region.

Furthermore, in our study, we found that the correlation coefficients between NDVI and precipitation in 40 out of 52 meteorological stations and the correlation coefficients between NDVI and temperature in 43 out of 52 meteorological stations are positive in Zhejiang, Fujian, and Guangdong in summer, while this result is not in line with the result generated by Cui (2010). Cui (2010) displayed that all of the correlation coefficients between NDVI and precipitation are negative in summer, except for three meteorological stations, and all of the correlation coefficients between NDVI and temperature are positive in summer in Zhejiang, Fujian, and Guangdong. On the one hand, the disagreement can be attributed to the data source, Cui (2010) adopted SPOT-4 VEGETATION NDVI with a 1 km spatial resolution to analyze the relationships between NDVI and climate variables, while we employed MODIS NDVI with a 250 m spatial resolution to be the data source in our study, and MODIS NDVI is considered to be a more precise and robust data source to reflect the long-term vegetation cover. On the other hand, the disagreement can be ascribed to the difference of the study period. Cui (2010) investigate the relationships between NDVI and climate variables from 1998 to 2008, but from 2001 to 2016 in our study.

Figure 3-5 shows that lands in Zhejiang, Fujian, and Guangdong are covered by evergreen broadleaf forest, while lands in Jiangsu, Shandong, Tianjin, the south of Hebei, and the west of Liaoning are dominated by farmlands and grasslands. As demonstrated by de Jong et al. (2013) and Shen et al. (2013) that the farmlands and grasslands showed a higher sensitivity to changes in temperature. Thus, the response of NDVI to temperature in the north of the study area is pronounced than that in the south of the study area, which is partly ascribed to the spatial distribution of the land use types.

Previous studies have concentrated on analyzing the response of vegetation cover change to a single force or on a single scale (Kileshye Onema and Taigbenu, 2009, Kong et al., 2017, Krishnaswamy et al., 2014, Bennie et al., 2006, Luck et al., 2009). The

relationships between NDVI and precipitation as well as NDVI and temperature and the time lag effects of vegetation variability to climate variables are less considered, which tend to increase the uncertainty of the research results. For instance, Peng et al., (2015) computed the correlation coefficients between NDVI and precipitation as well as NDVI and temperature for each meteorological station in eastern China on annual scale, but relationships between NDVI and precipitation as well as NDVI and temperature on seasonal scale and the lag time for maximum NDVI response to climate variation is not taken into consideration. In our study, the relationships between NDVI and precipitation as well as NDVI and temperature are investigated for each administrative unit and meteorological station both on annual and seasonal scales, and the lag time for maximum NDVI response to climate variation is investigated.

Regarding the maximum correlation coefficients between NDVI and temperature on seasonal scale, the response of NDVI to temperature is generally weaker in summer than in spring and autumn. Particularly, the maximum correlation coefficients between NDVI and temperature of some meteorological stations in the south of the study area are lower than 0, indicating a negative relationship between NDVI and temperature in these regions in summer. Figure A-6(c) shows that temperature in summer is higher in the south and lower in the north of the study area. Moreover, the overall precipitation and temperature are remarkably greater in summer than in spring and autumn across eastern China (Figure A-5 and Figure A-6). An optimum temperature can prolong the growing season and favor vegetation growth (Peng et al., 2011). However, along with the vegetation growth, the NDVI reaches its full potential in summer and the increasing temperature cannot continually promote the NDVI value (Kern et al., 2016). In addition, the high temperature can increase evapotranspiration and decrease soil moisture, thereby aggravating water stress and inhabiting the vegetation growth (Duan et al., 2011). This would be a reason why NDVI is weakly or even negatively correlated with the temperature in summer in some meteorological stations.

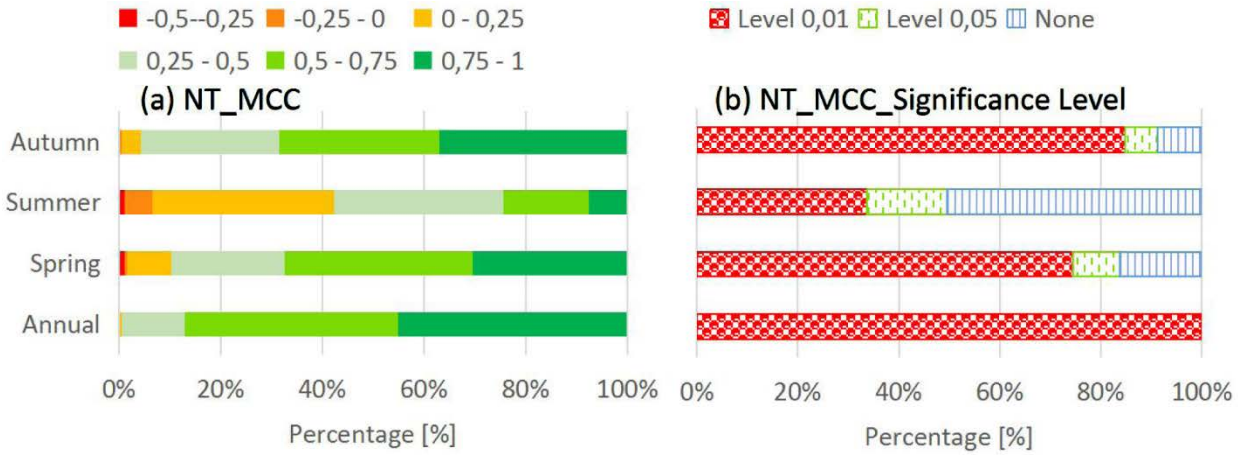

Figure 5-19. The statistical results of the maximum correlation coefficient between NDVI and temperature and the significance level of the maximum correlation coefficient on annual and seasonal scales

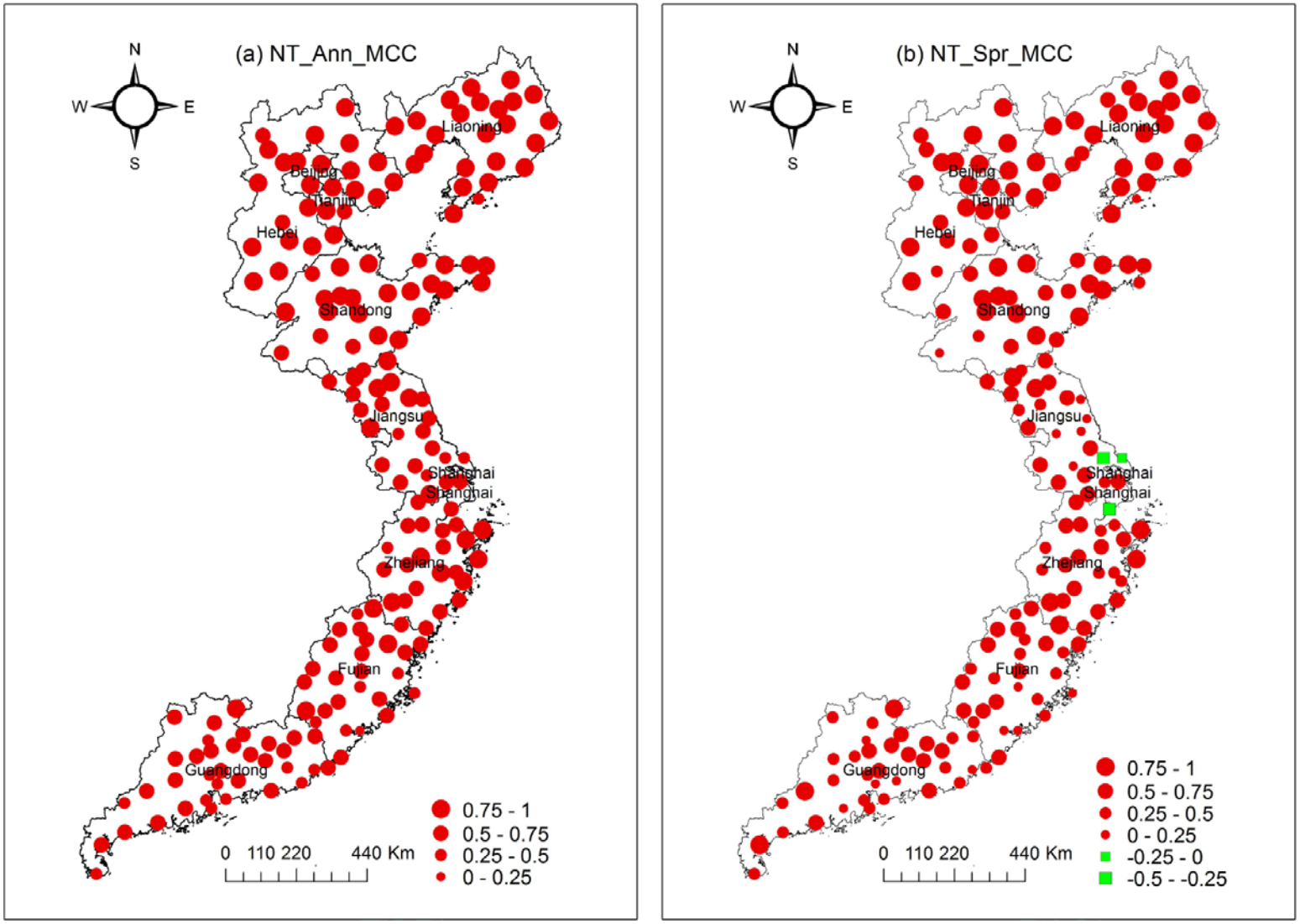

Figure 5-20. Spatial distribution of the maximum correlation coefficient between annual NDVI and temperature (a) as well as spring NDVI and temperature (b)

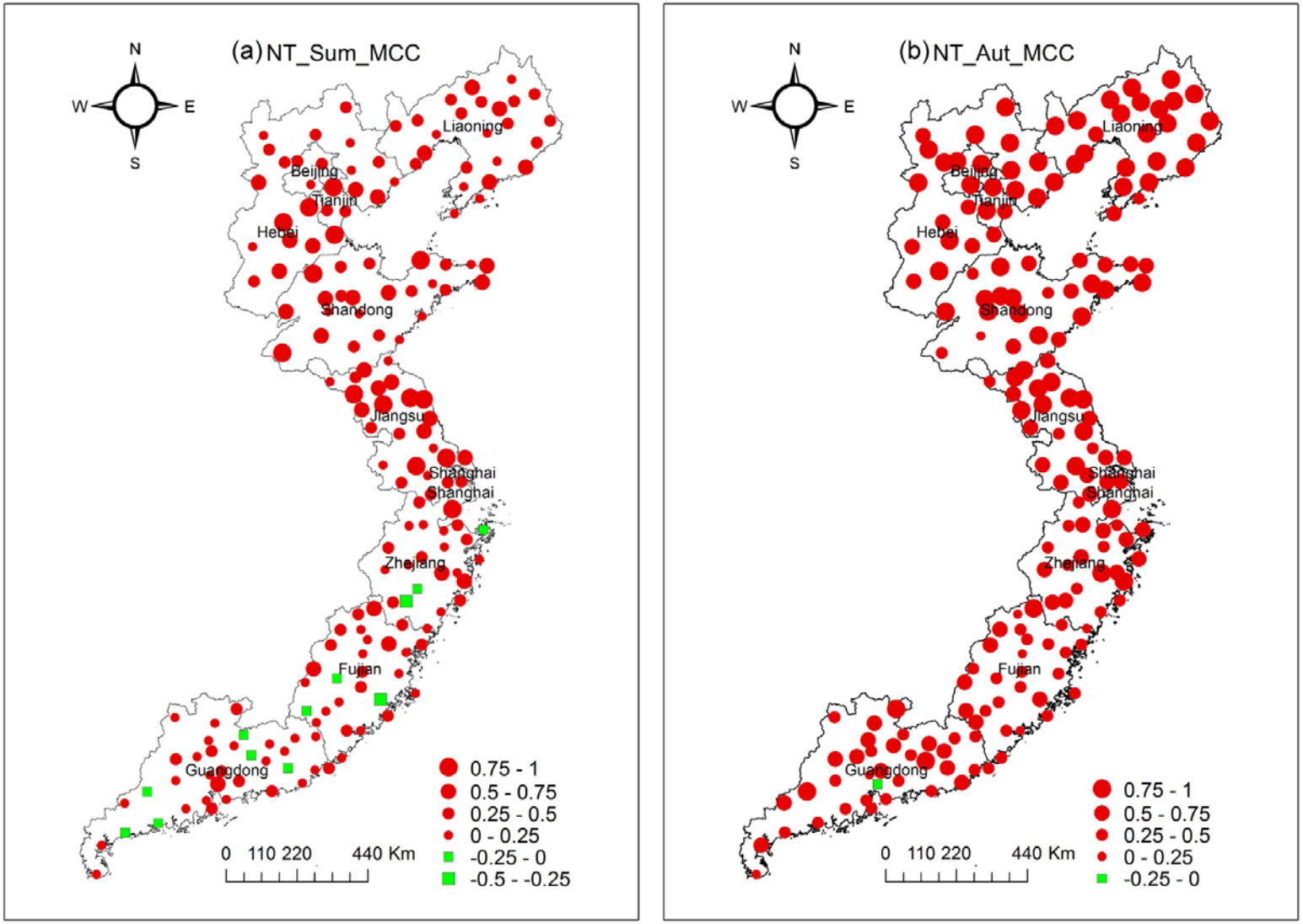

Figure 5-21. Spatial distribution of the maximum correlation coefficient between summer NDVI and temperature (a) as well as autumn NDVI and temperature (b)

5.2.3 The spatial pattern of lag time for maximum NDVI response to climate factors

5.2.3.1 The spatial patterns of lag time for maximum NDVI response to precipitation

Influenced by the spatial heterogeneity of Earth's ecosystems, the lag time for maximum NDVI response to precipitation and temperature is anticipated to show diverse spatial patterns (Wu et al., 2015, Braswell et al., 1997). In this chapter, the lag time between NDVI and precipitation as well as NDVI and temperature is investigated against the background of the maximum correlation coefficients for each meteorological station in eastern China both on annual and seasonal scales. The lag time for maximum NDVI response to precipitation and temperature is identified on the basis of the corresponding time period of the maximum correlation coefficient.

In eastern China, the lag time for maximum annual NDVI response to precipitation reports clear spatial differences (Figure 5-23(a)). Annual NDVI distributed from the middle of Jiangsu to Liaoning and in the eastern coastal areas of Zhejiang and Fujian shows no lag time on changes in precipitation, which accounts for 59% of the total meteorological stations (Figure 5-22), implying that the annual NDVI in these regions is mostly associated with the concurrent precipitation. However, the lag time between the annual NDVI and precipitation in the north of Zhejiang and northeast of Guangdong is dominated by a 1-month lag time. The annual NDVI presents 2- to 3-month lag time to changes in precipitation in many parts of Fujian and Guangdong. The lag time for maximum annual NDVI response to precipitation shows great geographic differences and less spatial patterns in Shanghai, Zhejiang, Fujian, and Guangdong, indicating that the precipitation of previous 2 to 3 months has considerable impacts on vegetation growth in these regions. It is worth noticing that the proportion of the 1-month, 2-month, and 3-month lag time for maximum annual NDVI response to precipitation account for 21%, 13%, and 7% of the total meteorological stations, respectively (Figure 5-22).

The lag time for maximum NDVI response to precipitation display complex spatial patterns on seasonal scale. NDVI in 39% in spring, 27% in summer, and 28% in autumn of the total meteorological stations show no lag time to changes in precipitation. The proportion of the 2-month and 3-month lag time for maximum NDVI response to

precipitation account for 21% and 33% of the total meteorological stations in summer, individually (Figure 5-22), which is considerably higher than in spring and autumn.

Figure 5-23(b) and Figure 5-24(b) shows that, in spring and autumn, the lag time for maximum NDVI response to precipitation in Liaoning, Beijing, Tianjin, Hebei, as well as in Shandong is generally dominated by 0- and 1-month lag time. Furthermore, in spring the vegetation growth is mostly associated with the precipitation of previous 2 to 3 months in Jiangsu, Shanghai, and Zhejiang. However, 3-month lag time for maximum NDVI response to precipitation is detected in a relative number of meteorological stations of Fujian and Guangdong in autumn, implying that NDVI is maximally affected by the precipitation of previous 3 months in these regions. Figure 5-24(a) shows that in summer the lag time of 0 to 3 months for maximum NDVI response to precipitation coexist across the study area, and the NDVI in the south of the study area tends to report a longer time lag to changes in precipitation, especially in Zhejiang, Fujian, and Guangdong.

The lag time for maximum NDVI response to precipitation has noticed by many scholars. The time lag effects of different vegetation types in response to the same climate factor and the same vegetation type in response to different climate factors are carried out (Braswell et al., 1997, Cui, 2010, Liang et al., 2015, Wu et al., 2015, Piao et al., 2006b, Potter and Brooks, 1998). In this study, we observe that the annual NDVI in the north of eastern China, including Liaoning, Beijing, Tianjin, Hebei, Shandong, as well as in most areas of Jiangsu, shows the greatest reaction with the concurrent precipitation, whereas the annual NDVI in Zhejiang, Fujian, and Guangdong shows 0- to 3-month lag time to changes in precipitation. These results are highly in line with the conclusions made by Liang et al. (2015) and Cui (2010) that the time lag period of the NDVI in response to precipitation in humid and semi-humid climate zones ranged from 1 to 3 months.

The NDVI in the north of eastern China was greatly associated with the concurrent precipitation, and this spatial characteristic was potentially determined by the spatial distribution of the land use types. Wu et al. (2015) demonstrated that evergreen broadleaf forest was expected to show a longer time lag period to changes in precipitation in comparison with the time lag effects of deciduous needle leaf forest, mixed forest, shrubs land, grassland, and farmland to changes in precipitation.

Coincidentally, lands in the south of eastern China such as Zhejiang, Fujian, and Guangdong are dominated by evergreen broadleaf forest, and lands in the north of eastern China are covered by grassland, deciduous needle leaf forest, and farmland.

NDVI shows finite lag time to changes in precipitation on seasonal scale. The NDVI tends to show a longer lag time to precipitation in summer than in spring and autumn across the study area, indicating that NDVI is not primarily correlated with the precipitation in the concurrent month, but the precipitation of previous 1 to 3 months in summer. Precipitation is more abundant in summer over the study area. The precipitation cannot be directly absorbed to promote the plant growth, a large amount of the precipitation flows off the surface of the land and a considerable part of that will be used to offset the soil moisture. The only part of the precipitation, which is retained in the soil, can be considered as “effective precipitation” to vegetation growth. It takes time from precipitation to shift into vegetation roots and then become available water resources for plant growth (Yang et al., 2014, Zeppel et al., 2014). The above explanation illustrates how precipitation affects the delay of the vegetation growth and why a longer lag time takes place between vegetation growth and precipitation in summer.

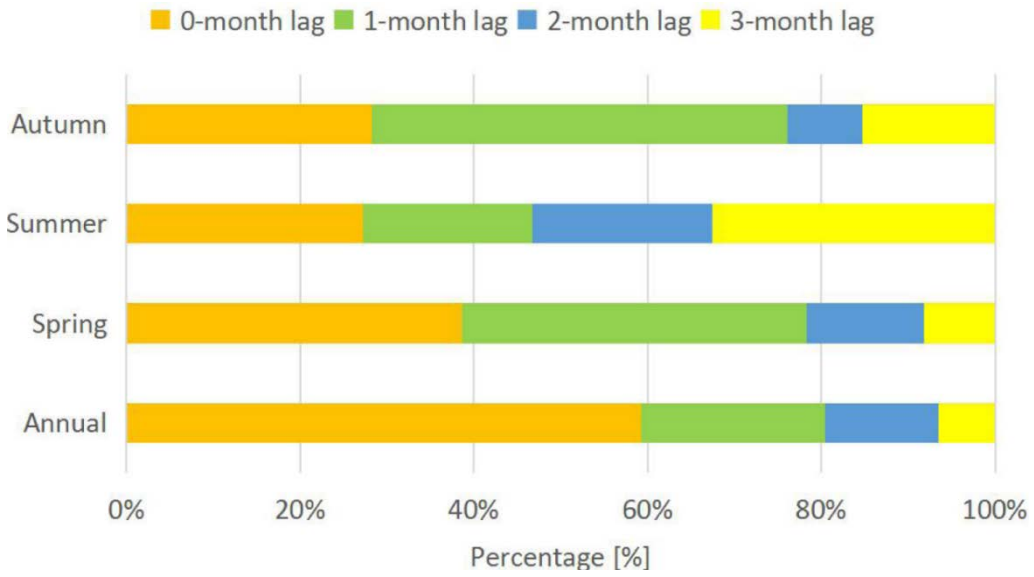

Figure 5-22. The statistical results of the lag time for maximum NDVI response to precipitation on annual and seasonal scales

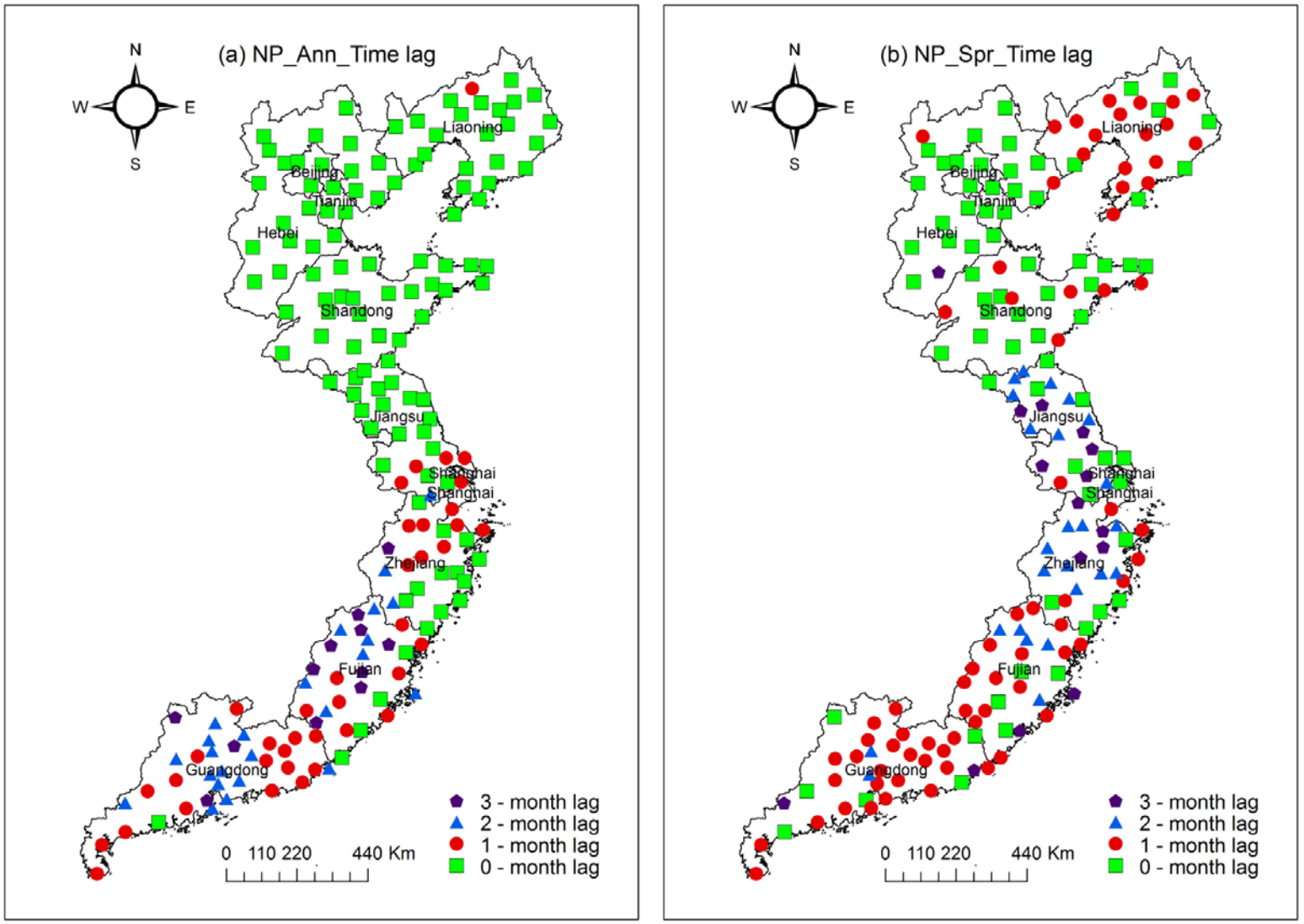

Figure 5-23. Spatial distribution of the lag time for maximum annual NDVI (a) and spring NDVI (b) response to precipitation

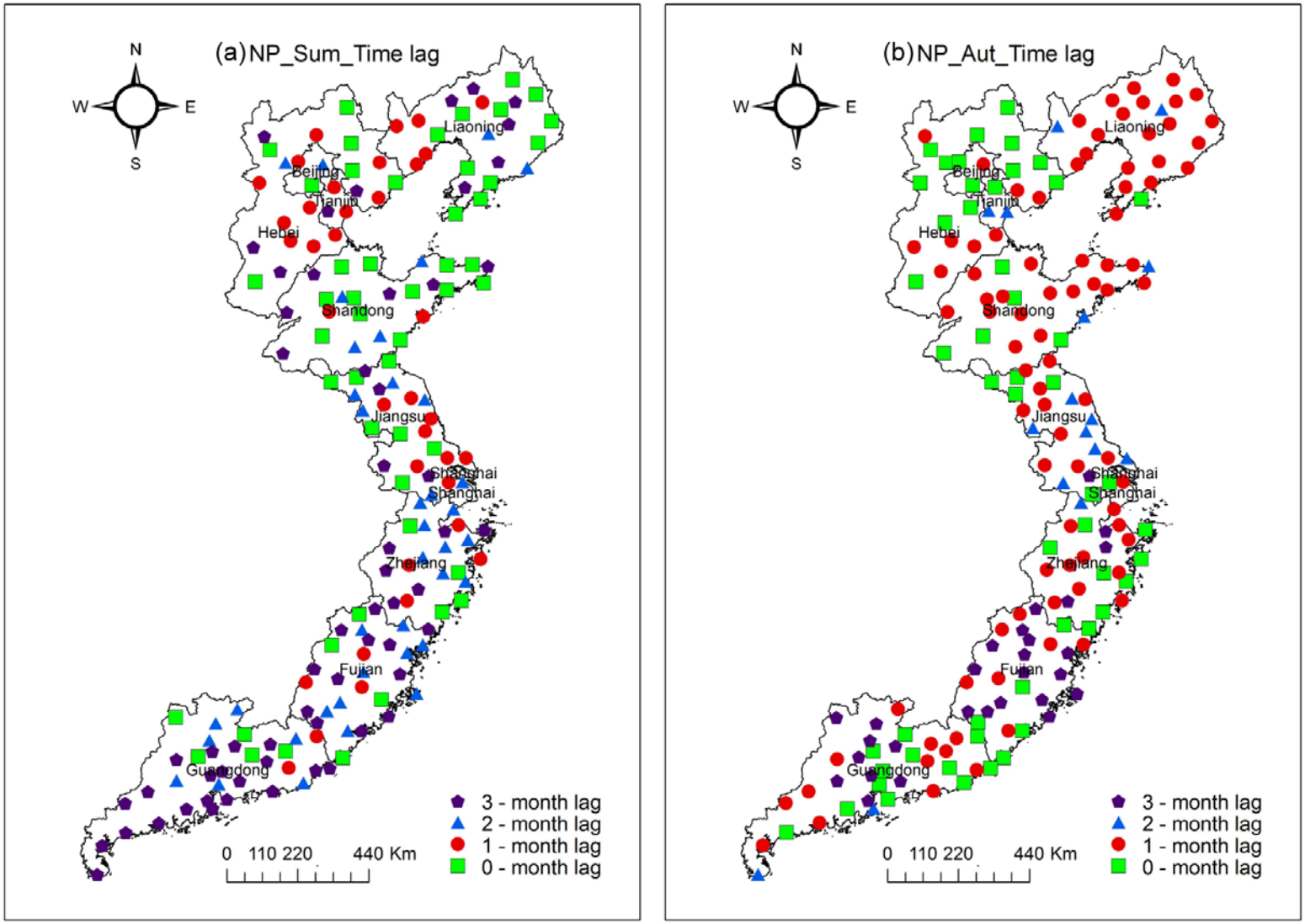

Figure 5-24. Spatial distribution of the lag time for maximum summer NDVI (a) and autumn NDVI (b) response to precipitation

5.2.3.2 The spatial patterns of lag time for maximum NDVI response to temperature

Spatially, comparing with the lag time between the annual NDVI and precipitation as well as the annual NDVI and temperature, the spatial differences for maximum annual NDVI response to temperature are less pronounced than that for maximum annual NDVI response to precipitation across eastern China. Figure 5-26(a) shows that annual NDVI is maximally related to the concurrent temperature over eastern China, except for the meteorological stations located in the middle of Liaoning, south of Fujian, as well as in the middle of Guangdong. The maximum correlation coefficients located in the above regions obtain when the temperature preceding NDVI by 1 month, suggesting a 1-month lag time for maximum annual NDVI response to changes in temperature in these regions. The proportion of the lag time between annual NDVI and temperature is statistically analyzed. It is detailed in Figure 5-25 that in eastern China the annual NDVI in 84% of the total meteorological stations shows no lag time to changes in temperature. The annual NDVI maximally responses to the temperature of previous 1 month accounting for 14% of the total meteorological stations. Only 2% of the total meteorological stations has a 2-month lag for maximum annual NDVI response to temperature.

The lag time for maximum NDVI response to temperature in spring, summer, and autumn is geographically heterogeneity, as displayed in Figure 5-26(b) and Figure 5-27(a) and (b). In spring and autumn, the maximum NDVI response to the temperature within the same month accounts for 58% and 66% of the total meteorological stations, respectively. These meteorological stations are basically evenly distributed across the study area. Figure 5-25 shows that 3-month lag time between NDVI and temperature accounts for 16% of the total meteorological stations in autumn, which is four times higher than in spring. These meteorological stations are mostly distributed in Fujian, the eastern coastal areas of Jiangsu, as well as in the south of Zhejiang, suggesting that the NDVI is markedly delayed to changes in temperature in autumn in these regions.

The lag time for maximum NDVI response to temperature is more pronounced in summer than in spring and autumn. In summer, the NDVI in 28% of the total meteorological stations maximally responses to the concurrent temperature, which are mainly distributed in the eastern coastal areas of the study area. Moreover, the proportion of 2- and 3-month lag time for maximum NDVI response to temperature

accounts for 33% and 22% of the total meteorological stations, individually. The meteorological stations with a 2-month lag time stretch from Fujian to Liaoning and the meteorological stations with a 3-month lag time are distributed from Guangdong to the north of Fujian and the middle of Shandong (Figure 5-27(a)).

Regarding the lag time for maximum annual NDVI response to temperature over the entire study area, the lag time of the annual NDVI to temperature can be negligible, which is in agreement with former studies. For example, Liang et al. (2015) investigated the time lag effects of NPP in response to temperature in China. The results of this study indicated that NPP was mostly influenced by concurrent temperature and the time lag period of NPP in response to changes in temperature can be ignored. Particularly in arid and semi-arid areas, temperature may not be a restricting factor for vegetation growth. Comparing with the response of vegetation growth to changes in precipitation and temperature, the response of vegetation growth to temperature is more rapid than that to precipitation (Cui, 2010, Liang et al., 2015), which is also confirmed in our study. Wang et al. (2003) detected the maximum response of NDVI to temperature and precipitation in Kansas, USA and pointed out that the temperature of previous 0 to 1 month had great impacts on vegetation growth and NDVI generally maximally responded to the precipitation of previous 1 to 2 months.

With regard to the lag time for maximum NDVI response to temperature on seasonal scale, the lag time in most of the meteorological stations is longer in summer than in spring and autumn. This result indicates that the temperature of the previous month has considerable effects on plants grown in summer. The possible reason is the high temperature in summer. The high temperature in summer is no longer the ideal temperature conditions for vegetation growth (Wu et al., 2015). On the one hand, the high temperature cannot constantly promote the vegetation growth due to the stage of maturity of plants in summer. On the other hand, soil moisture, trace elements, soil organic matters, and nutrient availability in the root zone might potentially affect the vegetation growth because of the unique water and nutrient requirements at different plant growth stages (Olson et al., 2010, Qian et al., 2016).

The explanations provided above answer why 2- and 3-month lag time show in summer in most of the meteorological stations in eastern China. Moreover, the lag time is closely

associated with the vegetation types, as demonstrated by Wu et al. (2015) that more than 60% of the deciduous broadleaf forest presents a 2-month lag time to changes in temperature throughout the world, which is longer than other vegetation types. Coincidentally, as mentioned previously, lands distributed in the southeast of China are mostly covered by deciduous broadleaf forest, which answers the question why the lag time for maximum NDVI response to changes in temperature in Zhejiang, Fujian, and Guangdong is more pronounced.

Furthermore, in our study, we detected that NDVI in most of the meteorological stations shows 2- to 3-month lag time to changes in precipitation and temperature in summer in Zhejiang, Fujian, and Guangzhou, which are not in line with the results generated by Cui (2010). Cui (2010) demonstrated that NDVI in most of the meteorological station shows no lag time to changes in precipitation and temperature within the same area. The differences can be ascribed to the data source and study period.

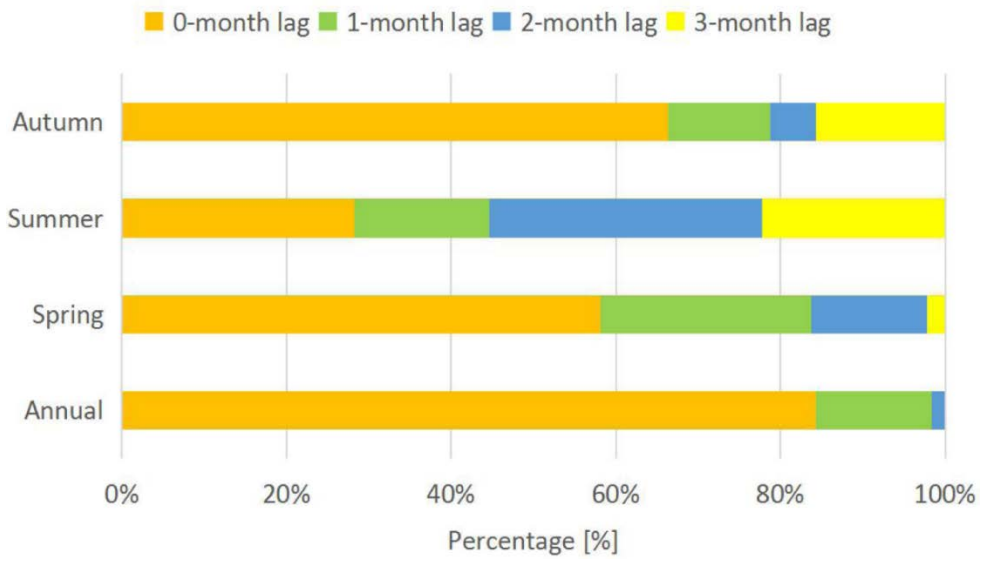

Figure 5-25. The statistical results of the lag time for maximum NDVI response to temperature on annual and seasonal scales

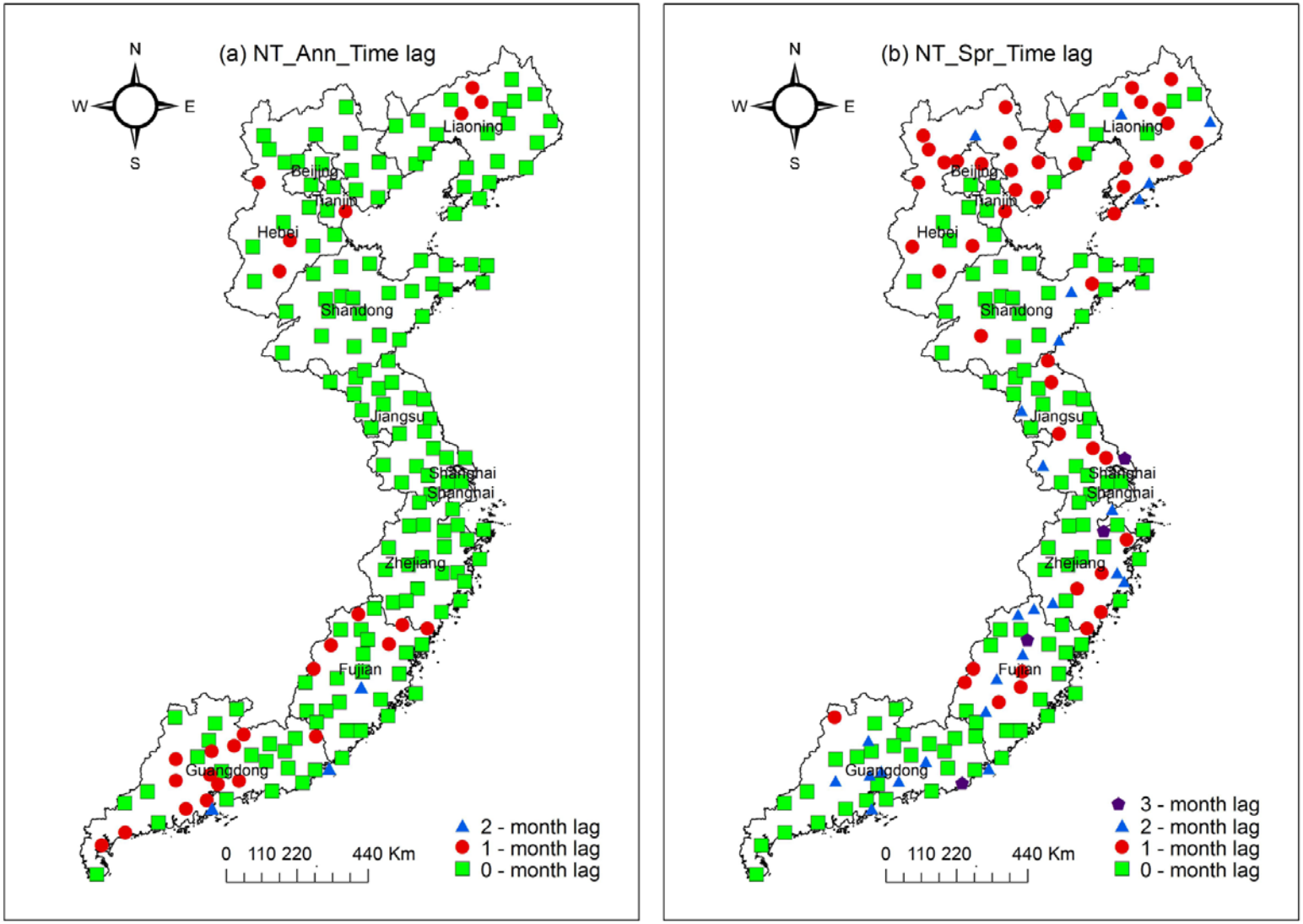

Figure 5-26. Spatial distribution of the lag time for maximum annual NDVI (a) and spring NDVI (b) response to temperature

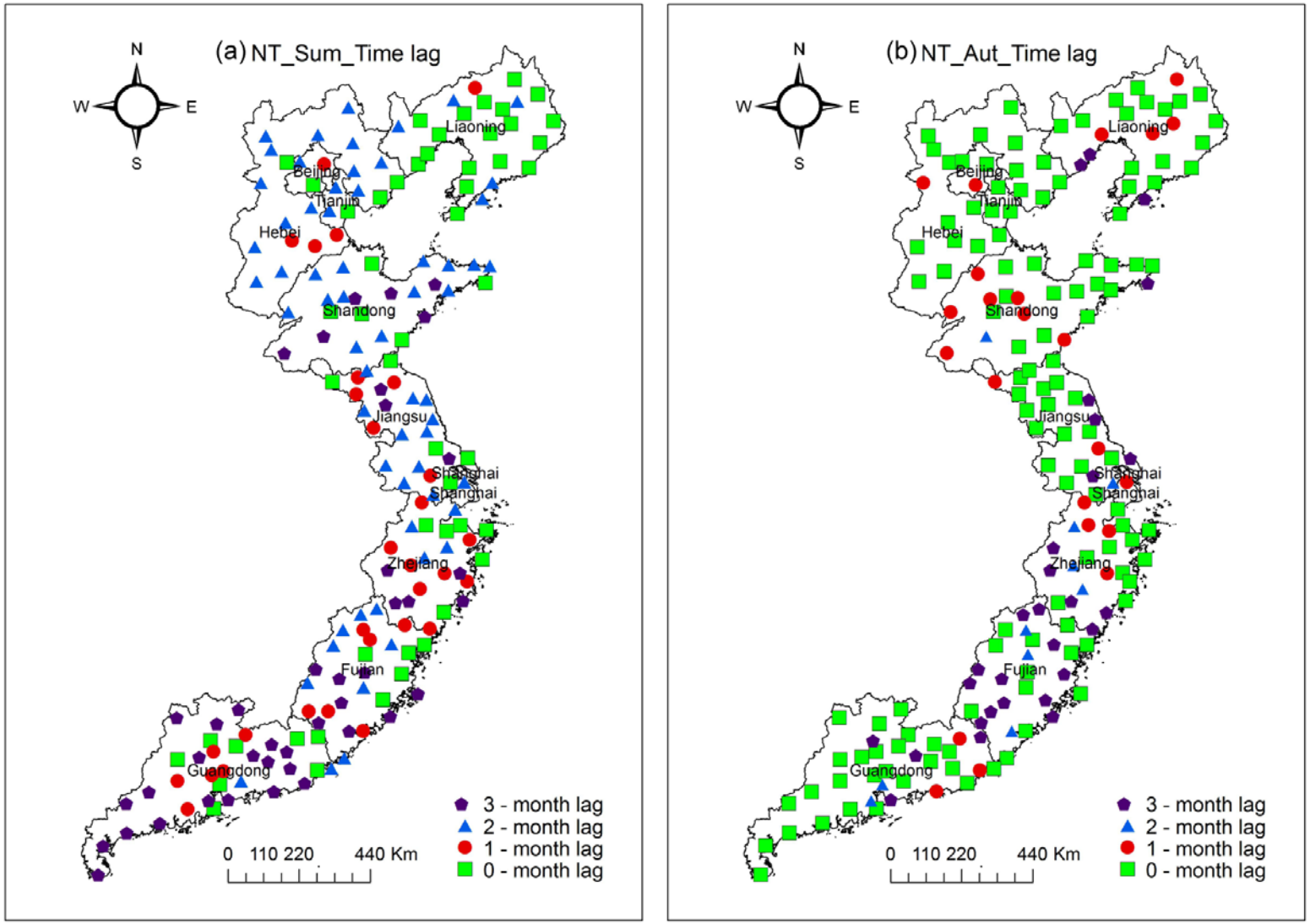

Figure 5-27. Spatial distribution of the lag time for maximum summer NDVI (a) and autumn NDVI (b) response to temperature

5.3 The relationship between annual NDVI and topographic factors in eastern China

5.3.1 The interaction between annual NDVI and elevation

For a better understanding of the relationship between vegetation cover change and terrain attributes is of critical importance for environment protection, biodiversity conservation, and vegetation restoration. Interrelationships between the vegetation cover change and the three topographic factors were investigated for eastern China from 2001 to 2016. In this study, three vegetation metrics such as the annual NDVI value, annual NDVI changing slope, and annual NDVI CV are used to quantitatively indicate the dynamic change of vegetation cover. To analyze the relationships between vegetation changing trend and the three topographic factors, the NDVI changing slopes were reclassified into three classes: decrease (significant and slight decreases), unchanged, and increase (significant and slight increases). The spatial coupling characteristics of elevation to the annual NDVI value, annual NDVI changing slope, and annual NDVI CV were carried out on the basis of Spatial Overlay Analysis using the platform of ArcGIS 10.3.

Elevation is a dominant element controlling the vertical distribution of vegetation cover. Figure 5-28(a) shows that the proportion of the NDVI values ranging from 0 to 0.2 occupies 34% when the elevation ranges from -284 to 0 m, which can be explained by the distribution of water body within this elevation range. The proportion of the NDVI values ranging from 0.2 to 0.4 decreases with the elevation increase from 0 to 500 m in eastern China. However, an opposite changing trend is observed in the proportion of the NDVI values ranging from 0.8 to 1 at the same elevation range, which increases with the elevation increase. Furthermore, the proportion of the NDVI values ranging from 0.6 to 0.8 increased by 32% and the proportion of NDVI values ranging from 0.4 to 0.6 decreased by 26% from the elevation ranges of 0 to 100 m to 200 to 300 m，indicating that the vegetation cover increases with the elevation increase from 0 to 300 m. It is worth mentioning that the proportion of the NDVI values ranging from 0.4 to 0.6 and from 0.6 to 0.8 occupy approximately 30% and 50% from the elevation ranges of 200 to 300 m to 400 to 500 m. Above conclusions suggest that the vegetation cover dramatically

increased from the elevation ranges of 0 to 200 m and kept stable from the elevation ranges of 200 to 500 m. All conclusions provided above further prove that elevation is a dominant factor controlling the vertical distribution of vegetation growth in eastern China, but the vegetation cover tends to be stable when the elevation is above 200 m.

Figure 5-28(b) shows that the proportion of the NDVI with a decreasing trend within the elevation ranges from 100 to 2849 m is roughly the same. The proportion of the NDVI with an increasing trend is relatively lower at the elevation range of 0 to 100 m than at other elevation ranges, suggesting that vegetation degradation is more serious at the elevation range of 0 to 100 m than at higher elevation ranges. The dynamic change of vegetation cover is dominated by an increasing trend when the elevation is higher than 100 m, and the NDVI with an increasing trend reaches the highest proportion at the elevation range of 500 to 2849 m. Namely, NDVI had improved more noticeably at higher elevation ranges, but remained fairly stable or even declined at lower elevation ranges from 2001 to 2016.

Figure 5-28(c) shows that vegetation cover is fairly stable within the elevation ranges from 100 to 500 m across the study area. It is obvious that the stability of the vegetation cover enhances with the elevation increase apparently and reaches its peak at the elevation range of 400 to 500m. All conclusions provided above is fairly in line with the results generated by Mokarram and Sathyamoorthy (2015), Jin (2015), and Li et al. (2015b). They demonstrated that vegetation activity and NDVI value increase with elevation increase and NDVI value reach its peak at the best elevation range for vegetation growth. Figure 5-28(a) and (c) show that the annual NDVI value and the stability of the annual NDVI are low at the elevation range of -282 to 0 m. Areas with the elevation of less than 0 m mostly consist of the eastern coastal areas, the estuary areas, and water body (Figure 3-4). These areas have no vegetation cover or rarely vegetation cover, and it is relatively vulnerable and sensitive to external disturbances. Above explanation explains the question of why the vegetation cover and vegetation stability are lower at the elevation range of -282 to 0 m than at higher elevation ranges.

The synergism between topographic factors and vegetation growth is correlated with the interaction between elevation ranges and land use types (Gouveia et al., 2014). In our study, areas at the elevations from 0 to 100 m account for 45% of the study area, where

the land is dominated by built-up land and farmland. Due to the unique attributes of these two land use types, frequent human activities and disturbances play a negative role in vegetation growth and succession. The species richness and diversity and the vegetation growth statues are closely associated with elevation range and human activities because of the intimate connection between ecological ecosystems and human activities and elevational gradients (Nogues-Bravo et al., 2008, Moura et al., 2016).

However, the frequency of human activity decreases and the species richness enhances with the elevation increase to a certain level (Li et al., 2015b). It has been demonstrated previously that the elevation and disturbance intensity (due to tourism and agriculture) play essential roles in affecting the spatial distribution of communities and diversity of plant species in the Baihua Mountain Reserve (Zhang et al., 2013a). Plant species richness presents a ‘‘humped’’ pattern with elevation and disturbance increases (Austrheim, 2002, Zhang and Ru, 2010, Rumpf et al., 2018). The maximum vegetation species diversity shows in the middle elevation, a place with lower disturbance intensity. Li et al. (2015a) also found that the vegetation cover has been most improved in the Yarlung Zangbo River Basin when the elevation is lower than 500 m. It is worth notifying that heat, moisture, soil fertility, and other factors may not favor the vegetation growth or even seem to be constraint factors limiting the vegetation activity at high elevational ranges (Li et al., 2015b). Above conclusions answer the questions why a more stable vegetation cover and a higher NDVI value presented at the elevation ranges from 100 to 500 m, and why the improving trends of vegetation cover reversed when the elevation is above 500 m.

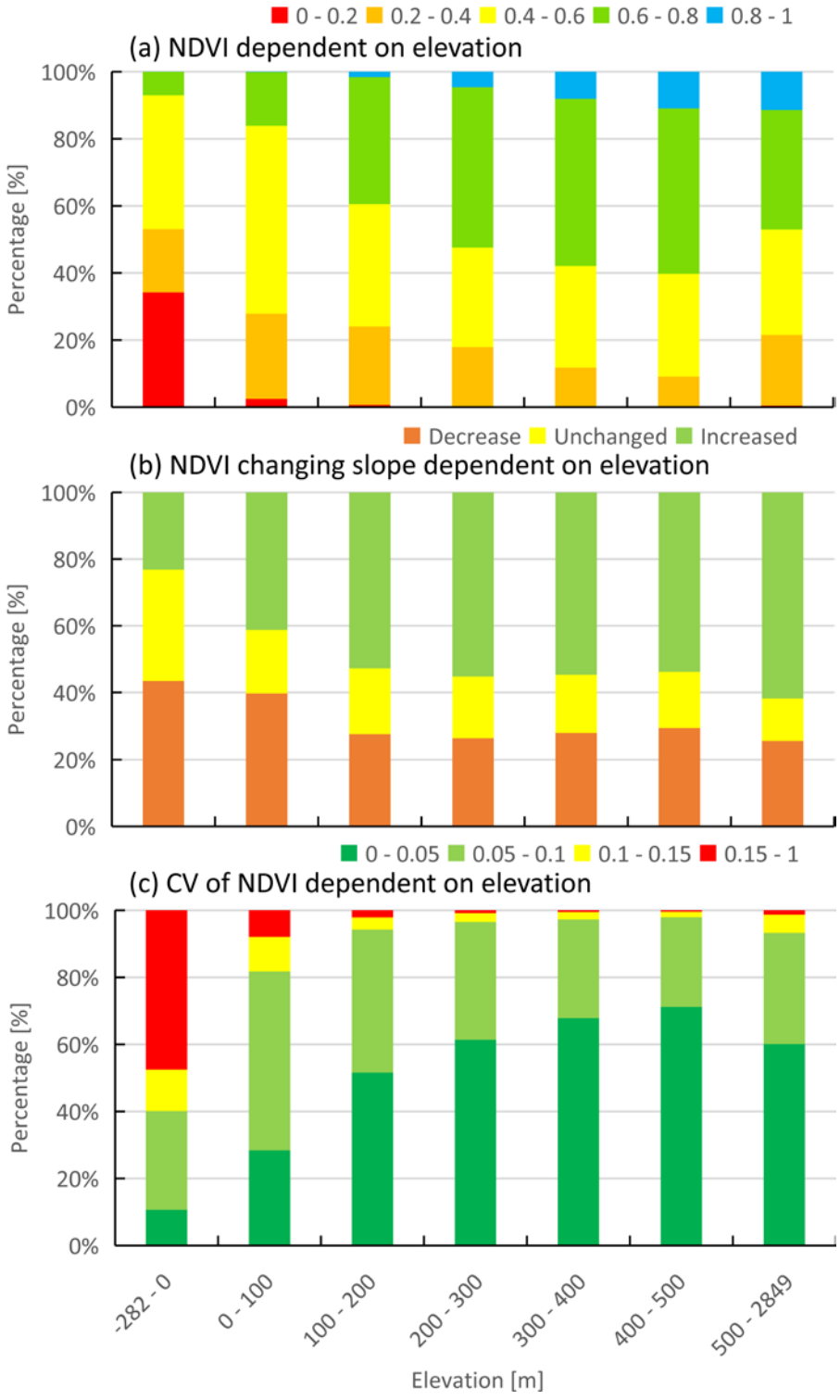

Figure 5-28. The statistical results of NDVI value, NDVI changing slope, and NDVI CV for different interval of elevation

5.3.2 The interaction between annual NDVI and aspect

This study detected the changes in vegetation cover on the NFS and SFS in eastern China using MODIS NDVI dataset from 2001 to 2016. A comparative analysis of the three vegetation metrics on the NFS and SFS was carried out. The corresponding maps of the spatial interaction between aspects and the three vegetation metrics are obtained based on the overlay analysis. A zonal statistic was used to calculate the proportion of the annual NDVI value, annual NDVI changing slope, as well as the annual NDVI CV in the context of the two aspects. The statistical results are shown in Figure 5-29(a), (b) and (c), respectively.

Directions of aspect contribute to the differences in solar radiation received by the vegetation in the middle and high latitudes (Toro Guerrero et al., 2016). The annual NDVI value shows a homogenous pattern on the NFS and SFS. The proportion of the NDVI value in each category on the NFS and SFS is quite similar. The proportion of the NDVI values ranging from 0.2 to 0.4, 0.4 to 0.6, and 0.6 to 0.8 accounts for approximately 21%, 44%, and 30%, respectively, both on the NFS and SFS.

Areas with a vegetation greening trend on the NFS and SFS account for half of the total area on its corresponding aspect. Areas with a vegetation browning trend account for 33% both on the NFS and SFS. With the above results, it can be inferred that the areas with a vegetation greening trend are larger than the areas with a vegetation browning trend both on the NFS and SFS. However, no statistical differences and magnitude differences of vegetation cover change are detected on the NFS and SFS.

No statistical differences in vegetation stability are observed on the NFS and SFS. The vegetation cover in the Pearl River Delta, Yangtze River Delta, Bohai Economic RIM, as well as in the northwest of Hebei is more sensitive and vulnerable. The vegetation cover in the east of Liaoning and most areas of Zhejiang, Fujian, and Guangdong shows the greatest vegetation stability. The proportion of the NDVI CV values ranging from 0 to 0.05 accounts for 46% both on the NFS and SFS, whereas the proportion of the NDVI CV values ranging from 0.05 to 0.1 accounts for 43% on these two aspects. Above results suggest that the majority of the vegetation cover remained stable or fluctuated at

a self-regulating range, and only a small part of the study area had undergone a strong vegetation oscillation from 2001 to 2016.

Against the background of the above conclusions, aspect cannot be regarded as a primary topographic factor influencing the vegetation variation over eastern China. This conclusion is against our initial assumptions. In the northern hemisphere, vegetation on the NFS is projected to receive several times more solar radiation than on the SFS, thereby resulting in differences in vegetation vitality on the NFS and SFS (Auslander et al., 2003). Many scholars have demonstrated that the vegetation growth and succession are apparently better on the NFS than on the SFS during the drying season due to warmer and drier conditions on the SFS in the northern hemisphere (Toro Guerrero et al., 2016, Deng et al., 2009, Dietz et al., 2007). Furthermore, Auslander et al. (2003) carried out that the plant traits were closely associated with the slope directions. The leaf size/plant height was greatly larger/taller on the NFS than on the SFS in Israel.

However, the result generated in our study is against most of the former studies. In our study, the dynamic changes of vegetation cover show no differences on the NFS and SFS, which is highly in line with Li et al. (2015b). Li et al. (2015b) addressed a conclusion of vegetation growth on the NFS and SFS, and the conclusion pointed out that no significant differences of vegetation cover were detected on the NFS and SFS in Henan, China. Differ to former studies, in our study, areas located in the south of eastern China are controlled by humid climate, a place with abundant precipitation, sufficient light, and warm temperature across a year, and no apparent wet season and dry season are detected in this region. Areas located in the north of eastern China are dominated by flat landscape. Vegetation on the NFS and SFS is, therefore, less restricted by the differences of light, heat, and water conditions. The explanations provided above are the reasons why vegetation shows no differences on the NFS and SFS in eastern China.

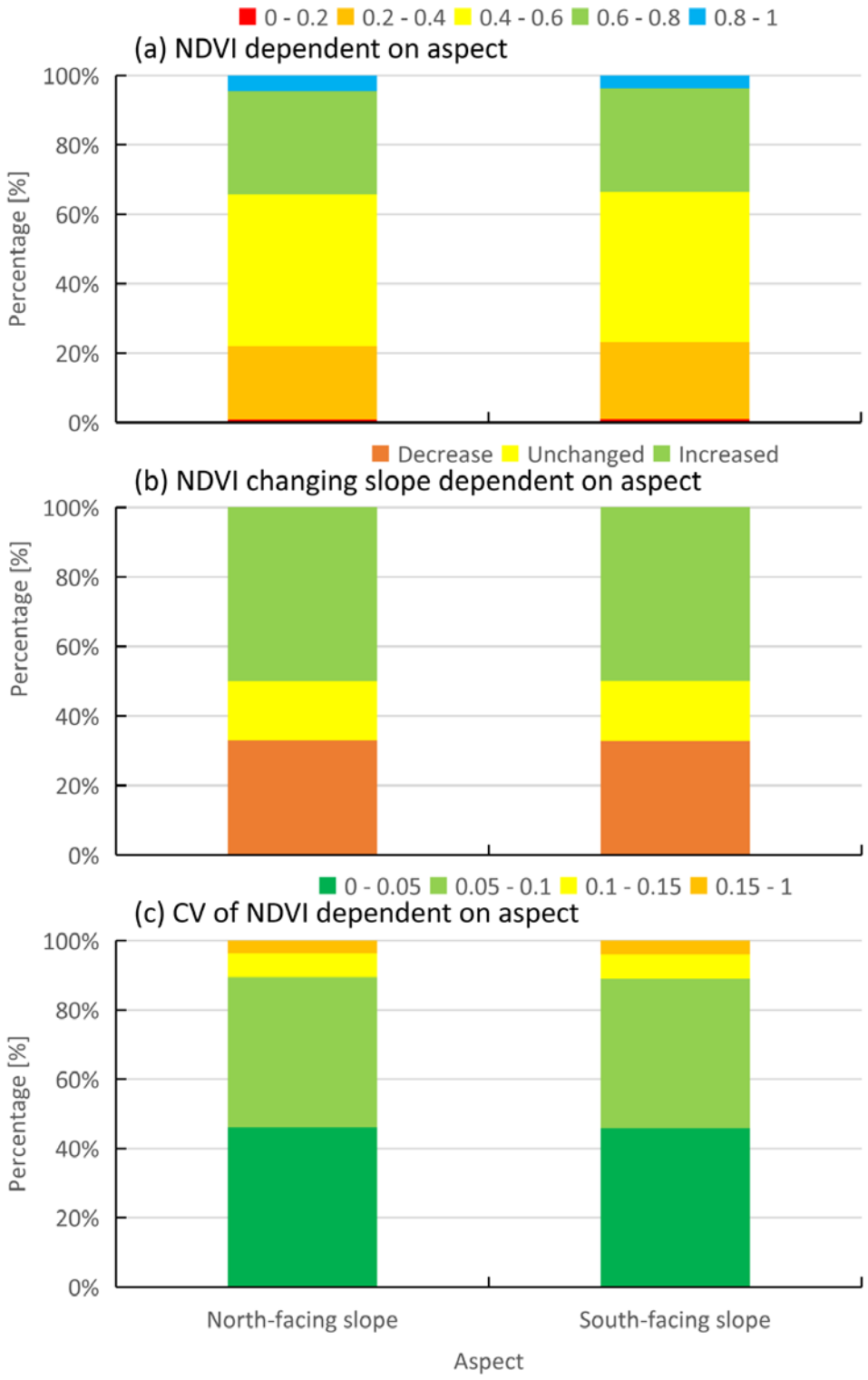

Figure 5-29. The statistical results of NDVI value, NDVI changing slope, and NDVI CV for different aspects

5.3.3 The interaction between annual NDVI and slope

The synergism between the presence of vegetation and the steepness of the slope is well known. On the one hand, vegetation affects the stability of the slope by changing the soil suction and soil-water content of the corresponding root zone of plants. On the other hand, the soil suction and soil-water content determine the matter and energy supply of vegetation growth. Spatial characteristics of the annual NDVI value, annual NDVI changing slope, and annual NDVI CV at each slope range were investigated on the basis of overlay analysis, respectively. The proportion of the annual NDVI value, annual NDVI changing slope, and annual NDVI CV in the background of each slope range were acquired on the basis of the zonal statistic. The results are shown in Figure 5-30(a), (b) and (c), respectively.

The landscape is mostly flat in eastern China, and areas with slope degree ranging from 0° to 2° and from 2° to 6° account for 30% and 25% of the study area, respectively. Particularly, vast plain areas are extending from Jiangsu to the north of eastern China. NDVI values are relatively lower in the middle of Liaoning, southeast of Hebei and Beijing, Tianjin, and eastern coastal areas of Guangdong at the slope range of 0° to 2° and 2° to 6°. A roughly similar spatial distribution of the NDVI value is observed at the slope ranges of 6° to 15°, 15° to 25°, and 25° to 90°. The NDVI values are basically higher in Zhejiang, Fujian, and Guangdong than in the middle of Shandong, east and west of Liaoning, as well as in the northwest of Hebei and Beijing.

As reported in Figure 5-30(a), the proportion of lower NDVI value (0.2 to 0.4 and 0.4 to 0.6) and the proportion of higher NDVI value (0.6 to 0.8 and 0.8 to 1) present an inverse trend with the slope degree increase. Areas with the NDVI values more than 0.6 account for only 9% and 16% at the slope ranges of 0° to 2° and 2° to 6°, separately, whereas areas with the same NDVI value range occupy 62% and 72% at the slope ranges of 15° to 25° and 25° to 90°, respectively. Above conclusions indicate that the vegetation cover is basically higher in the steeper regions and lower in the flat regions of the study area.

Regarding the spatial interplay between vegetation cover change and terrain slope variability, areas located in the junction areas of Shandong and Hebei, middle of Liaoning, and northwest of Hebei present a greening trend at the slope ranges of 0° to 2°

and 2° to 6°. Apart from these areas, the vegetation cover had gradually declined during the study period. Within the slope ranging from 6° to 90°, the vegetation cover is dominated by an increasing trend, which is mainly concentrated in the north and sparsely distributed in the south of the study area. Figure 5-30(b) shows that the proportion of the browning areas shows a “valley” pattern with the slope degree increase. The proportion of the browning areas declines to the valley-bottom when the slope degree ranges from 6° to 15°, whereas the proportion of the greening areas reports an opposite phenomenon and reaches the peak at the same slope range.

Vegetation cover displays high stability over the study area when slope degree is more than 6°, except for small areas located in the northwest of Hebei and west of Liaoning. Vegetation cover is pretty fragile within the slope range of 0° to 6°. Figure 5-30(c) indicates that the proportion of the NDVI CV values ranging from 0.1 to 1 accounts for 21% at the slope range of 0° to 2° and 16% at the slope range of 2° to 6°, which are remarkably higher than that at the slope range of 15° to 25° and 25° to 90°. In addition, the proportion of the NDVI CV values ranging from 0 to 0.05 increases with the slope degree increase, while the proportion of the NDVI CV values ranging from 0.15 to 1 declines with the slope degree increase, implying that, generally, the vegetation cover is more stable at higher slope ranges and relatively vulnerable at lower slope ranges.

The overall vegetation cover and vegetation stability at higher slope ranges are better than at lower slope ranges. China has been experiencing unparalleled socio-economic development, which leads to a huge amount of migration from rural areas to urban areas. In eastern China, in particular, a place has been highly developed in the last three decades and constantly develops at a fast speed. Moreover, the unprecedented development mostly took place in flat areas, which results in a sharp decline in farmland at the urban edge. Meanwhile, with rapid urbanization and industrialization, the construction of urban infrastructure is also exponentially growing, which further limits the vegetation growth. The negative influences gradually decline with the slope degree increase, which answers the question of why the vegetation cover and vegetation stability are relatively higher at high slope ranges. Klinge et al. (2015) further confirmed that no significant effects of the topographic pattern were detected in vegetation distribution when the slope degree is lower than 5◦. Namely, human activity and climate

variability are dominant elements controlling the vegetation activity in these regions. Topographically, with the rise in slope degree, terrain landscape turns progressively steeper. Areas with high slope degree, the human disturbances are being negligible. But most of the steep slopes accompany severe soil erosion, soil fertility loss. Consequently, high slope ranges may not favor the vegetation growth.

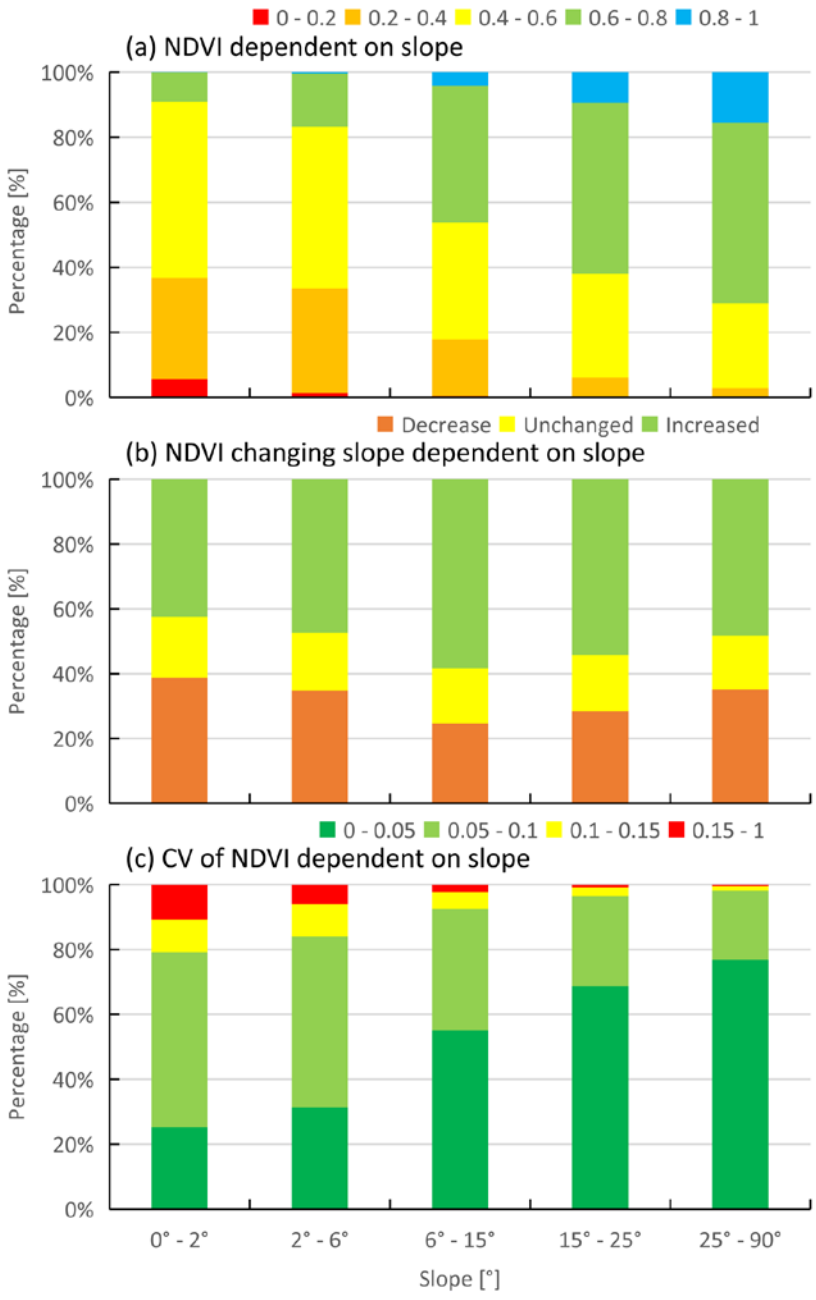

Figure 5-30. The statistical results of NDVI value, NDVI changing slope, and NDVI CV for different interval of slope

5.4 The relationship between annual NDVI and socio-economic factors in eastern China

5.4.1 The temporal characteristics of annual NDVI in response to socio-economic factors

5.4.1.1 The negative effects of socio-economic factors on annual NDVI

Vegetation cover has tremendously changed in the last century and this century at the global level, socio-economic factors along with the effects of climate factors and topographic factors are anticipated to contribute to the dynamic change of vegetation cover. In this study, the response of the annual NDVI to changes in socio-economic factors was quantitatively computed using Pearson's correlation analysis for each administrative unit. The correlation coefficients between the annual NDVI and the 13 socio-economic factors for each administrative unit are shown in Table 5-5. It has to be clarified that the correlation coefficient between the annual NDVI and the total employment in Hebei is absent due to lack of relevant data. To distinguish the relative roles of socio-economic development and population growth in vegetation change, the 13 socio-economic factors were divided into three classes: general economic vitality, consumption, and human population (Table 3-2).

All of the correlation coefficients between the annual NDVI and the 13 socio-economic factors are negative in Tianjin, Shanghai, Jiangsu, Zhejiang, Fujian, and Guangdong, suggesting that vegetation cover negatively responses to human activities in these administrative units, and human activities play an essential role in vegetation degradation. Especially, in Shanghai and Jiangsu, the negative effects of human activities on vegetation growth are more serious. Table 5-5 shows that most of the correlation coefficients in Shanghai and Jiangsu are significant at the $p<0.01$ level, implying a stronger negative relationship between the annual NDVI and the 13 socio-economic factors in Shanghai and Jiangsu than in Zhejiang, Tianjin, Fujian, and Guangdong.

Socio-economic development dominates the vegetation variability in Shanghai, Jiangsu, Zhejiang, and Guangdong because the correlation coefficients in these administrative

units between socio-economic development and vegetation variability are basically higher than that of between population growth and vegetation variability. Except for in Shanghai, the negative impact of primary industry product on vegetation growth is weaker than that other socio-economic factors. China is on the processes of transformation to a more productive, service-based economy body. Shanghai is a megacity of China and plays an irreplaceable role in China's socio-economic development. In 2016 the proportion of the primary industry product accounts for 0.38% of the total GDP in Shanghai. This proportion is significantly lower than that of other administrative units. For instance, the proportion of the primary industry product in Hebei, Liaoning, Fujian, and Shandong constitutes more than 7% of the total GDP in 2016. The primary industry is a land-based industry. Due to the scarcity of land resources in Shanghai, the local government prioritizes tertiary industries, which cause less damage to the local ecological system. In Shanghai, this initiative has achieved enormous positive results in socio-economic development and environmental protection.

In addition, in 2001 the urbanization rate reached 75.3% in Shanghai, which preceded only by Beijing. With the rapid socio-economic development and population growth, in 2016 the urbanization rate reached 87.9% in Shanghai, taking the first position and surpassing Beijing by a rate of 1.4% (Table 5-6 and Table B-10), which accounts for the conversion of farmland to urban areas. Above all, the above-mentioned changes answer the question of why the effects of primary industry product on changes of NDVI are smaller in Shanghai than the effects of other socio-economic factors on changes of NDVI.

The proportion of the areas with a vegetation browning trend distributed in Fujian, Zhejiang, Shanghai, and Jiangsu exceeds the proportion of these areas in other administrative units of the study area (Figure 5-8(a)). This browning trend is attributed to the combination of such effects as rapid economic development, urban expansion, and population growth. For example, in 2016 China's permanent urbanization rate is 57.4%, while the urbanization rate in Jiangsu, Zhejiang, and Fujian had increased respectively by 25.1%, 16.1%, and 20.8% from 2001 to 2016 and reached 67.7%, 67%, and 63.6% in 2016 (Table 5-6 and Table B-10). The extensive urbanization in Jiangsu, Zhejiang, and Fujian is at the cost of the transformation of a huge number of farmlands to urban areas and a large amount of farmland abandonment. Moreover, the proportion of the

secondary industry product had increased by 4.2% of the total GDP in Fujian from 2001 to 2016, and it accounts for 48.9% of the total GDP in 2016. Meanwhile, the proportion of the secondary industry product in the other nine administrative units had dropped during the same period, indicating that the secondary industry takes an irreplaceable role in socio-economic development in Fujian. The World Bank 2007 reported that population pressure may aggravate the vulnerable ecosystem degradation. Shanghai is considered the most densely populated region in mainland China. In 2016 the population density grows up to 3816 people/sq. km in Shanghai, which is almost three times higher than in Beijing (1324 people/sq. km) and Tianjin (1328 people/sq. km) and 13 times higher than in Liaoning (285 people/sq. km) (Table B-11), implying that heavy human population pressure could be a critical socio-economic factor for vegetation degradation in Shanghai.

Previous studies have demonstrated that human activities contribute to vegetation degradation in many parts of the world, the results generated in our study is highly in line with the above conclusions. For example, Dewan and Yamaguchi (2009) proposed that with the rapid socio-economic development and population growth, urban areas increased sharply, thereby causing to a manifest decline in the area of water bodies, cultivated lands, vegetation, and wetlands in Greater Dhaka, Bangladesh. De Freitas et al. (2013) evidenced that vegetation degradation and deterioration were closely associated with population pressure in the Upper Uruguay Basin, Brazil. Zhou et al. (2014) investigated the relationship between terrestrial vegetation cover and urban development intensity in 32 major cities of China and found that the vegetation cover declined dramatically with the urban land expansion for 28 of the 32 cities, including Beijing, Tianjin, Shijiazhuang, Jinan, Nanjing, Hangzhou, Fuzhou, and Guangzhou, which are located in our study area. Moreover, Zhao et al. (2017) evaluated the GDP spatialization and economic differences in the south of China on the basis of NPP-Visible Infrared Imaging Radiometer Suite (VIIRS) nighttime light imagery and showed that socio-economic development in the eastern coastal areas and low elevation plains of Guangdong were greater than in other regions of the study area (Zhao et al., 2017). The results of the study by Zhao et al. (2017) answered the questions why the NDVI value is

lower in the coastal areas of Guangdong than in inland areas and why the NDVI value had decreased in many parts of Guangdong.

The effects of human activities such as socio-economic development, urban expansion, and population growth on changes of vegetation cover cannot be quantitatively isolated and, for this reason, can be regarded as a combining effect. With sharp socio-economic development and frequent human activities after launching the program of reform and opening-up termed "Socialism with Chinese Characteristics" in China in 1978, urban expansion has encroached a huge amount of farmland and forest land in the Yangtze River Delta, Pearl River Delta, and Bohai Economic RIM in particular, thereby resulting in significant vegetation degradation and deterioration in these regions.

5.4.1.2 The positive effects of socio-economic factors on annual NDVI

The annual NDVI in Beijing, Hebei, Liaoning, and Shandong is positively related to the 13 socio-economic factors, and the relevant correlation coefficients are basically higher in Beijing, Hebei, and Liaoning than in Shandong. Moreover, in Beijing, Hebei, and Liaoning the correlation coefficients between the annual NDVI and the 13 socio-economic factors are significant at $p<0.01$ level, with the exception of the correlation coefficient between the annual NDVI and the total investment in fixed assets in Liaoning.

Beijing is the capital city of the People’s Republic of China and is political, economic, and cultural centers. From 2001 to 2016 the urbanization rate had increased by 8.44% in Beijing and reached 86.5% in 2016 (Table 5-6). The increasing magnitude of the urbanization rate in Beijing is particularly lower than in other administrative units during the study period. Meanwhile, the tertiary industry product had increased by 19.7% and reached 80.2% of the total GDP in 2016, which is significantly higher than in other administrative units. In comparison with the secondary industry, the development of the tertiary industry causes fewer adverse consequences to the local environment and ecological system. In addition, the primary industry plays a significant role in socio-economic development in Liaoning, Hebei, and Shandong. These are places where the primary industry product accounted for 9.8%, 10.9%, and 7.3% of their corresponding total GDP in 2016, respectively. As mentioned previously, the primary industry is a land-based industry, which in principle may contribute to the improvement of vegetation cover.

Economic development and population pressure are the principal controlling factors of vegetation degradation, characteristic of the developing countries. Due to the implementation of efficient agricultural activities and migration of labor forces from rural to urban areas, the regional economic and agricultural vitality, economic welfare, and quality of life have considerably improved in rural areas in particular, which could potentially result in the enhancement of local vegetation activity. Previous studies also demonstrated that, in rural areas, integrated ecosystem management could restore the deteriorated local social-ecological systems in a sustainable way. The improvement of socio-ecological systems could consequently minimize population pressure and promote social welfare, ultimately resulting in vegetation restoration and ecological rehabilitation (Xu et al., 2014, Wang et al., 2010). The explanations provided above explore the underlying cause of the vegetation cover improvement in many parts of eastern China from 2001 to 2016, particularly in rural areas.

Figure 5-8(a) shows that vegetation distributed in the north of the study area displays a comprehensive greening trend, particularly in Liaoning, Hebei, Beijing, and Shandong. These regions have benefited significantly from the implementation of large-scale reforestation and afforestation programs such as the NFCP, TNSFP, BTSSCP, and GGP. These programs have been evidenced to be the controlling element facilitating vegetation growth in many parts of China (Zhang et al., 2016, Viña et al., 2016, Piao et al., 2015, Zhou et al., 2009). These reforestation and afforestation programs not only promoted regional vegetation vitality but also offset the negative effects derived from socio-economic development, urban expansion, population growth, and natural resources over-exploitation. The vegetation cover change in Shaanxi was detected by Zhou et al. (2009) after launching the GGP in 1999. The results of this study indicated that the vegetation cover in the north of Shaanxi presented a considerable increasing trend from 1998 to 2005, which was mostly ascribed to the implementation of GGP. Viña et al. (2016) evaluated the vegetation cover in China from 2000 to 2010 in the context of the NFCP implementation and found that the vegetation cover had significantly improved over a huge number of China’s territories and the NFCP exerted a great impact on regional vegetation restoration and rehabilitation.

Combining the effects of the large-scale forest reforestation on the basis of the implementation of TNSFP, NFCP, GGP, and BTSSCP, which not only contributed to significant improvement for vegetation cover in project's corresponding areas, but also alleviated the problem of poverty reduction, livelihood improvement, and rural economic recovery by supplying farmers, whose cropland on steep slopes was transformed to forest land and grassland, with grain and cash subsidies directly. However, inappropriate reforestation in some parts of northern China generated an enduring reduction in soil moisture. Due to the positive effects of implementation of the BTSSCP, the vegetation cover has improved for nearly half of the Beijing–Tianjin dust and sandstorm source region (BTSSR) from 2000 to 2010, and the increasing trend tends to expand in the future (Wu et al., 2013, Li et al., 2015c). Furthermore, winning the right to host the 2008 Olympic Games contributed the vegetation improvement in Beijing (Duan et al., 2011).

Table 5-5. The correlation coefficient between annual NDVI and the 13 socio-economic factors for the ten administrative units

Category	Factor	Beijing	Tianjin	Hebei	Liaoning	Shanghai	Jiangsu	Zhejiang	Fujian	Shandong	Guangdong
General Economic Vitality	GDP	0.837**	-0.222	0.701**	0.687**	-0.679**	-0.730**	-0.534*	-0.347	0.443	-0.140
	Primary Industry Product	0.659**	-0.214	0.701**	0.719**	-0.166	-0.701**	-0.495	-0.342	0.474	-0.136
	Secondary Industry Product	0.817**	-0.146	0.712**	0.652**	-0.552*	-0.687**	-0.486	-0.323	0.513*	-0.102
	Tertiary Industry Product	0.839**	-0.283	0.678**	0.689**	-0.714**	-0.763**	-0.573*	-0.376	0.363	-0.171
	PCGDP	0.839**	-0.171	0.706**	0.688**	-0.711**	-0.726**	-0.536*	-0.340	0.454	-0.137
	Total Investment in Fixed Assets	0.816**	-0.280	0.638**	0.564*	-0.683**	-0.741**	-0.613*	-0.380	0.357	-0.193
Consumption	Household Consumption	0.863**	-0.262	0.687**	0.697**	-0.677**	-0.761**	-0.536*	-0.370	0.369	-0.140
	Rural Household Consumption	0.856**	-0.309	0.676**	0.668**	-0.632**	-0.773**	-0.606*	-0.398	0.292	-0.210
	Urban Household Consumption	0.867**	-0.260	0.678**	0.692**	-0.685**	-0.757**	-0.515*	-0.356	0.400	-0.108
Human Population	Population	0.783**	-0.226	0.693**	0.720**	-0.538*	-0.576*	-0.451	-0.367	0.475	-0.125
	Total Employment	0.807**	-0.183	-	0.636**	-0.719**	-0.466	-0.174	-0.347	0.566*	-0.090
	Population Density	0.784**	-0.226	0.69**	0.662**	-0.538*	-0.200	-0.451	-0.381	0.472	-0.050
	Urbanization	0.645**	-0.134	0.772**	0.729**	-0.435	-0.660**	-0.528*	-0.286	0.486	-0.094
* Significant at P < 0.05 * * Significant at P < 0.01											

Table 5-6. Differences of the socio-economic factors for the ten administrative units from 2001 to 2016

	Primary Industry Product [%]	Secondary Industry Product [%]	Tertiary Industry Product [%]	Urbanization Rate [%]	Population density [People/sq.km]	Rural Household Consumption [RMB/person]	Urban Household Consumption [RMB/person]
Beijing	-2.77%	-16.95%	19.72%	8.44	500	20454	42571
Tianjin	-3.04%	-6.83%	9.87%	10.52	474	18458	30202
Hebei	-5.49%	-2.04%	7.54%	32.97	42	6930	13174
Liaoning	-1.05%	-9.80%	10.85%	12.47	6	9605	21888
Shanghai	-1.34%	-17.75%	19.08%	12.6	1185	16737	38793
Jiangsu	-6.11%	-6.86%	12.97%	25.13	29	20592	34690
Zhejiang	-6.14%	-6.41%	12.56%	16.1	84	18594	25693
Fujian	-7.10%	4.15%	2.95%	20.84	35	11752	20612
Shandong	-7.16%	-3.24%	10.40%	19.82	53	13415	26093
Guangdong	-4.86%	-6.74%	11.61%	12.75	126	11902	24937

5.4.2 The spatial characteristics of annual NDVI in response to socio-economic factors

The ever-increasing extent and intensity of human activities have imposed vast ecological deterioration and vegetation degradation throughout the world. China is the biggest developing country and occupies one-fifth of the world's population. China is undergoing unprecedented economic growth in the world's history at the moment (Lu et al., 2015). Specifically, socio-economic development, urban expansion, and population growth are dramatically greater in eastern China than in other regions of China, thereby aggravating resource depletion, environmental pollution, ecological deterioration, vegetation degradation, and land-use transformation in eastern China (Lu et al., 2011, Shi et al., 2011). In this study, the raster data of GDP, urban areas (rural residential areas, industrial areas, and mining areas are not considered in this sector), and population density with a spatial resolution of 1 km in 2000 and 2015 were utilized to investigate the spatial characteristics of the annual NDVI in response to socio-economic development, urban expansion, and population growth in eastern China from 2001 to 2016.

GDP is regarded as the representative of the economic vitality of a country or a region. Figure 4-11(a) displays the spatial differences in GDP from 2000 to 2015 in eastern China. A positive value indicates an increase in GDP from 2000 to 2015 and vice versa. Statistically, areas with positive values account for 99% of the study area. The differences in the GDP in 11% of these areas are more than 10,000 RMB/sq. km, and these areas are mostly located in the Pearl River Delta, Yangtze River Delta, as well as in the Bohai Economic Rim. Figure 4-11(b) illustrates the spatial pattern of urban expansion from 2000 to 2015 and the urban marginal areas with distance ranges of 0 to 5 km, 5 to 10 km, and 10 to 15 km to urban areas. The urban areas had increased by 10,624 km^2 from 2000 to 2015, which is mainly ascribed to the usage of agricultural land, grassland, and forest land as urban areas. Figure 4-11(c) indicates that the population density had increased over 60% of the study area. The population density mostly and concentratedly increases in the three economic zones and city centers. It is worth noting that the differences of the population density gradually decrease from the city center toward its surrounding areas.

Areas with a GDP decrease and areas with a population density decline of more than 500 people/sq.km are highly and spatially coupled, which are basically distributed within the old urban areas. The unique spatial characteristic is caused by China's regional industrial transfer behavior on the basis of the conversion of industry upgrade and urban expansion under the pressure of population growth and aging infrastructure (Su, 2016, Schneider and Mertes, 2014). For instance, China started relocating Shougang Group, the biggest steelmaker in Beijing, from the western suburban district of Beijing to a rural part of Qian'an city in Hebei province in 2003 and shifted its business focusing on tertiary industry. This action not only reduced regional population density and GDP dramatically but also alleviated the sulfur-containing compound emission (Wu and Zeng, 2013).

Figure 5-31 quantitatively reveals the spatial coupling between the dynamic change of vegetation cover and socio-economic development, urban expansion, and population growth for eastern China. Figure 5-31(a) shows that the proportion of the NDVI values ranging from 0 to 0.4 shows no differences at the GDP difference ranges of 0 to 10,000 and 10,000 to 20,000 RMB/sq.km, whereas this proportion increases with the GDP difference increase steadily when the GDP difference is higher than 20,000 RMB/sq.km., indicating that the vegetation cover declines gradually when the GDP difference is higher than 20,000 RMB/sq.km. From Figure 5-31(b) and (c), we observed that the vegetation cover change is dominated by a decreasing trend and shows no differences at the GDP difference ranges from 10,000 to 40,000 RMB/sq.km, while the vegetation stability is negatively associated with the socio-economic development for the same GDP difference ranges in eastern China.

In general, the vegetation cover is slightly higher in the new urban areas than in the old urban areas. Figure 5-32(a) shows that the proportion of the NDVI values ranging from 0.6 to 0.8 and 0.8 to 1 is higher in the non-urban areas than in the urban areas (old urban areas and new urban areas). Especially, these proportions at the distance of 10 to 15 km to urban areas are higher than at the distance of 5 to 10 km to urban areas, followed by the distance of 0 to 5 km to urban areas, indicating a monotonic increase of the vegetation density from the new urban areas toward rural areas. Figure 5-32(b) indicates that the urban expansion had devastated the vegetation cover, particularly in the newly developed urban areas. The negative impacts derived from urban expansion

gradually decline at the distances of 0 to 5 km toward the distances of 10 to 15 km to urban areas. Areas with an increasing trend of vegetation cover reach 37% in old urban areas. This proportion is double larger than that in the newly developed urban areas. The vegetation stability decreased from old urban areas to new urban areas, and the decreasing trend reversed with the distance range increase afterward. The vegetation cover is more stable at the distance of 10 to 15 km to urban areas (Figure 5-32(c)).

As mentioned previously, areas with a population density reduction of more than 500 people/sq.km are mostly distributed in old urban areas. Consequently, the vegetation cover and vegetation stability in these areas are relatively lower. Figure 5-33(a) and (c) report that the vegetation cover and vegetation stability are negatively associated with population growth. The vegetation cover is relatively lower and most fragile for the population density difference from 500 to 50,218 people/sq.km. The overall vegetation cover had improved at the population density difference from -500 to 500 people/sq.km due to less population pressure and human activities in these areas for the study period. It is worth noticing that the vegetation degradation had alleviated at the GDP difference range of 40,000 to 2,042,300 RMB/sq. km and the population density difference range of 1,500 to 50,218 people/sq.km. These areas are located in old urban areas with a low vegetation density. Therefore, the continuous increase of GDP and population density cannot constantly decrease the vegetation activity, but vegetation cover has improved due to practical vegetation management and natural vegetation succession.

Geographically, the vegetation cover change is closely associated with socio-economic development. In this study, vegetation degradation can be primarily ascribed to the combing effects of socio-economic development, urban expansion, and population growth, which is in good agreement with previous studies (Esau et al., 2016, Wang et al., 2012). On the basis of MOD13Q1 NDVI data from 2000 to 2014, Esau et al. (2016) detected the spatial interaction between urban development and vegetation cover change in northern West Siberia. The results of this study indicated that urban expansion negatively affected the vegetation cover in the newly developed urban areas and the surrounding areas at approximately 5 to 10 km due to large-scale human disturbances such as new infrastructure development and rapid urbanization. Furthermore, the NDVI value within the urban areas is fairly lower than the surrounding areas. This result is line

with the results generated by Wang et al. (2012) that the negative effects of human disturbances on vegetation cover gradually decrease with distance increase from urban areas to rural areas.

China has been experiencing countrywide urbanization, which is at the cost of farmland, grassland, and forest land loss. For example, 33,080 km^2 of agricultural land had converted to built-up land due to rapid urban expansion from 2000 to 2013, and more than half of these areas are located in eastern China (Shi et al., 2016). Moreover, such as in Sichuan, Yunnan, Chongqing, Guizhou, and Shaanxi, forest land or grassland on the hillsides were cultivated to cropland to satisfy the food demand because of population growth in these regions (Lu et al., 2005, Lu et al., 2015), which accordingly accelerated the processes of vegetation browning and soil erosion.

The Yangtze River Delta and Pearl River Delta economic zones, two largest economic zones located in eastern China, have experienced rapid socio-economic development, large-scale urban expansion, as well as dramatical population growth for the last three decades. All these unparalleled changes have paid the price in massive farmland loss (with a decline of 6.12% and 6.05% of their total farmland in Yangtze River Delta and Pearl River Delta from 2000 to 2013, respectively) and environment contamination, thereby resulting in ecological deterioration and vegetation degradation (Qu et al., 2015, Shi et al., 2016, Shi et al., 2011). Piao et al. (2003) demonstrated that vegetation cover in the Pearl River Delta and Yangtze River Delta has experienced a significant browning trend because of rapid urbanization. Peng et al. (2015) quantitatively analyzed the differences in vegetation cover in urban areas and rural areas in eastern China in general and the three economic zones in particular from 1999 to 2008. The results of this study demonstrated that the vegetation cover was basically lower in the urban areas than in the rural areas, particularly the vegetation cover is lowest in the three economic zones. Regarding the vegetation cover changing trend, the vegetation cover enhanced in rural areas but declined in urban areas due to socio-economic development, rural-urban migration, and its cumulative effects.

Previous studies have focused on discussing the overall effects of human activities on vegetation variation. For Instance, Qu et al. (2015) discussed the effects of human activities on vegetation cover change in China from 1982 to 2011 and pointed out that the vegetation deterioration was mainly induced by land use change, urban expansion, and agricultural activities. Peng et al. (2015) demonstrated that the large-scale urbanization processes in eastern China were the negative factor accumulatively affecting the vegetation density from 1998 to 2011. Only a few studies quantitatively detected the relationships between vegetation cover change and socio-economic factors. For example, Lu et al. (2015) computed the correlation coefficients between vegetation cover and ten socio-economic factors (*e.g.,* total population, working-age population, total employment, urban employment, GDP, first industry product, total investments in fixed assets, household consumption expenditures, and per capita consumption expenditures of rural households) for China from 2000 to 2010. The result of this study demonstrated that the vegetation degradation is positively associated with the total population, working-age population, total employment, urban employment, and negatively related to primary industry product, total investments in fixed assets, and the per capita consumption expenditures of rural households.

However, in our study, the quantified relationships between the annual NDVI and the 13 socio-economic factors for each administrative unit were primarily taken into consideration. Then the spatial interaction of the vegetation variables in response to socio-economic development, urban expansion, and population growth was displayed. Furthermore, we quantitatively illustrated the quantified relationship of the three vegetation metrics along with socio-economic development, urban expansion, and population growth. In our study, we generated a whole picture of the dynamic changes of vegetation cover in related to socio-economic factors both on spatial and temporal scales in eastern China, which enhances the understanding of how vegetation cover reacts to human activities.

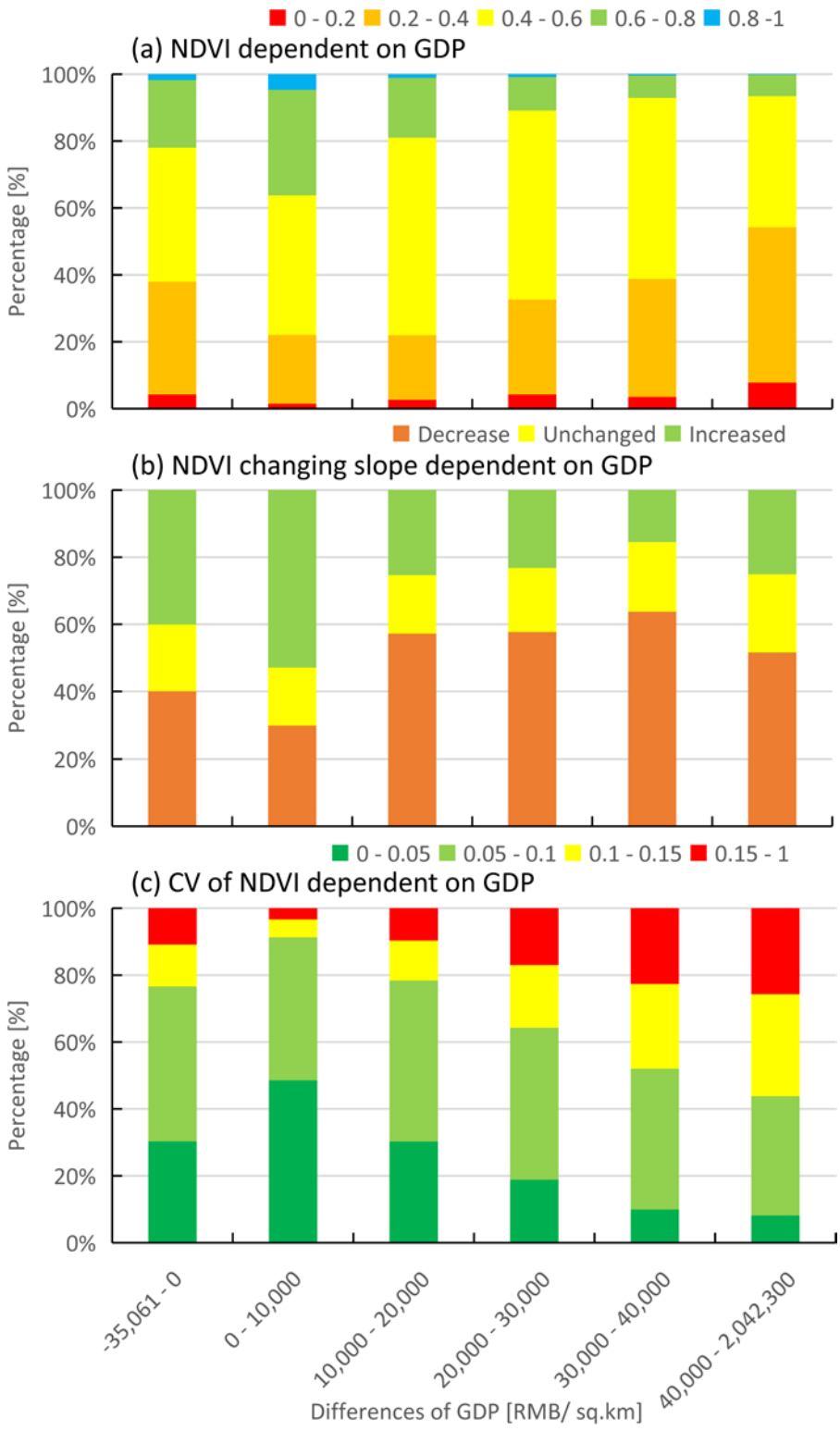

Figure 5-31. The statistical results of NDVI value, NDVI changing slope, and NDVI CV to difference range of GDP

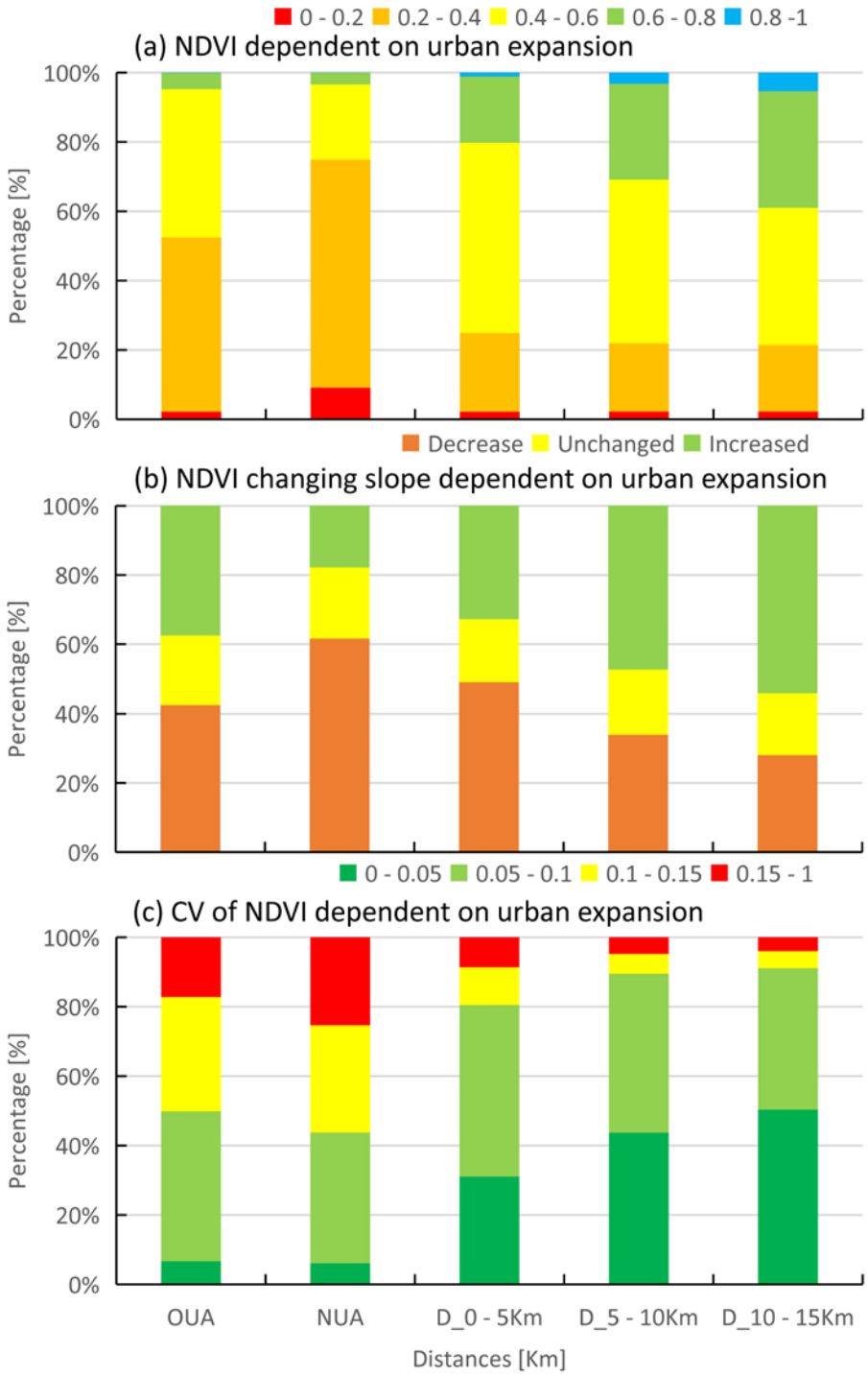

Figure 5-32. The statistical results of NDVI value, NDVI changing slope, and NDVI CV to urban expansion

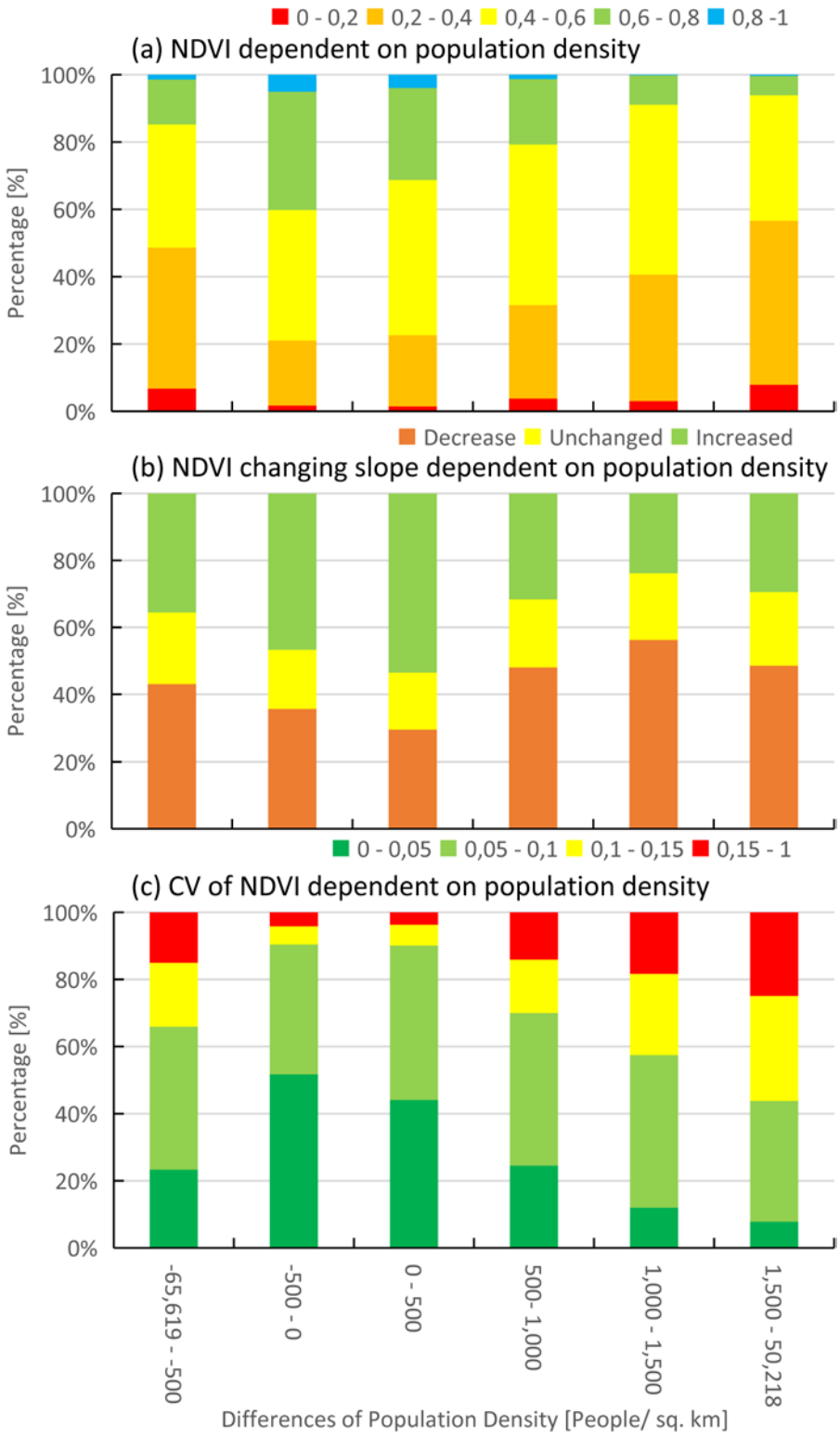

Figure 5-33. The statistical results of NDVI value, NDVI changing slope, and NDVI CV to difference range of population density

6 Summary and conclusion

Chapter 1 establishes the general background information of this study, incorporating research problem statement and motivation, research objectives, and key questions. The theoretical background and mathematical methods for monitoring of vegetation cover change and analyzing of vegetation cover in response to its driving forces such as climate forces, topographic forces, and socio-economic forces are outlined in chapter 2. Furthermore, the geographical location, socio-economic status, climate characteristics, population composition, and the land use status of the study area and the related data are introduced in chapter 3. Chapter 4 provides the methodological framework of this study by combining RS and GIS technologies, intending to carry out the objectives of this study. On the basis of multi-source data using multi-mathematical methods and platforms, the main findings and its relative discussions are distributed in chapter 5. In the following chapter, a summary of the research objectives is presented. Against the background of the results, the strengths and limitations of this study, and future research are proposed.

6.1 Summary

Vegetation cover change is a sensitive indicator of climate change, human activities, as well as natural disturbances. This study aims to quantitatively monitor the dynamic change of vegetation cover, investigate the relationships between NDVI and its driving forces such as climate forces, topographic forces, as well as socio-economic forces, and investigate the lag time for maximum NDVI response to climate variables in eastern China using multiple mathematical methods. MODIS NDVI time series, monthly meteorological data, DEM data, socio-economic statistical data, the vector map of eastern China, the map of land use types, the map of GDP, and the map of population density provided reliable data support for this study. Knowledge of the vegetation cover change and the relationships between NDVI and its driving factors can further improve the understanding of the basic biogeochemical processes, and their possible feedbacks to the surface vegetation evolution. The objectives of this study are fulfilled, and the research questions of this study are answered in the context. Moreover, the main findings of this study are summarized in the following four sections.

6.1.1 The spatiotemporal variation of vegetation cover in eastern China

Temporally, the annual NDVI shows an upward trend with a magnitude of 0.0003 $year^{-1}$ in eastern China, suggesting a slightly increasing trend during the study period. NDVI presents an increasing trend in spring and autumn but a decreasing trend in summer. Former research demonstrated that NDVI established an upward trend in all seasons in China (Piao et al., 2003). This difference might be caused by the differences in data source, study period, and the study area.

Spatially, the spatial distribution of the vegetation cover in spring, summer, and autumn follows the same pattern that the NDVI values are higher in the south and lower in the north of the study area. The overall NDVI value is higher in summer than in autumn, followed by spring. With an exception of the NDVI values in Jiangsu and the west part of Shandong is noticeably higher in spring than in autumn, which is ascribed to regional agricultural activities in the context of the winter wheat/paddy rice and rapeseed/paddy rice double cropping rotation system.

On annual scale, areas with a greening trend account for 49% of the study area. These greening areas are mostly distributed in the north of the study area. Areas with a browning trend account for 33% of the study area. Above results indicate that the areas showing vegetation improvement are larger than the areas showing vegetation degradation in eastern China. In terms of the vegetation variation on seasonal scale, the vegetation degradation is more critical in summer than in spring and autumn.

In term of the consistency of the vegetation cover on annual scale, areas expected to maintain the current changing trends and switch the current changing trends in the future accounting for 57% and 43% of the study area, respectively. Inconsistent with former research (Tong et al., 2018), in our study, we found that the degradation area will be larger than the improvement area for eastern China both on annual and seasonal scales in the future.

The vegetation cover is relatively stable during a year, particularly in Guangdong, Zhejiang, Fujian, and the east part of Liaoning. However, the vegetation cover had significantly fluctuated in the three economic zones due to the influences of socio-economic development, urban expansion, and population growth and the northwest part

of Hebei due to the implementation of large-scale reforestation programs, and practical forest management.

6.1.2 The relationship between NDVI and climate factors in eastern China

The relationship is more pronounced between NDVI and temperature than that of between NDVI and precipitation in eastern China both on annual and seasonal scales. In addition, the response of NDVI to changes in precipitation is strongest in autumn. The relationship between NDVI and temperature is higher in spring than in autumn, followed by in summer, which is not in line with previous research. Previous research evidenced that the correlation coefficient between NDVI and temperature is greatest in autumn in eastern China (Cui, 2010).

Considering the lag time for maximum NDVI response to changes in precipitation and temperature for eastern China on seasonal scale, NDVI maximally responses to the current temperature in spring and autumn but to the temperature of previous 1 month in summer. The maximum correlation coefficient between NDVI and precipitation is acquired when precipitation is preceding NDVI by 1 month in spring and autumn and 2 months in summer. Above results generated two statements that (1) the lag time for maximum NDVI response to precipitation is longer than that to temperature, and (2) both the lag time for maximum NDVI response to changes in temperature and precipitation is longer in summer than in spring and autumn.

Spatially, the maximum correlation coefficients between NDVI and precipitation as well as NDVI and temperature are generally higher in the north and lower in the south of the study area both on annual and seasonal scales, except for summer, suggesting that both precipitation and temperature play a higher-level control on vegetation growth in the north of the study area. Previous research evidenced that NDVI in most of the meteorological stations of Zhejiang, Fujian, and Guangdong is negatively associated with temperature in summer (Cui, 2010, Peng et al., 2015). But, in our study, we found that NDVI is positively related to temperature in 43 out of 52 meteorological stations in summer within the same region.

Generally, the annual NDVI is maximally associated with the concurrent temperature across eastern China. The annual NDVI shows distinctive geographical characteristics to

changes in precipitation: namely, the annual NDVI maximally responses to the concurrent precipitation in the north of the study area, but the annual NDVI presents complex lag time to precipitation in the south of the study area (*e.g.,* Zhejiang, Fujian, and Guangdong). Furthermore, in our study, we detected that NDVI in most of the meteorological stations show 2- to 3-month lag time to changes in precipitation and temperature in summer in Zhejiang, Fujian, and Guangzhou, but Cui (2010) evidenced that NDVI in most of the meteorological station shows no lag time to changes in precipitation and temperature in summer within the same region. The differences between Cui (2010) and our study can be ascribed to the differences of the data sources and study period.

6.1.3 The relationship between NDVI and topographic factors in eastern China

The vegetation cover and vegetation stability increase with an elevation increase constantly when elevation ranges from 0 to 500 m, but the upward trend of the vegetation cover and vegetation stability reversed afterward. Areas with a decreasing trend at the elevation range of -282 to 0 m and 0 to 100 m are relatively higher than at higher elevation ranges. Areas with vegetation improvement are larger than the areas with vegetation degradation when elevation ranges from 100 to 2849 m.

It is worth mentioning that the proportion of the annual NDVI value, annual NDVI changing trend, and annual NDVI CV in each category shows no statistical differences on the SFS and NFS. This result is against our initial hypothesis and former research results. In the northern hemisphere, plants on the SFS are expected to accept several times more solar radiation than on the NFS, and vice versa in the southern hemisphere. Differ to former studies, in our study, areas extending the south of Jiangsu to Guangdong are controlled by humid climate, a place with abundant precipitation, sufficient light, and warm temperature across a year, and no apparent wet season and dry season are detected in this region. Areas extending from the north of Jiangsu to Liaoning are predominated by flat landscape. Vegetation on the NFS and SFS is, therefore, less restricted by the differences of light, heat, and water conditions and shows no differences of vegetation growth on the NFS and SFS.

Similar to the relationships between the elevation-vegetation cover and elevation-vegetation stability, the vegetation cover and vegetation stability increase with slope range increase. The proportion of the areas with a greening trend shows a “humped” pattern with the slope degree increase. Meanwhile, the proportion of the browning areas shows a “valley” pattern. The “peak” and the “valley bottom” reach 58% and 25% of the corresponding area, respectively, when the slope degree ranges from 6° to 15°.

6.1.4 The relationship between NDVI and socio-economic factors in eastern China

Results derived from this study demonstrated that, temporally, vegetation cover is negatively associated with the 13 socio-economic factors in Tianjin, Shanghai, Jiangsu, Zhejiang, Fujian, and Guangdong but positively related to the 13 socio-economic factors in Beijing, Hebei, Liaoning, and Shandong. The vegetation degradation is primarily ascribed to socio-economic development, urban expansion, and population growth. However, the vegetation improvement in Beijing, Hebei, Liaoning, and Shandong is attributed to the implementation of large-scale reforestation and afforestation programs such as the NFCP, TNSDP, BTSSCP, and GGP at a certain level. Another reason for vegetation improvement in Beijing is winning the right to host the 2008 Olympic Games.

Spatially, the dynamic change of vegetation cover is negatively coupled with socio-economic development, urban expansion, and population growth in eastern China. The proportion of the browning areas increases with GDP difference increase, and the proportion reaches the peak with a magnitude of 64% of the corresponding area at the GDP difference range of 30,000 to 40,000 RMB/sq. km. Urban expansion is negatively correlated to vegetation growth, particularly in the new urban areas. we found that the negative influences of urban expansion on vegetation growth are strongest in the new urban areas but weaken with the distance from 0 to 15 km to urban areas gradually. Migration from rural to urban areas leads to a greening trend of vegetation cover in the rural areas and a browning trend of vegetation cover in the urban areas.

6.2 The answers to the research questions

Multiple data sources and approaches were utilized and integrated to monitor the dynamic change of vegetation cover from 2001 to 2016 and to investigate the

relationships between vegetation variation and its driving forces (*e.g.*, climate forces, topographic forces, and socio-economic forces) to answer five main scientific research questions of this study. The five research questions are produced with regarding metrics and approach selection, driving factors determination, and dominant factor detection. In the following sections, answers of the five research questions are distributed.

1) Which metrics can be used to reflect the long-term vegetation cover variation, and how to quantify the vegetation changing trend and vegetation cover stability?

MODIS NDVI (NDVI value) is used to monitor the dynamic change of vegetation cover; linear regression analysis is applied to assess the vegetation changing trend; and NDVI CV is considered as an efficient indicator for identifying the amplitude of the vegetation cover oscillation.

NDVI value is used to monitor the spatial distribution of vegetation cover on annual and seasonal scales. As mentioned in Chapter 1 that NDVI is a normalized ratio reflecting the different reaction of vegetation to the red and near-infrared reflectance, and it is applied to give a quantitative description of the earth's surface vegetation cover and vegetation growth status under certain conditions (Chen et al., 2014). It has been widely used to monitor the vegetation growth status, vegetation phenology variability, crop yield estimation, agricultural cropping pattern, and vegetation dynamic variation (Butt et al., 2011, Miao et al., 2015, Ren et al., 2008, Lunetta et al., 2010).

Linear regression analysis is utilized to reveal and estimate the vegetation changing trend of each grid over the study period against the background of NDVI time-series images. As intimated in chapter 2.1, linear regression analysis is more frequently and effectively implemented for monitoring the spatial pattern of long-term vegetation cover change. Although the non-linear regression analysis was proved to be more precise for inspecting the turning point of the vegetation cover change, linear regression analysis and their estimation turned out to be rough on temporal scale but much practical on spatial scale (Fensholt and Proud, 2012).

The coefficient of variation (CV) is diffusely used to evaluate the stability of the terrestrial vegetation cover under the combined effects of climate change, human activities, as well as natural forces for a certain region during a corresponding period (Peng et al., 2015).

As demonstrated in chapter 2.1, the stability of the terrestrial vegetation cover over a specified region during different time periods can be revealed by NDVI CV on pixel scale. NDVI CV is commonly applied to monitor the stability of vegetation cover and achieved good results (Fang et al., 2001, Peng et al., 2015, Barbosa et al., 2006). Therefore, in this study, the NDVI CV is regarded to be an indicator of NDVI stability related to the mean NDVI value on annual and seasonal scales.

2) How to quantitatively determine the relationships between NDVI and climate factors, and how to investigate the lag time for maximum NDVI response to changes in climate factors? Which climate factor is the dominant factor controlling the vegetation growth in eastern China?

The methodology of how to quantify the correlation coefficient between NDVI and climate variables and investigate the lag time for maximum NDVI response to changes in climate variables is introduced in chapter 4.2. Pearson's correlation analysis is applied to quantify the strength of the linear relationship between NDVI and climate variables. Regarding the lag time for maximum NDVI response to changes in precipitation and temperature, the correlation coefficients between NDVI and precipitation and temperature of previous 0 to 3 months are examined and reported for each administrative units and each meteorological station both on annual and seasonal scales. The maximum correlation coefficients of four (0 to 3 months) correlation coefficients of each corresponding administrative unit and meteorological station are selected, which suggests the maximum response of NDVI to precipitation and temperature variation. The corresponding month of the maximum correlation coefficient determines the lag time for maximum NDVI response to changes in precipitation and temperature.

At provincial level, temperature is regarded as the dominant factor controlling the vegetation cover variation throughout eastern China. In terms of the dominant factor in each meteorological station, 183 out of 184 meteorological stations are primarily controlled by temperature on annual scale. Furthermore, the vegetation cover variation is decisively influenced by temperature at 160 meteorological stations in spring, 124 meteorological stations in summer, and 170 meteorological stations in autumn, suggesting that the decisive influence of temperature on vegetation cover variation is weaker in summer than in spring and autumn.

3) How to map the spatial interaction and how to determine the quantitative relationships between vegetation variation and topographic factors and socio-economic factors?

Topographic factors (*e.g.*, elevation, aspect, and slope) are decisive for long-term vegetation evolution and succession, while, in the short term, the dynamic changes of vegetation cover are most directly and indirectly affected by socio-economic factors (*e.g.*, socio-economic development, urban expansion, and population growth). In this study, as mentioned in chapter 4.3 and chapter 4.4, overlay analysis is utilized to map the spatial characteristics between vegetation variation and topographic factors as well as vegetation variation and socio-economic factors, and zonal analysis is applied to obtain the regional statistical results.

To map the spatial pattern of the dynamic changes of vegetation cover in different categories of the elevation ranges, the dataset of elevation is employed to be overlapped on the three vegetation metrics (*e.g.,* annual NDVI, annual NDVI changing slope, and annual NDVI CV), respectively. For example, the annual NDVI was extracted on the basis of the reclassified elevation not only to map the spatial pattern of the annual NDVI along with the elevation gradient but also to statistically analyze the changing characteristics of the annual NDVI in terms of in different categories of elevation ranges. Theoretically, against the background of the above methods, the spatial interaction between the three vegetation metrics and the three topographic factors (*e.g.,* elevation, aspect, and slope) was illustrated, and then their quantitative relationships of the three vegetation metrics at each elevation, aspect, and slope ranges were determined, respectively. Based on the same methodology, the spatial interaction between the three vegetation metrics and the three socio-economic factors is displayed, and the quantitative relationships between the three vegetation metrics and the three socio-economic factors are computed.

4) Do all the socio-economic factors negatively affect the vegetation growth over eastern China from 2001 to 2016?

Human activities are anticipated to exert a stronger impact on the processes of vegetation evolution and succession than climate forces and topographic forces both in

speed and extent. In this study, the correlation coefficients between annual NDVI and the 13 socio-economic factors for each administrative unit are calculated.

The 13 socio-economic factors are negatively associated with the annual NDVI in Tianjin, Shanghai, Jiangsu, Zhejiang, Fujian, and Guangdong, particularly in Shanghai, Jiangsu, and Zhejiang, the negative effects of human activities on vegetation growth are more serious. However, the correlation coefficients between the annual NDVI and the 13 socio-economic factors are positive in Beijing, Hebei, Liaoning, and Shandong. Especially in Beijing, Hebei, and Liaoning, all of the correlation coefficients between the annual NDVI and the 13 socio-economic factors are significant at the $p<0.01$ level, which can be chiefly ascribed to the initiation of large-scale reforestation and afforestation programs such as the NFCP, TNSDP, BTSSCP, and GGP. These large-scale reforestation and afforestation programs not only exert the processes of the vegetation restoration but also offset the negative effects derived from human activities in its corresponding regions.

5) What is the underlying cause of the spatial heterogeneity of vegetation cover over eastern China?

The vegetation cover shows apparent spatial heterogeneity over eastern China both on annual and seasonal scales, which is not only produced by a single force but also attributed to the combined effects of local climate variation, local land use change, topographic forces, and human intervention. For instance, the spatial heterogeneity of vegetation cover is generally determined by the changes in precipitation and temperature and land use types. As displayed in Figure A-5 and Figure A-6, the precipitation and temperature show a gradient increase from the south of the study to the north of the study. Precipitation and temperature are recognized as primary factors controlling the rate of respiration and photosynthesis in plants, thereby affecting the vegetation vitality. Due to the uneven precipitation and temperature over eastern China, the vegetation cover presents a distinctive spatial heterogeneity. Furthermore, against the background of local land use types, the vegetation cover is generally higher in Zhejiang, Fujian, Guangdong, and the east of Liaoning but lower each city center, in the west of Liaoning, southeast of Beijing and Tianjin, and the northwest of Hebei.

Elevation is considered to be a dominant factor controlling the vertical distribution of vegetation cover. This study demonstrated that vegetation cover increases with the elevation and slope increase and reaches its peak at the elevation range of 400 to 500 m and 25° to 90°, respectively. However, the gradient changes of vegetation cover are not only dependent on the elevation and slope variations but also closely associated with the frequency of human activities. Due to the human intervention gradually weakening with the increase of elevation and slope ranges, the spatial heterogeneity of vegetation cover is considerably ascribed to the combined effects of topographic forces and human activities. It is worth noticing that the vegetation cover in each category shows no statistical differences on the SFS and NFS.

Human activities exert both positive and negative impacts on vegetation cover change, which contribute to the spatial heterogeneity of vegetation cover. For example, along with the socio-economic development, urban expansion, and population growth for the study period, the annual vegetation cover in Shanghai decreased with a changing rate of -0. 0036 $year^{-1}$, while the annual vegetation cover in Beijing increased with a changing rate of 0.0033 $year^{-1}$ during the same period. It has been evidenced that the vegetation cover improvement in Beijing is attributed to the implementation of large-scale reforestation and afforestation programs and winning the right to host the 2008 Olympic Games at a certain level.

6.3 Strengths and limitations

This study investigated the spatiotemporal characteristics of vegetation variation and explored the responding mechanisms of vegetation cover to the variability of its driving factors such as climate change, human activities, and natural forces in eastern China from 2001 to 2016. The results of this study contribute to a better understanding of the dynamic change of vegetation cover, the interplay between vegetation cover change and its driving forces, and the time lag effects of vegetation cover to climate variation in the context of global climate change, terrain evolution, socio-economic development, urban expansion, as well as population growth. This study further provides a theoretical framework for decision-making for future environmental protection, biodiversity conservation, as well as vegetation management.

6.3.1 Strengths

The emergence of NDVI time series from multiple satellite sensors such as NOAA AVHRR, MODIS, as well as SPOT VGT provides the foundation for studying on the dynamic change of vegetation cover from pixel scale, regional scale, and national scale to global scale. In this study, MODIS NDVI C6 is utilized to monitor the spatiotemporal variation of vegetation cover because the production of MODIS NDVI is on the basis of spectral bands, which include state-of-the-art navigation, atmospheric correction, reduced geometric distortions, and improved radiometric sensitivity. In addition, these spectral bands are especially projected for vegetation monitoring. In addition, as demonstrated by Zhang et al. (2017) that the accuracy and precision of the MODIS NDVI C6 are better than the MODIS NDVI C5 due to sensor upgrade. Consequently, the MODIS NDVI C6 is regarded to be an enhancement over the NDVI products derived from other sensors.

Previous studies have focused on investigating the response of vegetation cover change to a single force or on a single scale (Kileshye Onema and Taigbenu, 2009, Kong et al., 2017, Krishnaswamy et al., 2014, Bennie et al., 2006, Luck et al., 2009). The relationships between vegetation cover change and multi-forces and the time lag effects of vegetation cover change to climate factors such as precipitation and temperature are less considered, which tend to increase the uncertainty of the research results. In this study, (1) three NDVI metrics such as the NDVI value, NDVI changing slope, as well as NDVI CV are employed to detect the spatiotemporal variation of vegetation cover; (2) the underlying relationships between vegetation cover change and its driving factors and the responding mechanisms of vegetation cover to variability of driving factors in eastern China are analyzed; (3) the lag time for maximum NDVI response to climate factors is investigated for each administrative unit and each meteorological station, and the spatial patterns of the lag time for maximum NDVI response to precipitation and temperature are displayed both on annual and seasonal scales ; (4) the spatial interaction between the three vegetation metrics and the three topographic factors are illustrated; (5) furthermore, the relationships between the annual NDVI and the 13 socio-economic factors and the spatial interplay between the three vegetation metrics and socio-

economic development, urban expansion, and population growth are demonstrated in this study.

Taking multi-driving forces into consideration and including multiple factors in each force can promote an enhanced understanding of spatiotemporal interaction between vegetation cover change and its driving forces in eastern China. Our study can not only promote a way for evaluating the effectiveness of the reforestation program, but also can provide basic knowledge to urban planner, lawmaker, and authorities for environmental protection, ecological restoration, and vegetation reforestation during the processes of large-scale urbanization, reforestation program implementation and management.

6.3.2 Limitations

The overall relationships between vegetation cover and climate factors such as precipitation and temperature are obtained in this study, but the differences of different land use types in response to climate variability do not take into consideration. As mentioned in chapter 3 that the major land use types in eastern China are farmland, forest land, grassland, built-up land, and water body. Particularly, the three former land use types occupy a large proportion in eastern China. Wu et al. (2015) demonstrated that different vegetation types show clearly different lag time to changes in the same climate factors, and the same vegetation type presents significantly different lag time to different climate factors. For instance, the deciduous broadleaf forest shows the longest lag time to changes in temperature, while most of the grassland and cropland response to the concurrent month of temperature. However, the time lag effects of different vegetation types to precipitation show huge geographic differences and less distinct patterns. Regarding the grassland types, the relationships between NDVI and precipitation as well as NDVI and temperature are obviously varied (Piao et al., 2006b).

After applying the linear regression analysis, areas had experienced greening trends and browning trends are detected in eastern China from 2001 to 2016. Figure 5-8(a) shows that areas located in the three economic zones and its surrounding areas are undergoing a serious vegetation degradation, while areas distributed in Beijing, the north of Hebei, and many parts of Liaoning and Shandong are experiencing significant vegetation rehabilitation. Although these results are highly in line with previous studies (Cao et al.,

2017, Li et al., 2015c, Lu et al., 2015, Peng et al., 2015), verification of the main findings of this study is restricted by the availability of in situ observations. Fieldworks are therefore urgently needed to validate the main findings of this study and to improve the accuracy of the main findings of this study. For instance, the statistical vegetation cover change shows no differences on the NFS and SFS, which is not in line with some previous studies (Albaba, 2014, Maren et al., 2015, Toro Guerrero et al., 2016). Thus, field works can verify the differences and provide a better understanding of the underlying causes of the dynamic change of vegetation cover in eastern China.

It is well known that vegetation plays an important role in regulating climate systems in the long-term process. The MDO13Q1 NDVI data is available from February 2000 to the present. The use of MODIS satellite imageries and monthly meteorological data may propose a challenge to investigate the relationship between vegetation cover change and climate variation accurately. The 16-year study period is only available to generalize a whole picture of vegetation cover change responses to climate variation in this century, but cannot demonstrate the interaction mechanism between vegetation cover change and climate variation in the last century. The study period needs to be extended forward. Furthermore, the relationships between the annual NDVI and the 13 socio-economic factors are investigated at the administrative unit level, which cannot report the spatial characteristic of each socio-economic factor contributing to vegetation cover change.

6.4 Future research

The methodology framework, which proposed in chapter 4, has demonstrated to be practical in monitoring the dynamic change of vegetation cover and investigating the spatiotemporal characteristics of vegetation cover change in response to its driving factors. The main findings of this study contribute to a better understanding of the relationship between vegetation cover change and its driving forces and provide decision-making support for future project implementation. However, it is just a beginning to improve our insight into global vegetation variation, additional research issues need to be addressed in future study.

1) The relationship between different land use types and climate factors

This study generally accounts for the effects of climate factors on vegetation. It is well acknowledged that land use and land cover changes have performed a significant influence on vegetation variation. In addition, different land use types are expected to show different correlation and lag time to changes in climate factors. Eastern China possesses abundant ecosystems. Future work is needed to investigate the underlying mechanism of different land use types response to climate variation and the specific lag time of different land use types to changes in climate factors.

2) The interaction between groundwater storage dynamic and long-term vegetation variation

Satellite gravimetry is a unique RS technique capable to detect total water storage anomaly. The current Gravity Recovery and Climate Experiment (GRACE) satellite mission, launched in 2002, has provided valuable scientific data for hydrological applications particularly for large-scale total water storage resources monitoring and assessment. Vegetation growth is highly controlled by water availability, particularly in water-limited ecosystems (Yang et al., 2014, Xie et al., 2016). Drought events frequently occur in the north of the study area (Zhu et al., 2016). It is therefore of great practical value to examine the relationship between vegetation variation and total water storage variability in eastern China.

3) Spatial characteristic of NDVI in response to precipitation

Monthly precipitation and temperature data are applied to investigate the relationship between NDVI and climate variability based on 184 meteorological base stations in this study. The 184 meteorological stations are unevenly distributed in the study area, which may lead to a systematical error of spatial interplay between NDVI and climate variability. The Tropical Rainfall Measuring Mission (TRMM) satellite, launched in November 1997, provides a possibility to investigate the spatial pattern of the relationship and lag time for maximum NDVI response to precipitation evenly. Hence, the spatial pattern of the relationship between NDVI and precipitation and the lag time for maximum NDVI response to changes in precipitation is able to be detected evenly in the background of the TRMM satellite images.

References

AL-ABED, M., ZHOU, S., AHMAD YAGHI, A. & WANG, R. C. 2000. Application of GIS and remote sensing in soil degradation assessments in the Syrian coast. *Journal of Zhejiang University (Agriculture and Life Sciences),* 26**,** 191-196.

ALBABA, I. 2014. The effects of slope orientations on vegetation characteristics of Wadi Al Quf forest reserve (WAFR) West Bank-Palestine. *International Journal of Agricultural and Soil Science,* 2**,** 118-125.

ALBANI, M., MEDVIGY, D., HURTT, G. C. & MOORCROFT, P. R. 2006. The contributions of land-use change, CO2fertilization, and climate variability to the Eastern US carbon sink. *Global Change Biology,* 12**,** 2370-2390.

ALLEN, R. B. & PEET, R. K. 1990. Gradient Analysis of Forests of the Sangre-De-Cristo-Range, Colorado. *Canadian Journal of Botany-Revue Canadienne De Botanique,* 68**,** 193-201.

ANDERSON, L. O., MALHI, Y., ARAGAO, L. E., LADLE, R., ARAI, E., BARBIER, N. & PHILLIPS, O. 2010. Remote sensing detection of droughts in Amazonian forest canopies. *New Phytologist,* 187**,** 733-750.

ANGERT, A., BIRAUD, S., BONFILS, C., HENNING, C. C., BUERMANN, W., PINZON, J., TUCKER, C. J. & FUNG, I. 2005. Drier summers cancel out the CO2 uptake enhancement induced by warmer springs. *Proceedings of the National Academy of Sciences of the United States of America,* 102**,** 10823-10827.

ANYAMBA, A. & TUCKER, C. J. 2005. Analysis of Sahelian vegetation dynamics using NOAA-AVHRR NDVI data from 1981–2003. *Journal of Arid Environments,* 63**,** 596-614.

ARMESTO, J. A. & MARTINEZ, J. A. 1978. relations between vegetation structure and slope aspect in the mediterranean region of chili. *Journal of Ecology,* 66**,** 881-889

ARNETH, A., HARRISON, S. P., ZAEHLE, S., TSIGARIDIS, K., MENON, S., BARTLEIN, P. J., FEICHTER, J., KORHOLA, A., KULMALA, M., O'DONNELL, D., SCHURGERS, G., SORVARI, S. & VESALA, T. 2010. Terrestrial biogeochemical feedbacks in the climate system. *Nature Geoscience,* 3**,** 525-532.

ATKINSON, P. M., CUTLER, M. E. J. & LEWIS, H. 1997. Mapping sub-pixel proportional land cover with AVHRR imagery. *International Journal of Remote Sensing,* 18**,** 917-935.

AUSLANDER, M., NEVO, E. & INBAR, M. 2003. The effects of slope orientation on plant growth, developmental instability and susceptibility to herbivores. *Journal of Arid Environments,* 55**,** 405-416.

AUSTRHEIM, G. 2002. Plant diversity patterns in semi-natural grasslands along an elevational gradient in southern Norway. *Plant Ecology,* 161**,** 193-205.

BANK, T. W. 2007. Dhaka: Improving living conditions for the urban poor. *Sustainable Development Unit, South Asia Region.*

BAO, G., QIN, Z. H., BAO, Y. H., ZHOU, Y., LI, W. J. & SANJJAV, A. 2014. NDVI-based long-term vegetation dynamics and its response to climatic change in the Mongolian Plateau. *Remote Sensing,* 6**,** 8337-8358.

BARBER, V. A., JUDAY, G. P. & FINNEY, B. P. 2000. Reduced growth of Alaskan white spruce in the twentieth century from temperature-induced drought stress. *Nature,* 405**,** 668-673.

BARBOSA, H. A., HUETE, A. R. & BAETHGEN, W. E. 2006. A 20-year study of NDVI variability over the Northeast Region of Brazil. *Journal of Arid Environments,* 67**,** 288-307.

BENNIE, J., HILL, M. O., BAXTER, R. & HUNTLEY, B. 2006. Influence of slope and aspect on long-term vegetation change in British chalk grasslands. *Journal of Ecology,* 94**,** 355-368.

BENNIE, J., HUNTLEY, B., WILTSHIRE, A., HILL, M. O. & BAXTER, R. 2008. Slope, aspect and climate: Spatially explicit and implicit models of topographic microclimate in chalk grassland. *Ecological Modelling,* 216**,** 47-59.

BIEBL, R. & MCROY, C. P. 1971. Plasmatic resistance and rate of respiration and photosynthesis of Zostera-Marina at different salinities and temperatures. *Marine Biology,* 8**,** 48-56.

BOGAERT, J., ZHOU, L., TUCKER, C. J., MYNENI, R. B. & CEULEMANS, R. 2002. Evidence for a persistent and extensive greening trend in Eurasia inferred from satellite vegetation index data. *Journal of Geophysical Research-Atmospheres,* 107**,** ACL 4-1-ACL 4-14.

BOYD, D. S., FOODY, G. M. & RIPPLE, W. J. 2002. Evaluation of approaches for forest cover estimation in the Pacific Northwest, USA, using remote sensing. *Applied Geography,* 22**,** 375-392.

BRASWELL, B. H., SCHIMEL, D. S., LINDER, E. & MOORE, B. 1997. The response of global terrestrial ecosystems to interannual temperature variability. *Science,* 278**,** 870-872.

BROOKS, T. M., MITTERMEIER, R. A., DA FONSECA, G. A. B., GERLACH, J., HOFFMANN, M., LAMOREUX, J. F., MITTERMEIER, C. G., PILGRIM, J. D. & RODRIGUES, A. S. L. 2006. Global biodiversity conservation priorities. *Science,* 313**,** 58-61.

BROWN, M. E. & DE BEURS, K. M. 2008. Evaluation of multi-sensor semi-arid crop season parameters based on NDVI and rainfall. *Remote Sensing of Environment,* 112**,** 2261-2271.

BRYAN, B. A., GAO, L., YE, Y., SUN, X., CONNOR, J. D., CROSSMAN, N. D., STAFFORD-SMITH, M., WU, J., HE, C., YU, D., LIU, Z., LI, A., HUANG, Q., REN, H., DENG, X., ZHENG, H., NIU, J., HAN, G. & HOU, X. 2018. China's response to a national land-system sustainability emergency. *Nature,* 559**,** 193-204.

BUERMANN, W., PARIDA, B., JUNG, M., MACDONALD, G. M., TUCKER, C. J. & REICHSTEIN, M. 2014. Recent shift in Eurasian boreal forest greening response may be associated with warmer and drier summers. *Geophysical Research Letters,* 41**,** 1995-2002.

BUSING, R. T. & WHITE, P. S. 1993. Gradient analysis of old spruce-fir forest of the Great Smokey Mountains circa 1935. *Ecology,* 71**,** 951- 958.

BUTT, B., TURNER, M. D., SINGH, A. & BROTTEM, L. 2011. Use of MODIS NDVI to evaluate changing latitudinal gradients of rangeland phenology in Sudano-Sahelian West Africa. *Remote Sensing of Environment,* 115**,** 3367-3376.

BUYANTUYEV, A. & WU, J. 2009. Urbanization alters spatiotemporal patterns of ecosystem primary production: A case study of the Phoenix metropolitan region, USA. *Journal of Arid Environments,* 73**,** 512-520.

CAO, S. X. 2011. Impact of China's large-scale ecological restoration program on the environment and society in arid and semiarid areas of China: Achievements,

problems, synthesis, and applications. *Critical Reviews in Environmental Science and Technology,* 41**,** 317-335.

CAO, S. X., CHEN, L., SHANKMAN, D., WANG, C. M., WANG, X. B. & ZHANG, H. 2011. Excessive reliance on afforestation in China's arid and semi-arid regions: Lessons in ecological restoration. *Earth-Science Reviews,* 104**,** 240-245.

CAO, S. X., SHANG, D., YUE, H. & MA, H. 2017. A win-win strategy for ecological restoration and biodiversity conservation in Southern China. *Environmental Research Letters,* 12**,** 044004.

CHEN, T., DE JEU, R. A. M., LIU, Y. Y., VAN DER WERF, G. R. & DOLMAN, A. J. 2014. Using satellite based soil moisture to quantify the water driven variability in NDVI: A case study over mainland Australia. *Remote Sensing of Environment,* 140**,** 330-338.

CHEN, Y. H., LI, X. B., SHI, P. J. 2001. Variation in NDVI driven by climate factors across China, 1983-1992. *Chinese Journal of Plant Ecology,* 25**,** 716-720 (in Chinese).

COETZER, K. L., ERASMUS, B. F., WITKOWSKI, E. T. & REYERS, B. 2013. The race for space: tracking land-cover transformation in a socio-ecological landscape, South Africa. *Environmental Management,* 52**,** 595-611.

CUI, L. L., SHI, J. 2010. Temporal and spatial response of vegetation NDVI to temperature and precipitation in eastern China. *Journal of Geographical Sciences,* 20**,** 163-176.

CUI, X., GIBBES, C., SOUTHWORTH, J. & WAYLEN, P. 2013. Using Remote Sensing to Quantify Vegetation Change and Ecological Resilience in a Semi-Arid System. *Land,* 2**,** 108-130.

D'ARRIGO, R. D., KAUFMANN, R. K., DAVI, N., JACOBY, G. C., LASKOWSKI, C., MYNENI, R. B. & CHERUBINI, P. 2004. Thresholds for warming-induced growth decline at elevational tree line in the Yukon Territory, Canada. *Global Biogeochemical Cycles,* 18**,** GB3021.

DAI, S. P. & ZHANG, B. 2010. Ten-days response of vegetation NDVI to the variations of temperature and precipitation in Qilian Mountains based on GIS. *Ecology and Environmental Sciences,* 01**,** 140-145 (in Chinese).

DE FREITAS, M. W. D., SANTOS, J. R. D. & ALVES, D. S. 2013. Land-use and land-cover change processes in the Upper Uruguay Basin: linking environmental and socioeconomic variables. *Landscape Ecology,* 28**,** 311-327.

DE JONG, R., DE BRUIN, S., DE WIT, A. J., SCHAEPMAN, M. E. & DENT, D. L. 2011. Analysis of monotonic greening and browning trends from global NDVI time-series. *Remote Sensing of Environment,* 115**,** 692-702.

DE JONG, R., SCHAEPMAN, M. E., FURRER, R., DE BRUIN, S. & VERBURG, P. H. 2013. Spatial relationship between climatologies and changes in global vegetation activity. *Global Change Biology,* 19**,** 1953-1964.

DENG, Y. X., GOODCHILD, M. F. & CHEN, X. F. 2009. Using NDVI to define thermal south in several mountainous landscapes of California. *Computers & Geosciences,* 35**,** 327-336.

DEWAN, A. M. & YAMAGUCHI, Y. 2009. Land use and land cover change in Greater Dhaka, Bangladesh: Using remote sensing to promote sustainable urbanization. *Applied Geography,* 29**,** 390-401.

DIETZ, T., ROSA, E. A. & YORK, R. 2007. Driving the human ecological footprint. *Frontiers in Ecology and the Environment,* 5**,** 13-18.

DRAGONI, D., SCHMID, H. P., WAYSON, C. A., POTTER, H., GRIMMOND, C. S. B. & RANDOLPH, J. C. 2011. Evidence of increased net ecosystem productivity associated with a longer vegetated season in a deciduous forest in south-central Indiana, USA. *Global Change Biology,* 17**,** 886-897.

DUAN, H. C., YAN, C. Z., TSUNEKAWA, A., SONG, X., LI, S. & XIE, J. L. 2011. Assessing vegetation dynamics in the Three-North Shelter Forest region of China using AVHRR NDVI data. *Environmental Earth Sciences,* 64**,** 1011-1020.

ECKERT, S., HUSLER, F., LINIGER, H. & HODEL, E. 2015. Trend analysis of MODIS NDVI time series for detecting land degradation and regeneration in Mongolia. *Journal of Arid Environments,* 113**,** 16-28.

ESAU, I., MILES, V. V., DAVY, R., MILES, M. W. & KURCHATOVA, A. 2016. Trends in normalized difference vegetation index (NDVI) associated with

urban development in northern West Siberia. *Atmospheric Chemistry and Physics,* 16**,** 9563-9577.

FABRICANTE, I., OESTERHELD, M. & PARIDA, B. 2009. Annual and seasonal variation of NDVI explained by current and previous precipitation across Northern Patagonia. *Journal of Arid Environments,* 73**,** 745-753.

FANG, J. Y., PIAO, S. L., TANG, Z. Y., PENG, C. H. & WEI, J. 2001. Interannual variability in net primary production and precipitation. *Science,* 293**,** 1723a.

FENSHOLT, R., LANGANKE, T., RASMUSSEN, K., REENBERG, A., PRINCE, S. D., TUCKER, C., SCHOLES, R. J., LE, Q. B., BONDEAU, A., EASTMAN, R., EPSTEIN, H., GAUGHAN, A. E., HELLDEN, U., MBOW, C., OLSSON, L., PARUELO, J. M., SCHWEITZER, C., SEAQUIST, J. & WESSELS, K. 2012. Greenness in semi-arid areas across the globe 1981–2007—An Earth Observing Satellite based analysis of trends and drivers. *Remote Sensing of Environment,* 121**,** 144-158.

FENSHOLT, R. & PROUD, S. R. 2012. Evaluation of earth observation based global long term vegetation trends — Comparing GIMMS and MODIS global NDVI time series. *Remote Sensing of Environment,* 119**,** 131-147.

FENSHOLT, R., RASMUSSEN, K., NIELSEN, T. T. & MBOW, C. 2009. Evaluation of earth observation based long term vegetation trends — Intercomparing NDVI time series trend analysis consistency of Sahel from AVHRR GIMMS, Terra MODIS and SPOT VGT data. *Remote Sensing of Environment,* 113**,** 1886-1898.

FU, B. H. & BURGHER, I. 2015. Riparian vegetation NDVI dynamics and its relationship with climate, surface water and groundwater. *Journal of Arid Environments,* 113**,** 59-68.

GAMON, J. A., HUEMMRICH, K. F., STONE, R. S. & TWEEDIE, C. E. 2013. Spatial and temporal variation in primary productivity (NDVI) of coastal Alaskan tundra: Decreased vegetation growth following earlier snowmelt. *Remote Sensing of Environment,* 129**,** 144-153.

GAO, Q. & YU, M. 1998. A model of regional vegetation dynamics and its application to the study of Northeast China Transect (NECT) responses to global change. *Global Biogeochemical Cycles,* 12**,** 329-344.

GARONNA, I., DE JONG, R., DE WIT, A. J., MUCHER, C. A., SCHMID, B. & SCHAEPMAN, M. E. 2014. Strong contribution of autumn phenology to changes in satellite-derived growing season length estimates across Europe (1982-2011). *Global Change Biology,* 20**,** 3457-3470.

GAZOL, A., CAMARERO, J. J., VICENTE-SERRANO, S. M., SANCHEZ-SALGUERO, R., GUTIERREZ, E., DE LUIS, M., SANGUESA-BARREDA, G., NOVAK, K., ROZAS, V., TISCAR, P. A., LINARES, J. C., MARTIN-HERNANDEZ, N., MARTINEZ DEL CASTILLO, E., RIBAS, M., GARCIA-GONZALEZ, I., SILLA, F., CAMISON, A., GENOVA, M., OLANO, J. M., LONGARES, L. A., HEVIA, A., TOMAS-BURGUERA, M. & GALVAN, J. D. 2018. Forest resilience to drought varies across biomes. *Global Change Biology,* 24**,** 2143-2158.

GILL, A. L., GALLINAT, A. S., SANDERS-DEMOTT, R., RIGDEN, A. J., SHORT GIANOTTI, D. J., MANTOOTH, J. A. & TEMPLER, P. H. 2015. Changes in autumn senescence in northern hemisphere deciduous trees: a meta-analysis of autumn phenology studies. *Annuals of Botany,* 116**,** 875-888.

GOETZ, S. J., WRIGHT, R. K., SMITH, A. J., ZINECKER, E. & SCHAUB, E. 2003. IKONOS imagery for resource management: Tree cover, impervious surfaces, and riparian buffer analyses in the mid-Atlantic region. *Remote Sensing of Environment,* 88**,** 195-208.

GOUVEIA, S. F., VILLALOBOS, F., DOBROVOLSKI, R., BELTRAO-MENDES, R. & FERRARI, S. F. 2014. Forest structure drives global diversity of primates. *Journal of Animal Ecology,* 83**,** 1523-1530.

GU, X., ZHOU, S. & ZHANG, H. 2009. Region analysis of cultivated land pressure in Coalstal Regions of Jiangsu Province. *Chinese Journal of Agricultural Resources and Regional Planning,* 30**,** 32-38 (in Chinese).

GUAN, Q. Y., YANG, L. Q., PAN, N. H., LIN, J. K., XU, C. Q., WANG, F. F. & LIU, Z. Y. 2018. Greening and browning of the Hexi Corridor in Northwest China: Spatial patterns and responses to climatic variability and anthropogenic drivers. *Remote Sensing,* 10**,** 1270.

GUO, N., ZHU, Y. J., WANG, J. M. & DENG, C. P. 2008. The relationship between NDVI and climate elements for 22 years in different vegetation areas of Northwest China. *Journal of Plant Ecology,* 02**,** 319-327 (in Chinese).

GUTIÉRREZ RODRÍGUEZ, L., HOGARTH, N. J., ZHOU, W., XIE, C., ZHANG, K. R. & PUTZEL, L. 2016. China's conversion of cropland to forest program: a systematic review of the environmental and socioeconomic effects. *Environmental Evidence,* 5.

GUTMAN, G. & IGNATOV, A. 1998. The derivation of the green vegetation fraction from NOAA/AVHRR data for use in numerical weather prediction models. *International Journal of Remote Sensing,* 19**,** 1533-1543.

HAN, X. M., ZUO, D. P., XU, Z. X., CAI, S. Y. & GAO, X. X. 2018. Analysis of vegetation condition and its relationship with meteorological variables in the Yarlung Zangbo River Basin of China. *Innovative Water Resources Management - Understanding and Balancing Interactions between Humankind and Nature,* 379**,** 105-112.

HANSEN, M. C., DEFRIES, R. S., TOWNSHEND, J. R. G., MARUFU, L. & SOHLBERG, R. 2002. Development of a MODIS tree cover validation data set for Western Province, Zambia. *Remote Sensing of Environment,* 83**,** 320-335.

HATFIELD, J. L. & PRUEGER, J. H. 2015. Temperature extremes: Effect on plant growth and development. *Weather and Climate Extremes,* 10**,** 4-10.

HAZARIKA, M. K., YASUOKA, Y., ITO, A. & DYE, D. 2005. Estimation of net primary productivity by integrating remote sensing data with an ecosystem model. *Remote Sensing of Environment,* 94**,** 298-310.

HE, F. L. 2009. Price of prosperity: economic development and biological conservation in China. *Journal of Applied Ecology,* 46**,** 511-515.

HICKE, J. A., ASNER, G. P., RANDERSON, J. T., TUCKER, C., LOS, S., BIRDSEY, R., JENKINS, J. C. & FIELD, C. 2002. Trends in North American net primary productivity derived from satellite observations, 1982-1998. *Global Biogeochemical Cycles,* 16**,** 1-14.

HOU, Z., MA, Y. & GE, H. 2013. The vegetation cover change in Fen River Basin. *Journal of Arid Land Resources and Environment,* 27**,** 162-166 (in Chinese).

HU, Q., HUA, W., YIN, Y., ZHANG, X. K., LIU, L. J., SHI, J. Q., ZHAO, Y. G., QIN, L., CHEN, C. & WANG, H. Z. 2017. Rapeseed research and production in China. *Crop Journal,* 5**,** 127-135.

HUANG, X., SONG, Y., LI, M. M., LI, J. F. & ZHU, T. 2012. Harvest season, high polluted season in East China. *Environmental Research Letters,* 7**,** 044033.

HUETE, A., DIDAN, K., MIURA, T., RODRIGUEZ, E. P., GAO, X. & FERREIRA, L. G. 2002. Overview of the radiometric and biophysical performance of the MODIS vegetation indices. *Remote Sensing of Environment,* 83**,** 195-213.

HURST, H. E. 1951. Long-term storage capacity of reservoirs. *Transactions of the American Society of Civil Engineers,* 116**,** 770-799.

ICHII, K., YAMAGUCHI, Y. & KAWABATA, A. 2001. Global decadal changes in NDVI and its relationships to climate variables. *Igarss 2001: Scanning the Present and Resolving the Future, Vols 1-7, Proceedings***,** 1818-1819.

IPCC 2013. Working Group I contribution to the IPCC Fifth Assessment Report (AR5). *Climate Change 2013: The Physical Science Basis, Final Draft Underlying Scientific-Technical Assessment.*

JEONG, S. J., HO, C. H., BROWN, M. E., KUG, J. S. & PIAO, S. L. 2011. Browning in desert boundaries in Asia in recent decades. *Journal of Geophysical Research-Atmospheres,* 116**,** D02103.

JEYASEELAN, A. T., ROY, P. S. & YOUNG, S. S. 2007. Persistent changes in NDVI between 1982 and 2003 over India using AVHRR GIMMS (Global Inventory Modeling and Mapping Studies) data. *International Journal of Remote Sensing,* 28**,** 4927–4946.

JIANG, D., WANG, N. B., YANG, X. H. & LIU, H. H. 2002. Principles of the interaction between NDVI profile and the growing situation of crops. *Acta Ecologica Sinica,* 22**,** 247-253 (in Chinese).

JIANG, L., GULI, J., BAO, A., GUO, H. & NDAYISABA, F. 2017. Vegetation dynamics and responses to climate change and human activities in Central Asia. *Science of the Total Environment,* 599-600**,** 967-980.

JIN, H., SHEN, W. S. & YAN, Y. H. 2015. Study on sope-direct of vegetation coverage of Daqing Mount Nature Reserve Based on NDMVI. *Forest Resources Management,* 3**,** 59-64 (in Chinese).

JULIEN, Y., SOBRINO, J. A. & VERHOEF, W. 2006. Changes in land surface temperatures and NDVI values over Europe between 1982 and 1999. *Remote Sensing of Environment,* 103**,** 43-55.

KARLSEN, S. R., TOLVANEN, A., KUBIN, E., POIKOLAINEN, J., HOGDA, K. A., JOHANSEN, B., DANKS, F. S., ASPHOLM, P., WIELGOLASKI, F. E. & MAKAROVA, O. 2008. MODIS-NDVI-based mapping of the length of the growing season in northern Fennoscandia. *International Journal of Applied Earth Observation and Geoinformation,* 10**,** 253-266.

KERN, A., MARJANOVIC, H. & BARCZA, Z. 2016. Evaluation of the Quality of NDVI3g Dataset against Collection 6 MODIS NDVI in Central Europe between 2000 and 2013. *Remote Sensing,* 8**,** 955.

KILESHYE ONEMA, J. M. & TAIGBENU, A. 2009. NDVI–rainfall relationship in the Semliki watershed of the equatorial Nile. *Physics and Chemistry of the Earth, Parts A/B/C,* 34**,** 711-721.

KIM, Y. 2013. Drought and elevation effects on MODIS vegetation indices in northern Arizona ecosystems. *International Journal of Remote Sensing,* 34**,** 4889-4899.

KLINGE, M., BÖHNER, J. & ERASMI, S. 2015. Modeling forest lines and forest distribution patterns with remote-sensing data in a mountainous region of semiarid central Asia. *Biogeosciences,* 12**,** 2893-2905.

KOH, L. P., MIETTINEN, J., LIEW, S. C. & GHAZOUL, J. 2011. Remotely sensed evidence of tropical peatland conversion to oil palm. *Proceedings of the National Academy of Sciences of the United States of America,* 108**,** 5127-5132.

KONG, D. D., ZHANG, Q., SINGH, V. P. & SHI, P. J. 2017. Seasonal vegetation response to climate change in the Northern Hemisphere (1982–2013). *Global and Planetary Change,* 148**,** 1-8.

KRISHNASWAMY, J., JOHN, R. & JOSEPH, S. 2014. Consistent response of vegetation dynamics to recent climate change in tropical mountain regions. *Global Change Biology,* 20**,** 203-215.

KUTIEL, P. & LAVEE, H. 1999. Effect of slope aspect on soil and vegetation properities along an aridity trensect. *Israel Journal of Plant Sciences* 47**,** 169-178

LI, A., WU, J. G. & HUANG, J. H. 2012. Distinguishing between human-induced and climate-driven vegetation changes: a critical application of RESTREND in inner Mongolia. *Landscape Ecology,* 27**,** 969-982.

LI, D. K., FAN, J. Z. & WANG, J. 2010. Change characteristics and their causes of fractional vegetation coverage (FVC) in Shaanxi Province. *Chinese Journal of Applied Ecology,* 11**,** 2896-2903 (in Chinese).

LI, H. D., LI, Y. K., SHEN, W. S., LI, Y. A., LIN, J. K., LU, X. T., XU, X. & JIANG, J. 2015a. Elevation-dependent vegetation greening of the Yarlung Zangbo River Basin in the Southern Tibetan Plateau, 1999–2013. *Remote Sensing,* 7**,** 16672-16687.

LI, J. Z., LIU, Y. M., CAO, M. M. & XUE, B. 2015b. Space-time characteristics of vegetation cover and distribution: Case of the Henan Province in China. *Sustainability,* 7**,** 11967-11979.

LI, L. H., ZHANG, Y. H., LIU, L. S., WU, J. S., WANG, Z. F., LI, S. C., ZHANG, H. M., ZU, J. X., DING, M. J. & PAUDEL, B. 2018. Spatiotemporal patterns of vegetation greenness change and associated climatic and anthropogenic drivers on the Tibetan Plateau during 2000–2015. *Remote Sensing,* 10.

LI, S. S., YAN, J. P., LIU, X. Y. & WAN, J. 2013. Response of vegetation restoration to climate change and human activities in Shaanxi-Gansu-Ningxia Region. *Journal of Geographical Sciences,* 23**,** 98-112.

LI, X. B. & SHI, P. J. 2000. Sensitivity analysis of variation in NDVI, temperature and precipitation in typical vegetation types across China. *Acta Phytoecologica Sinica,* 24**,** 379-382 (in Chinese).

LI, X. S., WANG, H. Y., WANG, J. Y. & GAO, Z. H. 2015c. Land degradation dynamic in the first decade of twenty-first century in the Beijing–Tianjin dust and sandstorm source region. *Environmental Earth Sciences,* 74**,** 4317-4325.

LI, Y., XIE, Z. X., QIN, Y. C. & ZHENG, Z. C. 2019. Estimating relations of vegetation, climate change, and human activity: A case study in the 400 mm annual precipitation fluctuation zone, China. *Remote Sensing,* 11.

LI, Z. C., MA, M. G., ZHANG, F. & JIANG, Z. R. 2006. The dynamic analysis of vegetation pattern in the Northwest of China from 1982 to 2003. *Remote Sensing Technology and Application,* 21**,** 332-337 (in Chinese).

LIANG, W., YANG, Y. T., FAN, D. M., GUAN, H. D., ZHANG, T., LONG, D., ZHOU, Y. & BAI, D. 2015. Analysis of spatial and temporal patterns of net primary production and their climate controls in China from 1982 to 2010. *Agricultural and Forest Meteorology,* 204**,** 22-36.

LIN, D., XIA, J. & WAN, S. 2010. Climate warming and biomass accumulation of terrestrial plants: a meta-analysis. *New Phytologist,* 188**,** 187-198.

LIN, H., XIONG, Y. J. & WAN, L. F. 2007. Temporal and spatial variation of MODIS vegetation indices in Hunan province. *Chinese Journal of Applied Ecology,* 18**,** 581–585 (in Chinese).

LIN, Q., WU, Z., SINGH, V. P., SADEGHI, S. H. R., HE, H. & LU, G. 2017. Correlation between hydrological drought, climatic factors, reservoir operation, and vegetation cover in the Xijiang Basin, South China. *Journal of Hydrology,* 549**,** 512-524.

LINDERHOLM, H. W. 2006. Growing season changes in the last century. *Agricultural and Forest Meteorology,* 137**,** 1-14.

LIU, D. E., FU, N. & FAN, J. L. 2008a. Dynamic change of vegetation cover and its response to climate change in recent 20 years in Tianjin area. *Environmental Engineering,* 17**,** 798–801 (in Chinese).

LIU, J., LI, S., OUYANG, Z., TAM, C. & CHEN, X. 2008b. Ecological and socioeconomic effects of China's policies for ecosystem services. *Proceedings of the National Academy of Sciences of the United States of America,* 105**,** 9477-9482.

LIU, J. G. & DIAMOND, J. 2005. China’s environment in a globalizing world. *Nature,* 435**,** 1179–1186.

LIU, J. G. & DIAMOND, J. 2008. Science and government - Revolutionizing China's environmental protection. *Science,* 319**,** 37-38.

LIU, S., CHENG, F., DONG, S., ZHAO, H., HOU, X. & WU, X. 2017. Spatiotemporal dynamics of grassland aboveground biomass on the Qinghai-Tibet Plateau based on validated MODIS NDVI. *Science Report,* 7**,** 4182.

LIU, X. X., TIAN, Z., ZHANG, A. B., ZHAO, A. Z. & LIU, H. X. 2019. Impacts of climate on spatiotemporal variations in vegetation NDVI from 1982–2015 in Inner Mongolia, China. *Sustainability,* 11.

LOTSCH, A., FRIEDL, M. A., ANDERSON, B. T. & TUCKER, C. J. 2005. Response of terrestrial ecosystems to recent Northern Hemispheric drought. *Geophysical Research Letters,* 32**,** L06705.

LU, Q., SÖDERLUND, L., WU, P. & LI, J. 2005. Cultivated land loss arising from the rapid urbanization in China. *Agrifood Research Reports,* 68**,** 313-327.

LU, Y., FU, B., WEI, W., YU, X. & SUN, R. 2011. Major ecosystems in China: dynamics and challenges for sustainable management. *Environmental Management,* 48**,** 13-27.

LU, Y., ZHANG, L., FENG, X., ZENG, Y., FU, B., YAO, X., LI, J. & WU, B. 2015. Recent ecological transitions in China: greening, browning, and influential factors. *Scientific Reports,* 5**,** 8732.

LUCK, G. W., SMALLBONE, L. T. & O'BRIEN, R. 2009. Socio-economics and vegetation change in urban ecosystems: patterns in space and time. *Ecosystems,* 12**,** 604-620.

LUNETTA, R. S., SHAO, Y., EDIRIWICKREMA, J. & LYON, J. G. 2010. Monitoring agricultural cropping patterns across the Laurentian Great Lakes Basin using MODIS-NDVI data. *International Journal of Applied Earth Observation and Geoinformation,* 12**,** 81-88.

MA, M., DONG, L. & WANG, X. 2003. Study on the dynamically monitoring and simulating the vegetation cover in Northwest China in the past 21 years. *Journal of Glaciology and Geocryology,* 2*5***,** 232-236 (in Chinese).

MA, N., HU, H. F., ZHUANG, D. F. & ZHANG, X. L. 2012. Vegetation coverage distribution and its changes in Plan Blue Banner based on remote sensing data and dimidiate pixel model. *Scientia Geographica Sinica,* 32**,** 251-256 (in Chinese).

MADU, I. A. 2009. The impacts of anthropogenic factors on the environment in Nigeria. *Journal of Environmental Management,* 90**,** 1422-1426.

MÄND, P., HALLIK, L., PEÑUELAS, J., NILSON, T., DUCE, P., EMMETT, B. A., BEIER, C., ESTIARTE, M., GARADNAI, J. & KALAPOS, T. 2010. Responses of the reflectance indices PRI and NDVI to experimental warming and drought in European shrublands along a north–south climatic gradient. *Remote Sensing of Environment,* 114**,** 626-636.

MANDELBROT, B. B. & WALLIS, J. R. 1969. Some long-run properties of geophysical records. *Water resources research,* 5**,** 321-340.

MANN, C. C. 2009. Addicted to rubber. *Science,* 325**,** 564-566.

MAO, D. H., WANG, Z. M., LUO, L. & REN, C. Y. 2012. Integrating AVHRR and MODIS data to monitor NDVI changes and their relationships with climatic parameters in Northeast China. *International Journal of Applied Earth Observation and Geoinformation,* 18**,** 528-536.

MAREN, I. E., KARKI, S., PRAJAPATI, C., YADAV, R. K. & SHRESTHA, B. B. 2015. Facing north or south: Does slope aspect impact forest stand characteristics and soil properties in a semiarid trans-Himalayan valley? *Journal of Arid Environments,* 121**,** 112-123.

MATHER, A. S. 1992. The Forest Transition. *Area,* 24**,** 367-379.

MATHER, A. S. 2007. Recent Asian forest transitions in relation to foresttransition theory. *International Forestry Review,* 9**,** 491-502.

MIAO, L. J., LIU, Q., FRASER, R., HE, B. & CUI, X. F. 2015. Shifts in vegetation growth in response to multiple factors on the Mongolian Plateau from 1982 to 2011. *Physics and Chemistry of the Earth,* 87-88**,** 50-59.

MOKARRAM, M. & SATHYAMOORTHY, D. 2015. Modeling the relationship between elevation, aspect and spatial distribution of vegetation in the Darab Mountain, Iran using remote sensing data. *Modeling Earth Systems and Environment,* 1.

MOURA, M. R., VILLALOBOS, F., COSTA, G. C. & GARCIA, P. C. 2016. Disentangling the role of climate, topography and vegetation in species richness gradients. *PLoS One,* 11**,** e0152468.

MYNENI, R. B., KEELING, C. D., TUCKER, C. J., ASRAR, G. & NEMANI, R. R. 1997. Increased plant growth in the northern high latitudes from 1981 to 1991. *Nature,* 386**,** 698-702.

NEMANI, R. R., KEELING, C. D., HASHIMOTO, H., JOLLY, W. M., PIPER, S. C., TUCKER, C. J., MYNENI, R. B. & RUNNING, S. W. 2003. Climate-driven

increases in global terrestrial net primary production from 1982 to 1999. *Science,* 300**,** 1560-1563.

NOGUES-BRAVO, D., ARAUJO, M. B., ROMDAL, T. & RAHBEK, C. 2008. Scale effects and human impact on the elevational species richness gradients. *Nature,* 453**,** 216-219.

OLSON, K. A., MURRAY, M. G. & FULLER, T. K. 2010. Vegetation Composition and Nutritional Quality of Forage for Gazelles in Eastern Mongolia. *Rangeland Ecology & Management,* 63**,** 593-598.

PAN, Y., D., BIRDSEY, R. A., FANG, J. Y., HOUGHTON, R., KAUPPI, P. E., KURZ, W. A., PHILLIPS, O. L., SHVIDENKO, A., LEWIS, S. L., CANADELL, J. G., CIAIS, P., B. JACKSON, R. B., W. PACALA, S. W., MCGUIRE, D., PIAO, S. L., RAUTIAINEN, A., SITCH, S. & HAYES, D. 2011. A large and persistent carbon sink in the world's forests. *Science,* 333**,** 988-993.

PARK, H. S. & SOHN, B. J. 2010. Recent trends in changes of vegetation over East Asia coupled with temperature and rainfall variations. *Journal of Geophysical Research-Atmospheres,* 115**,** D14101.

PARMESAN, C. & YOHE, G. 2003. A globally coherent fingerprint of climate change impacts across natural systems. *Nature,* 421**,** 37-42.

PECH, R. P., GRAETZ, R. D. & DAVIS, A. W. 1986. Reflectance modeling and the derivation of vegetation indices for an Australian semi-arid shrubland. *International Journal of Remote Sensing,* 7**,** 389-403.

PENG, J., LI, Y., TIAN, L., LIU, Y. X. & WANG, Y. L. 2015. Vegetation Dynamics and Associated Driving Forces in Eastern China during 1999–2008. *Remote Sensing,* 7**,** 13641-13663.

PENG, J., LIU, Z. H., LIU, Y. H., WU, J. S. & HAN, Y. A. 2012. Trend analysis of vegetation dynamics in Qinghai-Tibet Plateau using Hurst Exponent. *Ecological Indicators,* 14**,** 28-39.

PENG, S. P., PIAO, S. L., CIAIS, P., MYNENI, R. B., CHEN, A., CHEVALLIER, F., DOLMAN, A. J., JANSSENS, I. A., PENUELAS, J., ZHANG, G. X., VICCA, S., WAN, S. Q., WANG, S. P. & ZENG, H. 2013. Asymmetric effects of daytime and night-time warming on Northern Hemisphere vegetation. *Nature,* 501**,** 88-92.

PENG, S. S., CHEN, A. P., XU, L., CAO, C. X., FANG, J. Y., MYNENI, R. B., PINZON, J. E., TUCKER, C. J. & PIAO, S. L. 2011. Recent change of vegetation growth trend in China. *Environmental Research Letters,* 6**,** 044027.

PIAO, S., CIAIS, P., FRIEDLINGSTEIN, P., PEYLIN, P., REICHSTEIN, M., LUYSSAERT, S., MARGOLIS, H., FANG, J., BARR, A., CHEN, A., GRELLE, A., HOLLINGER, D. Y., LAURILA, T., LINDROTH, A., RICHARDSON, A. D. & VESALA, T. 2008. Net carbon dioxide losses of northern ecosystems in response to autumn warming. *Nature,* 451**,** 49-52.

PIAO, S., CIAIS, P., HUANG, Y., SHEN, Z., PENG, S., LI, J., ZHOU, L., LIU, H., MA, Y., DING, Y., FRIEDLINGSTEIN, P., LIU, C., TAN, K., YU, Y., ZHANG, T. & FANG, J. 2010. The impacts of climate change on water resources and agriculture in China. *Nature,* 467**,** 43-51.

PIAO, S. L., FANG, J. Y., ZHOU, L. M., CIAIS, P. & ZHU, B. 2006a. Variations in satellite-derived phenology in China's temperate vegetation. *Global Change Biology,* 12**,** 672-685.

PIAO, S. L., FANG, J. Y., ZHOU, L. M., GUO, Q. H., HENDERSON, M., JI, W., LI, Y. & TAO, S. 2003. Interannual variations of monthly and seasonal normalized

difference vegetation index (NDVI) in China from 1982 to 1999. *Journal of Geophysical Research-Atmospheres,* 108**,** 4401.

PIAO, S. L., MOHAMMAT, A., FANG, J. Y., CAI, Q. & FENG, J. M. 2006b. NDVI-based increase in growth of temperate grasslands and its responses to climate changes in China. *Global Environmental Change-Human and Policy Dimensions,* 16**,** 340-348.

PIAO, S. L., WANG, X. H., CIAIS, P., ZHU, B., WANG, T. & LIU, J. 2011. Changes in satellite-derived vegetation growth trend in temperate and boreal Eurasia from 1982 to 2006. *Global Change Biology,* 17**,** 3228-3239.

PIAO, S. L., YIN, G. D., TAN, J. G., CHENG, L., HUANG, M. T., LI, Y., LIU, R. G., MAO, J., MYNENI, R. B., PENG, S. P., POULTER, B., SHI, X., XIAO, Z. Q., ZENG, N., ZENG, Z. Z. & WANG, Y. P. 2015. Detection and attribution of vegetation greening trend in China over the last 30 years. *Glob Chang Biol,* 21**,** 1601-1609.

POTTER, C. S. & BROOKS, V. 1998. Global analysis of empirical relations between annual climate and seasonality of NDVI. *International Journal of Remote Sensing,* 19**,** 2921-2948.

PRASANNAKUMAR, V., SHINY, R., GEETHA, N. & VIJITH, H. 2011. Applicability of SRTM data for landform characterisation and geomorphometry: a comparison with contour-derived parameters. *International Journal of Digital Earth,* 4**,** 387-401.

PRINCE, S. D., BECKER-RESHEF, I. & RISHMAWI, K. 2009. Detection and mapping of long-term land degradation using local net production scaling: Application to Zimbabwe. *Remote Sensing of Environment,* 113**,** 1046-1057.

QIAN, Y. Q., HE, F. P. & WANG, W. 2016. Seasonality, Rather than Nutrient Addition or Vegetation Types, Influenced Short-Term Temperature Sensitivity of Soil Organic Carbon Decomposition. *PLoS One,* 11**,** e0153415.

QU, B., ZHU, W. B., JIA, S. F. & LV, A. F. 2015. Spatio-temporal changes in vegetation activity and its driving factors during the growing season in China from 1982 to 2011. *Remote Sensing,* 7**,** 13729-13752.

RASMUSSEN, C., PELLETIER, J. D., TROCH, P. A., SWETNAM, T. L. & CHOROVER, J. 2015. Quantifying topographic and vegetation effects on the transfer of energy and mass to the critical zone. *Vadose Zone Journal,* 14.

RAYNOLDS, M. K., COMISO, J. C., WALKER, D. A. & VERBYLA, D. 2008. Relationship between satellite-derived land surface temperatures, arctic vegetation types, and NDVI. *Remote Sensing of Environment,* 112**,** 1884-1894.

REN, J. Q., CHEN, Z. X., ZHOU, Q. B. & TANG, H. J. 2008. Regional yield estimation for winter wheat with MODIS-NDVI data in Shandong, China. *International Journal of Applied Earth Observation and Geoinformation,* 10**,** 403-413.

RICHARDSON, A. D., BLACK, T. A., CIAIS, P., DELBART, N., FRIEDL, M. A., GOBRON, N., HOLLINGER, D. Y., KUTSCH, W. L., LONGDOZ, B., LUYSSAERT, S., MIGLIAVACCA, M., MONTAGNANI, L., MUNGER, J. W., MOORS, E., PIAO, S., REBMANN, C., REICHSTEIN, M., SAIGUSA, N., TOMELLERI, E., VARGAS, R. & VARLAGIN, A. 2010. Influence of spring and autumn phenological transitions on forest ecosystem productivity. *Philosophical Transactions of the Royal Society B: Biological Sciences,* 365**,** 3227-3246.

RUMPF, S. B., HULBER, K., KLONNER, G., MOSER, D., SCHUTZ, M., WESSELY, J., WILLNER, W., ZIMMERMANN, N. E. & DULLINGER, S. 2018. Range dynamics

of mountain plants decrease with elevation. *Proceedings of the National Academy of Sciences of the United States of America,* 115**,** 1848-1853.

RUNDQUIST, B. C. & HARRINGTON, J. A. 2000. The effects of climatic factors on vegetation dynamics of tallgrass and shortgrass cover. *Geocarto International,* 15**,** 33-38.

SALIM, H. A., CHEN, X. L. & GONG, J. Y. 2008. Analysis of Sudan vegetation dynamics using NOAA–AVHRR NDVI data from 1982–1993. *Asian Journal of Earth Sciences,* 1**,** 1-15.

SCHMIDT, H. & GITELSON, A. 2000. Temporal and spatial vegetation cover changes in Israeli transition zone: AVHRR-based assessment of rainfall impact. *International Journal of Remote Sensing,* 21**,** 997-1010.

SCHNEIDER, A. & MERTES, C. M. 2014. Expansion and growth in Chinese cities, 1978–2010. *Environmental Research Letters,* 9**,** 024008.

SHEN, X. J., JIN, W. Z. & DU, H. B. 2013. Variation of vegetation in the Northeast China and its response to meteorological factors. *Journal of Northeast Normal University (Natural Science Edition),* 45**,** 123-130 (in Chinese).

SHI, K. F., CHEN, Y., YU, B. L., XU, T. B., LI, L. Y., HUANG, C., LIU, R., CHEN, Z. Q. & WU, J. P. 2016. Urban expansion and agricultural land loss in China: A multiscale perspective. *Sustainability,* 8.

SHI, M. J., MA, G. X. & SHI, Y. 2011. How much real cost has China paid for its economic growth? *Sustainability Science,* 6**,** 135-149.

SU, Y. 2016. China's regional industrial transfer behavior based on evolutionary game theory. *Journal of Discrete Mathematical Sciences and Cryptography* 19**,** 677-690.

TESTA, S., MONDINO, E. C. B. & PEDROLI, C. 2017. Correcting MODIS 16-day composite NDVI time-series with actual acquisition dates. *European Journal of Remote Sensing,* 47**,** 285-305.

TIAN, H. J., CAO, C. X., DAI, S. M., ZHENG, S., LV, S. L., XU, M., CHEN, W., ZHAO, J., LIU, D. & ZHU, H. Y. 2014. Analysis of vegetation fractional cover in Jungar Banner based on time-series remote sensing data. *Journal of Geo-Information Science,* 1**,** 126-133 (in Chinese).

TONG, S. Q., ZHANG, J. Q., BAO, Y. H., LAI, Q., LIAN, X., LI, N. & BAO, Y. B. 2018. Analyzing vegetation dynamic trend on the Mongolian Plateau based on the Hurst exponent and influencing factors from 1982–2013. *Journal of Geographical Sciences,* 28**,** 595-610.

TORO GUERRERO, F. J. D., HINOJOSA-CORONA, A. & KRETZSCHMAR, T. G. 2016. A comparative study of NDVI values between north- and south-facing slopes in a semiarid mountainous region. *IEEE Journal of Selected Topics in Applied Earth Observations and Remote Sensing,* 9**,** 5350-5356.

VESALA, T., LAUNIAINEN, S., KOLARI, P., PUMPANEN, J., SEVANTO, S., HARI, P., NIKINMAA, E., KASKI, P., MANNILA, H., UKKONEN, E., PIAO, S. L. & CIAIS, P. 2010. Autumn temperature and carbon balance of a boreal Scots pine forest in Southern Finland. *Biogeosciences,* 7**,** 163-176.

VIÑA, A., MCCONNELL, W. J., YANG, H. B., XU, Z. C. & LIU, J. G. 2016. Effects of conservation policy on China’s forest recovery. *Science Advances,* 2**,** 1500965.

WANG, C., GAO, Q., WANG, X. & YU, M. 2015a. Decadal trend in agricultural abandonment and woodland expansion in an agro-pastoral transition band in Northern China. *PLoS One,* 10**,** e0142113.

WANG, C., GAO, Q., WANG, X. & YU, M. 2016a. Spatially differentiated trends in urbanization, agricultural land abandonment and reclamation, and woodland recovery in Northern China. *Scientific Reports,* 6**,** 37658.

WANG, C. C., YANG, Y. S. & ZHANG, Y. Q. 2010. Economic development, rural livelihoods, and ecological restoration: Evidence from China. *Ambio,* 40**,** 78-87.

WANG, J., RICH, P. M. & PRICE, K. P. 2003. Temporal responses of NDVI to precipitation and temperature in the central Great Plains, USA. *International Journal of Remote Sensing,* 24**,** 2345-2364.

WANG, J., WANG, H., CAO, Y., BAI, Z. & QIN, Q. 2016b. Effects of soil and topographic factors on vegetation restoration in opencast coal mine dumps located in a loess area. *Scientific Reports,* 6**,** 22058.

WANG, J., WANG, K. L., ZHANG, M. Y. & DUAN, Y. F. 2014. Temporal-spatial variation in NDVI and drivers in hilly terrain of Southern China. *Resources Science,* 8**,** 1712-1723 (in Chinese).

WANG, S. H., JIA, S. F. & LV, A. F. 2012. The relationship between NDVI and residential sites across “Three-River-Source” area. *Resources Science,* 34**,** 2045-2050 (in Chinese).

WANG, X., GAO, Q., WANG, C. & YU, M. 2017a. Spatiotemporal patterns of vegetation phenology change and relationships with climate in the two transects of East China. *Global Ecology and Conservation,* 10**,** 206-219.

WANG, X., PIAO, S., CIAIS, P., LI, J., FRIEDLINGSTEIN, P., KOVEN, C. & CHEN, A. 2011. Spring temperature change and its implication in the change of vegetation growth in North America from 1982 to 2006. *Proceedings of the National Academy of Sciences of the United States of America,* 108**,** 1240-1245.

WANG, X., TAN, K., CHEN, B. & DU, P. 2017b. Assessing the Spatiotemporal Variation and Impact Factors of Net Primary Productivity in China. *Scientific Reports,* 7**,** 44415.

WANG, Y. G., PENG, J., WEI, H., SONG, Z. H. & ZHANG, X. F. 2015b. Land ecological suitability assessment for forest coupled with the resilience perspective: A case study in Wangqing county, Jilin province, China. *Acta Geographica Sinica,* 70**,** 476-487 (in Chinese).

WANG, Y. G., ZHU, Y., ZHANG, Q. H. & ZHANG, F. 2006. Species diversity of wild vascular plants in Longjiao Mountain forest area. *Chinese Journal of Ecology,* 25**,** 1490-1494 (in Chinese).

WESSELS, K. J., PRINCE, S. D., MALHERBE, J., SMALL, J., FROST, P. E. & VANZYL, D. 2007. Can human-induced land degradation be distinguished from the effects of rainfall variability? A case study in South Africa. *Journal of Arid Environments,* 68**,** 271-297.

WU, C. G., ZHOU, Z. X. & XIAO, W. F. 2012. Dynamic monitoring of vegetation coverage in Three Gorges Reservoir area based on MODIS NDVI. *Scientia Silvae Sinicae,* 48**,** 22-28 in Chinese.

WU, D., ZHAO, X., LIANG, S., ZHOU, T., HUANG, K., TANG, B. & ZHAO, W. 2015. Time-lag effects of global vegetation responses to climate change. *Global Change Biology,* 21**,** 3520-3531.

WU, L. Y. & ZENG, W. H. 2013. Research on the contribution of structure adjustment on SO2 emissions reduction-case study Shijingshan district, Beijing. *2013*

International Symposium on Environmental Science and Technology (2013 Isest), 18**,** 849-855.

WU, Y., ZENG, Y., ZHAO, Y., WU, D. F. & WU, W. B. 2010. Monitoring and dynamic analysis of fractional vegetation cover in the Hai River Basin based on MODIS data. *Resources Science,* 32**,** 1417-1424 (in Chinese).

WU, Z. T., WU, J. J., LIU, J. H., HE, B., LEI, T. J. & WANG, Q. F. 2013. Increasing terrestrial vegetation activity of ecological restoration program in the Beijing–Tianjin Sand Source Region of China. *Ecological Engineering,* 52**,** 37-50.

XIAO, J. & MOODY, A. 2005. Geographical distribution of global greening trends and their climatic correlates: 1982–1998. *International Journal of Remote Sensing,* 26**,** 2371–2390.

XIAO, X., BOLES, S., FROLKING, S., SALAS, W., MOORE, B., LI, C., HE, L. & ZHAO, R. 2010. Observation of flooding and rice transplanting of paddy rice fields at the site to landscape scales in China using VEGETATION sensor data. *International Journal of Remote Sensing,* 23**,** 3009-3022.

XIE, Z., HUETE, A., RESTREPO-COUPE, N., MA, X., DEVADAS, R. & CAPRARELLI, G. 2016. Spatial partitioning and temporal evolution of Australia's total water storage under extreme hydroclimatic impacts. *Remote Sensing of Environment,* 183**,** 43-52.

XU, H., SU, H., SU, B. Y., HAN, X. G., BISWAS, D. K. & LI, Y. G. 2014. Restoring the degraded grassland and improving sustainability of grassland ecosystem through chicken farming: A case study in northern China. *Agriculture Ecosystems & Environment,* 186**,** 115-123.

XU, H. J., WANG, X. P. & YANG, T. B. 2017. Trend shifts in satellite-derived vegetation growth in Central Eurasia, 1982-2013. *Science of the Total Environment,* 579**,** 1658-1674.

XU, W. X., GU, S., ZHAO, X. Q., XIAO, J. S., TANG, Y. H., FANG, J. Y., ZHANG, J. & JIANG, S. 2011. High positive correlation between soil temperature and NDVI from 1982 to 2006 in alpine meadow of the Three-River Source Region on the Qinghai-Tibetan Plateau. *International Journal of Applied Earth Observation and Geoinformation,* 13**,** 528-535.

XU, X. K., LIN, Z. H. & XUE, F. 2003. Correlation analysis between meteorological factors and the ratio of vegetation cover. *Acta Ecologica Sinica,* 23**,** 221–230 (in Chinese).

YANG, G. H., BAO, A. M., CHEN, X., LIU, H. L., HUANG, Y. & DAI, S. Y. 2009. Study of the vegetation cover change and its driving factors over Xinjiang during 1998–2007. *Journal of Glaciology and Geocryology* 31**,** 436–445 (in Chinese).

YANG, Y., LONG, D., GUAN, H., SCANLON, B. R., SIMMONS, C. T., JIANG, L. & XU, X. 2014. GRACE satellite observed hydrological controls on interannual and seasonal variability in surface greenness over mainland Australia. *Journal of Geophysical Research: Biogeosciences,* 119**,** 2245-2260.

YIN, Y. H., MA, D. Y. & WU, S. H. 2018. Enlargement of the semi-arid region in China from 1961 to 2010. *Climate Dynamics*.

YUAN, L. H., JIANG, W. G., SHEN, W. M., LIU, Y. H., WANG, W. J., TAO, L. L., ZHENG, H. & LIU, X. F. 2013. The Spatio-temporal variations of vegetation cover in the Yellow River Basin from 2000 to 2010. *Acta Ecologica Sinica,* 33**,** 7798-7806 (in Chinese).

ZENG, F. W., COLLATZ, G. J., PINZON, J. E. & IVANOFF, A. 2013. Evaluating and quantifying the climate-driven interannual variability in Global Inventory Modeling and Mapping Studies (GIMMS) Normalized Difference Vegetation Index (NDVI3g) at global scales. *Remote Sensing,* 5**,** 3918-3950.

ZEPPEL, M. J. B., WILKS, J. V. & LEWIS, J. D. 2014. Impacts of extreme precipitation and seasonal changes in precipitation on plants. *Biogeosciences,* 11**,** 3083-3093.

ZHANG, G. L., DONG, J. W., XIAO, X. M., HU, Z. M. & SHELDON, S. 2012. Effectiveness of ecological restoration projects in Horqin Sandy Land, China based on SPOT-VGT NDVI data. *Ecological Engineering,* 38**,** 20-29.

ZHANG, J., WANG, T. & GE, J. 2015. Assessing vegetation cover dynamics induced by policy-driven ecological restoration and implication to soil erosion in Southern China. *PLoS One,* 10**,** e0131352.

ZHANG, J. T. & RU, W. M. 2010. Population characteristics of endangered species Taxus chinensis var. mairei and its conservation strategy in Shanxi, China. *Population Ecology,* 52**,** 407-416.

ZHANG, J. T., XU, B. & LI, M. 2013a. Vegetation patterns and species diversity along eevational and disturbance gradients in the Baihua Mountain Reserve, Beijing, China. *Mountain Research and Development,* 33**,** 170-178.

ZHANG, Y. & LIANG, S. 2014. Changes in forest biomass and linkage to climate and forest disturbances over Northeastern China. *Global Change Biology,* 20**,** 2596-2606.

ZHANG, Y., PENG, C. H., LI, W. Z., TIAN, L. X., ZHU, Q., CHEN, H., FANG, X. Q., ZHANG, G. L., LIU, G. B., MU, X. M., LI, Z. B., LI, S. Q., YANG, Y. Z., WANG, J. A. & XIAO, X. M. 2016. Multiple afforestation programs accelerate the greenness in the 'Three North' region of China from 1982 to 2013. *Ecological Indicators,* 61**,** 404-412.

ZHANG, Y. L., GAO, J. G., LIU, L. S., WANG, Z. F., DING, M. J. & YANG, X. C. 2013b. NDVI-based vegetation changes and their responses to climate change from 1982 to 2011: A case study in the Koshi River Basin in the middle Himalayas. *Global and Planetary Change,* 108**,** 139-148.

ZHANG, Y. L., SONG, C. H., BAND, L. E., SUN, G. & LI, J. X. 2017. Reanalysis of global terrestrial vegetation trends from MODIS products: Browning or greening? *Remote Sensing of Environment,* 191**,** 145-155.

ZHAO, M. S., CHENG, W. M., ZHOU, C. H., LI, M. C., WANG, N. & LIU, Q. G. 2017. GDP spatialization and economic differences in South China based on NPP-VIIRS nighttime light imagery. *Remote Sensing,* 9.

ZHAO, M. S., FU, C. B. & YAN, X. D. 2001. Study on the relationship between different ecosystems and climate in China using NOAA/AVHRR data. *Acta Geographica Sinica,* 56**,** 287–296 (in Chinese).

ZHOU, D., ZHAO, S., LIU, S. & ZHANG, L. 2014. Spatiotemporal trends of terrestrial vegetation activity along the urban development intensity gradient in China's 32 major cities. *Science of The Total Environment,* 488-489**,** 136-145.

ZHOU, D. C., ZHAO, S. Q., ZHANG, L. X. & LIU, S. G. 2016. Remotely sensed assessment of urbanization effects on vegetation phenology in China's 32 major cities. *Remote Sensing of Environment,* 176**,** 272-281.

ZHOU, H., VAN ROMPAEY, A. & WANG, J. A. 2009. Detecting the impact of the "Grain for Green" program on the mean annual vegetation cover in the Shaanxi province, China using SPOT-VGT NDVI data. *Land Use Policy,* 26**,** 954-960.

ZHU, B. W., XIE, X. H. & ZHANG, K. 2016. Identifying water deficit and vegetation response during the 2009/10 drought over North China: Implications for the South-to-North Water Diversion project. *Hydrology and Earth System Sciences***,** hess-2016-313.

ZOU, C. S. & SHEN, W. S. 2003. Research progress on ecological security. *Rural Eco-Environment,* 19**,** 56-59 (in Chinese).

Appendix A

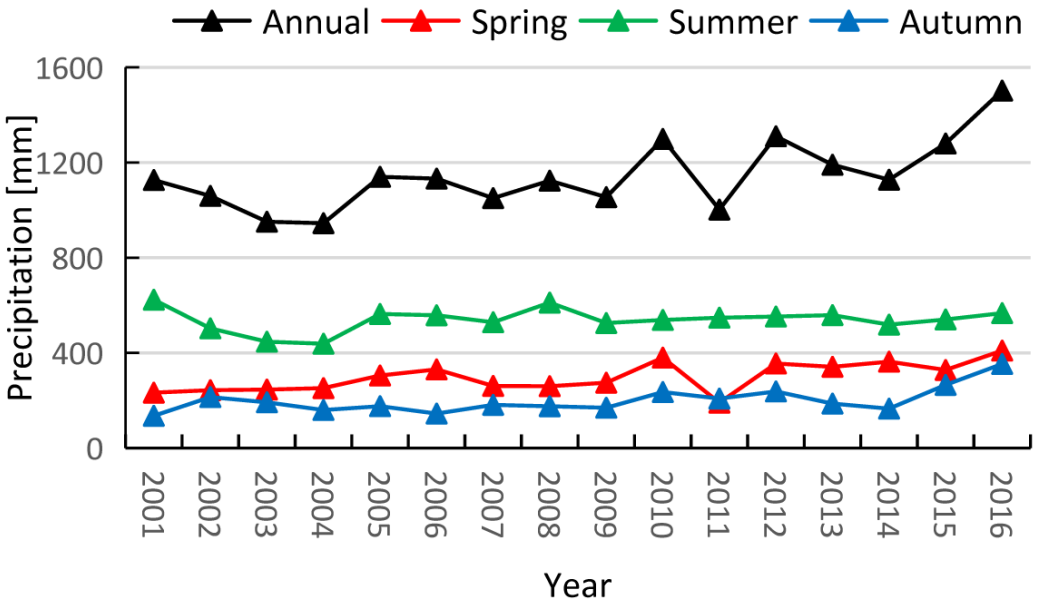

Figure A-1. The temporal variation of annual and seasonal precipitation in eastern China from 2001 to 2016

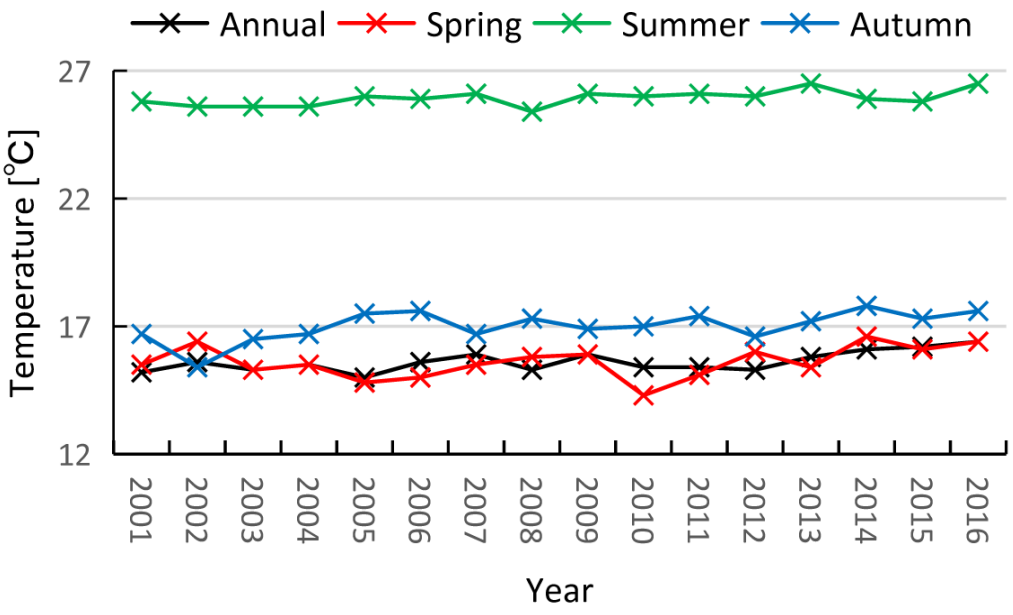

Figure A-2. The temporal variation of annual and seasonal temperature in eastern China from 2001 to 2016

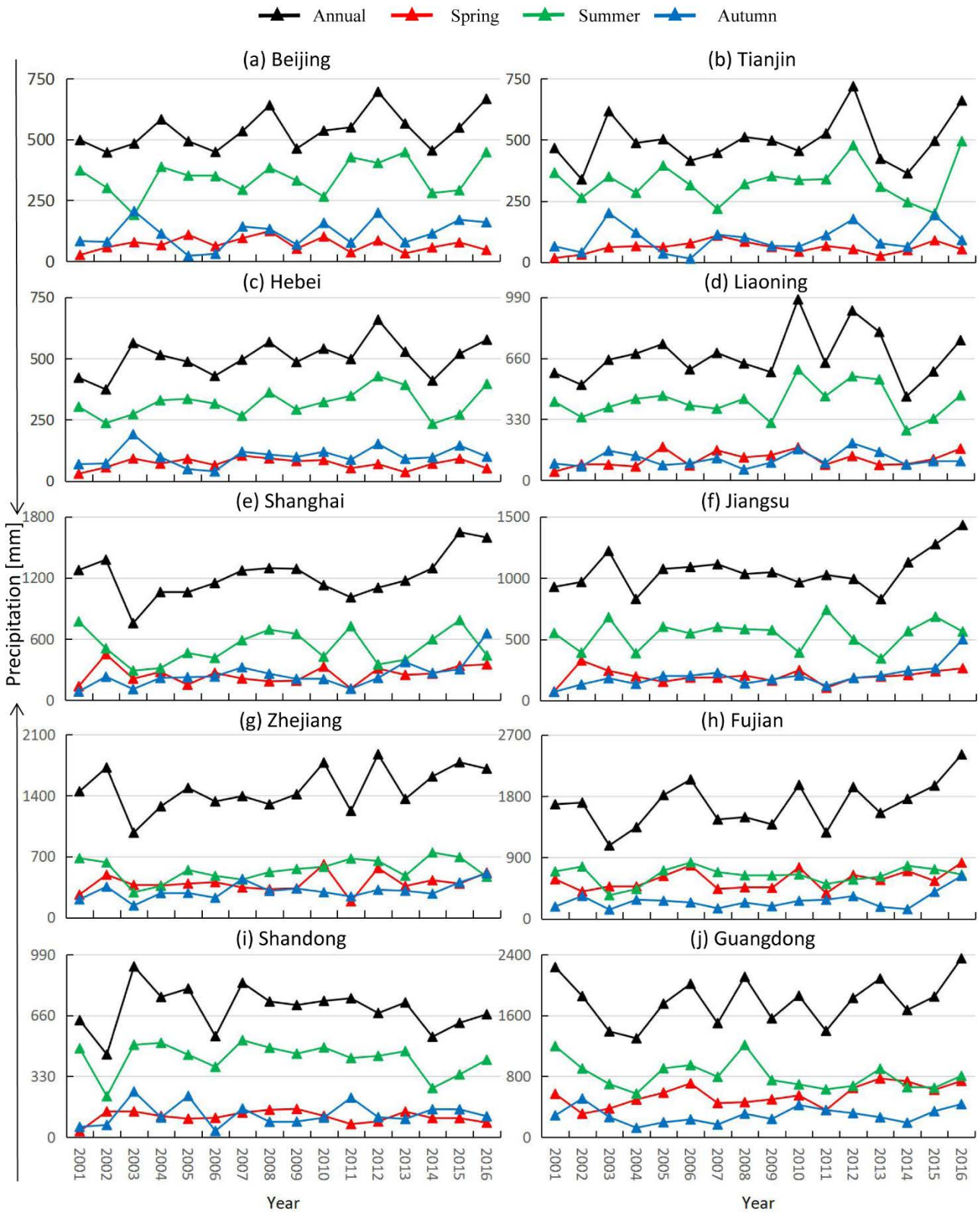

Figure A-3. The temporal variation of annual and seasonal precipitation in ten administrative units from 2001 to 2016

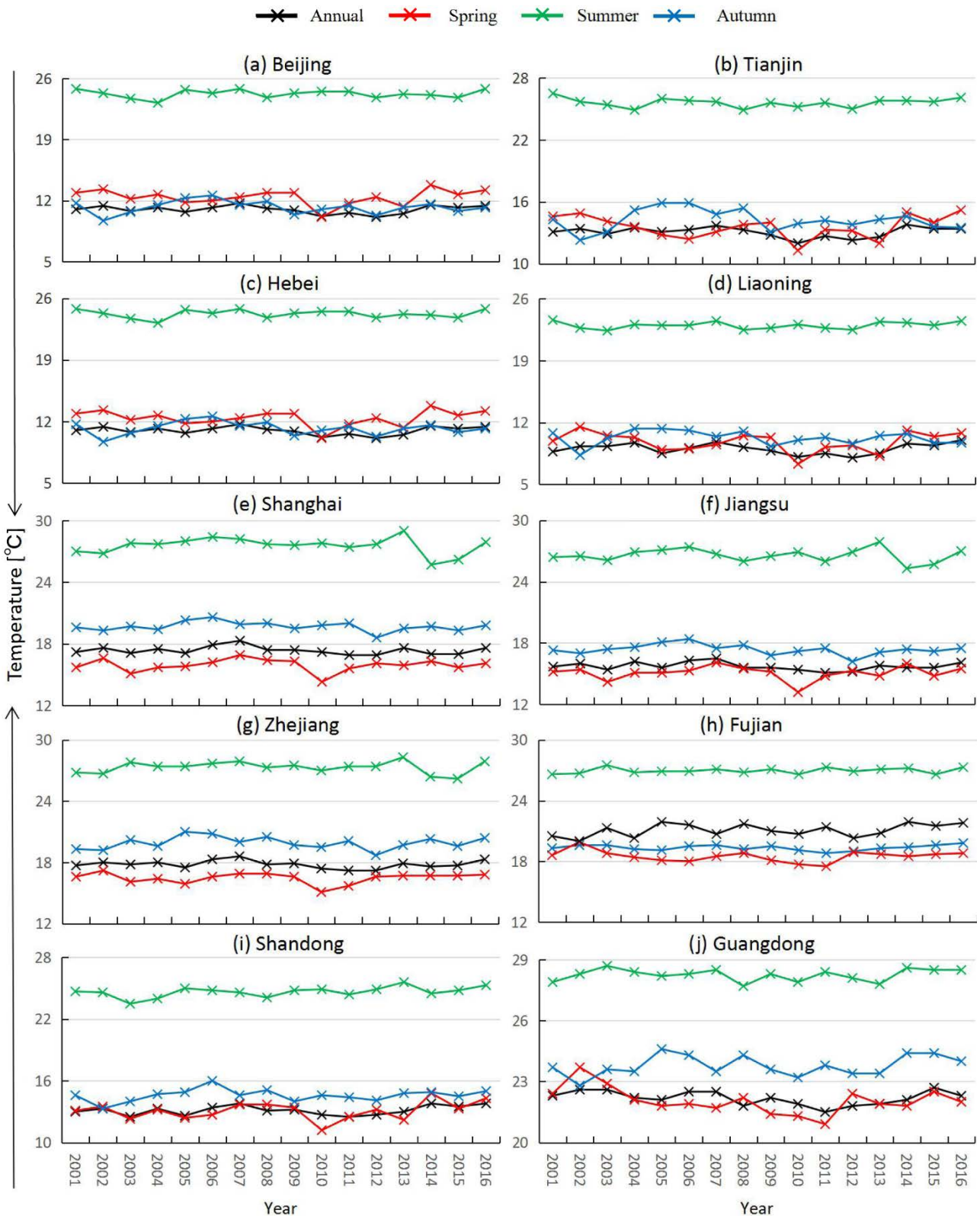

Figure A-4. The temporal variation of annual and seasonal temperature in ten administrative units from 2001 to 2016

Table A-1. The equation and R-squared value of annual and seasonal precipitation of eastern China and the ten administrative units (Unit: mm year^{-1})

Administrative unit	The equation and R-squared value of annual and seasonal precipitation			
	Annual	Spring	Summer	Autumn
Beijing	y = 7.5668x + 473.7 R^2 = 0.215	y = -0.4628x + 72.915 R^2 = 0.006	y = 4.6275x + 305.91 R^2 = 0.0938	y = 3.6109x + 83.87 R^2 = 0.0955
Tianjin	y = 5.3837x + 449.48 R^2 = 0.0649	y = 0.7076x + 53.61 R^2 = 0.02	y = 1.8465x + 313.23 R^2 = 0.0117	y = 2.5668x + 74.208 R^2 = 0.0491
Hebei	y = 6.2476x + 451.13 R^2 = 0.1709	y = -0.0462x + 71.755 R^2 = 0.0001	y = 4.2362x + 283.08 R^2 = 0.126	y = 1.8424x + 86.628 R^2 = 0.0524
Liaoning	y = 6.9581x + 616.35 R^2 = 0.0574	y = 3.0274x + 87.843 R^2 = 0.118	y = 2.1474x + 408.14 R^2 = 0.0128	y = 1.3721x + 101.34 R^2 = 0.0278
Shanghai	y = 21.195x + 1038.3 R^2 = 0.2143	y = 4.0234x + 217.85 R^2 = 0.0453	y = 4.3475x + 489 R^2 = 0.016	y = 17.068x + 106.72 R^2 = 0.3787
Jiangsu	y = 13.543x + 943.78 R^2 = 0.1691	y = 1.8597x + 183.28 R^2 = 0.0214	y = 2.8925x + 519.28 R^2 = 0.0142	y = 13.038x + 88.63 R^2 = 0.4355
Zhejiang	y = 23.45x + 1281 R^2 = 0.2058	y = 5.8562x + 346.89 R^2 = 0.0662	y = 8.609x + 476.17 R^2 = 0.1035	y = 9.9354x + 222.02 R^2 = 0.2739
Fujian	y = 32.302x + 1404.2 R^2 = 0.2029	y = 11.828x + 469.81 R^2 = 0.1595	y = 3.8515x + 608.26 R^2 = 0.0212	y = 11.206x + 169.41 R^2 = 0.188
Shandong	y = -2.911x + 720.56 R^2 = 0.0135	y = -0.4076x + 113.49 R^2 = 0.0036	y = -3.4387x + 457.51 R^2 = 0.0357	y = 1.1415x + 115.2 R^2 = 0.0078
Guangdong	y = 14.379x + 1674.4 R^2 = 0.0478	y = 17.765x + 402.54 R^2 = 0.3466	y = -15.64x + 944.05 R^2 = 0.1531	y = 3.8932x + 257.27 R^2 = 0.0316
Eastern China	y = 20.397x + 970.11 R^2 = 0.4387	y = 8.6357x + 224.97 R^2 = 0.4407	y = 1.9525x + 522.37 R^2 = 0.0367	y = 7.041x + 140.33 R^2 = 0.3882

Table A-2. The equation and R-squared value of annual and seasonal temperature of eastern China and the ten administrative units (Unit: ℃ year^{-1})

Administrative unit	The equation and R-squared value of annual and seasonal temperature			
	Annual	Spring	Summer	Autumn
Beijing	y = -0.0734x + 12.618 R^2 = 0.2597	y = -0.0643x + 14.19 R^2 = 0.0866	y = -0.0547x + 25.69 R^2 = 0.3037	y = -0.0825x + 12.783 R^2 = 0.1657
Tianjin	y = -0.0116x + 13.18 R^2 = 0.0123	y = -0.0075x + 13.645 R^2 = 0.001	y = -0.0034x + 25.635 R^2 = 0.0013	y = -0.0219x + 14.43 R^2 = 0.0103
Hebei	y = -0.0104x + 11.058 R^2 = 0.0117	y = -0.0037x + 12.425 R^2 = 0.0004	y = 0.0018x + 24.21 R^2 = 0.0003	y = -0.0132x + 11.35 R^2 = 0.0071
Liaoning	y = 0.0019x + 9.015 R^2 = 0.0002	y = -0.0226x + 9.9925 R^2 = 0.0095	y = 0.0132x + 22.888 R^2 = 0.0264	y = -0.0276x + 10.498 R^2 = 0.0263
Shanghai	y = -0.0172x + 17.503 R^2 = 0.0449	y = 0.0007x + 15.913 R^2 = 3E-05	y = -0.0207x + 27.733 R^2 = 0.0148	y = -0.0174x + 19.835 R^2 = 0.0328
Jiangsu	y = -0.0187x + 15.89 R^2 = 0.0508	y = 0.0054x + 15.048 R^2 = 0.0014	y = -0.0125x + 26.688 R^2 = 0.0081	y = -0.0274x + 17.608 R^2 = 0.0661
Zhejiang	y = -0.0134x + 17.92 R^2 = 0.0268	y = 0.0007x + 16.463 R^2 = 4E-05	y = -0.0019x + 27.335 R^2 = 0.0003	y = 0.0026x + 19.89 R^2 = 0.0004
Fujian	y = 0.0012x + 19.34 R^2 = 0.0004	y = -0.0194x + 18.665 R^2 = 0.0273	y = 0.0138x + 26.845 R^2 = 0.0561	y = 0.0547x + 20.623 R^2 = 0.1714
Shandong	y = 0.0282x + 12.898 R^2 = 0.0875	y = 0.0451x + 12.71 R^2 = 0.0606	y = 0.0528x + 24.208 R^2 = 0.2507	y = 0.026x + 14.373 R^2 = 0.0434
Guangdong	y = -0.0226x + 22.38 R^2 = 0.0981	y = -0.0563x + 22.535 R^2 = 0.1654	y = 0.0054x + 28.21 R^2 = 0.0075	y = 0.0304x + 23.523 R^2 = 0.082
Eastern China	y = 0.0551x + 15.15 R^2 = 0.4411	y = 0.0418x + 15.245 R^2 = 0.1002	y = 0.0381x + 25.608 R^2 = 0.3537	y = 0.0738x + 16.385 R^2 = 0.3538

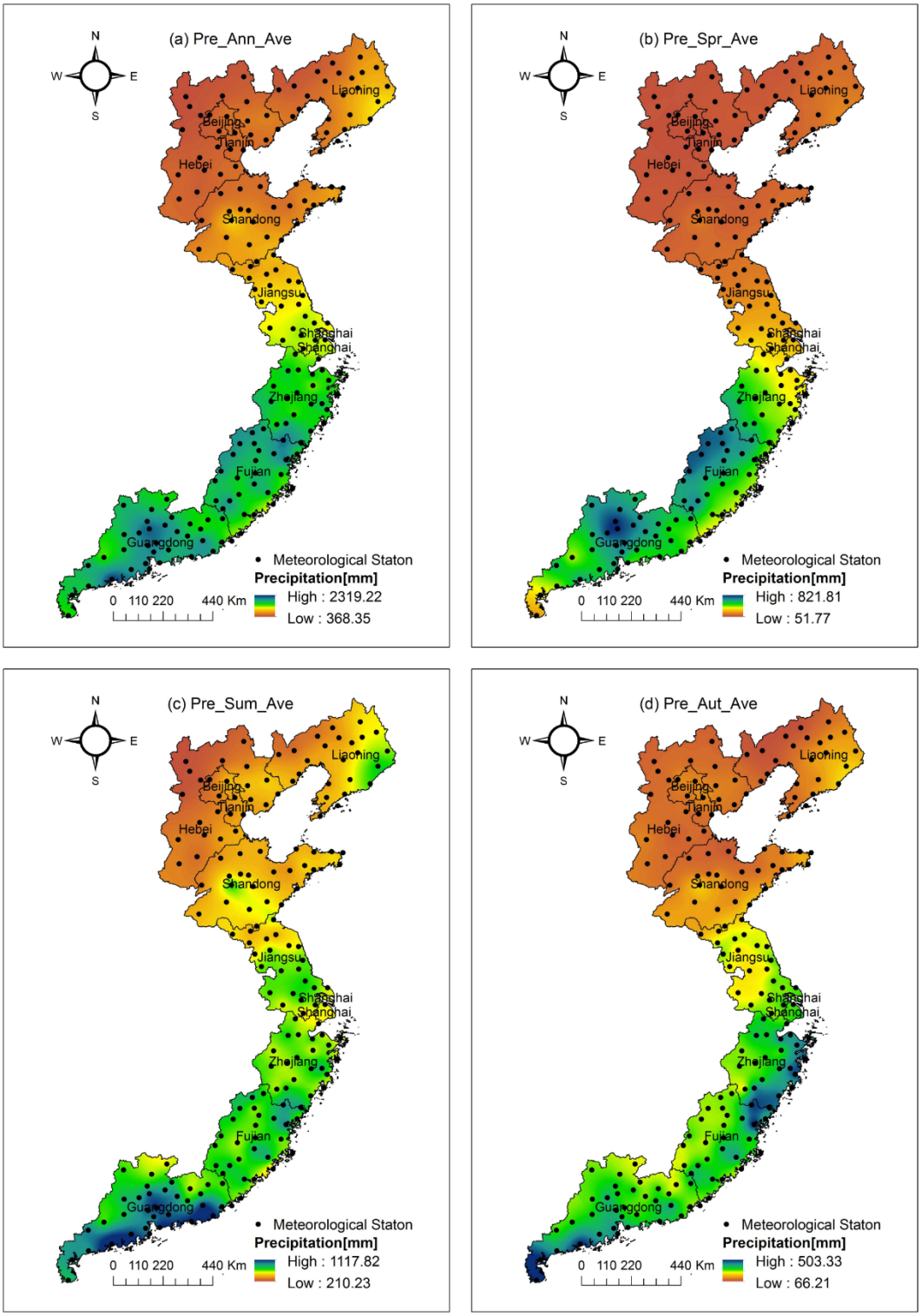

Figure A-5. The spatial pattern of mean annual and seasonal precipitation in eastern China from 2001 to 2016

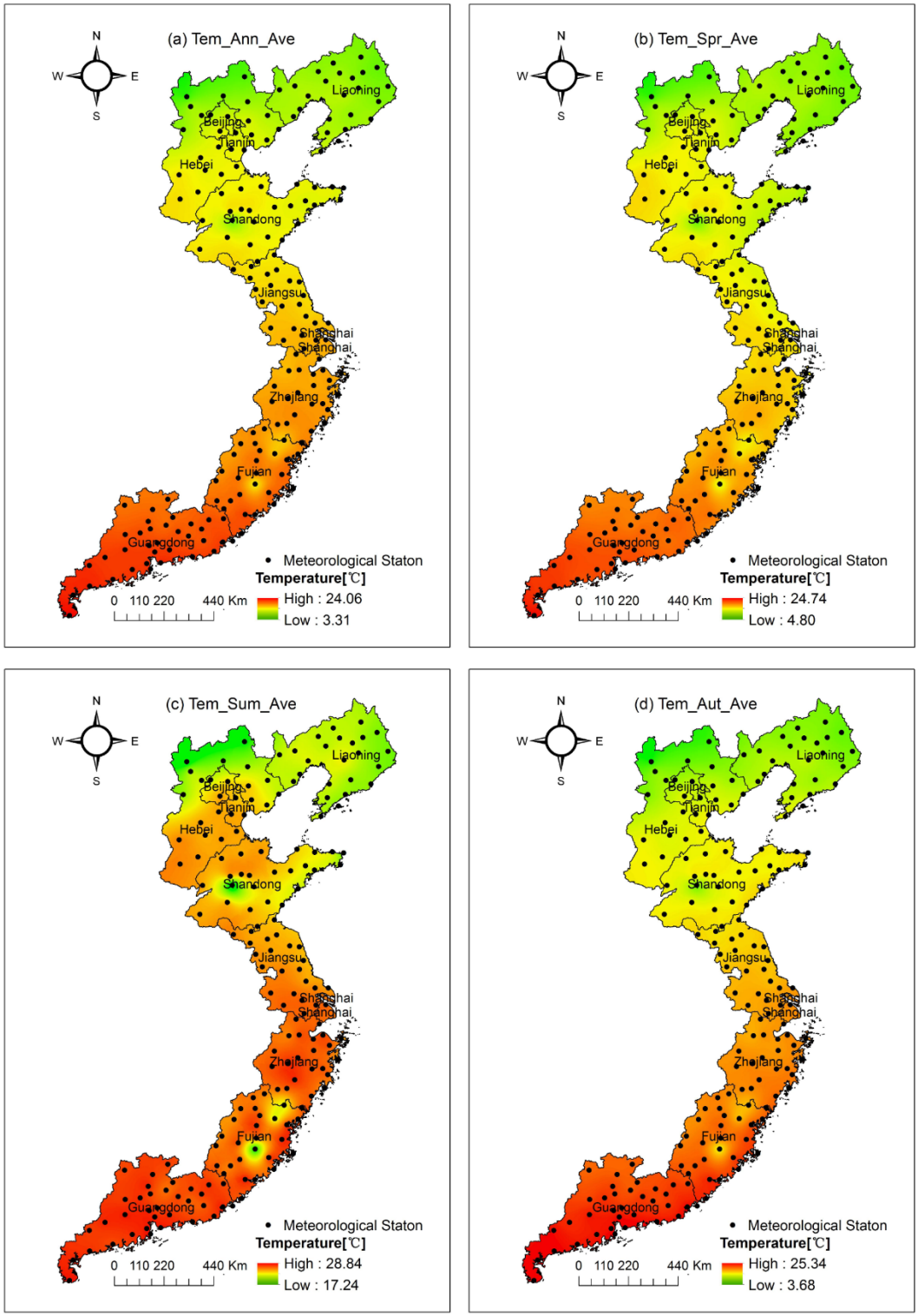

Figure A-6. The spatial pattern of mean annual and seasonal temperature in eastern China from 2001 to 2016

Appendix B

Table B-1. GDP for ten administrative units from 2001 to 2016 (Unit: 100 million RMB)

	Beijing	Tianjin	Hebei	Liaoning	Shanghai	Jiangsu	Zhejiang	Fujian	Shandong	Guangdong
2001	2845.65	1840.1	5577.78	5033.08	4950.84	9511.91	6748.15	4253.68	9438.31	10647.71
2002	3212.71	2051.16	6122.53	5458.22	5408.76	10631.75	7796	4682.01	10552.06	11769.73
2003	3663.1	2447.66	7098.56	6002.54	6250.81	12460.83	9395	5232.17	12435.93	13625.87
2004	4283.31	2931.88	8768.79	6872.65	7450.27	15403.16	11243	6053.14	15490.73	16039.46
2005	6886.31	3697.62	10096.11	8009.01	9154.18	18305.66	13437.85	6568.93	18516.87	22366.54
2006	7870.28	4359.15	11660.43	9251.15	10366.37	21645.08	15742.51	7614.55	22077.36	26204.47
2007	9353.32	5050.4	13709.5	11023.49	12188.85	25741.15	18780.44	9249.13	25965.91	31084.4
2008	10488.03	6354.38	16188.61	13461.57	13698.15	30312.61	21486.92	10823.11	31072.06	35696.46
2009	12153.03	7521.85	17235.48	15212.49	15046.45	34457.3	22990.35	12236.53	33896.65	39482.56
2010	14113.58	9224.46	20394.26	18457.27	17165.98	41425.48	27722.31	14737.12	39169.92	46013.06
2011	16251.93	11307.28	24515.76	22226.7	19195.69	49110.27	32318.85	17560.18	45361.85	53210.28
2012	17879.4	12893.88	26575.01	24846.43	20181.72	54058.22	34665.33	19701.78	50013.24	57067.92
2013	19500.56	14370.16	28301.41	27077.65	21602.12	59161.75	37568.49	21759.64	54684.33	62163.97
2014	21330.83	15726.93	29421.15	28626.58	23567.7	65088.32	40173.03	24055.76	59426.59	67809.85
2015	23014.59	16538.19	29806.11	28669.02	25123.45	70116.38	42886.38	25979.82	63002.33	72812.55
2016	25669.13	17885.39	32070.45	22246.9	28178.65	77388.28	47251.36	28810.58	68024.49	80854.91

Table B-2. Primary industry product for ten administrative units from 2001 to 2016 (Unit: 100 million RMB)

	Beijing	Tianjin	Hebei	Liaoning	Shanghai	Jiangsu	Zhejiang	Fujian	Shandong	Guangdong
2001	93.08	78.55	913.9	544.44	85.5	1082.43	695.15	651.11	1359.49	1004.35
2002	98.05	84	957.01	590.2	88.24	1119.12	694	664.78	1390	1032.8
2003	95.64	89.66	1064.33	615.8	90.64	1106.35	728	692.94	1480.67	1093.52
2004	102.9	102.29	1370.4	769.9	96.71	1315.38	816	777.87	1778.3	1245.42
2005	97.99	112.38	1503.07	882.41	80.34	1461.49	892.83	841.2	1963.51	1428.27
2006	98.04	118.23	1606.48	976.37	93.8	1545.01	925.1	896.17	2138.9	1577.12
2007	101.26	110.19	1804.72	1133.4	101.84	1816.24	986.02	1002.11	2509.14	1695.57
2008	112.81	122.58	2034.6	1302	111.8	2100	1095.43	1157.75	3002.65	1970.23
2009	118.29	128.85	2207.34	1414.9	113.82	2261.86	1163.08	1182.74	3226.64	2010.27
2010	124.36	145.58	2562.81	1631.08	114.15	2540.1	1360.56	1363.67	3588.28	2286.98
2011	136.27	159.72	2905.73	1915.57	124.94	3064.77	1583.04	1612.24	3973.85	2665.2
2012	150.2	171.6	3186.66	2155.82	127.8	3418.29	1667.88	1776.71	4281.7	2847.26
2013	161.83	188.45	3500.42	2321.63	129.28	3646.08	1784.62	1936.31	4742.63	3047.51
2014	158.99	199.9	3447.46	2285.75	124.26	3634.33	1777.18	2014.8	4798.36	3166.82
2015	140.21	208.82	3439.45	2384.03	109.82	3986.05	1832.91	2118.1	4979.08	3345.54
2016	129.79	220.22	3492.81	2173.06	109.47	4077.18	1965.18	2363.22	4929.13	3694.37

Table B-3. Secondary industry product for ten administrative units from 2001 to 2016 (Unit: 100 million RMB)

	Beijing	Tianjin	Hebei	Liaoning	Shanghai	Jiangsu	Zhejiang	Fujian	Shandong	Guangdong
2001	1030.6	904.64	2767.41	2440.55	2355.53	4907.46	3459.75	1904.21	4654.51	5341.61
2002	1116.53	1001.9	3046	2609.85	2564.69	5550.98	3982	2159.94	5309.54	5935.63
2003	1311.86	1245.29	3657.19	2898.89	3130.72	6787.11	4941	2492.73	6656.85	7307.08
2004	1610.37	1560.16	4635.23	3278.88	3788.22	8716.11	6045	2950.33	8724.52	8890.29
2005	2026.51	2051.17	5232.5	3953.28	4452.92	10355.03	7166.15	3200.26	10628.62	11339.93
2006	2191.43	2488.29	6115.01	4729.5	5028.37	12250.84	8509.57	3743.71	12751.2	13431.82
2007	2509.4	2892.53	7241.8	5853.1	5678.51	14306.4	10148.45	4549.42	14776.53	15939.1
2008	2693.15	3821.07	8777.42	7512.11	6235.92	16663.81	11580.33	5415.77	17702.17	18402.64
2009	2855.55	3987.84	8959.83	7906.34	6001.78	18566.37	11908.49	6005.3	18901.83	19419.7
2010	3388.38	4840.23	10707.68	9976.82	7218.32	21753.93	14297.93	7522.83	21238.49	23014.53
2011	3752.48	5928.32	13126.86	12152.15	7927.89	25203.28	16555.58	9069.2	24017.11	26447.38
2012	4059.27	6663.82	14003.57	13230.49	7854.77	27121.95	17316.32	10187.94	25735.73	27700.97
2013	4352.3	7276.68	14762.1	14269.46	8027.77	29094.03	18446.65	11315.3	27422.47	29427.49
2014	4544.8	7731.85	15012.85	14384.64	8167.71	30854.5	19175.06	12515.36	28788.11	31419.75
2015	4542.64	7704.22	14386.87	13041.97	7991	32044.45	19711.67	13064.82	29485.35	32613.54
2016	4944.44	7571.35	15256.93	8606.54	8406.54	34619.5	21194.61	14093.47	31343.67	35109.66

Table B-4. Tertiary industry product for ten administrative units from 2001 to 2016 (Unit: 100 million RMB)

	Beijing	Tianjin	Hebei	Liaoning	Shanghai	Jiangsu	Zhejiang	Fujian	Shandong	Guangdong
2001	1721.97	856.91	1896.47	2048.09	2509.81	3522.02	2593.25	1698.36	3424.31	4301.75
2002	1998.13	965.26	2119.52	2258.17	2755.83	3961.65	3120	1857.29	3852.52	4801.3
2003	2255.6	1112.71	2377.04	2487.85	3029.45	4567.37	3726	2046.5	4298.41	5225.27
2004	2570.04	1269.43	2763.16	2823.87	3565.34	5371.68	4382	2324.94	4987.91	5903.75
2005	4761.81	1534.07	3360.54	3173.32	4620.92	6489.14	5378.87	2527.47	5924.74	9598.34
2006	5580.81	1752.63	3938.94	3545.28	5244.2	7849.23	6307.85	2974.67	7187.26	11195.53
2007	6742.66	2047.68	4662.98	4036.99	6408.5	9618.52	7645.96	3697.6	8680.24	13449.73
2008	7682.07	2410.73	5376.59	4647.46	7350.43	11548.8	8811.17	4249.59	10367.23	15323.59
2009	9179.19	3405.16	6068.31	5891.25	8930.85	13629.07	9918.78	5048.49	11768.18	18052.59
2010	10600.84	4238.65	7123.77	6849.37	9833.51	17131.45	12063.82	5850.62	14343.14	20711.55
2011	12363.18	5219.24	8483.17	8158.98	11142.86	20842.21	14180.23	6878.74	17370.89	24097.7
2012	13669.93	6058.46	9384.78	9460.12	12199.15	23517.98	15681.13	7737.13	19995.81	26519.69
2013	14986.43	6905.03	10038.89	10486.56	13445.07	26421.64	17337.22	8508.03	22519.23	29688.97
2014	16627.04	7795.18	10960.84	11956.19	15275.72	30599.49	19220.79	9525.6	25840.12	33223.28
2015	18331.74	8625.15	11979.79	13243.02	17022.63	34085.88	21341.91	10796.9	28537.35	36853.47
2016	20594.9	10093.82	13320.71	11467.3	19662.9	38691.6	24091.57	12353.89	31751.69	42050.88

Table B-5. GDP per capita for ten administrative units from 2001 to 2016 (Unit: RMB)

	Beijing	Tianjin	Hebei	Liaoning	Shanghai	Jiangsu	Zhejiang	Fujian	Shandong	Guangdong
2001	25523	20154	8362	12041	37382	12922	14655	12362	10465	13730
2002	28449	22380	9115	12986	40646	14391	16838	13497	11645	15030
2003	32061	26532	10513	14258	46718	16809	20147	14979	13661	17213
2004	37058	31550	12918	16297	55307	20705	23942	17218	16925	19707
2005	45444	35783	14782	18983	51474	24560	27703	18646	20096	24435
2006	50467	41163	16962	21788	57695	28814	31874	21471	23794	28332
2007	58204	46122	19877	25729	66367	33928	37411	25908	27807	33151
2008	63029	55473	23239	31259	73124	39622	42214	30123	33083	37589
2009	70452	62574	24581	35239	78989	44744	44641	33840	35894	41166
2010	75943	72994	28668	42355	76074	52840	51711	40025	41106	44736
2011	81658	85213	33969	50760	82560	62290	59249	47377	47335	50807
2012	87475	93173	36584	56649	85373	68347	63374	52763	51768	54095
2013	93213	99607	38716	61686	90092	74607	68462	57856	56322	58540
2014	99995	105231	39984	65201	97370	81874	73002	63472	60879	63469
2015	106497	107960	40255	65354	103796	87995	77644	67966	64168	67503
2016	118198	115053	43062	50791	116562	96887	84916	74707	68733	74016

Table B-6. Household consumption ten administrative units from 2001 to 2016 (Unit: RMB)

	Beijing	Tianjin	Hebei	Liaoning	Shanghai	Jiangsu	Zhejiang	Fujian	Shandong	Guangdong
2001	8197	6802	2785	4789	12562	4322	4772	4611	3751	5038
2002	9291	7162	3054	5095	14295	4704	5515	4900	3952	5683
2003	10584	7836	3452	5159	15866	5274	6451	5324	4385	6190
2004	12405	8765	3858	5561	18382	6159	6844	5913	4966	7286
2005	14835	9484	4311	6449	18396	7163	9701	6793	5899	9821
2006	16770	10564	4945	6929	20944	8302	11161	7826	7025	10829
2007	18911	11957	5674	7965	24260	9659	12569	8772	8075	12663
2008	20346	14000	6570	9625	27343	11013	13893	10361	9573	14390
2009	22154	15149	7193	10848	29572	11993	15790	10950	10494	15291
2010	25015	17784	8057	12934	32271	14035	18097	12871	11611	17218
2011	27760	20624	9551	15635	35439	17167	21346	14958	13565	19578
2012	30350	22984	10749	17999	36893	19452	22845	16144	15095	21823
2013	33337	26261	11557	20156	39223	23585	24771	17115	16728	23739
2014	36057	28492	12171	22260	43007	28316	26885	19099	19184	24582
2015	39200	32595	12829	23693	45816	31682	28712	20828	20684	26365
2016	48883	36257	14328	23670	49617	35875	30743	23355	25860	28495

Table B-7. Rural household consumption for ten administrative units from 2001 to 2016 (Unit: RMB)

	Beijing	Tianjin	Hebei	Liaoning	Shanghai	Jiangsu	Zhejiang	Fujian	Shandong	Guangdong
2001	3831	3736	1967	2540	6923	2867	3434	3901	2555	2882
2002	4390	3974	2120	2643	7516	3109	4017	4104	2681	3001
2003	5041	4321	2305	2630	8141	3293	4665	4358	2943	3086
2004	5498	4716	2644	2817	9085	3517	4677	4831	3318	3374
2005	6635	4360	2449	3267	9157	4207	5476	3730	3078	3947
2006	7655	4771	2725	3458	10136	4915	6301	4290	3537	4205
2007	9063	5334	3090	3634	11235	5775	7077	4808	4126	4490
2008	10043	6389	3553	4321	12202	6461	7665	5633	4859	5176
2009	11483	7075	3606	4909	13748	7147	8324	6037	5395	5239
2010	12886	7814	3867	5739	13609	8196	9878	6879	5733	5880
2011	13659	9658	4893	7221	17758	10164	12371	8436	7063	7854
2012	14664	11936	5766	8652	18512	11721	13724	9596	8212	8898
2013	17663	14954	6460	10417	20221	14571	15458	10147	9224	9914
2014	20506	16949	7023	12178	22803	17780	17281	11908	11215	12674
2015	22315	19922	7667	13707	23005	20428	19953	13631	12651	13344
2016	24285	22194	8897	12145	23660	23459	22028	15653	15970	14784

Table B-8. Urban household consumption for ten administrative units from 2001 to 2016 (Unit: RMB)

	Beijing	Tianjin	Hebei	Liaoning	Shanghai	Jiangsu	Zhejiang	Fujian	Shandong	Guangdong
2001	10150	8979	6102	7366	14447	7267	9459	7247	6923	9730
2002	11365	9403	6604	7874	16457	7742	10481	7779	7145	10890
2003	12775	10266	7082	7147	18175	8126	11688	8731	7740	10471
2004	14971	11369	7757	7717	20795	9065	12782	9686	8526	11447
2005	16683	11394	7927	8688	19573	10199	14097	10296	9453	13624
2006	18508	12554	9008	9357	22294	11530	15877	11710	11193	14913
2007	20729	14140	9941	10950	25919	13165	17486	13006	12633	17448
2008	22207	16301	10955	13216	29250	14930	18515	15223	14851	19743
2009	24044	17475	12195	14774	31608	15965	21251	15739	16027	21098
2010	27071	20466	13619	17489	34588	18243	23624	17920	17726	23511
2011	30037	23360	15331	20561	37558	21598	26856	19762	19984	25527
2012	32857	25569	16554	23065	39095	24101	28259	20722	21528	28269
2013	35836	28779	17198	25161	41464	28753	30101	21725	23358	30439
2014	38515	31000	17589	27282	45352	34074	32186	23642	25869	30216
2015	41846	35290	17924	28567	48750	37515	33359	25202	26993	32393
2016	52721	39181	19276	29254	53240	41957	35152	27859	33016	34667

Table B-9. Total investment in fixed assets for ten administrative units from 2001 to 2016 (Unit: 100 million RMB)

	Beijing	Tianjin	Hebei	Liaoning	Shanghai	Jiangsu	Zhejiang	Fujian	Shandong	Guangdong
2001	1513.32	705	1912.53	1421.19	2004.64	2823.2	2834.94	1172.91	2788.68	3484.43
2002	1796.14	807.51	2020.38	1605.55	2213.72	3450.12	3477.47	1253.08	3483.31	3850.78
2003	2169.26	1039.39	2477.98	2076.36	2499.14	5233	4740.27	1496.37	5315.14	4813.2
2004	2528.2	1245.7	3218.8	2979.6	3050.3	6557.1	5781.4	1892.9	6970.6	5870
2005	2827.2	1495.1	4139.7	4200.4	3509.7	8165.4	6520.1	2316.7	9307.3	6977.9
2006	3296.4	1820.5	5470.2	5689.6	3900	10069.2	7590.2	2981.8	11111.4	7973.4
2007	3907.2	2353.1	6884.7	7435.2	4420.4	12268.1	8420.4	4287.8	12537.7	9294.3
2008	3814.7	3389.8	8866.6	10019.1	4823.1	15300.6	9323	5207.7	15435.9	10868.7
2009	4616.9	4738.2	12269.8	12292.5	5043.8	18949.9	10742.3	6231.2	19034.5	12933.1
2010	5403	6278.1	15083.4	16043	5108.9	23184.3	12376	8199.1	23280.5	15623.7
2011	5578.9	7067.7	16389.3	17726.3	4962.1	26692.6	14185.3	9910.9	26749.7	17069.2
2012	6112.4	7934.8	19661.3	21836.3	5117.6	30854.2	17649.4	12439.9	31255.9	18751.5
2013	6847.1	9130.2	23194.2	25107.7	5647.8	36373.3	20782.1	15327.4	36789.1	22308.4
2014	6924.2	10518.2	26671.9	24730.8	6016.4	41938.6	24262.8	18177.9	42495.5	26293.9
2015	7496	11832	29448.3	17917.9	6352.7	46246.9	27323.3	21301.4	48312.4	30343
2016	7943.9	12779.4	31750	6692.2	6755.9	49663.2	30276.1	23237.4	53322.9	33303.6

Table B-10. Urbanization rate for ten administrative units from 2001 to 2016 (Unit: %)

	Beijing	Tianjin	Hebei	Liaoning	Shanghai	Jiangsu	Zhejiang	Fujian	Shandong	Guangdong
2001	78.06	72.41	20.35	54.9	75.3	42.6	50.9	42.76	39.2	56.45
2002	78.56	72.87	31.86	55	76.4	44.7	51.9	45.66	40.3	57.42
2003	79.05	73.45	33.52	56	77.6	46.8	53	46.37	41.8	58.45
2004	79.53	74.21	35.83	56	81.2	48.2	54	47.63	43.5	59.6
2005	83.62	75.11	37.69	58.7	84.5	50.11	56.02	47.3	45	60.68
2006	84.33	75.73	38.44	58.99	85.8	51.9	56.5	48	46.1	63
2007	84.5	76.31	40.25	59.2	86.8	53.2	57.2	51.4	46.75	63.14
2008	84.9	77.23	41.9	60.05	87.5	54.3	57.6	53	47.6	63.37
2009	85	78.01	43.74	60.35	88.6	55.6	57.9	55.1	48.32	63.4
2010	85.96	79.55	44.5	62.1	89.3	60.58	61.62	57.1	49.7	66.17
2011	86.2	80.5	45.6	64.05	88.9	61.9	62.3	58.1	50.95	66.5
2012	86.2	81.55	46.8	65.65	89.3	63	63.2	69.6	52.43	67.4
2013	86.3	82.01	48.12	66.45	89.6	64.11	64	60.77	53.75	67.76
2014	86.35	82.27	49.33	67.05	89.6	65.21	64.87	61.8	55.01	68
2015	86.5	82.64	51.33	67.35	87.6	66.52	65.8	62.6	57.01	68.71
2016	86.5	82.93	53.32	67.37	87.9	67.73	67	63.6	59.02	69.2

Table B-11. Population density for ten administrative units from 2001 to 2016 (Unit: Person/sq.km.)

	Beijing	Tianjin	Hebei	Liaoning	Shanghai	Jiangsu	Zhejiang	Fujian	Shandong	Guangdong
2001	824	854	356	279	2631	717	465	278	577	486
2002	847	856	359	280	2702	722	469	280	580	492
2003	867	860	361	279	2785	727	477	282	582	499
2004	910	870	363	281	2894	733	484	285	586	507
2005	937	887	365	282	2981	740	490	287	589	511
2006	976	914	368	284	3098	746	498	289	592	525
2007	1021	948	370	285	3255	753	506	291	596	537
2008	1079	1000	373	286	3376	756	512	293	599	550
2009	1133	1044	375	287	3486	761	518	296	603	563
2010	1196	1105	384	287	3632	767	535	298	610	581
2011	1230	1152	386	287	3702	770	537	300	613	584
2012	1261	1202	389	286	3754	772	538	302	616	590
2013	1289	1252	391	286	3809	774	540	304	619	592
2014	1311	1290	394	286	3826	776	541	307	620	597
2015	1323	1315	396	285	3809	777	544	310	624	604
2016	1324	1328	398	285	3816	780	549	313	630	612

Table B-12. Population for ten administrative units from 2001 to 2016 (Unit: Ten thousand)

	Beijing	Tianjin	Hebei	Liaoning	Shanghai	Jiangsu	Zhejiang	Fujian	Shandong	Guangdong
2001	1385	1004	6668	4182	1668	7359	4739	3445	9041	7783
2002	1423	1007	6735	4203	1713	7406	4776	3476	9082	7859
2003	1456	1011	6769	4210	1766	7458	4857	3502	9125	7954
2004	1493	1024	6809	4217	1835	7523	4925	3529	9180	8304
2005	1538	1043	6851	4221	1890	7588	4991	3557	9248	9194
2006	1601	1075	6898	4271	1964	7656	5072	3585	9309	9442
2007	1676	1115	6943	4298	2064	7723	5155	3612	9367	9660
2008	1771	1176	6989	4315	2141	7762	5212	3639	9417	9893
2009	1860	1228	7034	4341	2210	7810	5276	3666	9470	10130
2010	1962	1299	7194	4375	2303	7869	5447	3693	9588	10441
2011	2019	1355	7241	4383	2347	7899	5463	3720	9637	10505
2012	2069	1413	7288	4389	2380	7920	5477	3748	9685	10594
2013	2115	1472	7333	4390	2415	7939	5498	3774	9733	10644
2014	2152	1517	7384	4391	2426	7960	5508	3806	9789	10724
2015	2171	1547	7425	4382	2415	7976	5539	3839	9847	10849
2016	2173	1562	7470	4378	2420	7999	5590	3874	9947	10999

Table B-13. Total employment for ten administrative units from 2001 to 2016 (Unit: Ten thousand)

	Beijing	Tianjin	Hebei	Liaoning	Shanghai	Jiangsu	Zhejiang	Fujian	Shandong	Guangdong
2001	628.9	488.34	-	2069.3	752.26	4436.45	2796.65	1677.79	5475.3	4058.63
2002	679.2	492.61	-	2025.3	792.04	4472.84	2858.56	1711.32	5527	4134.37
2003	703.3	510.9	-	2018.9	813.05	4499.97	2918.74	1756.71	5620.6	4395.93
2004	854.1	527.78	-	2097.3	836.87	4537.07	2991.95	1814.03	5728.1	4681.89
2005	878	542.52	-	2120.3	863.32	4578.75	3100.76	1868.5	5840.7	5022.97
2006	919.7	562.92	-	2128.1	885.51	4628.95	3172.38	1949.58	5960	5177.02
2007	942.7	613.93	-	2180.7	1 024.33	4677.88	3405.01	2015.33	6081.4	5341.5
2008	980.9	647.32	-	2198.2	1 053.24	4700.96	3486.53	2079.78	6187.6	5471.72
2009	998.3	677.13	-	2277.1	1 064.42	4726.54	3591.98	2168.86	6294.2	5688.62
2010	1031.6	728.7	-	2317.5	1 090.76	4754.68	3636.02	2241.59	6401.9	5870.48
2011	1069.7	763.16	-	2364.9	1 104.33	4758.23	3674.11	2459.99	6485.6	5960.74
2012	1107.3	803.14	-	2432.8	1 115.50	4759.53	3691.24	2568.93	6554.3	5965.95
2013	1141	847.46	-	2518.9	1 368.91	4759.89	3708.73	2555.86	6580.4	6117.68
2014	1156.7	877.21	-	2562.2	1 365.63	4760.83	3714.15	2648.51	6606.5	6183.23
2015	1186.1	896.8	-	2409.9	1 361.51	4758.5	3733.65	2768.41	6632.5	6219.31
2016	1220.1	902.42	-	2301.2	1 365.24	4756.22	3760	2797.03	6649.7	6279.22

EIDESSTATTLICHE VERSICHERUNG

Hiermit versichere ich an Eides statt, dass ich die vorliegende Dissertationsschrift zum Thema

"Study of the Vegetation Cover Change and Its Driving Forces"

selbstständig verfasst und keine anderen als die angegebenen Quellen benutzt habe. Alle Stellen, die wörtlich oder sinngemäß aus Quellen entnommen wurden, habe ich als solche gekennzeichnet.

Des Weiteren erkläre ich an Eides statt, dass diese Arbeit weder in gleicher noch in ähnlicher Fassung einer akademischen Prüfung vorgelegt wurde.

Dortmund, 15.06.2019 Yong Xu